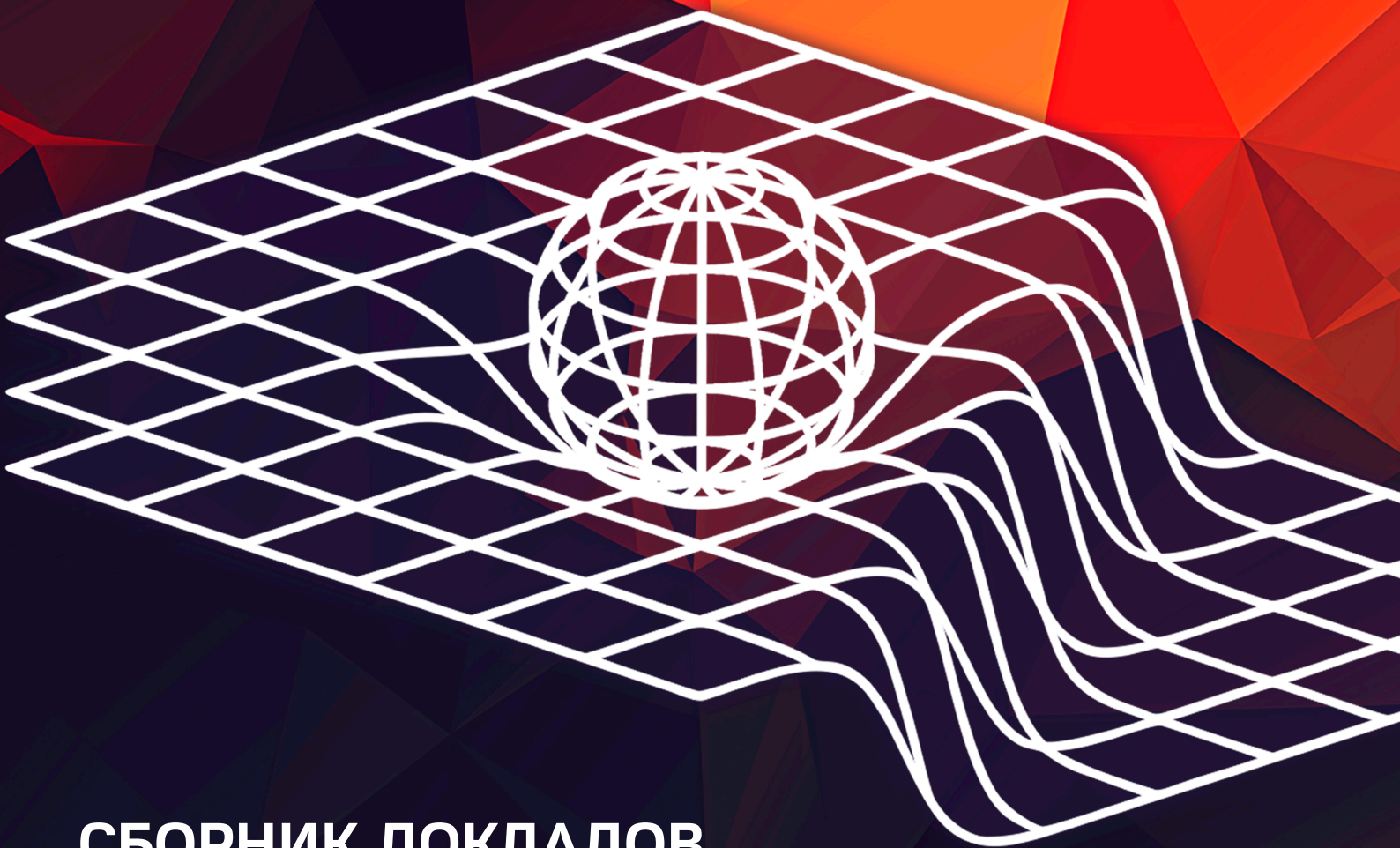


СЕДЬМАЯ МЕЖДУНАРОДНАЯ КОНФЕРЕНЦИЯ

ПРОБЛЕМЫ МАТЕМАТИЧЕСКОЙ ФИЗИКИ И МАТЕМАТИЧЕСКОЕ МОДЕЛИРОВАНИЕ



СБОРНИК ДОКЛАДОВ

25-27 ИЮНЯ 2018 ГОДА
МОСКВА, РОССИЯ

Ministry of Education and Science
Russian Federation
National Research Nuclear University MEPhI

7th International conference
“Problems of Mathematical Physics
and Mathematical Modelling”

Book of abstracts
(Moscow, NRNU MEPhI, 25–27 June 2018)

Moscow, Russia

УДК 51(06)+53(06)
ББК 22.1г+22.3г
I73

7th International conference “Problems of Mathematical Physics and Mathematical Modelling”: Books of abstracts (Moscow, NRNU MEPhI, 25–27 June). / M.B. Kochanov. M.: Moscow, 2018. — 216p.
ISBN 978-5-7262-2487-9

The book contains abstracts of 7th International conference “Problems of Mathematical Physics and Mathematical Modelling”

The contributions are reproduced directly from the originals
presented by the authors

УДК 51(06)+53(06)
ББК 22.1г+22.3г

ISBN 978-5-7262-2487-9

© *National Research Nuclear University MEPhI, 2018*

Co-chairs

V.V. Kozlov, Member of the Russian Academy of Science, Russia

N.A. Kudryshov, Head of department of Applied Mathematics NRNU MEPhI, Russia

O.V. Nagornov, Head of department of Higher Mathematics of NRNU MEPhI, Russia

Program committee

V.V. Kozlov, Member of the Russian Academy of Science, Russia

N.A. Kudryshov, Head of department of Applied Mathematics NRNU MEPhI, Russia

O.V. Nagornov, Head of department of Pure Mathematics of NRNU MEPhI, Russia

A.V. Aksenov, Lomonosov Moscow State University, Russia

V. Arakelyan, Professor, Institut National des Sciences Appliques, France

P. Bedrikovetsky, Professor of Petroleum Engineering, University of Adelaide, Australia

O.I. Vinogradova, Lomonosov Moscow State University, Russia

Y. Efendiev, Director of Institute for Scientific Computation, Texas AM University, USA

V. S. Gerdjikov, Institute of Mathematics and Informatics, Bulgarian Academy of Sciences

S.A. Kaschenko, Yaroslavl State University, Russia

R. Conte, Condensed Matter Laboratory, CEA Saclay, France

A.V. Kryanev, NRNU MEPhI, Russia

R. Lazarov, Professor of Mathematics, Texas A&M University, USA

S.Yu. Misyurin, Director of Institute of Cyber Intelligence Systems NRNU MEPhI, Russia

N. Pogorelov, Professor, University of Alabama in Huntsville

A.D. Polyanin, IPMech RAS, Russia

V.L. Savatorova, Professor, University of Nevada, Las Vegas, USA

Organizing committee

N.A. Kudryshov, Head of department of Applied Mathematics NRNU MEPhI, Russia

O.V. Nagornov, Head of department of Higher Mathematics of NRNU MEPhI, Russia

S.Yu. Misyurin, Director of Institute of Cyber Intelligence Systems NRNU MEPhI, Russia

E.V. Antonova, NRNU MEPhI, Russia

M.B. Kochanov, NRNU MEPhI, Russia

P.N. Ryabov, NRNU MEPhI, Russia

D.I. Sinelschikov, NRNU MEPhI, Russia

Y.E. Semenova, NRNU MEPhI, Russia

M.A. Chmyhov, NRNU MEPhI, Russia

A.G. Shinkaryuk, NRNU MEPhI, Russia

Table of contents

Section “Methods of mathematical physics”

<i>Adzhiev S.Z., Melikhov I.V., Vedenyapin V.V.</i> Kinetic models of the coalescence-fragmentation: the derivation of equations, the determination of the coefficients of the equations by the experimental distribution functions	11
<i>Aksenov A.V., Chicherina A.D., Chicherin I.S.</i> Self-similar solution for the problem of power-law liquid flow along an inclined plane	12
<i>Aksenov A.V., Druzhkov K.P.</i> Symmetries of the system of two-dimensional shallow water over a rough bottom equations	14
<i>Aleshin S.V., Glyzin S.D., Kaschenko S.A.</i> Computational aspects of the wave distribution problem in the logistic equation with spatial deviation	16
<i>Antonov I.D., Porubov A.V.</i> Influence of compressibility on the foam fracture modeling	18
<i>Averina V.V., Kudryashov N.A.</i> Numerical simulation of Fermi-Pasta-Ulam model, its discrete and continuous approximations	19
<i>Bagderina Y.Y.</i> Equivalence of second-order ODEs to the Painleve equations	21
<i>Bulatov V.V., Vladimirov Y.V., Vladimirov I.Y.</i> Far surface gravity waves fields generated by a rapidly moving oscillating source	23
<i>Butuzov V.F., Nefedov N.N., Omel’chenko O.E., Recke L.</i> Partially dissipative system with multizonal initial and boundary layers	25
<i>Davydova M.A., Nefedov N.N.</i> Multidimensional singularly perturbed reaction-diffusion-advection problems with balanced nonlinearity and their applications in the theory of nonlinear heat conductivity	26
<i>Demina M.V.</i> Invariant algebraic curves and Liouvillian first integrals for polynomial dynamical systems in the plane	28
<i>Demina M.V., Kudryashov N.A., Safonoova D.V.</i> Stationary vortex configurations on a cylindrical surface	29
<i>Dobrokhotov S.Y., Nazaikinskii V.E.</i> Pair of Lagrangian manifolds and asymptotic solutions of nonhomogeneous partial (pseudo)differential equations with localized right hand side	31
<i>Dorodnitsyn V., Kozlov R., Meleshko S., Winternitz P.</i> Lie group classification of first and second order delay ordinary differential equations	32
<i>Dryuma V.</i> On geometric applications of nonlinear integrable equations	33
<i>Gaiur I.Y., Sinelshchikov D.I., Kudryashov N.A.</i> Lax representation and quadratic first integrals for a family of non-autonomous second-order differential equations	35
<i>Garashchuk I.R., Sinelshchikov D.I., Kudryashov N.A.</i> Multistability in a model of oscillations of an encapsulated microbubble contrast agent close to an elastic wall	36
<i>Gavrikov M.B., Taiurskii A.A.</i> Traveling Waves and Plasma Acceleration in Quasi-Steady Plasma Accelerators (QSPAs) with Longitudinal Field	38
<i>Glyzin S.D., Kolesov A.Y., Rozov N.K.</i> Quasi-Stable Structures of the Repressilator Model	40
<i>Golovin A.V., Lagodiski V.M.</i> Functions of differential operators and the relativistic Schrödinger equation	42
<i>Grigorieva E.V., Kaschenko S.A., Glazkov D.V.</i> Normal forms for the model of optoelectronic oscillator with delay	45
<i>Kashchenko A.A.</i> Dynamical properties of one model with delay and large parameter	46
<i>Kashchenko I.S.</i> Dynamics of spatially distributed delay logistic equation	47
<i>Kasimov A.R.</i> Supersonic waves of spin reversal in molecular magnets	49
<i>Khakimova Z.N.</i> The replenishment method and new solvable cases of third-order nonlinear differential equations of Emden – Fowler type	49
<i>Kozlov V.K., Chmykhov M.A.</i> Mathematical modeling of free convection problems in a gravity field in OpenFOAM	51
<i>Kudryashov N.A., Kutukov A.A.</i> On the connection between the mKdV-sinh-Gordon hierarchy and the generalized hierarchy of the second Painleve equation	54

<i>Kudryashov N.A., Muratov R.V., Ryabov P.N.</i> Statistical features of plastic flow localization in dipolar materials	56
<i>Kudryashov N.A., Muratov R.V., Ryabov P.N.</i> On shear strain localization in composites	58
<i>Kuznetsov N.V., Mokaev T.N.</i> Hidden Attractors in Fundamental Problems and Applied Models	60
<i>Lavrova S.F., Kudryashov N.A., Sinelshchikov D.I.</i> Analytical properties and numerical modelling of the coupled FitzHugh-Nagumo equations	61
<i>Petrov P.N., Dobrokhotov S.Y.</i> Semiclassical asymptotics of the solution of the Helmholtz equation in a three-dimensional layer of variable thickness with a localized right-hand side	62
<i>Polyanin A.D., Shingareva I.K.</i> The method of nonlocal transformations: Applications to singularly perturbed boundary-value problems with a small parameter	64
<i>Prosviryakov E.Y.</i> Exact Polynomial Solutions for the Navier-Stokes Equations	66
<i>Romanov O.</i> Modeling of laser-induced acoustic signals in layered nanostructures	67
<i>Savel'ev V.V., Shutov I.V.</i> Nonlinear waves in the Hall magnetohydrodynamics in isothermal approximation	67
<i>Sekerzh-Zen'kovich S.Y., Tolchennikov A.A.</i> Comparison of tsunami heights calculated by asymptotic formulas with known numerical results for the transoceanic tsunami propagation.	69
<i>Sergeev S.A., Tolchennikov A.A., Petrov P.S.</i> Simulation of the propagation of acoustic pulse signal propagation in a shallow sea with penetrable bottom with the Maslov's canonical operator	70
<i>Shargatov V.A., Il'ichev A., Gorkunov S.V., Artamonov I.A.</i> Stability of phase transition evaporation interfaces in the form of travelling fronts	71
<i>Sinelshchikov D.I., Kudryashov N.A.</i> Integrable non-autonomous Li'enard-type equations	72
<i>Sorokin V.G., Polyanin A.D.</i> Nonlinear delay partial differential equations: Linear and nonlinear instability of solutions and numerical integration	72
<i>Sultanov O.A.</i> Lyapunov functions and asymptotics for near-Hamiltonian systems	75
<i>Teterev A.V., Rudak L.V., Mandrik P.A.</i> Modeling of a pulse detonation chamber	75
<i>Tsegel'nik V.</i> Qualitative and analytical properties of solutions belonging to a family of three-dimensional four-component conservative dynamical systems with two quadratic nonlinearities	78
<i>Tsvetkova A.V.</i> On a pair of Lagrangian manifolds connected with the asymptotics of Hermite polynomials	79
<i>Vazhenin G.A., Banov S.M., Dalechina A.V.</i> Using Machine Learning to predict survival in patients with brain metastases after Gamma Knife radiosurgery.	80
<i>Vedenyapin B.V., Adzhiev S.Z., Kazantseva V.V., Melikhov I.V.</i> The chemical kinetics and the connection between the hydrodynamic and kinetic descriptions	82

Section "Mathematical modelling"

<i>Barmenkov A., Barmenkov N.</i> On the application of systems of functions of special kind in mathematical physics	85
<i>Baskakov A.V., Volkov N.P.</i> Refinement of the Reactor Dynamics Mathematical Model	86
<i>Belendryasova E.G., Gani V.A., Moradi Marjaneh A., Askari A., Saadatmand D.</i> A new look at the double sine-Gordon kink-antikink scattering	88
<i>Bogdanova Y.A., Mamedov Z., Kudinov A.V.</i> The influence of potential parameters of a binary mixture components on the calculation accuracy by the Monte Carlo simulations	89
<i>Bukharova T.I., Kamynin V.L., Tonkikh A.P.</i> On Inverse Problem of Determination of the Coefficient in Strongly Degenerate Parabolic Equation	91
<i>Dashevskiy I.N.</i> Dependence of micromobility of dental implants on its thread geometry	92
<i>Dashevskiy I.N., Gribov D.A.</i> On personification of the evaluation of stress-strain state in a mandible according to CT data for different dental implantation schemes	94
<i>Dats E.P., Murashkin E.V.</i> Governing Equations of the Thermoelastoplasticity in Toroidal Coordinates	96
<i>Fedotova A.D., Kolybasova V.V., Krutitskii P.A.</i> Computation of potential of a single layer for Helmholtz equation in three-dimensional case by quadrature formulas of increased accuracy	98

<i>Gorkunov S.V., Bogdanova Y.A., Karabulin A.V.</i> An approximate analytical solution for the shock wave structure in a duct with a pseudo-perforated wall	100
<i>Gubin S.A., Victorov S.B.</i> The accuracy of the theories based on statistical physics for the thermodynamic modeling of state parameters of dense pure gases (fluids).	102
<i>Ivanova T.M.</i> Axial closed form texture component approximating the canonical normal distribution	105
<i>Kamynin V.L., Kostin A.B.</i> Determination of the right-hand term in degenerate parabolic equation with two independent variables	106
<i>Kazakov K.E., Manzhirov A.V.</i> Plane contact problem for foundation with multilayer nonuniform coating .	108
<i>Kondratyev I.A., Moiseenko S.G.</i> Basic operators method extension for 3D stationary problems on unstructured tetrahedral meshes	110
<i>Kostin A.B., Sherstyukov V.B.</i> Calculation of sums of Rayleigh type by zeros of equation containing Bessel function and its derivative	112
<i>Kozlov I.M., Misuchenko N.I., Teterev A.V.</i> Modeling of acetylene detonation in a shock tube by the large particle method with TVD correction	114
<i>Kukudzhanov K.V., Levitin A.L.</i> On the mechanism of electroplasticity of a metal under the action of a pulsed high-energy electromagnetic field	116
<i>Leonov A.S.</i> Application of M.Riesz potentials for solving a 3D inverse problem of acoustic sounding	118
<i>Mitrofanov M.S., Nagovitsyna O.A., Sergievskii V.V.</i> Description of liquid-vapor equilibria in binary associated of nonelectrolyte systems	120
<i>Murashkin E.V., Radayev Y.N.</i> Heat transport modelling in hemitropic micropolar continuum	122
<i>Nagornov O.V., Dunin S.Z.</i> Cooling effect for evaporating of drops situated at high-conductivity substrate	125
<i>Nagornov O.V., Tyuftin S.A., Mikhalevko V.N., Chernyakov G.A.</i> Determination of paleotemperature for the Elbrus glacier based on the inverse problem solution	126
<i>Nikabadze M.</i> Application of eigenvalue problems for tensor and tensor-block matrices for mathematical modeling of micropolar thin bodies	128
<i>Nikabadze M., Ulukhanyan A., Sakhvadze G.</i> To mathematical modeling of deformation of micropolar thin bodies with two small sizes	129
<i>Nikitaev V.G., Nagornov O.V., Pronichev A.N., Polyakov E.V., Dmitrieva V.V.</i> Optical radiation sensor signal distortion model in the computer microscopy system	130
<i>Orlovsky D.G.</i> Inverse Problem for a Differential Equation with Caputo fractional derivative in a Hilbert Space	132
<i>Parshin D.A., Manzhirov A.V.</i> Mathematical model of additively formed solids for the mechanical analysis of layer-by-layer manufacturing viscoelastic materials on rotating cylindrical substrates	134
<i>Peregoudov D.V.</i> Relativistic length contraction and time dilation as dynamical phenomena	137
<i>Perelmuter M.N.</i> Boundary integral equations for stress analysis of technical structures (from jet blades to tooth implants)	139
<i>Petrov S.V., Prostokishin V.M.</i> An Example of a None-zero Walsh Series with Riesz-spaces' Coefficients and Vanishing Partial Sums S_{2^k}	141
<i>Stadnik N.E., Klindukhov V.V.</i> On Simulation of Blood Vessels Growth	144
<i>Stepin E.V.</i> Steady trans-Alfvénic and sub-Alfvénic MHD flows in coaxial channels with longitudinal magnetic field	146
<i>Sumskoi S.I.</i> Simulation of gas release from trunk pipelines using a new numerical method based on the Godunov approach	148
<i>Telyakovskii D.S.</i> On the Holomorphy of Functions that Define Mappings with Asymptotically Constant Stretching	149
<i>Tkachenko D.S., Soloviev V.V.</i> Global uniqueness of the compact support source identification problem	151
<i>Vasilyev S.A., Kolosova I.S.</i> Tikhonov-type Cauchy problem for Relativistic Schrodinger Equation	152
<i>Zaluzhnaya G., Zagrebayev A.</i> Mathematical modelling and optimization of High-Power Channel-Type Reactor's core charge	154

Section “Mathematical methods of processing and data analysis”

<i>Apreutesey A.Y., Korolkova A.V.</i> A Simple Model of Active Queue Management System According to the RED Algorithm	155
<i>Bychovets E., Klimanov S.G., Klimov V.V., Kryanov A.V., Sliva D.E.</i> Mathematical model for predicting the resource allocation within a system in the course of a transition process	157
<i>Bykova N.D.</i> Study of the dynamics of a system with delay that described of the operation of a nuclear reactor	159
<i>Demidova A.V., Demidova T.S., Sobolev A.A.</i> Stochastic modeling of spreading of computer viruses	160
<i>Dobrovolsky M.N., Getmanov V.G., Soloviev A.A., Butirskiy E.Y., Dmitrieva A.N.</i> Method of anomaly recognition in time series of matrix data based on confidence interval systems and space-time filtering ..	162
<i>Druzhinina O.V., Sevastianov L.A., Vasilyev S.A., Vasilyeva D.G.</i> Numerical analysis of Kurzanov bearing oscillation	164
<i>Filipenkov N., Petrova M.</i> Data Mining of Changing Rules in Time Series	167
<i>Gayduk E.V.</i> About periodic solutions for certain functional equation	169
<i>Getmanov V.G., Sidorov R.V.</i> A method of two-dimensional filtering of modulated matrix data sequences .	170
<i>Gevorkyan M.N., Demidova A.V., Kulyabov D.S., Korolkova A.V.</i> Statistically significant performance testing of Julia scientific programming language	172
<i>Golubtsov P.V.</i> Information spaces: optimizing sequential and parallel processing for big data	173
<i>Gostev I., Malykh M., Sevastianov L.</i> On the Identification of the Objects Shape Invariant to Projective Transformation	176
<i>Iulev V.I., Misyurin S.Y., Nosova N.Y.</i> Comparison of piston, vane and perspective scroll air motors performance	177
<i>Korotkov E.V., Korotkova M.A.</i> Mathematical method for search of a multi alignment of DNA sequences with weak similarity	179
<i>Kryanov A.V., Pavlov U.G., Sliva D.E., Ulyanin U.A.</i> Effective portfolio formation of business dimensions of organizations on the basis of statistical forecasts	180
<i>Kulikov A.N.</i> On the possibility of implementing the Landau-Hopf-Sell scenario for a transition to turbulence	182
<i>Kulikov D.A.</i> The generalized Solow model	184
<i>Kulyabov D.S., Korolkova A.V., Sevastianov L.A.</i> Algebraic structure of special relativity	185
<i>Loginov D.O.</i> Bifurcation as the Coefficients of the Boundary Conditions Change in the Logistic Equation with Delay and Diffusion	187
<i>Malykh M., Sevastianov L., Nikolaev N.</i> On the representation of electromagnetic fields in closed waveguides with discontinuous filling using four continuous potentials	187
<i>Malykh M., Sevastianov L., Ying Y.</i> The construction of explicit conservative difference schemes for autonomous systems of differential equations	189
<i>Marushkina E.A.</i> Complex behavior of solutions of the system of three Hutchinson equations with a delayed broadcast connection	190
<i>Misyurin S.Y., Potapov M.A., Nelyubin A.P.</i> Integrated control of a robotic group with partial dominance of decision variants	191
<i>Ovchinnikova A.O., Savjolova T.I.</i> Application of the improved polycrystalline model in the framework of the EBSD experiment simulation	192
<i>Peregoudov D.V., Gvishiani A.D., Yashin I.I., Shutenko V.V.</i> Application of the statistical tests method for calculation of the hardware function model estimates for streamer detector systems	195
<i>Preobrazhenskaia M.M.</i> Stability of Antiphase Regime in a System of Two Coupled Nonlinear Relaxation Oscillators	197
<i>Shchetinin E.Y., Berezhkov M.S.</i> Electricity load forecasting with clustering consumers in smart energy grids	198
<i>Shchetinin E., Rassakhan N.</i> On Some Properties of Tail Dependence Coefficient Nonparametric Estimators	200

<i>Sirotnin D.M.</i> Numerical analysis of invariant characteristics of buckling beam driven oscillations	201
<i>Statnikov I.N., Firsov G.I.</i> Regression analysis of the results of planned computer experiments in machine mechanics	202
<i>Suvorova Y.M., Skryabin K.G., Korotkov E.V.</i> A new method for triplet periodicity change point detection	205
<i>Tolmacheva N.S., Savyolova T.I.</i> The Monte-Carlo method for modeling of grains, their disorientation for polycrystal	206
<i>Zavozina A.V., Velieva T.R., Korolkova A.V.</i> The determination of the coefficients of harmonic linearization for deterministic nonlinear system with control	208
<i>Zhukov V.V., Aleksandrova L.V., Mardashev A.M., Petrov V.A., Tolmachev I.L.</i> Issues of medical datasets classification	210
<i>Zhurov A.I.</i> New functional-separable solutions to unsteady axisymmetric boundary-layer equations in terms of elementary functions	213

Section “Methods of mathematical physics”

Kinetic models of the coalescence-fragmentation: the derivation of equations, the determination of the coefficients of the equations by the experimental distribution functions

S.Z. Adzhiev^{1,a)}, I.V. Melikhov^{1,b)}, V.V. Vedenyapin^{2,c)}

¹*Lomonosov Moscow State University*

²*Keldysh Institute of Applied Mathematics of Russian Academy of Sciences*

The kinetic equations of the evolution of particles distinguishing by properties are considered. The aim is to determine the coefficients of the equations by the distribution function from ones, which are obtained in experiments.

The considered problem is the creation of mathematical models of the kinetics of the emergence, the growth and the aggregation of particles which distinguish by their properties. The results of the experiments should be presented in the form of a mathematical model. The first step here is to create an a priori model containing unknown functions as parameters, which should be later defined. A priori model is the writing of correct equations containing unknown parameters. The model should answer the questions: what are the conditions of the experiment, how and in what range they should be varied and what should be determined in the experiment to obtain these unknown functions of the priori model? We answer these questions for our problem. On the basis of experiments these unknown functions are determined, and a posteriori model arises.

We investigate the issue of determination of the coefficients of the coalescence-fragmentation kinetic equations for the distribution function by their properties from ones, which are obtained in experiments. The first problem that arises is the obtaining of correct equations, and, hence, the derivation of the equations from each other: the transition from a description with multiple parameters to a reduced one: for instance, the derivation of equations on the particle size distribution function from the generalized Boltzmann-type equations for the distribution function of bodies by sizes and velocities of their centers of mass [1]; the consideration of the connection between the discrete and continuum equations.

From the continuum coalescence-fragmentation equation we derived the Becker–Döring system of equations and the continuum equation of the Fokker–Planck type (or of the Einstein–Kolmogorov type, or of the diffuse approximation). Thus we have established the connection between the discrete equations and the continuum one. The Becker–Döring system of equations [2] is the model when the only one molecule attaches or separates. It describes the first stage of the aggregation process.

We determine the coefficients of the equations by the stationary and non-stationary distribution functions. The distribution functions obtained in experiments are modeled by the classes of functions, depending on parameters, which are time-depending functions. We substitute these classes of distribution functions in the equation of the Fokker–Planck type and determine the connection between the coefficients of the equations and the parameters of modeling distribution functions. Our consideration corresponds to the notion of the morphological memory (see, e.g., [3]) and confirms it.

^{a)}Email: sergeyadzhiev@yandex.ru

^{b)}Email: melikhov@radio.chem.msu.ru

^{c)}Email: vicveden@yahoo.com

References

- [1] Adzhiev S.Z., Vedenyapin V.V., Volkov Yu.A., Melikhov I.V. Generalized Boltzmann-Type Equations for Aggregation in Gases. *Computational Mathematics and Mathematical Physics*, 2017, 57 (12), 2017–2029.
- [2] Becker R., Döring W. Kinetische Behandlung der Keimbildung in übersättigten Dampfer. *Ann. Phys.*, 1935, 24, 719–752.
- [3] Melikhov I.V., Rudin V.N., Kozlovskaya E.D., Adzhiev S.Z., Alekseeva O.V. Morphological memory of polymers and their use in developing new materials technology. *Theoretical Foundations of Chemical Engineering*, 2016, 50 (3), 260–269.

Self-similar solution for the problem of power-law liquid flow along an inclined plane

A.V. Aksenov^{1,a)}, A.D. Chicherina^{1,b)}, I.S. Chicherin^{1,c)}

¹*Lomonosov Moscow State University*

Within the Stokes film approximation, unsteady plane-parallel spreading of a thin layer of a heavy non-Newtonian fluid along an inclined solid surface is studied. The forced spreading regime induced by mass supply is considered. An evolution equation for the film thickness is derived not taking into account surface tension. The group classification problem is solved. Self-similar solution is constructed for the power time dependence on mass supply.

In different applications it is necessary to consider motion of non-Newtonian fluids. Such fluids often occur in nature and are used in industry. Mudflow, volcanic lava, oil, paint and lacquer, polymer melts and solutions, granulated material are the examples of non-Newtonian liquids. Nonlinear dependence of shear rate at each point of liquid volume on shear stress at the same point characterizes liquids with complex rheology properties. Fundamental characteristics of liquidous and solid-like objects, methods of experimental determination of rheology properties and detailed description of hydraulic flows are given in [1]. Determination of the principles of the non-Newtonian laminar flow is presented in [2]. The reference of rheological equations for different materials is stated in [3].

The present work is devoted to the investigation of the two-dimension motion of a thin non-newtonian layer on an inclined solid surface. The angle of inclination of the layer equals α . The forced spreading regime induced by mass supply is considered. We align coordinates so that the plane occupies $z = 0$, and x points downslope. The fluid velocity field is $(u(x, z, t), w(x, z, t))$, $p(x, z, t)$ is pressure and $h(x, t)$ is the layer thickness. The surface tension effects is neglected. The flow is considered slow and laminar. The dimensionless equations of mass and momentum conservation then read

$$u_x + w_z = 0, \quad p_x = S + \tau_{xz,z}, \quad p_z = -1.$$

^{a)}Email: aksenov.av@gmail.com

^{b)}Email: chicerina@imec.msu.ru

^{c)}Email: chicherin-ivan@rambler.ru

A rheological equation is formulated in invariant terms [3]

$$\tau_{ij} = 2KI_2^{\frac{n-1}{2}} e_{ij}, \quad I_2 = e_{ij}e^{ij}, \quad e_{ij} = \frac{1}{2} \left(\frac{\partial v_i}{\partial x_j} + \frac{\partial v_j}{\partial x_i} \right),$$

where τ_{ij} are the components of the viscous stresses tensor, I_2 is the second invariant of the deformation rate tensor, K and n are empirical constants, $n > 0$. The boundary conditions at the solid wall and free surface are

$$z = 0, \quad u = 0, \quad w = 0; \quad z = h, \quad \tau_{xz} = 0, \quad \tau_{zz} = 0.$$

The statement of the problem for finding the surface shape $h(t, x)$ is completed by the formulation of an integral condition following from the mass supply law and the requirement of zero film thickness at the leading front of the wetted area

$$\int_0^{x_f} h(x, t) dx = Q(t), \quad h(t, x_f) = 0.$$

The evolution equation for the film thickness is derived

$$(2n + 1)h_t + B^{\frac{1}{n}}(S - h_x)^{\frac{1}{n}-1}h^{\frac{1}{n}+1}((2n + 1)(S - h_x)h_x - hh_{xx}) = 0, \quad B = Const, \quad S \sim tg\alpha.$$

The group classification problem is solved. Applying the criterion of invariance [4] we obtain the system of the determining equations. The analysis of the system solution shows that the kernel of the symmetry operators consists of the symmetry operator

$$X_1 = x \frac{\partial}{\partial x} - \frac{t}{n} \frac{\partial}{\partial t} + h \frac{\partial}{\partial h}.$$

Self-similar solution form is found in case when the law of mass supply in the film is a power function of time $h = t^{-n}F(\eta)$, where $\eta = Cxt^n$, $C = Const$. The ordinary differential equation is obtained.

$$(2n + 1)n(\eta F' - F) + (2n + 1)CB^{\frac{1}{n}}(S - CF')^{\frac{1}{n}}F'F^{\frac{1}{n}+1} - C^2B^{\frac{1}{n}}(S - CF')^{\frac{1}{n}}F''F^{\frac{1}{n}+2} = 0.$$

It has the second order and it is solved numerically using Runge–Kutta method.

References

- [1] *W.L. Wilkinson* Non-Newtonian Fluids. Fluid Mechanics, Mixing and Heat Transfer [Russian translation]. Moscow. 1964.
- [2] *Z.P. Shul'man, V.I. Baikov* Rheodynamics and Heat and Mass Transfer in Film Flows [in Russian]. Minsk. 1979.
- [3] *A.Ya. Malkin, A.I. Isayev* Rheology – Concepts, Methods and Applications. Chem. tech. Publ. Toronto. 2005.
- [4] *L. V. Ovsianikov* Group Analysis of Differential Equations. Academic Press. New York. 1982.

Symmetries of the system of two-dimensional shallow water over a rough bottom equations

A.V. Aksenov^{1,a)}, K.P. Druzhkov^{1,b)}

¹*Lomonosov Moscow State University*

The system of equations of two-dimensional shallow water over a rough bottom is considered. An overdetermined system of equations for finding the allowed symmetries is obtained. Compatibility of the obtained overdetermined system of equations is investigated. A general view of the system solution is obtained. The kernel of the symmetry operators is found. Cases in which kernel extensions of symmetry operators exists are presented. The corresponding classifying equations are given. Based on the results of the group classification, it is concluded that the system of equations of two-dimensional shallow water over a rough bottom cannot be linearized by point change of variables in contrast to the system of equations of one-dimensional shallow water in cases of horizontal and inclined bottom profiles.

The system of equations of one-dimensional shallow water over a rough bottom is considered in [1, 2] and the group classification problem is solved.

The system of equations of two-dimensional shallow water over a rough bottom in dimensionless form is follows [3]

$$\begin{aligned} u_t + uu_x + vv_y + \eta_x &= 0, \\ v_t + uv_x + vv_y + \eta_y &= 0, \\ \eta_t + [u(\eta + h)]_x + [v(\eta + h)]_y &= 0. \end{aligned} \tag{1}$$

Here $z = -h(x, y)$, $h(x, y) \geq 0$ is the bottom profile, $u = u(x, y, t)$, $v = v(x, y, t)$ are velocity components, $\eta = \eta(x, y, t)$ is free surface displacement.

The group classification problem consists of finding Lie groups that are allowed by the considered system of equations for every bottom profile [4].

We seek the symmetry operators of the system of equations (1) as follows

$$\begin{aligned} X = \xi^1(x, y, t, u, v, \eta) \frac{\partial}{\partial x} + \xi^2(x, y, t, u, v, \eta) \frac{\partial}{\partial y} + \xi^3(x, y, t, u, v, \eta) \frac{\partial}{\partial t} + \\ + \eta^1(x, y, t, u, v, \eta) \frac{\partial}{\partial u} + \eta^2(x, y, t, u, v, \eta) \frac{\partial}{\partial v} + \eta^3(x, y, t, u, v, \eta) \frac{\partial}{\partial \eta}. \end{aligned} \tag{2}$$

An overdetermined system of equations for finding the allowed symmetries is obtained with using of the invariance criterion [4]. The system is omitted as it is lengthy.

Investigation of the compatibility of the obtained overdetermined system gives

$$\begin{aligned} \xi^1 = -\dot{a}x - 2By + 2k(t), & \quad \eta^1 = (\dot{a} + 2C)u - 2Bv - \ddot{a}x + 2\dot{k}, \\ \xi^2 = -\dot{a}y + 2Bx + 2l(t), & \quad \eta^2 = (\dot{a} + 2C)v + 2Bu - \ddot{a}y + 2\dot{l}, \\ \xi^3 = -2a(t) - 2Ct, & \quad \eta^3 = (2\dot{a} + 4C)\eta + \frac{x^2 + y^2}{2} \ddot{a} - 2\ddot{k}x - 2\ddot{l}y + \dot{f}, \end{aligned} \tag{3}$$

^{a)}Email: aksenov.av@gmail.com

^{b)}Email: Konstantin.Druzhkov@gmail.com

where the functions $a(t), k(t), l(t), f(t)$ and constants B, C for all $h(x, y)$ are determined from classifying equation

$$\begin{aligned} &(-\dot{a}x - 2By + 2k(t))h_x + (-\dot{a}y + 2Bx + 2l(t))h_y - (2\dot{a} + 4C) \cdot h(x, y) = \\ &= -\frac{x^2 + y^2}{2} \cdot \ddot{a} + 2x \cdot \ddot{k} + 2y \cdot \ddot{l} - \dot{f} \end{aligned} \quad (4)$$

The group classification results are presented below.

1. $h(x)$ is arbitrary function.

$$X_1 = \frac{\partial}{\partial t}. \quad (5)$$

The symmetry operator (5) determines the symmetry operators kernel.

Direct calculation shows that extended Lie algebras of symmetries can change only at following bottom profiles

2. $h(x) = H(x) + a_0y^2 + b_0y$. In this case the unknown functions $a(t), k(t), l(t), f(t)$ and constants B, C can be found from the following equations

$$\begin{aligned} &8a_0\dot{a} + 8a_0C = \ddot{a}, \\ &-2BH' - 3\dot{a}b_0 + 4a_0Bx + 4a_0l(t) - 4b_0C = 2\ddot{l}, \\ &(-\dot{a}x + 2k(t))H' + (2Bx + 2l(t))b_0 - (2\dot{a} + 4C)H(x) = -\frac{x^2}{2} \cdot \ddot{a} + 2x \cdot \ddot{k} - \dot{f}. \end{aligned}$$

3. $h(x) = H(y - a_0x) + b_0x^2 + c_0xy + d_0x$. In this case the unknown functions $a(t), k(t), l(t), f(t)$ and constants B, C can be found from the following equations

$$\begin{aligned} &(1 + a_0^2)\ddot{a} - 8(b_0 + a_0c_0)(\dot{a} + C) = 4B(a_0^2c_0 - c_0 + 2a_0b_0), \\ &2B(1 + a_0^2)H' - (4c_0\dot{a} + 4c_0C + 4B(b_0 + a_0c_0) - a_0\ddot{a})z = \\ &= -2(2b_0 + a_0c_0)k(t) - 2c_0l(t) + 2\ddot{k} + 2a_0\ddot{l} + d_0(2a_0B + 3\dot{a} + 4C), \\ &((2a_0B - \dot{a})z - 2a_0k(t) + 2l(t))H' - (2\dot{a} + 4C)H(z) = \\ &= \left(-\frac{1}{2}\ddot{a} + 2c_0B\right)z^2 + (2\ddot{l} - 2c_0k(t) + 2d_0B)z - 2d_0k(t) - \dot{f}, \end{aligned}$$

where $z = y - a_0x$.

4. $h(x) = \frac{1}{(x - a_0)^2} \cdot H\left(\frac{y - b_0}{x - a_0}\right) + c_0(x^2 + y^2) + d_0x + e_0y + f_0$. In this case the unknown functions $a(t), k(t), l(t), f(t)$ and constants B, C can be found from the following equations

$$\begin{aligned} &\ddot{a} = 8c_0(\dot{a} + C), \\ &\ddot{l} - 2c_0l(t) = -2e_0C - d_0B - \frac{3}{2}e_0\dot{a}, \\ &\ddot{k} - 2c_0k(t) = e_0B - 2d_0C - \frac{3}{2}d_0\dot{a}, \\ &\dot{f} = 2f_0\dot{a} - 2d_0k(t) - 2e_0l(t) + 4f_0C, \\ &((1 + z^2)H' + 2z \cdot H(z)) \cdot B - 2C \cdot H(z) = 0, \\ &\left(2a_0Bz^2 + z(-a_0\dot{a} - 2b_0B + 2k(t)) + b_0\dot{a} - 2l(t)\right)H' + \\ &+ \left(4a_0Bz - 2a_0\dot{a} - 4a_0C - 4b_0B + 4k(t)\right)H(z) = 0, \end{aligned}$$

where $z = (y - b_0)/(x - a_0)$.

5. $h(x)$ is the solution of the equation $(A_1x + A_2y + A_3)h_x + (A_1y - A_2x + A_4)h_y + A_5h = A_6(x^2 + y^2) + A_7x + A_8y + A_9$ for constants A_1, \dots, A_9 , not all equals zero.

This work was supported by the Russian Foundation for Basic Research, project no. 18-01-00890.

References

- [1] Aksenov A.V., Druzhkov K.P. Zakony sokhraneniya, simmetrii i tochnye resheniya sistemy uravnenij melkoj vody nad nerovnym dnom [Conservation Laws, Symmetries, and Exact Solutions of the System of Equations of Shallow Water over an Irregular Bottom]. Vestnik Nacional'nogo issledovatel'skogo yadernogo universiteta MIFI, 2016, vol. 5, no. 1, pp. 38–46.
- [2] Aksenov A.V., Druzhkov K.P. Conservation laws and symmetries of the shallow water system above rough bottom. J. Phys.: Conf. Ser. 2016, v. 722, pp. 1–7.
- [3] Stoker J.J. Water Waves. The Mathematical Theory With Applications. Interscience Publishers, Inc., New York, 1957, 609 p..
- [4] Ovsyannikov L.V. Gruppyvoj analiz differencialnykh uravnenij. M.: Nauka, 1978. 400 p. (in Russian).

Computational aspects of the wave distribution problem in the logistic equation with spatial deviation

S.V. Aleshin^{1,2,a)}, S.D. Glyzin^{1,2,b)}, S.A. Kaschenko^{1,3,c)}

¹*P.G. Demidov Yaroslavl State University*

²*Scientific Center in Chernogolovka RAS*

³*National Research Nuclear University MEPhI*

We consider the problem of density wave propagation in a logistic equation with spatial deviation and diffusion (Fisher–Kolmogorov equation with spatial deviation). The numerical analysis of wave propagation shows that for a sufficiently small deviation this equation has a solution similar to the solution of a classical Fisher–Kolmogorov equation. The deviation increasing leads to existence of the oscillatory component in spatial distribution of solutions. A further increase of deviation leads to destruction of the traveling wave. Finally, when the deviation is sufficiently large we observe intensive spatio-temporal fluctuations in the whole area of wave propagation.

The most common form of logistic equation that accounts the dependency from time and spatial shifts was proposed by Gourley and Britton [3, 5]:

$$\frac{\partial u(t, x)}{\partial t} = \Delta u(t, x) + u(t, x)[1 + \alpha u(t, x) - (1 + \alpha(g * u))(t, x)]. \quad (1)$$

^{a)}Email: fktiby@yandex.ru

^{b)}Email: glyzin@uniyar.ac.ru

^{c)}Email: kasch@uniyar.ac.ru

where convolution $(g * u)(t, x) = \int_{-\infty}^t \int_{\Omega} g(t - \tau, x - y)u(\tau, y)dyd\tau$. If we take delta-function in the integral and move focusing point by time or spatial axis we may get equation with delay[1] or equation with spatial deviation [2]. We considered the process of density wave propagation in a logistic equation with diffusion (Fisher-Kolmogorov equation[6, 4]) and spatial deviation in two form. The first form is:

$$\frac{\partial u}{\partial t} = \frac{\partial^2 u}{\partial x^2} + u[1 - u(t, x - y)]. \quad (2)$$

Here $u(t, x)$ is a solution, which is a population density of FK-problem at time $t > 0$ in some point x of a habitat; $y > 0$ is spatial deviation. The second form is:

$$\frac{\partial u}{\partial t} = \frac{\partial^2 u}{\partial x^2} + u \left[1 - \frac{1}{\sqrt{\pi}} \int_{-\infty}^{+\infty} u(t, y) \frac{e^{-\left(\frac{y-(x-h)}{\sigma}\right)^2}}{\sigma} dy \right] \quad (3)$$

$$\frac{1}{\sqrt{\pi}} \int_{-\infty}^{+\infty} \frac{e^{-\left(\frac{y-(x-h)}{\sigma}\right)^2}}{\sigma} dy = 1 \quad (4)$$

A research of qualitative behavior of solutions of Fisher–Kolmogorov equation starts with the analysis of the wave equation profile, for which the conditions of appearance of oscillatory regimes are found. The second problem was the analysis of Fisher–Kolmogorov equation with periodic boundary conditions. We studied the stability loss problem of a spatially homogeneous equilibrium state and found spatially inhomogeneous oscillatory regimes branching from it. The last part of the research contains the results of a large numerical experiment for this equation in the case of an unbounded domain. Numerical analysis was performed at the cluster of massive and parallel computations with the use of the OpenMP and Nvidia Cuda parallel computing technology. A numerical analysis of the wave propagation process showed that for sufficiently small values of the spatial deviation, this equation has solutions close to the solutions of the standard Fisher–Kolmogorov equation. At first the increase of the deviation parameter leads to the appearance of a damped oscillatory component in the spatial distribution of the solution. Further growth of this parameter leads to the destruction of the traveling wave. This is expressed by the fact that undamped in time and propagated slowly along space oscillations are close to the solutions of the corresponding boundary-value problem with periodic boundary conditions in the propagation wave region opposite to the direction of deviation. Finally, if the value of deviation is sufficiently large, then intense spatiotemporal oscillations are observed throughout the wave propagation region. Also we got some interesting analytical results for numerical experiments in case of periodic boundary conditions related with computational artifacts.

This work was supported by the Russian Science Foundation (project nos. 14-21-00158).

References

- [1] Aleshin S.V., Glyzin S.D., and Kaschenko S.A., Spatially inhomogeneous structures in the solution of Fisher-Kolmogorov equation with delay, *Journal of Physics: Conference Series* 681 (2016) 012023
- [2] Aleshin S.V., Glyzin S.D., and Kaschenko S.A., Dynamic Properties of the Fisher–Kolmogorov–Petrovskii–Piscounov Equation with the Deviation of the Spatial Variable, *Automatic Control and Computer Sciences*, 2016, Vol. 50, No. 7, pp. 1–14
- [3] Britton N. 1990, Spatial structures and periodic travelling waves in an integro-differential reaction-diffusion population model, *SIAM J. Appl. Math.* **50:6** 1663–88

- [4] Fisher R., 1937, The Wave of Advance of Advantageous Genes, *Annals of Eugenics* **7** 355–69
- [5] Gourley S. and Kuang Y. 2003, Wavefronts and global stability in a time-delayed population model with stage structure, *Proc. R. Soc. Lond. A* **459** 1563–79
- [6] Kolmogorov A., Petrovsky I. and Piscounov N., 1937, Étude de l'équation de la diffusion avec croissance de la quantité de matière et son application, à un problème biologique *Moscou Univ. Bull. Math.* **1** 1–25

Influence of compressibility on the foam fracture modeling

I.D. Antonov^{1,2,a)}, A.V. Porubov^{1,2,b)}

¹*Peter the Great St. Petersburg Polytechnic University (SPbPU), Saint-Petersburg*

²*Institute of Problems in Mechanical Engineering of the RAS, Saint-Petersburg*

A new nonlinear model of foam hydraulic fracturing is developed with both compressibility and rheology being taken into account. The scaling analysis is performed to obtain a simplified model. Numerical simulations reveal an influence of compressibility and rheology on the temporal evolution both the width and length of the fracture opening.

The foam fracturing technique looks promising in comparison with other hydraulic fracturing methods due to several important industrial advantages. However, the modeling of foam faces with serious difficulties. Besides foam saturation and stability, it is necessary to take into account compressibility and non-Newtonian character of the foam viscosity. Moreover, foam contains both liquid and gas parts. Taking into account all these factors is a difficult task.

In this paper, the model of foam considers it as an isothermal compressible liquid where the gas part provides compressibility and rheology. The impact of compressibility is introduced by the fluid density-pressure relation [1], while the density of the liquid phase is assumed to be constant,

$$\rho = \frac{(1 - \Gamma_0)p\rho_l + \Gamma_0 p_0 \rho_g}{\Gamma_0 p_0 + (1 - \Gamma_0)p}, \quad (1)$$

where p_0 and Γ_0 are the injection pressure and foam quality respectively. The quality of foam is defined as the volume fraction of the gas phase in the fracturing fluid,

$$\Gamma = \frac{V_g}{V_g + V_l}. \quad (2)$$

The apparent viscosity of the foam is modeled by the non-Newtonian power law where the value of the exponent also depend on the foam quality [2]. Simultaneous accounting of compressibility in all above mentioned places represents the novelty of our foam fracturing model.

The scaling analysis is performed to reduce the solution of the initial 3D problem to the solution of a 1D model equation for a fracture opening or a pressure. The scales are taken from the available experimental data.

^{a)}Email: antoidco@gmail.com

^{b)}Email: alexey.porubov@gmail.com

An implicit FDM is used to solve the model equation. The calculations show significant differences in the final fracture geometry for the low and high qualities of the foam.

This work was supported by Ministry of Education and Science of the Russian Federation within the framework of the Federal Program «Research and development in priority areas for the development of the scientific and technological complex of Russia for 2014 – 2020» (activity 1.2), grant No. 14.575.21.0146 of September 26, 2017, unique identifier: RFMEFI57517X0146.

References

- [1] Ikoku, C. U. (1978). Transient flow of non-Newtonian power-law fluids in porous media.
- [2] Khade, S. D. and Shah, S. N. (2004). New Rheological Correlations for Guar Foam Fluids. SPE Production and Facilities, 19(2), 77–85.

Numerical simulation of Fermi-Pasta-Ulam model, its discrete and continuous approximations

V.V. Averina^{1,a)}, N.A. Kudryashov¹

¹*National Research Nuclear University MEPhI*

In this paper we study the Korteweg-de Vries equation obtained from the Fermi-Pasta-Ulam problem. We use the potential of interaction between neighbouring masses with quadratic term. We get the fifth-order nonlinear evolution equation for description of perturbation in the mass chain. We obtained exact solutions of both equations. Solitary wave solution of the fifth-order equation is found and discussed, compared to the Korteweg-de Vries solution. We use the pseudospectral method for the numerical simulation of wave processes, described by the equations. We studied the Fermi-Pasta-Ulam paradox using numerical simulation. We demonstrate the Fermi-Pasta-Ulam paradox in the case of the Korteweg-de Vries equation and we tested the existence of a return to initial state in the case of a fifth-order equation

It is well known that the Fermi-Pasta-Ulam (FPU) problem played a major role in the history of computer simulation because it introduced the concept of the numerical experiment for the first time [1],[2]. It describes perturbation in the chain of nonlinear coupling among masses.

$$m \frac{d^2 y_i}{dt^2} = F_{i,i+1} - F_{i-1,i}, \quad (1)$$

where y_i denotes the displacement of the i -th mass from its original position, the force $F_{i+1,i}$ describes the nonlinear interaction between masses. [5]

$$F_{i-1,i} = k(\Delta l) + \alpha(\Delta l)^2 + \beta(\Delta l)^3, \quad \Delta l = y_i - y_{i-1}, \quad (2)$$

and k, α are constant parameters of system.

It is shown [1] that energy remains in very few modes and the long-time dynamics of the system is recurrent. This fact was called the FPU paradox. We demonstrate the FPU paradox

^{a)}Email: lera_averina@mail.ru

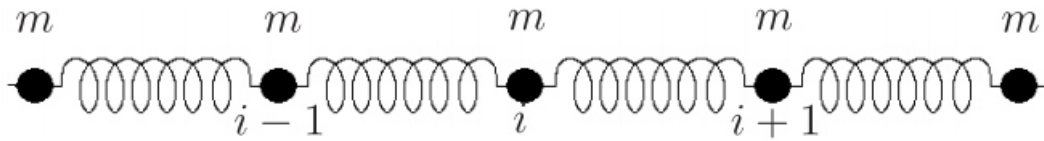


Fig. 1: Fermi-Pasta-Ulam model

using the Korteweg-de Vries equation obtained from the FPU problem. The equation is derived using the continuous limit (four terms in the Taylor series for the displacement):

$$u_t + \alpha uu_x + \delta u_{xxx} = 0 \quad (3)$$

and its solution:

$$u(x, t) = 2k^2 ch^{-2} \left\{ \frac{k\alpha}{6\delta} (x - C_0 t - x_0) \right\}. \quad (4)$$

We tested the existence of the FPU paradox using a fifth-order equation obtained from the FPU problem. The equation is derived using the continuous limit (six terms in the Taylor series for the displacement):

$$u_t + uu_x + \delta^2 u_{xxx} + 2\delta^2 u_x u_{xx} + \delta^2 uu_{xxx} + \frac{2}{5}\delta^4 u_{xxxxx} = 0 \quad (5)$$

and its solution:

$$u(x, t) = \delta^2 k^2 - \frac{1}{2} - \frac{3\delta^2 k^2}{2} \tanh^2 \left(\frac{k(x - x_0 - C_0 t)}{2} \right), \quad C_0 = -\frac{\delta^4 k^4}{10} - \frac{1}{2}. \quad (6)$$

References

- [1] *Fermi E, Pasta J, Ulam S.* Studies of nonlinear problems // Los Alamos Report - LA-1940; 1955. p.978-988.
- [2] *Zabusky N.J., Kruskal M.D.* Interaction of "solitons" in a collisionless plasma and the recurrence of initial states // Phys. Rev. Lett. 1965. V. 15. № 6. P. 240.
- [3] *Ford J.* Equipartition of energy for nonlinear systems // J. Math. Phys., 1961, vol. 2, no. 3, pp. 387-393.
- [4] *Kudryashov N.A., Volkov A.K.* The fifth-order partial differential equation for the description of the $\alpha + \beta$ Fermi-Pasta-Ulam model // Commun Nonlinear Sci Numer Simulat - 2017. - V.42. - P.491-501.
- [5] *Kudryashov N.A.* Analytical properties of nonlinear dislocation equation // Applied Mathematics Letters - 2017. - V.69. - P.29-34.
- [6] *Kudryashov N.A.* Refinement of the Korteweg-de Vries equation from the Fermi-Pasta-Ulam model // Phys. Lett. A. - 2015. - V.379. - P.2610-2614.
- [7] *Kassam A-K, Trefethen LN.* Fourth-Order Time-Stepping for Stiff PDEs // SIAM J Sci Comput 2005, 26(4):1214-33

Equivalence of second-order ODEs to the Painlevé equations

Y.Y. Bagderina^{1,a)}

¹*Institute of Mathematics with Computer Center UFRC RAS*

Equivalence problem for a projective type scalar second-order ODEs with respect to invertible point changes of variables is considered. Basis of invariants of this family of equations has been constructed. We use the invariants of a second-order ODE to find the necessary conditions of its equivalence to the six Painlevé equations. Sufficiency of these conditions are proved for PI-PIV equations. Difficulties of such a proof for PV and PVI equations are discussed. Results are illustrated with a few examples.

Problem of equivalence of the second-order equations

$$\frac{d^2y}{dx^2} = S(x, y) \left(\frac{dy}{dx}\right)^3 + 3R(x, y) \left(\frac{dy}{dx}\right)^2 + 3Q(x, y) \frac{dy}{dx} + P(x, y) \quad (1)$$

with respect to point change of variables

$$z = \xi(x, y), \quad w = \eta(x, y), \quad \det \frac{\partial(\xi, \eta)}{\partial(x, y)} \neq 0 \quad (2)$$

can be solved with the use of invariants of the equivalence transformation group of this family of equations, generated by transformations (2). If two equations of the form (1) are related by a change of variables (2), then all invariants of these equations are equal. The problem of constructing invariants of the family (1) was under study many times, beginning with R. Liouville and A. Tresse. Here the corresponding result from [1] is used. The Painlevé equations PI–PVI, and equation P34 as well, related to PII by a Miura type substitution, fall into degenerate types of equations (1). For them, the basis consists of two invariants

$$I_1(x, y), \quad I_2(x, y). \quad (3)$$

Arbitrary invariant can be obtained from the basis ones by applying the invariant differentiations D_1 , D_2 and algebraic operations.

Necessary conditions of the equivalence to a Painlevé equation (written in variables z , w) are found in the following way. One should calculate the basis invariants $I_1(z, w)$, $I_2(z, w)$ of this equation and a number of derivative invariants $D_j I_k$, $D_i D_j I_k$, $i, j, k = 1, 2$. A part of the invariants is used for eliminating z , w and constant parameters of the Painlevé equation. This allows to obtain the formulas of the change of variables (2), where the right-hand side is given by a function of invariants (3) of equation (1) and their derivatives. As a result the relations remain, which connect the invariants only and represent the necessary equivalence conditions. To prove the sufficiency, these conditions are applied to an equation

$$\frac{d^2y}{dx^2} = f(x, y). \quad (4)$$

Let this lead to a canonical form of the corresponding Painlevé equation, up to the transformations preserving the form of equations (4). This means the sufficiency of the equivalence conditions applied to (4). Canonical forms of the Painlevé equations defined by ODE with right-hand side, that does not depend on the first derivative, have been found in [2] (PI and PII are just in the canonical form).

^{a)}Email: bagderinayu@yandex.ru

Conditions of the equivalence to the first Painlevé equation with respect to the point transformations (2) have been obtained in [4] and later in [5]. Some necessary equivalence conditions for PI–PIV are constructed in [6] in terms of the invariants introduced by R. Liouville. Non-complete necessary conditions of the equivalence to PII, PIV, P34 are found in [5, 7, 8]. In [1] the complete set of necessary conditions of the equivalence to PI, PII, PIV and P34 were obtained. Then in [9] some conditions were added to necessary equivalence conditions for PII and P34 found earlier in [5, 8]. But their sufficiency has not been proved.

Today the criteria of equivalence to the PI–PIV and P34 equations are proved [3, 10, 11]. Necessary conditions of the equivalence to PV equation are stated as a system of relations in invariants J_m (series of modified Liouville's invariants), variable w and an auxiliary variable H . In theory, variables H and w can be eliminated, but this leads to cumbersome relations useless to solve the problem of equivalence of an ODE (1) to PV. Instead of this we propose the procedure of eliminating H and factorizing the remaining overdetermined system, that allows to find the expression for w in the change of variables (2). Substitution of such found H and w should turn the relations of the system into identities. Necessary conditions of the equivalence to PVI equation are stated as a system of relations in invariants J_m and variables z , w and H . We apply to it similar procedure of eliminating H and finding the expressions for z , w in the change of variables (2).

References

- [1] Bagderina Yu.Yu. Invariants of a family of scalar second-order ordinary differential equations. *J. Phys. A: Math. Theor.* 2013. V. 46. 295201.
- [2] Babich M.V., Bordag L.A. Projective differential geometrical structure of the Painlevé equations. *J. Differ. Equations.* 1999. V. 157, №2. P. 452–485.
- [3] Bagderina Yu.Yu. Equivalence of second-order ordinary differential equations to Painlevé equations. *Theor. Math. Phys.* 2015. V. 182, №2. P. 211–230.
- [4] Bocharov A.V., Sokolov V.V., Svinolupov S.I. On some equivalence problems for differential equations. Preprint ESI-54. Int. Erwin Schrödinger Inst. for Math. Phys. Vienna, 1993. 12 pp.
- [5] Kartak V.V. Explicit solution of the problem of equivalence for some Painleve equations. *Ufa Math. J.* 2009. V. 1, №3. P. 46–56.
- [6] Hietarinta J., Dryuma V. Is my ODE a Painlevé equation in disguise? *J. Nonlin. Math. Phys.* 2002. V. 9, Suppl. 1. P. 67–74.
- [7] Kartak V.V. Solution of the equivalence problem for the Painlevé IV equation. *Theor. Math. Phys.* 2012. V. 173, №2. P. 1541–1564.
- [8] Kartak V.V. "Painleve 34" equation: equivalence test. Preprint arXiv: math.CA/1302.2419. 2013. 7 pp.
- [9] Kartak V.V. "Painlevé 34" equation: equivalence test. *Commun. Nonlin. Sci. Numer. Simul.* 2014. V. 19. P. 2993–3000.
- [10] Bagderina Yu.Yu. Equivalence of second-order ODEs to equations of first Painlevé equation type. *Ufa Math. J.* 2015. V. 7, №1. P. 19–30.

- [11] Bagderina Yu.Yu., Tarkhanov N.N. Solution of the equivalence problem for the third Painlevé equation. *J. Math. Phys.* 2015. V. 56. 013507.

Far surface gravity waves fields generated by a rapidly moving oscillating source

V.V. Bulatov^{1,a)}, Y.V. Vladimirov^{1,b)}, I.Y. Vladimirov^{2,c)}

¹*Ishlinsky Institute for Problems in Mechanics RAS, Moscow*

²*Shirshov Institute of Oceanology RAS, Moscow*

In the paper, the far fields of surface wave perturbations excited by an oscillating localized source rapidly moving in a heavy liquid of infinite depth are studied. It is shown that the excited fields are a sum of two wedge-like ship waves located inside the corresponding Kelvin wave wedges. Each of the excited two waves is a complicated wave system of transverse and longitudinal perturbations. The properties of the dispersion curves are studied and the phase pictures describing the structure of wave surface perturbations are calculated. The characteristics of the excited wave fields are studied depending on the basic parameters of the wave generation such as the velocity of motion of the perturbation source and the frequency of its oscillations. Uniform asymptotic solutions are constructed in terms of the Airy function and its derivative, which permits describing the far fields of surface perturbations both outside and inside the corresponding wave wedges.

The surface wave motions in the marine environment can either originate due to natural causes (wind waves, flow past underwater obstacles, bottom relief variations, density and flow fields) or be generated by the flow past natural obstacles (platforms, underwater pipelines, complex hydraulic facilities). The goal in the present paper is to construct uniform asymptotics of far fields of surface perturbations excited by the fast motion of a localized oscillating source of perturbations in a heavy homogeneous liquid of infinite depth. We consider the steady-state pattern of wave perturbations on the surface of an ideal heavy liquid of infinite depth when the perturbation source moves with velocity V in the positive direction of the axis x . The waves are generated by a moving oscillating point source of perturbations located at the depth H (the axis z is directed upwards from the unperturbed liquid) whose capacity varies by the law $q = \exp(i\omega t) \exp(\varepsilon t)$ ($-\infty < t < \infty$). Further, we seek the limit as $\varepsilon \rightarrow 0$ in the obtained solution. The perturbation of the potential $\Phi(x, y, z, t)$ with respect to the homogeneous flow moving with velocity V ($\nabla\Phi = (u, v, w)$, where u, v, w are components of the vector of perturbations of the velocity $(V, 0, 0)$) is described by the following equation with an appropriate linearized boundary condition on the surface of the liquid

$$\begin{aligned} \Delta\Phi(x, y, z, t) &= \exp(i\omega t) \exp(\varepsilon t) \delta(x) \delta(y) \delta(z + H), \quad z < 0 \\ \left(\frac{\partial}{\partial t} + V \frac{\partial}{\partial x} \right)^2 \Phi + g \frac{\partial \Phi}{\partial z} &= 0, \quad z = 0 \end{aligned}$$

^{a)}Email: internalwave@mail.ru

^{b)}Email: vladimyura@yandex.ru

^{c)}Email: iyuvladimirov@rambler.ru

Here Δ is the three-dimensional Laplace operator, and $\delta(x)$ is the Dirac delta function. Then for free surface elevation $\eta(x, y, t)$ we can obtain

$$\eta(x, y, t) = \frac{i \exp(i\omega t)}{4\pi^2} \int_{-\infty}^{\infty} \exp(-i\nu y) d\nu \int_{-\infty}^{\infty} \frac{(\omega - \mu V) \exp(-kH - i\mu x) d\mu}{(\varepsilon + i(\omega - \mu V))^2 + gk}.$$

The zeros of the denominator in the integrand determine the dispersion relation: $B(\omega, \mu, \nu) \equiv (\omega - \mu V)^2 - g\sqrt{\mu^2 + \nu^2} = 0$. The set of values of the parameter $V\omega/g > 0$ is divided by two characteristic values $1/4$ and $\sqrt{6}/9$ into three intervals. For $V\omega/g < 1/4$, the dispersion curve consists of three branches, one closed and two nonclosed. In this case, the wave picture is a sum of two wedge-like (longitudinal) waves with half-opening angle of the wave wedge less than $\pi/2$ and the annular-like (transverse) waves around the source. For $V\omega/g > \sqrt{6}/9$, the dispersion curve consists of two unclosed branches without extrema. In this case, the wave picture is a sum of two wedge-like ship waves with the half-opening angle of the wave wedge less than $\pi/2$. If $1/4 < V\omega/g < \sqrt{6}/9$, then the dispersion curve consists of two unclosed curves one of which has two local extrema. One branch of the dispersion curve corresponds to the usual wedge-like waves with the half-opening angle of the wave wedge less than $\pi/2$, and the second branch corresponds to the ship waves with the half-opening angle of the wave wedge greater than $\pi/2$ (the wave front is directed upstream away from the source). This system of hybrid waves simultaneously has the features of both the annular (transverse) and wedge-like (longitudinal) waves. We consider the case $V\omega/g > \sqrt{6}/9$. Then the integrand in the inner integral has two real poles $\mu_{1,2}$. For $x > 0$, the contour of integration over μ becomes closed in the lower half-plane and, taking into account the contributions of the poles, we obtain

$$\eta(x, y, t) = I_1(x, y, t) + I_2(x, y, t), \quad I_m(x, y, t) = \int_{-\infty}^{\infty} F(\mu_m(\nu), \nu) \exp(-ixS_m(\nu, \alpha)) d\nu,$$

$$F(\mu_m(\nu), \nu) = \frac{\exp(i\omega t)}{2\pi} \frac{(\omega - \mu V) \exp(-kH)}{2V(\omega - \mu V) + \mu g/k}, \quad S_m(\nu, \alpha) = \mu_m(\nu) + \nu \tan \alpha,$$

$$\tan \alpha = y/x, \quad m = 1, 2.$$

For large value of $x > 0$, the asymptotic behavior of the integrals in the sum is completely determined by the stationary points of the phase function $S_m(\nu, \alpha)$ which are determined from the equation $\mu'_m(\nu) = -\tan \alpha$. The uniform asymptotics of $I_1(x, y, t)$ for $x > 0$ applicable at far distance from the wave front and near it has the form

$$I_1(x, y, t) \approx \frac{2\pi \exp(i(r\lambda(\alpha) + \omega t))}{x^{1/3}} \left(\frac{G(\sqrt{\sigma(\alpha)}) + G(-\sqrt{\sigma(\alpha)})}{2} \text{Ai}(x^{2/3}\sigma(\alpha)) - \right. \\ \left. - i \frac{G(\sqrt{\sigma(\alpha)}) - G(-\sqrt{\sigma(\alpha)})}{2x^{1/3}\sqrt{\sigma(\alpha)}} \text{Ai}'(x^{2/3}\sigma(\alpha)) \right),$$

$$\lambda(\alpha) = (S_1(\nu_1(\alpha), \alpha) + S_1(\nu_2(\alpha), \alpha))/2, \quad \sigma(\alpha) = (3(S_1(\nu_2(\alpha), \alpha) - S_1(\nu_1(\alpha), \alpha))/4)^{2/3},$$

$$G(\sqrt{\sigma(\alpha)}) = F(\mu_1(\nu_1(\alpha)), \nu_1(\alpha)) \sqrt{\frac{-2\sqrt{\sigma(\alpha)}}{\mu_1''(\nu_1(\alpha))}},$$

$$G(-\sqrt{\sigma(\alpha)}) = F(\mu_1(\nu_2(\alpha)), \nu_2(\alpha)) \sqrt{\frac{2\sqrt{\sigma(\alpha)}}{\mu_1''(\nu_2(\alpha))}},$$

where $\text{Ai}(\tau) = \frac{1}{2\pi} \int_{-\infty}^{\infty} \cos(\tau t - t^3/3) dt$ is the Airy function and $\text{Ai}'(\tau)$ is the derivative of the Airy function. The asymptotic becomes non-uniform if the Airy function and its derivative

are replaced by the corresponding expansions for large values of the argument. The uniform asymptotics of the integral $I_2(x, y, t)$ for large $x > 0$ are estimated similarly. We note that the waves described by the integral I_2 significantly (approximately by a factor of three) exceed in amplitudes the waves determined by the integral I_1 . The above numerical calculations show that an increase in the velocity V of motion of the source (for a fixed frequency ω of the source oscillations) leads to a decrease in the half-opening angles of both of the wave wedges. In this case, the distance between the neighboring wave crests increases; in particular, there is an increase in the lengths of transverse waves λ_1 and λ_2 along the axis x . We have shown that the far fields of surface perturbations due to a rapidly moving localized oscillating source in a heavy liquid of infinite depth are sums of two wedge-like (ship) waves each of which is contained inside the corresponding Kelvin wave wedge. It is shown that the amplitude of one wave is several times greater than the amplitude of the other wave. Each of the excited two waves is a complex wave system of transverse and longitudinal wave perturbations. The characteristics of the excited surface perturbations were studied depending on the basic parameters of the wave generation such as the velocity of motion of the source of perturbations and the frequency of its oscillations. The constructed asymptotic solutions permit describing the far-range fields of surface perturbations excited by a moving localized unsteady source both outside and inside the corresponding wave wedges. The obtained asymptotics of far-range fields of surface wave perturbations allow one efficiently to calculate the basic characteristics of wave fields and, in addition, qualitatively to analyze the obtained solutions, which is important for obtaining the well-posed statements of mathematical models of wave dynamics of surface perturbations of real natural environment. The research was carried out in the framework of the Federal target program of FASO Russia, projects No. 0149-2018-0003) (I.Yu.Vladimirov) and No. 0051-2016-0005 (V.V.Bulatov, Yu.V.Vladimirov).

Partially dissipative system with multizonal initial and boundary layers

V.F. Butuzov^{1,a)}, N.N. Nefedov^{1,b)}, O.E. Omel'chenko³, L. Recke²

¹*Faculty of Physics, Lomonosov Moscow State University, 119991 Moscow Russia*

²*HU Berlin, Institut für Mathematik, Rudower Chaussee 25, 12489 Berlin-Adlershof, Germany,*

³*Weierstrass Institute for Applied Analysis and Stochastics, Mohrenstr. 39, 10117 Berlin, Germany*

We consider a system of the form

$$\varepsilon^2 \left(\frac{\partial u}{\partial t} - \frac{\partial^2 u}{\partial x^2} \right) = F(u, v, x, \varepsilon), \quad (1)$$

$$\varepsilon \frac{\partial v}{\partial t} = f(u, v, x, t, \varepsilon), \quad (x, t) \in D := (0; 1) \times (0, T], \quad (2)$$

with Neumann boundary conditions

$$\frac{\partial u}{\partial x}(0, t, \varepsilon) = \frac{\partial u}{\partial x}(1, t, \varepsilon) = 0, \quad t \in (0, T] \quad (3)$$

^{a)}Email: butuzov@phys.msu.ru

^{b)}Email: nefedov@phys.msu.ru

and initial conditions

$$u(x, 0, \varepsilon) = u^o(x), \quad v(x, 0, \varepsilon) = v^o(x), \quad x \in [0; 1]. \quad (4)$$

Here $\varepsilon > 0$ is a small parameter; F, f, u^o, v^o are sufficiently smooth functions.

Systems of the form (1), (2) are called *partially dissipative* reaction - diffusion systems, because the diffusion term appears only in the first of these equations. Such systems are used for mathematical modeling in chemical kinetics, theoretical biology and other applied sciences.

Our goal is to construct the asymptotics as $\varepsilon \rightarrow 0$ for boundary layer solution to problem (1) - (4) in the case when the degenerative equation

$$F(u, v, x, t, 0) = 0$$

obtained from equation(1) for $\varepsilon = 0$, has a double root

$$u = \varphi(v, x, t).$$

It turns out that standart singular perturbation techniques developed for the case a simple root of the degenerate equation must be substantially modified in the case of a double root. The main difference is concerned with a more complicated multizonal structure of the initial and boundary layers.

In problem (1) - (4) close to the initial time moment two different time scales appear:

$$\sigma = t/\varepsilon \quad \text{and} \quad \tau = t/\varepsilon^2.$$

Respectively, two types of corner layer functions appear in the vicinity of the corner points $(x, t) = (0, 0)$ and $(x, t) = (1, 0)$. The initial layer functions which depend of (x, τ) , the corner layer functions which depend of (ξ, τ) , where $\xi = x/\varepsilon^{3/4}$, and also the corner layer functions depending of $(\tilde{\xi}, \tau)$, where $\tilde{\xi} = (1 - x)/\varepsilon^{3/4}$, are constructed by special method which was developed for singular perturbed problems with multiple roots of the degenerate equation.

We also formulate the assumptions which permit to construct and justify the asymptotics of the boundary layer solution to problem (1) - (4).

Multidimensional singularly perturbed reaction-diffusion-advection problems with balanced nonlinearity and their applications in the theory of nonlinear heat conductivity

M.A. Davydova^{1,a)}, N.N. Nefedov^{1,b)}

¹*Faculty of Physics, Lomonosov Moscow State University, 119991 Moscow Russia*

We construct an asymptotic approximation of the arbitrary-order accuracy to solutions with internal transition layers in multidimensional nonlinear singularly perturbed problems of the reaction-diffusion-advection type in the case of balanced advection and reaction and prove the existence theorem. We use this result to describe the thermal structures in the nonlinear dissipative media.

^{a)}Email: m.davydova@physics.msu.ru

^{b)}Email: nefedov@phys.msu.ru

The present paper is aimed to studying the question of the existence of solutions with internal transition layers (contrast structures) in multidimensional singularly perturbed reaction-diffusion-advection problems

$$\varepsilon^2 \Delta u - f(\varepsilon \nabla u, u, x) = 0, \quad x = (x_1, \dots, x_N) \in D \subset R^N, \quad (1)$$

$$u(x, \varepsilon) = g(x), \quad x \in S \quad (2)$$

in the case of balanced nonlinearity. Here $\varepsilon > 0$ is a small parameter, the functions f , g and the boundary S are assumed to be sufficiently smooth. The notation $\varepsilon \nabla u$ implies the dependence of the function f on the arguments $\varepsilon \partial u / \partial x_k$, $k = \overline{1, N}$, and the function f satisfies the condition of the most quadratic growth with respect to ∇u .

The problem (1), (2) can describe the stationary stable states of the dissipative media, characterized by the existence of the spatial structures. In particular, the thermal structures arising in the homogeneous dissipative medium with nonlinear characteristics at the intensive thermal influence [1] are described by the model problem of the type (1), (2):

$$\begin{aligned} \varepsilon^2 (\Delta u - A(u)(\nabla u)^2) &= B(u, x), \quad x \in D \subset R^3, \\ u(x, \varepsilon) &= g(x), \quad x \in S, \end{aligned} \quad (3)$$

where $u(x)$ is a value of the dimensionless temperature at the point x , the function $A(u)$ is expressed in the terms of thermal conductivity $k(u) > \delta_0 > 0$, δ_0 is a certain value, the function $B(u, x)$ describes the process of energy release, the function $g(x)$ determines the edge regime at the boundary S .

In the present paper, the problem (1), (2) is investigated in the framework of the scheme described in [2, 3, 4, 5], and is illustrated by the application (3).

The research was supported by the Russian Science Foundation (project no. 18-11-00042).

References

- [1] M.A.Davydova, S.A. Zakharova. Modeling and Analysis of Information Systems, 25:1 (2018), pp. 83-91.
- [2] Davydova M.A., Nefedov N.N. Numerical Analysis and Its Applications, Lecture Notes in Comput. Sci. 2017. Vol. 10187, pp. 277-285.
- [3] Nefedov N. N., Davydova M. A. Differ. Equations 48:5, (2012), pp. 745-755.
- [4] Davydova M. A. Math. Notes 98:6,(2015) pp. 909-919.
- [5] Nefedov N. Numerical Analysis and Its Applications, Lecture Notes in Comput. Sci. 2013. Vol. 8236, pp. 62-72.

Invariant algebraic curves and Liouvillian first integrals for polynomial dynamical systems in the plane

M.V. Demina^{1,a)}

¹*National Research Nuclear University MEPhI*

In this talk we shall discuss the problem of finding irreducible invariant algebraic curves and Liouvillian first integrals for polynomial dynamical systems in \mathbb{C}^2 .

Establishing integrability or non-integrability of a dynamical system is an important problem of analysis. A universal definition of integrability for dynamical systems seems intangible. In this talk we shall deal with the Liouvillian integrability.

Let us consider the polynomial dynamical system

$$x_t = P(x, y), \quad y_t = Q(x, y) \tag{1}$$

with coprime polynomials $P(x, y)$ and $Q(x, y)$. The vector field associated to dynamical system (1) can be written as $X = P\partial_x + Q\partial_y$. A non-constant C^1 function $I(x, y): D \rightarrow \mathbb{C}$ is called a first integral of the polynomial vector field X on an open subset $D \subset \mathbb{C}^2$ if $XI(x(t), y(t)) = 0$ for all values of t such that the solution $(x(t), y(t))$ of X is defined on D . We say that the vector field X is Liouvillian integrable if there exists a Liouvillian first integral I of X . Generally speaking, a function is Liouvillian if it can be expressed via quadratures of elementary functions.

An algebraic curve $F(x, y) = 0$ with a non-constant polynomial $F(x, y)$ is an invariant algebraic curve (or a Darboux polynomial) of the vector field X if it satisfies the following equation $XF = \lambda(x, y)F$, where $\lambda(x, y)$ is a polynomial called the cofactor of the invariant curve $F(x, y)$. It can be observed that an invariant algebraic curve of the vector field X is formed by solutions of the latter. A solution of X has either empty intersection with the zero set of F or it is entirely contained in $F = 0$. It is straightforward to show that if $F(x, y)$ is an invariant algebraic curve of the vector field X , then so do all the polynomials $F^n(x, y)$, where $n \in \mathbb{N}$.

The function $E = \exp(g/f) \notin \mathbb{C}$ with coprime polynomials $g(x, y)$ and $h(x, y)$ is an exponential factor of the vector field X whenever it satisfies the equation $XE = \varrho(x, y)E$. The polynomial $\varrho(x, y)$ is called the cofactor of the exponential factor E .

It is known that the problem of proving Liouvillian integrability or non-integrability of a polynomial vector field X and associated dynamical system (1) can be reduced to the problem of constructing all irreducible invariant algebraic curves of X and all exponential factors of X [1, 2]. The main difficulty in finding irreducible invariant algebraic curves lies in the fact that bounds on the degree of $F(x, y)$ are as a rule a priori unknown.

Our aim is to derive a relationship between irreducible invariant algebraic curves of the vector field X and Puiseux series satisfying the ordinary differential equation $P(x, y)y_x - Q(x, y) = 0$. We shall present the general structure of any irreducible invariant algebraic curve of X and develop a method, which can be used to find all irreducible invariant algebraic curves and exponential factors explicitly [3, 4].

As an application of our results we shall solve completely the problem of Liouvillian integrability for a number of physically relevant dynamical systems including the famous Duffing and Duffing–van der Pol oscillators [3, 4].

^{a)}Email: mvdemina@mephi.ru

References

- [1] *Singer M.F.* Liouvillian first integrals of differential systems, *Trans. Amer. Math. Soc.* 333 (1992) 673–688.
- [2] *Christopher C.* Liouvillian first integrals of second order polynomial differential equations, *Electron. J. Differential Equations* 49 (1999) 1–7.
- [3] *Demina M.V.* Invariant algebraic curves for Liénard dynamical systems revisited, *Applied Mathematics Letters* 84 (2018) 42–48.
- [4] *Demina M.V.* Novel algebraic aspects of Liouvillian integrability for two–dimensional polynomial dynamical systems, *Physics Letters A* 382 (20) (2018) 1353–1360.

Stationary vortex configurations on a cylindrical surface

M.V. Demina^{1,a)}, N.A. Kudryashov^{1,b)}, D.V. Safonova^{1,c)}

¹*National Research Nuclear University MEPhI*

In this paper we study the problem of constructing and classifying stationary equilibria of point vortices on a cylindrical surface. Introducing polynomials with roots at vortex positions, we derive an ordinary differential equation satisfying by the polynomials. We prove that this equation can be used to finding any stationary configuration. The multivortex systems containing point vortices with circulation Γ_1 and Γ_2 ($\Gamma_2 = -\mu\Gamma_1$) are considered in detail. All stationary configurations with the number of point vortices less than five are constructed. Several theorems on existence of polynomial solutions of the ordinary differential equation under consideration are proved. The values of the parameters of the mathematical model for which there is an infinite number of non–equivalent vortex configurations on a cylindrical surface are found. New point vortex configurations are obtained.

It is known that stationary equilibria of simply periodic arrangements of point vortices are governed by the following system [1, 2]

$$\frac{1}{2\pi i} \sum_{j=1}^M \Gamma_j \left\{ \frac{\pi}{L} \cot \frac{\pi}{L} (s_k - s_j) \right\} = 0, \quad k = 1, \dots, M, \quad (1)$$

where L is the principle period and pairwise distinct points s_k belong to a stripe of periods. The prime in this expression means that we exclude the case $j = k$. Simply periodic arrangements of point vortices are regarded as vortices on a cylinder [2, 3, 4].

In new variables $z_k = \exp[2\pi i s_k / L]$, $z_k \neq 0$ system (1) can be rewritten as

$$2z_k \sum_{j=1}^M \frac{\Gamma_j}{z_k - z_j} + \Gamma_k - \sum_{j=1}^M \Gamma_j = 0, \quad k = 1, \dots, M. \quad (2)$$

^{a)}Email: mvdemina@mephi.ru

^{b)}Email: nakudr@gmail.com

^{c)}Email: Safonovadashav@gmail.com

Using the polynomial method [1, 4] we derive the ordinary differential equation

$$\mu z(z-1) \frac{d^2 W(z)}{dz^2} - (\{\mu(n-1) + 1\}z + \mu(1-n) + 1) \frac{dW(z)}{dz} + nW(z) = 0 \quad (3)$$

describing stationary equilibria of point vortex systems consisting of $n + 1$ point vortices on a cylindrical surface with one vortex of circulation Γ_1 and n vortices of circulation $\Gamma_2 = -\mu\Gamma_1$. Any polynomial $W(z)$ of degree n without multiple roots that solves equation (3) and satisfies the condition $W(0) \neq 0$ gives a configuration of point vortices in stationary equilibria.

Theorem. *If $n, \nu = 1/\mu$ are natural numbers and $n > 2\nu$, then equation (3) possesses two linearly independent polynomial solutions.*

There exist an infinite number of nonequivalent vortex configurations on a cylinder whenever conditions of the theorem are satisfied. In this case a free parameter is present in the polynomial solution of equation (3). This parameter affects the positions of the vortices. Nonequivalent vortex configurations are obtained by changing the free parameter.

Using this theorem we are able to find new stationary vortex configurations on a cylindrical surface. Examples of configurations with a free parameter are shown in the Figure 1

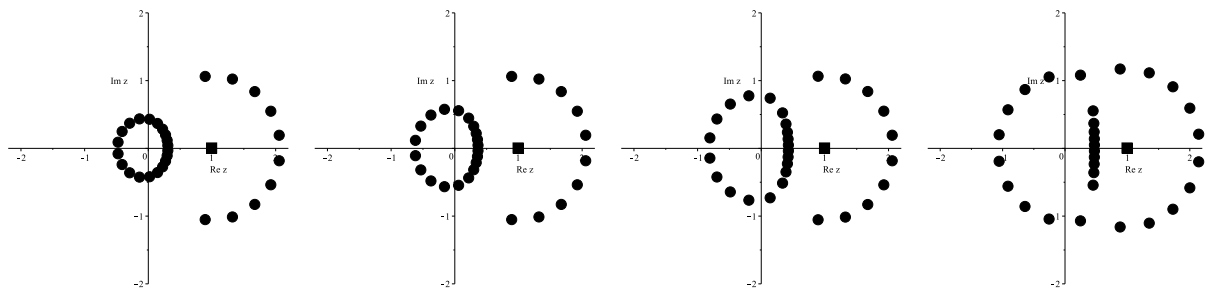


Fig. 1: : Plots of vortex positions in stationary equilibrium. Squares denote vortices with circulations Γ_1 , Circles denote vortices with circulation Γ_2 , $n = 30$, $\nu = 10$, $C_1 = 1$, $C_2 = 0.001, 0.1, 10, 1000$.

References

- [1] O'Neil K.A., Minimal Polynomial Systems for Point Vortex Equilibria, *Physica D*, 2006, vol. 219, pp. 69-79.
- [2] Aref H., Paul K. Newton, Mark A. Stremler, Tadashi Tokieda and Dmitri L. Vainchtein, Vortex Crystals, *Advances in Applied Mechanics*, 2003, vol. 39, p. 79
- [3] Borisov A.V., Mamayev I.S. *Matematicheskie metody dinamiki vikhrevykh struktur*. [Mathematical methods of dynamics of vortex structures.] Institut kompiuternykh issledovaniy, Moscow-Izhevsk, 2005, p. 368. (in Russian)
- [4] Demina M.V., Kudryashov N.A., Point Vortices and Classical Orthogonal Polynomials, *Regular and Chaotic Dynamics*, 2012, vol. 17, no. 5, pp. 371-384. doi: 10.1134/S1560354712050012

Pair of Lagrangian manifolds and asymptotic solutions of nonhomogeneous partial (pseudo)differential equations with localized right hand side

S.Y. Dobrokhotov^{1,2,a)}, V.E. Nazaikinskii^{1,2,b)}

¹*Ishlinsky Institute for Problems in Mechanics of Russian Academy of Sciences*

²*Moscow Institute of Physics and Technology*

We discuss the method of construction asymptotic solutions of linear partial differential and pseudodifferential problems with spatially localized right hand side. Our main observation is that such type asymptotics are based on a pair of Lagrangian manifolds. One of them is connected with the right hand side, and the second one defines so called wave part (far field) of the asymptotics. As examples we consider the Helmholtz equation and the equations from the water wave theory.

Rapidly changing asymptotic solutions describing the linear wave field in inhomogeneous media outside a neighbourhood of the caustic (and of the singularities of more General type) could be presented in the form WKB-functions $A(x, t)e^{\frac{i}{h}S(x, t)}$, $x = (x_1, \dots, x_n) \in \mathbb{R}^n$ or their linear combinations. Here the phase $S(x, t)$ and the amplitude $A(x, t)$ are (locally) smooth functions. In the presence of caustics (or singularities of a more complex form) in considered problems the WKB - asymptotics stop working and the asymptotic solutions are represented in a form of the Maslov canonical operator given on a suitable Lagrangian manifold in $2n$ -dimensional phase space. We consider inhomogeneous differential or pseudo-differential equations $\hat{L}u = f$ with spatially localized right-hand sides (sources). For stationary problems such a source is represented as $f(\frac{x-\xi}{h})$, where $f(y)$ is a smooth fast-decreasing function, ξ is a given vector and h is a small parameter. For evolution equations the source is represented in the form $f(\frac{x-\xi}{h}, t)$, where $f(y, t)$ is a smooth rapidly decreasing function on variable y , $\xi(t)$ is a given smooth vector-function that determines the dynamics of the center of the source. Thus, the source can move over time and change its shape. In the limit at $h \rightarrow 0$ the sources pass to δ -functions. The source functions are represented as the canonical Maslov operator on the "vertical" Lagrangian manifold $\Lambda_0 = x = \xi(t)$ and the problems under consideration have the form of equations with "canonically representable" right-hand sides. If the symbol $smbL$ of the operator \hat{L} is not equal to zero on Λ_0 , then the operator \hat{L} is reversed on f ("elliptic case") and the asymptotics of the solution of the problem are also determined by localized function. However, if the symbol $smbL$ of the operator \hat{L} vanishes on a subset $\tilde{\Lambda}$ from the manifold Λ_0 , the solution produces a fast-oscillating "wave" part that is associated with another Lagrangian manifold Λ_+ obtained by shifts $\tilde{\Lambda}$ along the trajectories of a suitable Hamiltonian system. The canonical operator on Λ_+ defines the mentioned "wave part" of the asymptotic solution of the corresponding inhomogeneous problem. Thus, the asymptotic solution to inhomogeneous equations with localized right-hand sides is determined by a *pair of Lagrangian manifolds*. In our talk we discuss the general method (algorithm) for constructing the manifold Λ_+ and asymptotic solution on a pair of manifolds Λ_0, Λ_+ . As examples, we consider the inhomogeneous Helmholtz equation and the problem of an analogue of the famous Kelvin wedge in the water waves theory.

The work was supported by the Russian Science Foundation (project N 16-11-10282).

^{a)}Email: dobr@iomnet.ru

^{b)}Email: nazaikinskii@googlemail.com

References

- [1] A. Yu. Anikin, S. Yu. Dobrokhotov, V. E. Nazaikinskii, and M. Rouleux, Dokl. Ross. Akad. Nauk 475 (6), 624–628 (2017); Engl. transl.: Dokl. Math. 96 (1), 406–410 (2017)]
- [2] Dobrokhotov S. Yu. and V. E. Nazaikinskii Waves on the Free Surface Described by Linearized Equations of Hydrodynamics with Localized Right-Hand Sides Russian Journal of Mathematical Physics, Vol. 25, No. 1, 2018, pp. 1–16.

Lie group classification of first and second order delay ordinary differential equations

V. Dorodnitsyn^{1,a)}, R. Kozlov^{2,b)}, S. Meleshko^{3,c)}, P. Winternitz^{4,d)}

¹*Keldysh Institute of Applied Mathematics, Russian Academy of Science, Miusskaya Pl. 4, Moscow, 125047, Russia*

²*Department of Business and Management Science, Norwegian School of Economics, Helleveien 30, 5045, Bergen, Norway*

³*School of Mathematics, Institute of Science, Suranaree University of Technology, 30000, Thailand*

⁴*Département de mathématiques et de statistique, Université de Montréal, Montréal, QC, H3C 3J7, Canada*

Lie group classification of first-order and second-order delay ordinary differential equations is presented. A delay ordinary differential system (DODS) is a delay ordinary differential equation (DODE) accompanied by a delay relation, i.e. an equation which describes a delay parameter.

A subset of such systems (delay ordinary differential systems or DODSs), which consists of linear DODEs and solution-independent delay relations, have infinite-dimensional symmetry algebra - as do nonlinear ones that are linearizable by an invertible transformation of variables. Genuinely nonlinear first order DODSs have symmetry algebras of dimension n , $0 \leq n \leq 3$.

It is shown how exact analytical solutions of invariant DODSs can be obtained using symmetry reduction.

References

- [1] Vladimir Dorodnitsyn, Roman Kozlov, Sergey Meleshko and Pavel Winternitz, Lie group classification of first-order delay ordinary differential equations, Journal of Physics A: Mathematical and Theoretical, Volume 51, Number 20, 2018

^{a)}Email: Dorodnitsyn@Keldysh.ru

^{b)}Email: Roman.Kozlov@nhh.no

^{c)}Email: sergey@math.sut.ac.th

^{d)}Email: wintern@crm.umontreal.ca

- [2] Vladimir Dorodnitsyn, Roman Kozlov, Sergey Meleshko and Pavel Winternitz, Linear or linearizable first-order delay ordinary differential equations and their Lie point symmetries, *Journal of Physics A: Mathematical and Theoretical*, Volume 51, Number 20, 2018.
- [3] Vladimir Dorodnitsyn, Roman Kozlov, Sergey Meleshko and Pavel Winternitz, Lie group classification of second-order delay ordinary differential equations, in preparation.

On geometric applications of nonlinear integrable equations

V. Dryuma^{1,a)}

¹*IMI AS RM, Academy str 5, MD2001, Kishinev, Moldova*

The Riemannian spaces associated with the 3D-Darboux system of equations and its generalizations are constructed, their applications in General Relativity and differential geometry are discussed.

1. The surfaces of projective spaces RP^3 and RP^4 that have families of conjugate lines are studied by means of solutions of a system of equations of the form

$$\hat{H}\Psi = 0, \quad \hat{L}_1\Psi = 0, \quad \hat{L}_2\Psi = 0,$$

where \hat{H} is the Laplace operator $\hat{H} = D_{xy} - a(x, y)D_x - b(x, y)D_y - c(x, y)$ and \hat{L}_1, \hat{L}_2 are linear the second order differential operators (in case of RP^3 -space) and the third order operators (in case of RP^4 -space [1]. If the relations $[\hat{H}, \hat{L}_1] = a_1\hat{L}_1 + b_1\hat{L}_2$, $[\hat{H}, \hat{L}_2] = a_2\hat{L}_1 + b_2\hat{L}_2$ between these operators are hold they form "weakly commuting" family and corresponding nonlinear differential equations on the coefficients of operators can be integrated by the IST-method.

As example, the operators $\hat{H} = D_{xy} - Q(x, y)/3$, $\hat{L}_1 = D_{xxx} - Q_{xy}D_x$ and $\hat{L}_2 = D_{yyy} - Q_{yy}D_y$ form "weakly commuting" family of operators at the condition $R_{xy} = 1/3 \exp(R) + \alpha \exp(-2R)$, where $Q_{xy} = \exp(R(x, y))$ that is well known integrable equation on the function $R(x, y)$. From here followed existension of 2D-surfaces in RP^4 -space defined by solutions of given integrable equation.

2. As another example, consider 3-sub-varieties of RP^4 -space having the families of 3-triply conjugate lines. They are described by the solutions of the system

$$\Psi_{xy} = u_y\Psi_x + v_x\Psi_y, \quad \Psi_{xz} = u_z\Psi_x + w_x\Psi_z, \quad \Psi_{yz} = v_z\Psi_y + w_y\Psi_z, \quad (1)$$

which is compatible under conditions

$$u_{yz} + u_yu_z - u_zw_y - u_yv_z = 0, \quad v_{xz} + v_xv_z - u_zv_x - w_xv_z = 0, \quad w_{xy} + w_xw_y - v_xw_y - u_yw_x = 0. \quad (2)$$

This system of equations is closely related to the Darboux system of equations

$$bca_{yz} - bc_ya_z - cb_za_y = 0, \quad acb_{xz} - ac_xb_z - ca_zb_x = 0, \quad abc_{xy} - ba_yc_x - ab_xc_y = 0, \quad (3)$$

which is condition of compatibility of the linear system with respect to the function $\phi(x, y, z)$

$$bc\phi_{yz} = cb_z\phi_y + bc_y\phi_z, \quad ac\phi_{xz} = ca_z\phi_x + ac_x\phi_z, \quad ab\phi_{xy} = ba_y\phi_x + ab_x\phi_y, \quad (4)$$

^{a)}Email: valdryum@gmail.com

and which is the part of complete Darboux-Lame system, on which classification of triply orthogonal curvilinear coordinates in three-dimensional Euclidean space R^3 is based. Applicability of the IST-method to the system (3) was shown first by the author [2-3] and with help of corresponding the Lax- presentation $[\hat{L}_1, \hat{L}_2] = (a_{xz} - a_{zx})\hat{L}_1 + (a_{xy} - c_{x,y})\hat{L}_2 + (b_{xx} - c_{xx})\hat{L}_3$, $[\hat{L}_1, \hat{L}_3] = (a_{yz} - b_{yz})\hat{L}_1 + (a_{yy} - c_{yy})\hat{L}_2 + (b_{xy} - c_{xy})\hat{L}_3$, $[\hat{L}_2, \hat{L}_3] = (a_{zz} - b_{zz})\hat{L}_1 + (a_{zy} - c_{zy})\hat{L}_2 + (c_{xz} - b_{xy})\hat{L}_3$, was detail investigated and it particular solutions [3-4] derived. Corresponding solutions were used to the study various problems of differential geometry and in General Relativity. Here we will discuss a properties of the Ricci-flat 4D-space with the orthogonal metric

$$ds^2 = L^2 e^{2 a_3 x + 2 b_1 y + 2 c_1 z} (dx)^2 + M^2 e^{3 b_1 y} (dy)^2 + N^2 e^{2 a_3 x + 2 b_1 y + 2 c_1 z} (dz)^2 - F^2 (dt)^2 e^{-b_1 y},$$

with parameters which is constructed with the help of solutions of the Darboux system and it the linear presentation (4).

3. To integrating of the nonlinear system (2) we apply multidimensional generalization of the Monge-Ampere transformation on base of parametric presentation of the functions and variables.

On such a way we bring a following example solution of the system (2)

$$u(x, y, z) = \ln(A(x, y, z)), \quad v(x, y, z) = \ln(B(x, y, z)), \quad w(x, y, z) = \ln(C(x, y, z)),$$

with the functions $A(x, y, z)$, $B(x, y, z)$ and $C(x, y, z)$ of the form

$$A(x, y, z) = 4 \frac{\mu (C_2 + H(x, z))}{-4 C_2 - 2 \mu C_1 y + \mu y^2 - 4 H(x, z)},$$

$$B(x, y, z) = \mu + 4 \frac{\mu (C_2 + H(x, z))}{-4 C_2 - 2 \mu C_1 y + \mu y^2 - 4 H(x, z)},$$

$$C(x, y, z) = \frac{F(x, z)}{-4 C_2 - 2 \mu C_1 y + \mu y^2 - 4 H(x, z)},$$

which depend on two arbitrary functions $F(x, z)$ and $H(x, z)$ of two variables connected by one relation

$$F(x, z) = F_1(z) e^{\int \frac{\left(\frac{\partial^2}{\partial x \partial z} H(x, z)\right) C_2 + \left(\frac{\partial^2}{\partial x \partial z} H(x, z)\right) H(x, z) - \left(\frac{\partial}{\partial x} H(x, z)\right) \frac{\partial}{\partial z} H(x, z}}{\left(\frac{\partial}{\partial z} H(x, z)\right) (C_2 + H(x, z))} dx}.$$

References:

1. E.P. Lane, *A Treatise on projective differential geometry*. Chicago: The University of Chicago Press, 1942, 528 p.
2. V. Dryuma, *A Projective properties of "weakly-commuting" family of operators*. The IX-Geometric Conference. Theses, Kishinev, 20-22 Septembrie, "Stiintsa", (1988), p.124-125.
3. V. Dryuma, *Three-dimensional integrable system of nonlinear differential equations ant its applications*. Mathematical Research. Kishinev, "Stiintsa".v.124 (1992), p. 56-68.
4. V. Dryuma, *Geometrical properties of the multidimensional Nonlinear differential equations and the Finsler metrics of phase spaces of dynamical systems*. Theoretical and Mathematical. Physics, v.99, No.2, pp.241-249, (1994), p. 56-68.

Lax representation and quadratic first integrals for a family of non–autonomous second–order differential equations

I.Y. Gaiur^{1,a)}, D.I. Sinelshchikov^{1,b)}, N.A. Kudryashov^{1,c)}

¹*National Research Nuclear University MEPhI*

We consider a family of non–autonomous second–order differential equations, which generalizes the Liénard equation. We explicitly find the necessary and sufficient conditions for members of this family of equations to admit a quadratic, with the respect to the first derivative, first integral. We show that these conditions are equivalent to the conditions for the considered family of equations to possess a Lax representation. This provides a connection between the existence of a quadratic first integral and a Lax representation for dissipative systems, which may be considered as an analogue to the theorem that connects Lax integrability and Arnold-Liouville integrability of Hamiltonian systems. We illustrate our results by several examples of dissipative equations that simultaneously have a quadratic first integral and a Lax representation.

In this work we study the following family of equations

$$y_{zz} + f(z, y)y_z + g(z, y) = 0, \tag{1}$$

which generalizes the Liénard equation. Here $f(z, y)$ and $g(z, y)$ are arbitrary functions, which do not vanish, i.e. $f \neq 0$ and $g \neq 0$.

In the case of $f_z = g_z = 0$ from (1) we obtain the classical Liénard equation

$$y_{zz} + f(y)y_z + g(y) = 0, \tag{2}$$

while at $f_z = 0$ we get

$$y_{zz} + f(y)y_z + g(z, y) = 0. \tag{3}$$

Equations of type (1) play an important role in various fields of science, such as nonlinear dynamics, mechanics and biology. In addition, equations from family (1) often appear as symmetry reductions of second and third order nonlinear partial differential equations.

The main aim of this work is to study equation (1) as a Lax integrable system and obtain the necessary and sufficient conditions for equation (1) to possess a fist integral, which is quadratic with respect to the first derivative. Lax integrability requires a differential system to have a Lax representation, which also called the Lax pair.

The knowledge of a Lax pair for an equation from family (1) leads to the corresponding quadratic first integral. On the other hand, one can consider the problem of finding all equations from family (1), which admits a quadratic first integral. Below, we solve this problem and provide explicit correlations on functions f and g , which provide the necessary and sufficient conditions for the existence of a quadratic first integral. Finally, we show that these conditions are equivalent to conditions for the existence of a Lax representation for an equation from family (1).

^{a)}Email: iygayur@gmail.com

^{b)}Email: disine@gmail.com

^{c)}Email: nakudr@gmail.com

Multistability in a model of oscillations of an encapsulated microbubble contrast agent close to an elastic wall

I.R. Garashchuk^{1,a)}, D.I. Sinelshchikov^{1,b)}, N.A. Kudryashov^{1,c)}

¹*NRNU "MEPhI"*

Contrast agents are bubbles with radius on the order of several micrometers with a gas core and encapsulated in a shell. Depending on the application, shell is made from different materials (e.g. lipid monolayer, biodegradable polymer protein thick shell, etc.), and has different thickness and other properties [1, 2]. Contrast agents can be applied in several areas: improvement of medical ultrasound imaging (including molecular imaging), targeted drug delivery and non-invasive therapy (see [1] and references therein). They are injected into the blood flow intravenously or intra-arterially. Afterwards, an external ultrasound field is applied. Microbubble response to the ultrasound acoustic wave is non-linear. Complex dynamics can occur in the models of bubble behavior. Interesting and the least studied problem is the multistability phenomenon arising in the bubble dynamics. It is known that multistability takes place in the models of contrast agent dynamics, both non-shelled [3, 4] and shelled [5]. The dependence of the type of dynamics of a contrast agent on the control parameters (pressure magnitude and frequency of the ultrasound field) is important for applications. Thus, an accurate investigation of emergence of the multistability in these models is an important issue. We demonstrate that coexisting attractors presence in the models under investigation at physically relevant values of the control parameters. Dynamical systems, corresponding to the models of contrast agent oscillations have no fixed points. If there is only one attractor, the system will converge to it starting from any acceptable initial conditions. However, if two attractors coexist, the initial values problem becomes non-trivial. We tried applying two powerful tools to overcome this problem: the perpetual points method (or higher order critical points method) [8, 10] and the continuation method [8, 9, 5, 4]. Unfortunately, the perpetual points method does not give us the desirable results when applied to these models, because of lack of required points in a reasonable subset of the initial conditions space (the missing points do not exist for the equations considered or are located in an unacceptable area of the initial conditions space and cannot be used). On the other hand, the numerical continuation approach is very efficient, if a good starting point can be found [5, 8, 9]. By means of the numerical continuation method, one can move from areas of the control parameters where the structure of attractors is simpler and easier to identify to other regions, where it can be more complicated. Also it can be used to observe ranges of existence of each of the attractors along with their bifurcation structure. We provide regions of the control parameters, where different types of dynamics take place (periodic, chaotic, multistability). Basins of the coexisting attractors have complicated geometry and it is hard to tell for any given point in the initial conditions space in which of the manifolds of attraction it lays without calculating these basins directly. While building the basins of each attractor is a very resource-intensive problem. We consider the multistability to be adverse for applications because it can lead to unpredictable behavior, especially if coexistence of a periodic and a chaotic attractor takes place.

^{a)}Email: ivan.mail4work@yandex.ru

^{b)}Email: disine@gmail.com

^{c)}Email: nakudr@gmail.com

After the contrast agents are injected into the blood flow, their state is not controlled by experimenter anymore. Thus, the initial conditions at the moment of activation of the ultrasound field are quite random, and it is uncertain, to which of the coexisting attractors the system will converge. Consequently, the resulting type of oscillations might differ from the one expected by experimenter. Moreover there are a lot of sources of external perturbations which can force the system to unpredictably switch from one attractor to another. We consider this kind of abrupt shifts between attractors (for example, between chaotic and periodic motion modes and vice versa) not beneficial for applications too.

References

- [1] A.L. Klibanov, Microbubble contrast agents: targeted ultrasound imaging and ultrasound-assisted drug-delivery applications., *Invest. Radiol.* 41 (2006) 354-362.
- [2] A.A. Doinikov, A. Bouakaz, Review of shell models for contrast agent microbubbles, *IEEE Trans. Ultrason. Ferroelectr. Freq. Control.* 58 (2011) 981-993.
- [3] U. Parlitz, V. Englisch, C. Scheffczyk, W. Lauterborn, Bifurcation structure of bubble oscillators, *J. Acoust. Soc. Am.* 88 (1990) 1061-1077.
- [4] I.R. Garashchuk, N.A. Kudryashov, D.I. Sinelshchikov, Hidden Attractors in a Model of a Bubble Contrast Agent Oscillating Near an Elastic Wall, *European Journal of Physics: Web of Conferences*, 173, 06006 (2018)
- [5] I.R. Garashchuk, N.A. Kudryashov, D.I. Sinelshchikov, Nonlinear Dynamics of a Bubble Contrast Agent Oscillating Near an Elastic Wall, *Regular and Chaotic Dynamics*, 2018, Vol. 23, No. 3, pp. 257–272.
- [6] L. Hoff, *Acoustic characterization of contrast agents for medical ultrasound imaging*, Springer, Berlin, 2001.
- [7] A.A. Doinikov, L. Aired, A. Bouakaz, Acoustic scattering from a contrast agent microbubble near an elastic wall of finite thickness, *Phys. Med. Biol.* 56 (2011) 6951-6967.
- [8] D. Dudkowski, A. Prasad, S. Jafari, T. Kapitaniak, N.V. Kuznetsov, G.A. Leonov, G. A., Hidden attractors in dynamical systems, *Physics Reports*, vol. 637, 2016
- [9] G.A. Leonov, N.V. Kuznetsov and T.N. Mokaev, Homoclinic orbits, and self-excited and hidden attractors in a Lorenz-like system describing convective fluid motion, *Eur. Phys. J.*, v. 224, Special Topics, 2015
- [10] D. Dudkowski, A. Prasad and T. Kapitaniak, Perpetual points: New tool for localization of co-existing attractors in dynamical systems, *arxiv.org*, 1702.03419v1

Traveling Waves and Plasma Acceleration in Quasi-Steady Plasma Accelerators (QSPAs) with Longitudinal Field

M.B. Gavrikov^{1,a)}, A.A. Taiurskii^{1,b)}

¹*Keldysh Institute of Applied Mathematics RAS*

We find and classify plane traveling waves in hot magnetized plasma in the case of zero transverse electric field (in the reference frame of background plasma motion). On the basis of these results, we evaluate the possibilities of using QSPAs with longitudinal magnetic field for plasma acceleration in plasma accelerator channels.

A plane traveling wave is defined as a flow of a continuous medium whose parameters, at each time instant, depend on a single spatial coordinate x , while the profile of each parameter is moving as a whole along the axis x with a common constant phase velocity a . Such waves are solutions of the equations of motion of continuous media and have the form $f(\theta)$, where $\theta = x - at$ is the phase of the wave. In a plasma continuum subject to the equations of electromagnetic hydrodynamics (EMHD) [1], traveling waves are solutions of the following system of equations for the dimensionless functions $\mathbf{H}_\perp(\theta)$, $u(\theta) = U_\parallel(\theta) - a$ [2]:

$$\left(\frac{|u|}{2} - \beta^2\right) \mathbf{H}_\perp - \xi^2 |u| \frac{d}{d\theta} \left(|u| \frac{d\mathbf{H}_\perp}{d\theta}\right) + \Lambda \xi \beta |u| \left[\mathbf{k}, \frac{d\mathbf{H}_\perp}{d\theta}\right] + \mathbf{p} = 0, \quad (1)$$

$$|u| + K/|u|^\gamma + H_\perp^2 = 2, \quad (2)$$

where \mathbf{k} is the unit vector along the axis x ; all vectors have two components: along (\parallel) and across (\perp) the vector \mathbf{k} ; $\xi > 0$, $K \geq 0$, β are similarity numbers; $\mathbf{p} \perp \mathbf{k}$ is an arbitrary vector; $\Lambda = (\lambda_+/\lambda_-)^{1/2} - (\lambda_-/\lambda_+)^{1/2}$, $\lambda_\pm = m_\pm/e_\pm$, m_\pm , e_\pm are masses and absolute values of the charges of plasma components. The parameter β is proportional to the longitudinal magnetic field; K is the plasma temperature; ξ^2 is inversely proportional to the number of plasma particles per unit length. In some special cases [3, 4, 5], system (1), (2) has exact solutions. In this paper, we obtain its solutions in the case of $\mathbf{p} = 0$, $K > 0$, assuming that the electrons and ions are ideal polytropic gases with a common adiabatic index $\gamma > 1$, and it is also assumed that $u > 0$. The integration of system (1), (2) is based on the following result.

Theorem 1. 1) Any solution of system (1), (2) satisfies the identity

$$\xi^2 u^2 \left(\dot{H}_y^2 + \dot{H}_z^2 \right) + u^2/8 + \beta^2 (H_y^2 + H_z^2) + \gamma K / \left(4(\gamma - 1) |u|^{\gamma-1} \right) - H_y p_y - H_z p_z = \text{const},$$

where $\mathbf{H}_\perp = (H_y, H_z)$, and the dot indicates differentiation in θ .

2) For $\mathbf{p} = 0$, any solution of system (1), (2) satisfies the identity

$$|u| \left(\dot{H}_y H_z - \dot{H}_z H_y \right) + \Lambda \beta (H_y^2 + H_z^2) / (2\xi) = \text{const}.$$

Any solution $w(\theta) = (H_y(\theta), H_z(\theta), u(\theta))$ of system (1), (2) lies on a spheroid S^2 obtained by revolving the curve $\Gamma : u + K/u^\gamma + H^2 = 2$ on the plane (H, u) about the axis u . **Theorem 1** allows us to integrate system (1), (2), with $\mathbf{p} = 0$, in spherical coordinates on $S^2 : H_y = S(\psi) \cos \varphi$, $H_z = S(\psi) \sin \varphi$, $u = C(\psi)$, where ψ and φ are, respectively, the altitude and the longitude of a point on S^2 , and $(S(\psi), C(\psi))$ are the coordinates of the point at which the curve

^{a)}Email: mbgavrikov@yandex.ru

^{b)}Email: tayurskiy2001@mail.ru

Γ is crossed by the ray issuing from the point $(0, u_*)$ on the plane (H, u) and forming the angle ψ with the positive direction of the axis u . Here, $u_* = (\gamma K)^{1/(\gamma+1)}$ is the point of minimum of the function $u + K/u^\gamma$. In spherical coordinates, the general solution of system (1), (2) with $\mathbf{p} = 0$ has the form

$$\pm \xi \int \frac{S'(\psi)C(\psi)d\psi}{\sqrt{2(\mathcal{E} - \Phi(\psi))}} = \theta + \text{const}, \quad \frac{d\varphi}{d\theta} = \frac{I + (\Lambda\beta/2)S^2(\psi)}{\xi S^2(\psi)C(\psi)}, \quad (3)$$

where \mathcal{E} , I are arbitrary constants, the prime indicates differentiation in ψ , and $\Phi(\psi)$ is the potential function

$$\Phi(\psi) = \frac{\beta^2}{2} \left(1 + \frac{\Lambda^2}{4}\right) S^2(\psi) + \frac{C^2(\psi)}{8} + \frac{\gamma}{4(\gamma-1)} \frac{K}{C(\psi)^{\gamma-1}} + \frac{I^2}{2S^2(\psi)}.$$

The solution $\psi(\theta)$ lies in the potential well $\Phi(\psi) \leq \mathcal{E}$ and is obtained as a certain combination of the \pm -arcs defined by the integral in (3). Knowing $\psi(\theta)$, we can find $\varphi(\theta)$ from the second relation in (3). The said combination of the arcs depends on the sign of $S'(\psi)$ in the potential well. If the sign of $S'(\psi)$ alternates, then the derivative of the altitude $\psi(\theta)$ becomes infinite at some points and the traveling wave has singularities. Smooth (of class C^2) traveling waves can be divided into three classes: cold (the curve $w(\theta)$ lies on the northern hemisphere $u \geq u_*$); hot (the curve $w(\theta)$ lies in the southern hemisphere $u \leq u_*$), and hybrid (the curve $w(\theta)$ lies on both hemispheres). Cold and hot waves can be studied by the methods of [5]. It has been shown that there are 4 types of hybrid waves (see Fig. 1).

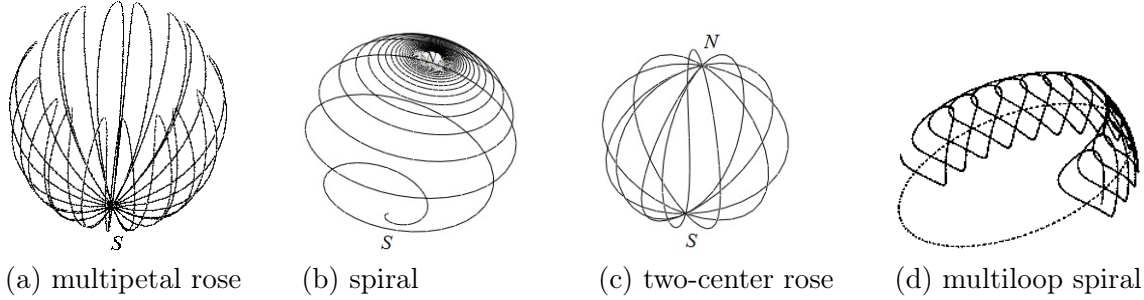


Figure 1

Traveling waves with zero phase velocity $a = 0$ determine steady regimes of plasma flow in quasi-steady plasma accelerators (QSPAs) with plane electrodes and longitudinal magnetic field. At the entrance of a plasma channel, for $x = 0$, the following plasma parameters are given: ρ_0 , p_0 , H_0 (transverse magnetic field), U_0 (longitudinal velocity), \dot{H}_y , \dot{H}_z (current density), $H_y(0) = H_0 \cos \varphi_0$, $H_z(0) = H_0 \sin \varphi_0$. If the flow entering the channel is subsonic, then the following conditions are necessary and sufficient for the plasma flow to be supersonic at its exit:

$$2\beta^2(1 + \Lambda^2/4) > u_* + 2I^2/H_{\max}^4, \quad \mathcal{E} = \Phi(\pi/2), \quad H_{\max}^2 = 2 - (\gamma + 1)u_*/\gamma,$$

where $I = \xi(M_A \sqrt{2C})^{-1}(\dot{H}_z \cos \varphi_0 - \dot{H}_y \sin \varphi_0) - \Lambda\beta/(4CM_A^2)$,

$$\mathcal{E} = \xi^2(\dot{H}_y \cos \varphi_0 + \dot{H}_z \sin \varphi_0)^2/2 + \Phi(\psi_0),$$

$$\Phi(\psi_0) = \beta^2(1 + \Lambda^2/4)/(4CM_A^2) + (8C^2)^{-1} + \gamma KC^{\gamma-1}/(4(\gamma-1)) + I^2 CM_A^2.$$

Here, ψ_0 is the initial altitude, $M = U_0(\gamma p_0/\rho_0)^{-1/2}$ is the (common) Mach number, $M_A = (U_0/H_0)\sqrt{4\pi\rho_0}$ is the Alfvénic Mach number, $C = (1 + (\gamma M^2)^{-1} + (2M_A^2)^{-1})/2$, $\beta = (H_{\parallel}/H_0)(M_A \sqrt{2C})^{-1}$, $K = (\gamma M^2 C^{\gamma+1})^{-1}$, $\xi = c\sqrt{\lambda_+\lambda_-}/(\sqrt{4\pi\rho_0}L_0) \cdot (C/2)^{1/2}$, L_0 is the length of the channel, H_{\parallel} is the longitudinal magnetic field.

This work has been supported by the Russian Scientific Foundation (Project No. 16-11-10278).

References

- [1] Gavrikov, M. B. Linear waves in nonrelativistic magnetohydrodynamics. Keldysh Institute of Applied Mathematics. Preprint 199, 1988.
- [2] Gavrikov M.B., Savel'jev V.V., and Tayurskii, A.A. Solitons in two-fluid magnetohydrodynamics with nonzero electron inertia. *Izvestiya VUZ, Applied Nonlinear Dynamics* 2010. Vol. 18, No. 4. P. 132–147.
- [3] Adlam J.H., Allen J.E. // *Phil. Mag.* 1958. Vol. 3 P. 448.
- [4] Lüst R. *Fortschritter der Physik.* // **7**. 503–558. (1959).
- [5] Gavrikov, M. B. Aperiodic vibrations of cold plasma. Keldysh Institute of Applied Mathematics. Preprint 33, 1991.

Quasi-Stable Structures of the Repressilator Model

S.D. Glyzin^{1,2,a)}, A.Y. Kolesov^{1,b)}, N.K. Rozov^{3,c)}

¹*P.G. Demidov Yaroslavl State University*

²*Scientific Center in Chernogolovka RAS*

³*M.V. Lomonosov Moscow State University*

A new mathematical model is proposed for a circular gene network representing a system of unidirectionally coupled ordinary differential equations. The existence and stability of special periodic motions (traveling waves) for this system is studied. It is shown that, with a suitable choice of parameters and an increasing number m of equations in the system, the number of coexisting traveling waves increases indefinitely, but all of them (except for a single stable periodic solution for odd m) are quasistable. The quasi-stability of a cycle means that some of its multipliers are asymptotically close to the unit circle, while the other multipliers (except for a simple unit one) are less than unity in absolute value.

The simplest genetic oscillator, known as a repressilator, was proposed in [1]. It consists of three elements A_j , $j = 1, 2, 3$ each unidirectionally inhibiting its neighbor. More specifically, A_1 inhibits the synthesis of A_2 , A_2 inhibits the synthesis of A_3 , and A_3 , which closes the cycle, inhibits the synthesis of A_1 .

The mathematical model of this gene network has the form

$$\dot{p}_j = -p_j + \frac{\alpha}{1 + u_{j-1}^\gamma} + \alpha_0, \quad \dot{u}_j = \beta(p_j - u_j), \quad j = 1, 2, 3, \quad u_0 = u_3. \quad (1)$$

Following [1], we assume that each element is a set of mRNA (message RNA) of concentration p_j and protein of concentration u_j . Furthermore, the time variation in p_j is assumed to be characterized by synthesis and degradation. The former of these processes is described by the

^{a)}Email: glyzin.s@gmail.com

^{b)}Email: andkolesov@mail.ru

^{c)}Email: fpo.mgu@mail.ru

function $\alpha/(1+u_{j-1}^\gamma)$, where u_{j-1} is the concentration of the repressor protein for the j th mRNA, $\gamma = \text{const} > 0$ is the cooperativity coefficient, and $\alpha = \text{const} > 0$ is the transcription rate in the absence of the repressor. The latter process is described by the linear term $-p_j$. Finally, the additive term $\alpha_0 > 0$ in the equation for p_j describes the leakiness of the promoter.

The problem of self-excited oscillations in (1) and similar systems arising in the modeling of gene networks has been extensively investigated (see, e.g., [2] – [7]).

The interaction of the concentrations u_j and p_j described above is surprisingly similar to the interaction of six ecological populations – three predators and three preys. Indeed, suppose that u_j ($j = 1, 2, 3$) and p_j ($j = 1, 2, 3$) are the population densities of the predators and preys, respectively. Then, by virtue of (1), each predator u_j feeds on only one prey p_j (for $p_j \equiv 0$, u_j decays exponentially) and, at the same time, exerts pressure only on the prey p_{j+1} . The last means that the growth rate of p_{j+1} decreases with increasing u_j . Additionally, if the repressor predator is absent ($u_j \equiv 0$), then p_j tends to the threshold value as $t \rightarrow +\infty$.

In view of this ecological interpretation, the gene network can be modeled using Kolesov's approach [8]. In the case of an arbitrary number of elements A_j , $j = 1, 2, \dots, m$ interacting according to the circular principle, this approach yields the system

$$\dot{p}_j = \frac{r_1}{1+a} [1 + a(1 - u_{j-1}) - p_j] p_j + \alpha, \quad \dot{u}_j = r_2 [p_j - u_j] u_j, \quad j = 1, 2, \dots, m, \quad u_0 = u_m, \quad (2)$$

where r_1, r_2, a , and α are positive constants. It should be emphasized that the term $+\alpha$, which is similar to the addition α_0 in (1), was intentionally added to the equation for p_j , thereby violating its Volterra structure. The condition $\alpha > 0$ cannot be omitted in our case, in contrast to system (1), where we can set $\alpha_0 = 0$. The new mathematical model of repressilator (2) can be simplified. Specifically, assume first that $r_2 \gg 1$ and $r_1 = r \sim 1$. Then, according to the Tikhonov reduction principle, as $r_2 \rightarrow +\infty$, we have $p_j = u_j$, $j = 1, 2, \dots, m$. For the component u_j , we obtain the system

$$\dot{u}_j = \frac{r}{1+a} [1 + a(1 - u_{j-1}) - u_j] u_j + \alpha, \quad j = 1, 2, \dots, m, \quad u_0 = u_m,$$

which, after making the normalizations $u_j/(1+a) \rightarrow u_j$, and $\alpha/(1+a) \rightarrow \alpha$ becomes

$$\dot{u}_j = r[1 - u_j - a u_{j-1}] u_j + \alpha, \quad j = 1, 2, \dots, m, \quad u_0 = u_m. \quad (3)$$

By traveling waves of system (3), we mean special periodic solutions (see [9, 10]) that can be represented in the form

$$u_j = u(t + (j - 1)\Delta), \quad j = 1, 2, \dots, m, \quad \Delta = \text{const} > 0. \quad (4)$$

Below, the existence and stability of such solutions are analyzed in the case where $r \gg 1$, $\alpha \ll 1$ and the parameter a is on the order of unity. More precisely, we assume throughout that

$$a = \text{const} > 1, \quad \alpha = r \exp(-br), \quad r \gg 1, \quad b = \text{const} > 0. \quad (5)$$

We prove that, under conditions (5), the number of coexisting periodic solutions (4) to system (3) increases indefinitely as $r \rightarrow +\infty$ and $m \rightarrow +\infty$ consistently. However, all of them (except for a single stable solution for odd m) are quasi-stable. Namely, the stability spectrum of each of these periodic solutions contains a nonempty group of multipliers $\nu \in \mathbb{C}$, $\nu \neq 1$ lying at a distance of order $\exp(-cr)$, $c = \text{const} > 0$ from the unit circle.

Acknowledgments. This work was supported by the Russian Science Foundation (project nos. 14-21-00158).

References

- [1] M. B. Elowitz and S. Leibler, A synthetic oscillatory network of transcriptional regulators, *Nature* 403, 335–338 (2000).
- [2] E. P. Volokitin, On limit cycles in the simplest model of a hypothetical genetic network, *Sib. Zh. Ind. Mat.* 7 (3), 57–65 (2004).
- [3] O. Buse, A. Pérez, and A. Kuznetsov, Dynamical properties of the repressilator model, *Phys. Rev. E* 81 (066206) 066206-1–066206-7 (2010).
- [4] V. A. Likhoshvai, G. V. Demidenko, S. I. Fadeev, Yu. G. Matushkin, and N. A. Kolchanov, Mathematical simulation of regulatory circuits of gene networks, *Comput. Math. Math. Phys.* 44 (12), 2166–2183 (2004).
- [5] S. D. Glyzin, A. Yu. Kolesov, and N. Kh. Rozov, Existence and stability of the relaxation cycle in a mathematical repressilator model, *Math. Notes* 101 (1), 71–86 (2017).
- [6] S. D. Glyzin, A. Yu. Kolesov, N. Kh. Rozov, An approach to modeling artificial gene networks, *Theoret. and Math. Phys.*, 194(3), 471–490 (2018).
- [7] S. D. Glyzin, A. Yu. Kolesov, and N. Kh. Rozov, Quasi-Stable Structures in Circular Gene Networks, *Computational Mathematics and Mathematical Physics.* 58(5), 659–679(2018).
- [8] A. Yu. Kolesov and Yu. S. Kolesov, *Relaxation Oscillations in Mathematical Models of Ecology* (Am. Math. Soc., Providence, 1997).
- [9] S. D. Glyzin, A. Yu. Kolesov, and N. Kh. Rozov, Periodic traveling-wave-type solutions in circular chains of unidirectionally coupled equations, *Theor. Math. Phys.* 175 (1), 271–312 (2013).
- [10] S. D. Glyzin, A. Yu. Kolesov, and N. Kh. Rozov, The buffer phenomenon in ring-like chains of unidirectionally connected generators, *Izv. Math.* 78 (4), 708–743 (2014).

Functions of differential operators and the relativistic Schrödinger equation

A.V. Golovin^{1,a)}, V.M. Lagodiski^{2,b)}

¹*Sankt-Petersburg State University, Physics faculty*

²*Saint-Petersburg State University of Aerospace Instrumentation*

A new definition of the function of the differential operator, which leads to local operators of infinite order, allows us to obtain an expression for the square root of the differential operator (Hamiltonian of a free spinless particle) and to determine the relativistic Schrödinger equation as a close analogue of the nonrelativistic Schrödinger equation. The spectral theory of various boundary value problems corresponding to some physical problems is constructed, and there are no difficulties typical for relativistic quantum mechanics based on the Klein-Gordon equation.

^{a)}Email: golovin50@mail.ru

^{b)}Email: lagodinskiy@mail.ru

It is known that the Klein-Gordon equation (KGE) leads to significant difficulties, for example, to solutions corresponding to the states of a free particle with negative energy, complex values of the energy of a pion atom with a nucleus charge $Z > 68$, and others. Two-particle KGE is impossible. It is easy to see that such a sharp difference between the KGE and the nonrelativistic Schrödinger equation (NSE) is due to the fact that the latter is based on a formal replacement

$$\varepsilon \rightarrow i \frac{\partial}{\partial t}, \quad \mathbf{p} \rightarrow -i \nabla$$

(we use the system of units in which the speed of light c and the Planck constant \hbar are equal to one) in the expression of the energy through the pulse, and in KGE — the same replacement is in the expression of **square energy** through the pulse. As a result, KGE is an equation of hyperbolic type, while NSE is of parabolic type. It can be assumed that the KGE describes the physical field, which as is known, has no place for NSE. So KGE is the basis of quantum field theory, but not relativistic quantum mechanics (RQM). Apparently, the basis of the RQM should be an equation similar to NSE, that is, it should be determined using a standard replacement not in the expression for square of energy, but in the expression for energy:

$$\varepsilon = \sqrt{m^2 + \mathbf{p}^2}.$$

Attempts are known [1, 2] to determine the square root of a differential operator by means of a pulse representation. However, such operators are pseudo-differential operators rather than differential operators. They're nonlocal. A local operator is a linear operator that transforms any function equal to zero on any interval into a function equal to zero on the same interval. The definition of the differential operator function leading to the local operator is proposed by one of the co-authors [3].

Let the analytic function $f(z)$ is holomorphic in some neighborhood of zero, has branching points, each of which is connected by a cut to an infinitely remote point, and the continuation of cuts beyond the branching points intersect at the origin, D — linear local differential operator (ordinary or partial derivatives), and $u(x)$ — a function, such that at Q are defined all its images $(D^n u)(x)$, moreover, the set of limit points of the sequence

$$\{\gamma_n(x_0)\} = \left\{ |(D^n u)(x_0)|^{1/n} \exp\left(i \frac{\varphi_n}{n}\right) \right\},$$

where $\varphi_n = \arg[(D^n u)(x_0)]$, is bounded and does not intersect with the set of cut points of the function $f(z)$ for all $x_0 \in Q$. Then the function $(f(D)u)(x)$ is defined on Q by analytic continuation of the function

$$(f(\alpha D)u)(x) = \sum_{n=0}^{\infty} \frac{f^{(n)}(0)}{n!} \alpha^n (D^n u)(x), \quad \forall x \in Q$$

by the real parameter α from $\alpha = 0$ to $\alpha = 1$. We assume $f(z) = \sqrt{m^2 + z^2}$ and $D = -i \nabla$. The corresponding equation has the form:

$$\left[i \frac{\partial}{\partial t} - \sqrt{m^2 - \nabla^2} \right] \Psi(t, \mathbf{r}) = 0.$$

In work [3] it is shown that this equation is relativistically invariant. It should be called the relativistic Schrodinger equation (RSE). It follows the continuity equation:

$$\begin{aligned} \frac{\partial}{\partial t} \rho(t, \mathbf{r}) &= \frac{\partial}{\partial t} \left[|\Psi(t, \mathbf{r})|^2 + \left| \frac{m}{\sqrt{m^2 - \nabla^2}} \Psi(t, \mathbf{r}) \right|^2 + \left| \frac{\nabla}{\sqrt{m^2 - \nabla^2}} \Psi(t, \mathbf{r}) \right|^2 \right] = \\ &= -\nabla \cdot \mathbf{j}(t, \mathbf{r}) = -i \nabla \cdot \left[\Psi^*(t, \mathbf{r}) \frac{\nabla}{\sqrt{m^2 - \nabla^2}} \Psi(t, \mathbf{r}) - \Psi(t, \mathbf{r}) \frac{\nabla}{\sqrt{m^2 - \nabla^2}} \Psi^*(t, \mathbf{r}) \right]. \end{aligned}$$

In the expression for the stream enters the speed operator

$$\mathbf{V} = -i \frac{\nabla}{\sqrt{m^2 - \nabla^2}} = i \left(\sqrt{m^2 - \nabla^2} \mathbf{r} - \mathbf{r} \sqrt{m^2 - \nabla^2} \right)$$

in full compliance with the principles of quantum mechanics. The analogy with NSE allowed in [3] to construct the theory of boundary value problems for stationary one-dimensional RSE. It is quite similar to the Sturm-Liouville theory.

Some physical problems, including S -states of a hydrogen-like pion atom, are solved with the help of this theory [4] (the use of KGE in the application to this problem leads to complex values of energy at the atomic number $Z > 68$) and the spectrum to which the RSE leads is real and bounded from below. For small Z , it is close to the spectrum of a similar problem for NSE [5]. It is also possible to construct a multiparticle RSE. The problems of reflection of a particle from an ideal mirror of finite mass [6] and elastic collision of two spinless electrically neutral particles [7] and some other problems have been solved. All solutions are accurate, without divergences.

Apparently, the RSE can be regarded as a basis of mathematically correct and physically plausible relativistic quantum mechanics.

References

- [1] C. Tzara. A study of relativistic Coulomb problem in momentum space. *Phys. Lett.* 1985, A111, p. 343-348.
- [2] W. Lucha, H. Rupprecht and F.F. Schoberl. Spinless Salpeter equation as a simple matrix eigenvalue problem. *Phys. Rev. D.* **45**. 1992, p. 1233.
- [3] V.M. Lagodinskiy. Holomorphic functions of differential operators and differential equations of infinite order. Thesis for the degree of candidate of physical and mathematical Sciences, SPb, pp. 110, 2005.
- [4] A.V. Golovin and V.M. Lagodinski, The Problem of the s -States of the pion atom in relativistic quantum mechanics without taking into account the strong interaction. *Vestnik SPbGU ser. 4, Physics, Chemistry*, iss. 2, p. 143, 2009.
- [5] L.D. Landau, E.M. Lifshits. *Quantum mechanics. Nonrelativistic theory.* M.: FIZMATLIT, 2001.
- [6] A.V. Golovin and V.M. Lagodinski, The problem of collision of an undisputed particle with an ideal mirror of finite mass in relativistic quantum mechanics without taking into account the strong interaction. *Vestnik SPbGU ser. 4, Physics, Chemistry*, iss. 4, pp. 3-14, 2012.
- [7] A.V. Golovin and V.M. Lagodinski, The problem of elastic collision of two spinless particles in relativistic quantum mechanics. *Vestnik SPbGU ser. 4, Physics, chemistry*, vol. 4 (62), pp. 249-263, 2017.

Normal forms for the model of optoelectronic oscillator with delay

E.V. Grigorieva^{1,a)}, S.A. Kaschenko^{2,b)}, D.V. Glazkov^{2,c)}

¹Belarus State Economic University, 220070, Partizanski av. 26, Minsk, Belarus

²Yaroslavl State University, 150000 Sovetskaya av. 14, Yaroslavl, Russia

In this paper we present the bifurcation analysis of the system

$$\begin{cases} \varepsilon \frac{dx}{d\zeta} = y - x + \beta [\cos^2(x(\zeta - \nu) + \phi) - \cos^2 \phi], \\ \frac{dy}{d\zeta} = -x, \end{cases} \quad (1)$$

with the phase space $C^1[-\nu, 0] \times R$. Our aim is to find the normal equations for the amplitudes of unstable modes in the case of $\varepsilon \rightarrow 0$ since typical experimental value is $\varepsilon \sim 10^{-6}$. It appears that these normal forms can serve as a justification for the space-time representation (STR) of the delayed dynamics, that was discussed firstly due to an intuitive interpretation of the delay as the size of one *quasispace* variable.

In the vicinity of the zero solution, the system (1) after the substitution $\zeta = \nu t$ is transformed into the second-order equation

$$\varepsilon \nu^{-1} \ddot{x} + \dot{x} + \nu x = b_1 \dot{x}(t-1) + b_2 \dot{x}^2(t-1) + b_3 \dot{x}^3(t-1) + \dots, \quad (2)$$

where $b_1 = -\beta \sin(2\phi)$, $b_2 = -\beta \cos(2\phi)$, $b_3 = (2/3) \beta \sin(2\phi)$. Stability of the zero state is determined by the roots of the characteristic equation

$$\varepsilon \nu^{-1} \lambda^2 + \lambda + \nu = b_1 \lambda e^{-\lambda}. \quad (3)$$

If $\varepsilon \rightarrow 0$ and $b_1 = b_0(1 + \varepsilon^{2\alpha} b_{10})$, where $|b_0| = 1$, then the characteristic equation (3) has infinitely many roots $\lambda_k(\varepsilon)$ ($k \in Z$) whose real parts tend to zero as $\varepsilon \rightarrow 0$. Two critical cases of infinite dimension arises in dependence on the value of α .

1) Let $\alpha = 1$. The solution $x(t)$ can be represented as a series

$$x = \varepsilon^{3/4} [\xi(\tau, r) \exp(i\Omega(\varepsilon)t) + c.c.] + \varepsilon^1 u_2(t, \tau, r) + \varepsilon^{7/4} u_3(t, \tau, r) + \dots,$$

where $\Omega(\varepsilon) = \nu \varepsilon^{-1/2} + \theta - 2\varepsilon \nu^{-1} + \varepsilon^{3/2} \theta \nu^{-2}$, the parameter $\theta = \theta(\varepsilon) \in [0, 2\pi)$ completes the value $\nu \varepsilon^{-1/2}$ up to an integer multiple of 2π (if $b_0 = 1$), or of π (if $b_0 = -1$). The complex functions $\xi(\tau, r)$, $u_j(t, \tau, r)$ are periodic in the argument $r = [1 - 2\varepsilon \nu^{-1} + 2\varepsilon^{3/2} \theta \nu^{-2} + O(\varepsilon^{5/2})]t$ with period 1, $\tau = \varepsilon^2 t$. For the function $\xi(\tau, r)$ we find the normal equation with periodic boundary conditions:

$$\begin{aligned} \frac{\partial \xi}{\partial \tau} &= \alpha_2 \frac{\partial^2 \xi}{\partial r^2} + \alpha_1 \frac{\partial \xi}{\partial r} + \alpha_0 \xi + d |\xi|^2 \xi, \\ \xi(\tau, r+1) &= \xi(\tau, r) \end{aligned} \quad (4)$$

where $\alpha_2 = -i/\nu^2$, $\alpha_1 = 2\theta/\nu^2$, $\alpha_0 = i\theta^2/\nu^2$, $d = \nu(-4b_2^2/3 - 3ib_3)$.

2) Let $1/2 < \alpha < 1$. Consider the solution of the system as series

$$x = \varepsilon^{\alpha-1/4} \left(\sum_{k=-\infty}^{\infty} \xi_k(\tau) \exp(\tilde{\lambda}_k(\varepsilon)t) + c.c. \right) + \varepsilon^{3\alpha-7/4} u_2 + \dots,$$

^{a)}Email: grigorieva@tut.by

^{b)}Email: kasch@uniyar.ac.ru

^{c)}Email: d.glazkov@uniyar.ac.ru

where $\tau = \varepsilon^{2\alpha} t$, $r = [\varepsilon^{\alpha-1} \omega (1 - \varepsilon \nu^{-1}) + \theta] t$. Here $\omega \neq 0$ is arbitrarily assigned real value, the parameter $\theta = \theta(\varepsilon) \in [0, 2\pi)$ completes the value $\omega \varepsilon^{\alpha-1}$ up to an integer multiple of 2π . For the function $\xi(\tau, r)$ we get the the normal equation with periodic boundary conditions:

$$\begin{aligned} \frac{\partial \xi}{\partial \tau} &= \nu^{-2} \omega^2 (i + 2\varepsilon^{1/2}) \frac{\partial^2 \xi}{\partial r^2} + \nu^{-3} \omega^3 \varepsilon^{\alpha-1/2} \frac{\partial^3 \xi}{\partial r^3} + b_{10} \xi + d F(\xi), \\ \xi(\tau, r+1) &= \xi(\tau, r). \end{aligned} \quad (5)$$

The obtained normal forms are non-linear boundary-value problems of parabolic type and, thus, STR can be justified. The parameter $\theta(\varepsilon)$ indicates the high sensitivity of their dynamic properties to the change of the small parameter ε : for $\varepsilon \rightarrow 0$ this value varies infinitely many times from 0 to 1 , and hence, the process of direct and inverse bifurcations is possible. Also, the normalized equations contain the continuum parameter ω that imply various steady-state solutions, i.e. multistability is possible.

Dynamical properties of one model with delay and large parameter

A.A. Kashchenko^{1,a)}

¹ *Yaroslavl State University*

We consider nonlocal dynamics of a model of two coupled oscillators with delayed feedback. This model has form of a system of two differential equations with delay. The feedback function is non-linear, compactly supported, smooth, and contains a large parameter. The coupling between oscillators is sufficiently small. We study behaviour of relaxation solutions of this model by a special analytical method of large parameter. For this purpose we construct a certain set in the phase space of original system. Then we build an asymptotics of solutions of the given system with initial conditions from this set. Using this asymptotics, a special mapping is constructed. Dynamics of this mapping describes dynamics of the original problem in general. As a result we prove that initial model has a two-parameter family of non-rough inhomogeneous relaxation periodic asymptotic (with respect to the residual) solutions.

^{a)} Email: sa-ahr@yandex.ru

Dynamics of spatially distributed delay logistic equation

I.S. Kashchenko^{1,a)}

¹ *Yaroslavl State University*

The local dynamics of spatially distributed delay logistic equation (Hutchinson equation) . In critical cases, which all have infinite dimension, systems of parabolic equations are built, which play the role of normal forms.

Hutchinson equation

$$\frac{dN}{dt} = r[1 - N(t - h)]N \quad (r, h > 0)$$

plays an especial role in modeling of mathematical ecology problems [1]). In the present work we will study more complex model for description of quantity $N = N(t, x)$, which depends also on spatial variable $x \in (-\infty, \infty)$:

$$\frac{\partial N}{\partial t} = r \left[1 - \int_{-\infty}^{\infty} F(s)N(t - h, x + s) ds \right] N + \delta^2 \frac{\partial^2 N}{\partial x^2}. \quad (1)$$

Here as above $r, h > 0$. We will consider that $N(t, x)$ is periodic in second variable, i.e. boundary conditions are met

$$N(t, x + 2\pi) \equiv N(t, x). \quad (2)$$

The aim of present work is to study system (1), (2) dynamics in the neighborhood of the equilibrium state. We will focus our attention below on two particular classes of kernel functions $F(s)$, each having a specified biological meaning. The first one (“one-peak”) is defined by formula

$$F(x) = \frac{\sigma}{\sqrt{\pi}} e^{-\sigma^2 x^2}, \quad (\sigma > 0). \quad (3)$$

For the second type (“three-peak”) we have

$$F(x) = \frac{\alpha\sigma_0}{\sqrt{\pi}} e^{-\sigma_0^2 x^2} + \frac{1 - \alpha}{2\sqrt{\pi}} \left(\sigma_1 e^{-\sigma_1^2 (x - \beta_1)^2} + \sigma_2 e^{-\sigma_2^2 (x - \beta_2)^2} \right). \quad (4)$$

Parameters satisfy next conditions: $0 < \alpha < 1$, $\sigma_0, \sigma_1, \sigma_2 > 0$, β_1 and β_2 are arbitrary. Note that in both cases the normalizing constants are chosen so that

$$\int_{-\infty}^{\infty} F(x) dx = 1.$$

Base assumption that allows us applying asymptotic methods to analyze the behavior of solutions of (1), (2) in a neighborhood of the state of equilibrium is as follows

$$\delta = \varepsilon d, \quad \sigma = \varepsilon^{-1} a, \quad \sigma_j = \varepsilon^{-1} a_j, \quad \beta_j = \mu b_j, \quad \text{where } 0 < \varepsilon, \mu \ll 1.$$

Therefore, we assume that the diffusion coefficient in (1) is a small parameter, and the values of $F(x)$ are small if x is not in the small neighborhood zero.

^{a)} Email: ikashchenko@yandex.ru

The method of research based is based on the special method of quasynormal forms [2]. The main idea of this method is to build special nonlinear equation, which dynamics describes behavior of initial equation's solutions in small neighbourhood of steady state.

Let, for example, $F(x)$ is defined by (3). If $rh < \pi/2$ then equilibrium $N = 1$ is stable and if $rh > \pi/2$ then it is unstable.

Let r_0 and h_0 be positive and such that $r_0h_0 = \frac{\pi}{2}$. Let us assume that

$$r = r_0 + \varepsilon^p r_1, \quad h = h_0 + \varepsilon^p h_1. \quad (5)$$

Consider for any $z > 0$ Ginzburg-Landau equation

$$\frac{\partial u}{\partial \tau} \left(1 + \frac{\pi}{2}i\right) = z^2 \left(d^2 + \frac{r_0}{4a^2}i\right) \frac{\partial^2 u}{\partial x^2} + \left(r_0 \frac{\pi h_1}{2h_0} + r_1 i\right)u + \frac{r_0(1-3i)}{5}u|u|^2, \quad (6)$$

$$u(\tau, x) \equiv u(\tau, x + 2\pi). \quad (7)$$

Let for some $z > 0$ $u(\tau, x)$ be a periodic solution of (6), (7). Then

$$N(t, x) = 1 + \varepsilon^{p/2} \left(u(\varepsilon^p t, y) \exp\left(i \frac{\pi}{2h_0} t\right) + \varepsilon \bar{u}(\varepsilon^p t, y) \exp\left(-i \frac{\pi}{2h_0} t\right) \right) + \varepsilon^p \left(\frac{2-i}{5} \exp\left(i \frac{\pi}{h_0} t\right) u^2(\varepsilon^p t, y) + \frac{2+i}{5} \exp\left(-i \frac{\pi}{h_0} t\right) \bar{u}^2(\varepsilon^p t, y) \right), \quad (8)$$

satisfy (1), (2) with residual $O(\varepsilon^{3p/2})$ uniformly by $t \geq 0$.

So, we have special nonlinear parabolic Ginzburg-Landau type equations (that does not contain asymptotically small or large parameters) to find the main terms of asymptotics of initial equation's solutions.

References

- [1] Leven S., Segel L. Patern generation in space and aspect, *SIAM Review* 27 (1985), 45–67.
- [2] Kashchenko I.S. Local dynamics of spatially distributed Hutchinson equation, *Communications in Nonlinear Science and Numerical Simulation*, 16 (2011). 3520-3524.

Supersonic waves of spin reversal in molecular magnets

A.R. Kasimov^{1,a)}

¹*Tamm Theory Department, Lebedev Physical Institute, Russian Academy of Sciences*

We investigate the dynamics of supersonic waves of spin reversal in molecular magnets in continuum framework that generalizes the steady-state model introduced in [1] to include unsteady effects. The theory is based on the reactive Euler equations with a non-ideal equation of state, wherein the reaction is that of exothermic spin reversal releasing the Zeeman energy of spin states in an external magnetic field. A forced Burgers equation is derived asymptotically that turns out to share much in common with both the nonlocal toy model in [2] and the asymptotic model in [3]. We discover that the solutions of the model in the form of traveling shock waves can become unstable when the magnet's initial temperature and the strength of the imposed external magnetic field are sufficiently low. Beyond the stability threshold, the wave dynamics is found to be either periodic or irregular.

This is a joint work with Luiz M. Faria and Rodolfo R. Rosales of MIT, USA.

References

[1] M. Modestov, V. Bychkov, and M. Marklund. Ultrafast spin avalanches in crystals of nanomagnets in terms of magnetic detonation. *Physical Review Letters*, 107(20):207208, 2011.

[2] A. R. Kasimov, L. M. Faria, and R. R. Rosales. Model for shock wave chaos. *Physical Review Letters*, 110(10):104104, 2013.

[3] L. M. Faria, A. R. Kasimov, and R. R. Rosales. Theory of weakly nonlinear self-sustained detonations. *J. Fluid Mech.*, 784, 163-198, 2015.

The replenishment method and new solvable cases of third-order nonlinear differential equations of Emden – Fowler type

Z.N. Khakimova^{1,a)}

¹*Military space Academy named A.F. Mozhaisky*

Using the method of replenishment and discrete transformation groups, a multiparameter class of ordinary differential equations of the third order with power nonlinearity is constructed. New third-order nonlinear differential equations of Emden–Fowler type are found.

^{a)}Email: aslankasimov@gmail.com

^{a)}Email: zilya-khakimova@mail.ru

1 Introduction

The main idea of the replenishment method lies in the fact that the investigated class of ordinary differential equations expands to a new wider class of equations on which some discrete transformations are closed.

Example 1. The class of generalized Emden–Fowler equations [1]

$$y''_{xx} = Ax^k y^l (y'_x)^m, \quad (1)$$

special cases of which are found in hydrodynamics, chemical technology and astrophysics, can be extended to a class of equations

$$y''_{xx} = Ax^k y^l (y'_x)^m (xy'_x - y)^n, \quad (2)$$

proceeding from the requirement of closure of a point transformation s : $x = \frac{1}{t}$, $y = \frac{u}{t}$.

It can be shown that the group of transformations of the dihedron D_6 (see below) is closed on the class (2). As a result it was possible to describe 400 solvable equations of the form (2) and 18 new solvable equations of the form (1) [2].

2 The class of third-order differential equations of the Emden–Fowler type and its extension

Let us consider a class of third-order nonlinear ordinary differential equations of the Emden–Fowler type

$$y'''_{xxx} = Ax^k y^l (y'_x)^m (y''_{xx})^p, \quad (3)$$

which is scarce in groups (still not found no transformations closed on the whole class of equations (3)). We note that special cases of the equation (3) take place in boundary layer theory and some partitions of physics.

Let us find an extension of the class of equations (3) so that the dihedral group is closed on this new class:

$$D_6 = \{E, h, h^2, h^3, h^4, h^5, r, hr, h^2r, h^3r, h^4r, h^5r\}, \quad (4)$$

where E is the identity transformation, and the generators r and h are defined as follows:

$$r: \quad x = u, \quad y = t; \quad h: \quad x = \frac{1}{u'_t}, \quad y = \frac{tu'_t - u}{u'_t} \quad (r^2 = h^6 = (hr)^2 = E).$$

The minimal expansion required is the 11-parameter class of equations

$$\prod_{i=1}^{11} z_i^{k_i} = B, \quad (5)$$

where $z_1 = x$, $z_2 = y$, $z_3 = y'_x$, $z_4 = xy'_x - y$, $z_5 = y''_{xx}$, $z_6 = y'''_{xxx}$, $z_7 = xy'''_{xxx} + 3y''_{xx}$, and z_8, z_9, z_{10}, z_{11} – polynomial homogeneous functions that depend on $x, y, y'_x, y''_{xx}, y'''_{xxx}$ (in view of their cumbersomeness these functions are omitted). The constants B and k_i in (5) can change.

The equations class (5) in an implicit form is convenient because it contains not only (3) (for $k_4 = k_7 = k_8 = k_9 = k_{10} = k_{11} = 0$, $k_6 = -1$) but also equations (1) and (2).

3 Solvable cases of third-order equations. Examples

The method described in Section 2 made it possible to find several hundred new solvable third-order differential equations with power right-hand side that are absent in [1].

For $k = 0$ or $l = 0$ the class of equations (3) is reduced to (1) [1]. Using the transformations of the group D_6 (4) the class of equations (3) is reduced to 11 other four-parameter classes of equations with power right-hand side.

In particular, we have

$$y'''_{xxx} = Ax^k y^l (y'_x)^m (y''_{xx})^p \xrightarrow{r} y'_x y'''_{xxx} - 3(y''_{xx})^2 = Bx^l y^k (y'_x)^{5-m-3p} (y''_{xx})^p,$$

$$y'''_{xxx} = Ax^k y^l (y'_x)^m (y''_{xx})^p \xrightarrow{s=h^2 r} xy'''_{xxx} + 3y''_{xx} = Bx^{-k-l+3p-4m} y^l (xy'_x - y)^m (y''_{xx})^p.$$

Thus integrable cases of the class of equations (3) induce solvable equations in these 11 classes.

In addition, for $k, l \neq 0$ there are several integrable cases in the class (3) [1]. They as well generate solvable third-order equations in the class (5).

Example 2. The general solution of the equation $y'''_{xxx} = Ax^{-\frac{3}{2}} y^{-\frac{1}{2}}$ is expressed in terms of the second Painlevé transcendent [1]. So the general solution of the appropriate equation $xy'''_{xxx} + 3y''_{xx} = Ax^{-6} y^{-\frac{1}{2}}$ as well is expressed in terms of the Painlevé transcendent.

Example 3. The equation $xy'''_{xxx} + 3y''_{xx} = A(xy)^l$ is integrable for $l = -\frac{7}{2}, -\frac{5}{2}, -2, -\frac{4}{3}, -\frac{5}{4}, -\frac{7}{6}, -\frac{1}{2}, 0, 1$ [1]. Therefore appropriate equation $y'''_{xxx} = Ax^{-2l} y^l$ is solvable at the same values l .

References

- [1] Polyanin A. D., Zaitsev V. F. Handbook of Ordinary Differential Equations: Exact Solutions, Methods, and Problems. CRC Press, Boca Raton–London, 2018.
- [2] Khakimova Z. N. The choice of the class of differential equations for finding new solvable cases // Some actual problems of modern mathematics and mathematical education, 2017. Pp. 112–117.

Mathematical modeling of free convection problems in a gravity field in OpenFOAM

V.K. Kozlov^{1,a)}, M.A. Chmykhov^{1,b)}

¹*National Research Nuclear University MEPhI (Moscow Engineering Physics Institute)*

A mathematical model of natural convection in the gravity field, using Boussinesq approximation, has been presented. This model contains the continuity equation, where density variations are ignored, the Navier-Stokes equation and the equation for heat flow. Rayleigh-Benard-convection in a rectangular box, with different types

^{a)}Email: viktorkozlovkonst@gmail.com

^{b)}Email: MAChmykhov@mephi.ru

of border conditions, has been investigated. The equations solved numerically by an original solver with the use of object-oriented programming language OpenFOAM. Solver is based on PISO(Pressure-Implicit with Splitting of Operators) algorithm and finite volume method.

The Prandtl number, Grashof number and Rayleigh number has been examined. Rayleigh-Benard-convection between parallel planes of different temperatures, steady convection in horizontal fluid layer and natural convection flow in a square box, enclosed by non-isothermal wall has been used for solver verification. Results has been visualized with the use of open source application ParaView.

A mathematical model of natural convection in the gravity field is determined by the continuity equation, where density variations are ignored, the Navier-Stokes equation and the equation for heat flow. In the Boussinesq approximation they have the following form [1].

$$\begin{cases} \operatorname{div} \vec{U} = 0, \\ \rho \left(\frac{\partial \vec{U}}{\partial t} + (\vec{U} \nabla) \vec{U} \right) - \nu \Delta \vec{U} = -\nabla p + g[\beta(T - T_0)], \\ \frac{\partial T}{\partial t} + \vec{U} \nabla T - \alpha \Delta T = 0, \end{cases} \quad (1)$$

where β – coefficient of thermal expansion of fluid, T_0 – temperature, α – the thermal diffusivity, ν – effective kinematic viscosity, ρ – the density of the fluid.

This equations solved numerically by an original solver with the use of object-oriented programming language OpenFOAM. To solve Navier-Stokes equation, PISO(Pressure-Implicit with Splitting of Operators) algorithm has been used [2]. It splits the operators into an implicit predictor and multiple explicit corrector steps, without iterations.

Analytical solution of steady free convection in an infinite vertical fluid layer between parallel planes of different temperatures, has already been investigated[1]. It was used in comparison with

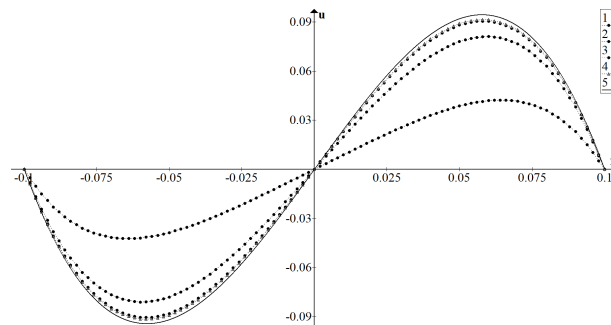


Fig. 1: Comparison between numerical and exact solution, where 1 – numerical solution for $h/l = 1$, 2 – $h/l = 2$, 3 – $h/l = 4$, 4 – $h/l = 8$, 5 – exact solution and $l = 0,2$ m.

numerical solution for solver verification. Test case considered a rectangular enclosure of height h and length l , with different ratio ($\frac{h}{l} = 1; 2; 4; 8$). Results confirmed the validity of the solver as shown in Fig. 1.

As for horizontal fluid layer, the onset of steady convection has been calculated. It was determined by critical value of Rayleigh number. The Rayleigh number is defined as the product of the Grashof number and the Prandtl number. When the Rayleigh number is below a critical value, heat transfer is primarily in the form of conduction, when it exceeds the critical value, heat transfer is primarily in the form of convection. Was established, that critical value of Rayleigh number belongs to the range of values between 1949 and 1952 (theoretical value 1708, experimental value Oertel[3] 1820).

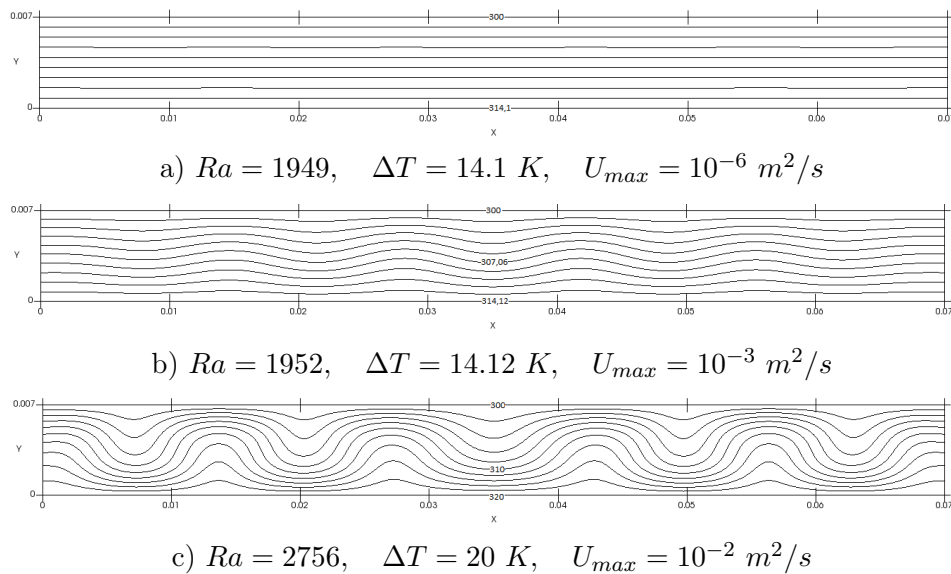


Fig. 2: Horizontal fluid layer, top wall cooler then the bottom one. Rayleigh number Ra , temperature difference ΔT and maximum speed U_{max} specified under the pictures.

A square enclosure with inhomogeneous boundary conditions has been considered. For the case of flow in a non-porous medium without heat generation the solutions are in agreement with [4].

The processes of natural convection in the field of gravity in the Boussinesq approximation has been examined. A mathematical model and numerical simulation has been made. Original solver and test cases were implemented using OpenFOAM. Simulation results for solver verification has been presented.

This work was supported by the Ministry of Education and Science of the Russian Federation (base part of state task, project no. 1.9746.2017/BCh).

References

- [1] Gershuni G.Z., Zhukhovitskii E.M. *Convective Stability of Incompressible Fluids*. Published by I.P.S.T. (1976) ISBN: 0706515625
- [2] R.I.Issa Solution of the implicitly discretised fluid flow equations by operator-splitting. *Journal of Computational Physics* (ISSN 0021-9991), vol. 62, Jan. 1986, p. 40-65.
- [3] Buhler K., Kirchartz K.R., Oertel H. Steady convection in a horizontal fluid layer *Acta Mechanica* (1979) 31: 155
- [4] Hossain M.A., Wilson M., Natural convection flow in a fluid-saturated porous medium enclosed by non-isothermal walls with heat generation. *International Journal of Thermal Sciences*. 41 (2002) pp. 447–454

On the connection between the mKdV-sinh-Gordon hierarchy and the generalized hierarchy of the second Painleve equation

N.A. Kudryashov¹, A.A. Kutukov^{1,a)}

¹*National Research Nuclear University MEPhI (Moscow Engineering Physics Institute)*

The fourth-order equation for the description of dislocations in a crystal lattice is considered. The generalization of this equation is the hierarchy of mKdV-sinh-Gordon equations. We consider the Lax pair for this hierarchy and discuss the connection between the hierarchy and the generalized hierarchy of the second Painleve equation.

1 Introduction

Let us consider the fourth-order nonlinear differential equation [1]

$$u_{xt} + \alpha u_x u_{xx} + 3\beta u_x^2 u_{xx} + \gamma u_{xxxx} = \delta \sin u \quad (1)$$

Equation (1) is a generalization of the mKdV equation and the sinh-Gordon equation. It was first presented in [1] to describe the chain of nonlinearly interacting masses. In addition, equation (1) describes dislocations in the crystal lattice [2], physical models for describing light pulses [3], etc. In [2] the analytical properties of equation (1) are investigated, in particular, the Painleve test was applied, and traveling wave solutions are found. Equation (1) for $\alpha = 0, \gamma = 2\beta$ is generalized by the mKdV-sinh-Gordon hierarchy [4]

$$u_{xt} + 2\beta(t) \frac{\partial}{\partial x} \left(u_x - i \frac{\partial}{\partial x} \right) L_n \left[\frac{i u_{xx}}{2} + \frac{u_x^2}{4} \right] + \gamma e^u + \delta e^{-u} = 0 \quad (2)$$

where $L_n[w]$ is the Lenard operator, which is given in [4]. Higher-order equations of this hierarchy describes mathematical models for various physical phenomena more exactly.

2 The Lax pair for the mKdV-sinh-Gordon hierarchy

The algorithm for obtaining Lax pairs by means of the AKNS scheme [5] for the mKdV equation and for the sine-Gordon equation is given in [6]. By combining these calculations, we obtain the Lax pair for the hierarchy (2). Consider the system of equations

$$\psi_x = \hat{P}\psi, \quad \psi_t = \hat{Q}\psi. \quad (3)$$

where $\psi = \begin{pmatrix} \psi_1 \\ \psi_2 \end{pmatrix}$, $\hat{P} = \begin{pmatrix} -i\lambda & -\frac{1}{2}u_x \\ \frac{1}{2}u_x & i\lambda \end{pmatrix}$, $\hat{Q} = \begin{pmatrix} A & B \\ C & -A \end{pmatrix}$ and $A = A(x, t, \lambda)$, $B = B(x, t, \lambda)$, $C = C(x, t, \lambda)$, $u = u(x, t)$. We look for A , B и C in the form

$$A = \sum_{k=0}^{2n+2} \lambda^{2n-k+1} a_k(x, t), \quad B = \sum_{k=1}^{2n+2} \lambda^{2n-k+1} b_k(x, t), \quad C = \sum_{k=1}^{2n+2} \lambda^{2n-k+1} c_k(x, t). \quad (4)$$

^{a)}Email: alexkutuk@gmail.com

From the condition of compatibility $(\psi_x)_t = (\psi_t)_x$ follows equations the sequentially solution of which leads to the following expressions

$$\begin{aligned} a_{2n+2} &= -\frac{i}{4}\gamma e^u + \frac{i}{4}\delta e^{-u}, \quad b_{2n+2} = c_{2n+2} = -\frac{i}{4}\gamma e^u - \frac{i}{4}\delta e^{-u}, \quad a_0 = -(2i)^{2n+1} \beta(t), \\ b_{2l} &= c_{2l} = (2i)^{2n-2l+1} 2\beta(t) \frac{\partial}{\partial x} \left(u_x - i \frac{\partial}{\partial x} \right) L_{l-1} \left[\frac{i u_{xx}}{2} + \frac{u_x^2}{4} \right], \quad l = 1, 2, \dots, n \\ b_{2l+1} &= -c_{2l+1} = (2i)^{2n-2l} 2\beta(t) \left(u_x - i \frac{\partial}{\partial x} \right) L_l \left[\frac{i u_{xx}}{2} + \frac{u_x^2}{4} \right], \quad l = 0, 1, \dots, n \\ a_{2l,x} &= -b_{2l} u_x, \quad l = 1, 2, \dots, n; \quad a_{2l+1} = 0, \quad l = 0, 1, \dots, n \end{aligned} \quad (5)$$

Two equations of this AKNS hierarchy give the mKdV-sinh-Gordon hierarchy (2). The solution of the Cauchy problem for the fourth-order equation from the hierarchy (2) by means of the inverse scattering problem is shown in [4].

3 The connection between the hierarchy (2) and the generalized hierarchy of the second Painlevé equation

Among the second-order differential equations, there are six equations, the solution of which is expressed in terms of special functions called Painlevé transcendent. At present, there is a problem of finding differential equations of high order that are analogues of the Painleve equations and defining new transcendents [8, 9]. The hierarchy of equations representing a generalization of the second and third Painleve equations is given in [7]

$$\frac{d}{dz} (z y_z) + 2\varepsilon \frac{d}{dz} \left(y_z + \frac{d}{dz} \right) L_n \left[\frac{y_{zz}}{2} - \frac{y_z^2}{4} \right] + \gamma e^y + \delta e^{-y} = 0. \quad (6)$$

Let in hierarchy (2) $\beta(t) = \frac{\varepsilon i}{t^{2n+2}}$, then after changing the variables $u(x, t) = y(z)$, $z = xt$, we get hierarchy (6). Therefore, hierarchy (2) is of great interest for study, since it allows to describe physical phenomena, and also probably has solutions in the form of new transcendents with a certain choice of parameters in equation.

4 Conclusion

The AKNS scheme is presented for obtaining the Lax pair for the mKdV-sinh-Gordon hierarchy. The connection between the mKdV-sinh-Gordon hierarchy and the generalized hierarchy of the second Painleve equation is shown.

This work is supported by the Russian Science Foundation under grant 18-11-00209 and by the Ministry of Education and Science of the Russian Federation (base part of state task, project no. 1.9746.2017/BCh)

References

- [1] Konno K., Kameyama W., Sanuki H. Effect of weak dislocation potential on nonlinear wave propagation in anharmonic cristal. *J. Phys. Soc. Japan*, 1974, vol. 37, pp. 171–176.
- [2] Kudryashov N.A. Analytical properties of nonlinear dislocation equation. *Applied Mathematics Letters*, 2017, vol. 69, pp. 29–34.
- [3] Leblond H., Mihalache D. Few-optical-cycle solitons: modified Kortevæg–de Vries sine–Gordon equation versus other non-slowly-varying-envelope approximation models *Phys. Rev. A.*, 2009, vol. 79, p. 063835

- [4] Kudryashov N.A. Integrable model of nonlinear dislocations. *ArXiv Preprint*, 2016, arXiv:1611.06813
- [5] Ablowitz M. J., Kaup, D. J., Newell, A. C., Segur, H. The Inverse Scattering Transform-Fourier Analysis for Nonlinear Problems. *Studies in Applied Mathematics*, 1974, vol. 53(4), pp. 249–315.
- [6] Kudryashov N.A. Analiticheskaya teoriya nelineinykh differentsial'nykh uravnenii (Analytical Theory of Nonlinear Differential Equations) *Moscow-Izhevsk: RCD*, 2004, 2nd ed.
- [7] Kudryashov N.A. One generalization of the second Painleve hierarchy. *J. Phys. A: Math. Gen.*, 2002, vol. 35, pp. 93–99.
- [8] Kudryashov N.A. Transcendents defined by nonlinear fourth-order ordinary differential equations. *J. Phys. A: Math. Gen.*, 1999, vol. 32(6), pp. 999–1013.
- [9] Kudryashov N.A. Fourth-order analogies to the painleve equations. *J. Phys. A: Math. Gen.*, 2002, vol. 35(21), pp. 4617–4632.

Statistical features of plastic flow localization in dipolar materials

N.A. Kudryashov¹, R.V. Muratov¹, P.N. Ryabov^{1,a)}

¹*National Research Nuclear University MEPhI*

We consider the processes of plastic flow localization in dipolar materials undergoing high speed shear deformations. The mathematical model of the processes of plastic flow localization is formulated taking into account dipolar effect. We introduce the new numerical algorithm and perform the series of numerical tests to show the accuracy and efficiency of the proposed algorithm. We show that dipolar effect changes average characteristics of the processes considered as average temperature, stress and etc. Moreover this effect leads to increase in initiation time, changes the widths of localization zones and distances between them. We obtain the statistical distributions of the width and distance for different strength of dipolar effect.

1 Mathematical formulation of the problem considered

We consider the infinite slab of incompressible thermoviscoplastic material undergoing to simple shear deformation at the initial strain rate $\dot{\epsilon}_0$. The direction of shear coincides with x -axis. Slab occupies the region $0 \leq y \leq H$. The lower boundary of the slab is fixed the upper boundary is moving at the constant velocity $v_{up} = H\dot{\epsilon}_0$. Also we take into account the dipolar effect and effect of strain hardening of material. So, the mathematical model of the process of slab deformation in the above mentioned suggestions can be expressed by the following system of nonlinear equations [1]

$$v_t = \frac{1}{\rho} (s - \sigma_y)_y, \tag{1}$$

^{a)}Email: pnryabov@mephi.ru

$$s_t = \mu (v_y - \dot{\varepsilon}), \quad (2)$$

$$\sigma_t = l\mu \left(v_{yy} - \frac{1}{l} \dot{d} \right), \quad (3)$$

$$\psi_t = \frac{s_e \dot{\varepsilon}_e}{\kappa(\psi)}, \quad (4)$$

$$C\rho T_t = (kT_y)_y + s_e \dot{\varepsilon}_e, \quad (5)$$

where $s(y, t), \sigma(y, t)$ are polar and dipolar stress respectively, $v(y, t)$ is the velocity, $T(y, t)$ is a temperature, $\dot{\varepsilon}^p(y, t)$ is the plastic strain rate, $\psi(y, t)$ is a strain hardening variable, $d(y, t)$ is a dipolar strain, l is a characteristic length of material, ρ is a mass density. We use the following notations in (1) – (5)

$$s_e = \sqrt{s^2 + \sigma^2}, \quad \dot{\varepsilon}_e = \sqrt{\dot{\varepsilon}^2 + \dot{d}^2}, \quad \varepsilon_e = \int_0^t \dot{\varepsilon}_e(\tau) d\tau, \quad (6)$$

Effective variables listed in (6) are connected by the plastic flow law $D(s_e, \psi, T) \geq 0$. We have the following relations between variables

$$\dot{\varepsilon} = \frac{s}{s_e} \dot{\varepsilon}_e, \quad \dot{d} = \frac{\sigma}{s_e} \dot{\varepsilon}_e, \quad \dot{\varepsilon}_e = D(s_e, \psi, T). \quad (7)$$

So, closing the system of equations (1) – (7) by boundary and initial conditions we obtain the mathematical model of the problem considered.

2 Results of the direct numerical simulation of the problem

Here we study the statistical properties of the process of plastic flow localization in two materials deformed at $\dot{\varepsilon}_0 = 10^5 \text{ s}^{-1}$. One of them is low alloy steel HY-100 and another one is oxygen free high thermal conductivity (OFHC) copper. To generate the localization processes we use the inhomogeneity in initial stress distribution [2, 3]. Also we suppose that plastic flow obeys the Litonski's flow law.

First we explore the behavior of the average characteristics of the problem considered such as average temperature and average stress. It is shown that we time the value of average temperature tends to a constant which increases with an increase of parameter l . For example in the case of HY-100 steel the value of $T_{\text{avg}} \sim 320 \text{ }^\circ\text{C}$ at $l = 0$ and $T_{\text{avg}} \sim 620 \text{ }^\circ\text{C}$ when $l = 10$. From the obtained dependencies we see that dipolar effect also changes the localization time. This time could be defined at the moment when the abrupt decrease of average stress is observed. So, at that moment $\varepsilon_{\text{nom}} = 0.6, 1.1, 1.3$ for HY-100 steel and $\varepsilon_{\text{nom}} = 4, 6, 7.6$ for OFHC copper at $l = 0, 5, 10$ respectively, where $\varepsilon_{\text{nom}} = t\dot{\varepsilon}_0$.

Since we consider the collective behavior of plastic flow localization the statistical distributions of the width and distance between localization areas were obtained. We use the Parzen–Rosenblatt window method with the Gaussian kernel to obtain the probability density function. We show that an increase of value of l leads to the appearance of several modes in the obtained distributions. The corresponding numerical estimates in that case were obtained. The dipolar effect influence on the width w of each localization zone and distance L between them. To understand the dependence of parameters w and L from parameter l we rolled up the distributions corresponding to $l = 0, 5, 10 \text{ } \mu\text{m}$ in a so-called box-plots. In Fig. 1 we illustrate the box-plot for HY-100 steel. From Fig. 1 we see that the value of w linearly increases with an increase in l . We observe the following effect for both materials. In turn, in the case of HY-100 steel the value of the L increases for small values of l but after a while tends to constant. However, for OFHC copper, this parameter does not significantly change.

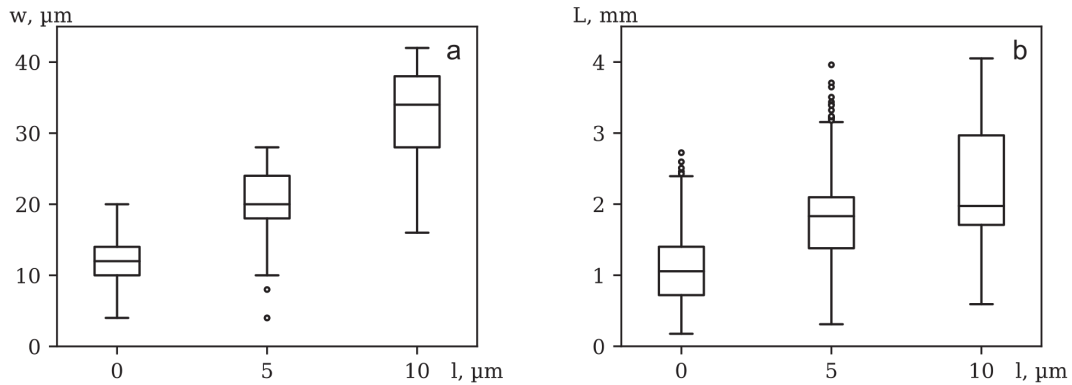


Fig. 1: Distributions of widths (a) and distances (b) for dipolar and nonpolar HY-100 steel.

Acknowledgment

This work was supported by the Grant for support of young Russian scientists MK-6044.2018.1 and by the Grant of Russian Science Foundation 18-11-00209.

References

- [1] R.C. Batra, C.H. Kim, The interaction among adiabatic shear bands in simple and dipolar materials, *Int. J. Engng. Sci.* 28:9 (1990) 927–942.
- [2] N.A. Kudryashov, P.N. Ryabov, A.S. Zakharchenko, Self-organization of adiabatic shear bands in OFHC copper and HY-100 steel, *J. Mech. Phys. Solids* 76 (2015) 180–192.
- [3] P.N. Ryabov, N.A. Kudryashov, R.V. Muratov, Adiabatic shear bands localization in materials undergoing deformations. *J. Phys.: Conf. Ser.* 788 (2017) 012031.

On shear strain localization in composites

N.A. Kudryashov¹, R.V. Muratov¹, P.N. Ryabov^{1,a)}

¹*National Research Nuclear University MEPHI*

The process of shear strain localization in composite materials undergoing high speed deformations is considered. The mathematical model of the shear strain localization is proposed. Numerical algorithm that allows one to investigate the process of shear strain localization from initial to final stage is proposed. The influence of initial strain rate on the process of shear strain localization is studied. Also the influence of the components height of the composite on the localization process is explored.

^{a)}Email: pnryabov@mephi.ru

1 Statement of the problem and numerical algorithm

We consider the simple shearing of the infinite specimen which consists of two thermoviscoplastic blocks. The height of the first block is equal to y_1 and the height of the second one is equal to y_2 . The specimen occupies the region between two planes $0 < y < H$, where $y = y_1 + y_2$. The lower plane is fixed and the upper plane is moving under the constant velocity along the x axis. In such suggestions the mathematical model of the problem considered has the following form

$$\rho v_t = \tau_y, \quad (1)$$

$$\tau_t - \mu v_y = -\mu \dot{\varepsilon}^p, \quad (2)$$

$$\tau = \kappa_0 g(T) \left(1 + \left(\frac{\psi}{\psi_0} \right)^n \right) \left(1 + \frac{\dot{\varepsilon}^p}{\dot{\varepsilon}_y} \right)^m \quad (3)$$

$$\psi_t = \frac{\tau \dot{\varepsilon}^p}{\kappa(\psi)}, \quad (4)$$

$$C \rho T_t = (k T_y)_y + \beta \tau \dot{\varepsilon}^p, \quad (5)$$

where τ is a stress, v is a velocity, T is a temperature, ψ is a strain hardening variable, ρ, k, C, μ are the density, thermal conductivity, specific heat, shear module respectively, $g(T)$ is a thermal softening function. We note that parameters ρ, k, C, μ are functions of spatial variable y and the explicit form of function $g(T)$ depends on the materials are used.

Initially the specimen is free of strain, with the strain rate equal to $\dot{\varepsilon}_0$. Initial distribution of the velocity has the linear form $v(y, 0) = y \dot{\varepsilon}_0$. All other initial conditions are equal to zero. We use zero boundary conditions for problem considered.

The proposed mathematical model was solved numerically. We solve the system (1)-(3) with the help of the Courant-Isaacson-Rees scheme with the Newton linearization method. The Cauchy problem for equation (4) was solved using the Runge-Kutta method and mixed boundary value problem for the heat equation (5) was solved using the implicit numerical scheme. The accuracy of the proposed algorithm was shown.

2 Results of mathematical modeling

Here we consider the composite specimen which consists of steel and copper parts. Let us define as a y_1 the height of the steel part of the specimen and y_2 the height of the copper part.

Numerical experiments show that plastic strain localizes in a copper part of the specimen. This fact does not depend of the magnitude of the $\dot{\varepsilon}_0$. However the value of initial strain rate $\dot{\varepsilon}_0$ influence on the number of localization zones formed in the copper part of the composite. Numerical experiments showed that there is a characteristic depth, the value of which is inversely proportional to the initial strain rate, on which the plastic flow localizes. We show that for relatively small values of $\dot{\varepsilon}_0 < 2 \cdot 10^4 \text{ s}^{-1}$ we observe the formation of one localization zone in the copper part of the specimen. This zone can be localized in the center, left or right boundary of copper block. However if the value of $\dot{\varepsilon}_0 \sim 10^5 \text{ s}^{-1}$ the multiple zones of shear strain localization could occur.

To answer the question about where the plastic strain localizes in the case when $500 \text{ s}^{-1} < \dot{\varepsilon}_0 < 2 \cdot 10^4 \text{ s}^{-1}$ we plot the map of the areas of localization. This map is illustrated in Fig. 1.

Acknowledgment

This work was supported by the Grant for support of young Russian scientists MK-6044.2018.1.

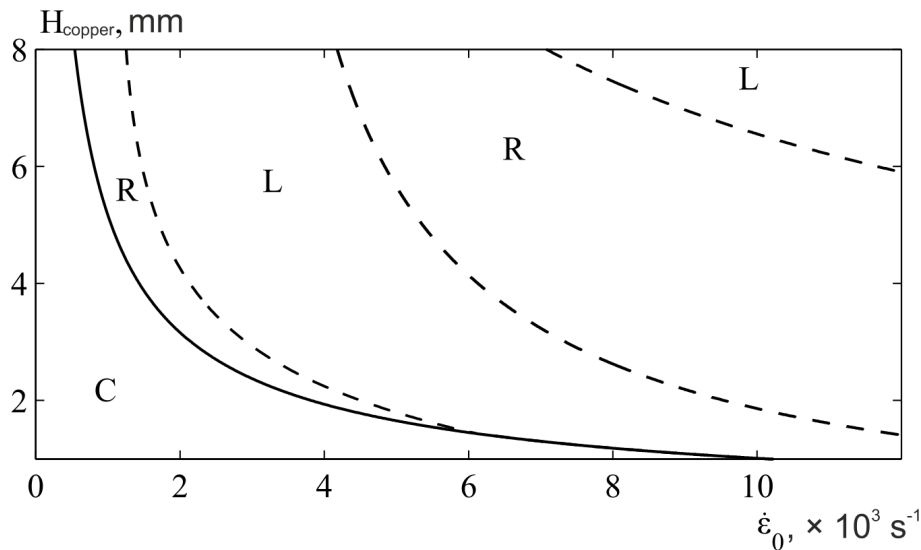


Fig. 1: The map of the areas of localization. C - shear strain localization zone based in the center of the copper block, L and R- shear strain localization zone based on the left and right boundaries respectively. The height of the steel part is equal to 2 mm

Hidden Attractors in Fundamental Problems and Applied Models

N.V. Kuznetsov^{1,2,a)}, T.N. Mokaev^{1,b)}

¹*Saint-Petersburg State University, Russia*

²*University of Jyväskylä, Finland*

The lecture is devoted to recent results on self-excited and hidden attractors in dynamical systems. The classification of attractors as being *hidden* either *self-excited* was proposed in 2009 and combined the notions of a transient process (engineering), a visualization (numerical analysis), and basins of attraction and stability (dynamical systems). An attractor is called a *self-excited attractor* if its basin of attraction intersects with any vicinity of an equilibrium, otherwise it is called a *hidden attractor* [1, 2, 3, 4, 5]. For example, hidden attractors are attractors in systems with no equilibria or with only one stable equilibrium (a special case of multistability and coexistence of attractors). While coexisting self-excited attractors can be found using the standard computational procedure, there is no standard way of prediction the existence or coexistence of hidden attractors in a system.

While many classical attractors, e.g. Lorenz and Hénon attractors, are self-excited and were localized numerically by trajectories from the unstable equilibria, there are a number of physical dynamical systems which possess hidden chaotic attractors, namely, the Rabinovich system (describes the interaction of plasma waves) the Glukhovskiy-Dolghansky system (describes convective fluid motion in a rotating cavity) and others.

The concept of hidden attractor arises in a number of fundamental problems [2]. One of the first well-known problems of analyzing hidden periodic oscillations is

^{a)}Email: nkunetsov239@gmail.com

^{b)}Email: t.mokaev@spbu.ru

connected with the second part of Hilbert's 16th problem on the number and mutual disposition of limit cycles in two-dimensional polynomial systems. Later, in the 1950s and 1960s, the study of the well-known Aizerman's and Kalman's conjectures on absolute stability led to the discovery of the possible coexistence of a hidden periodic oscillation and a unique stable stationary point in automatic control systems.

Hidden oscillations and hidden attractors also appear in various applied models: phase-locked loops (PLL), electromechanical models with the Sommerfeld effect, drilling systems, aircrafts control systems, and others.

References

- [1] V. Bragin, V. Vagitsev, N. Kuznetsov, G. Leonov, Algorithms for finding hidden oscillations in nonlinear systems. The Aizerman and Kalman conjectures and Chua's circuits, *Journal of Computer and Systems Sciences International* 50 (4) (2011) 511–543. doi:10.1134/S106423071104006X.
- [2] G. Leonov, N. Kuznetsov, Hidden attractors in dynamical systems. From hidden oscillations in Hilbert-Kolmogorov, Aizerman, and Kalman problems to hidden chaotic attractors in Chua circuits, *International Journal of Bifurcation and Chaos* 23 (1), art. no. 1330002. doi:10.1142/S0218127413300024.
- [3] G. Leonov, N. Kuznetsov, T. Mokaev, Homoclinic orbits, and self-excited and hidden attractors in a Lorenz-like system describing convective fluid motion, *Eur. Phys. J. Special Topics* 224 (8) (2015) 1421–1458. doi:10.1140/epjst/e2015-02470-3.
- [4] N. Kuznetsov, G. Leonov, T. Mokaev, A. Prasad, M. Shrimali, Finite-time Lyapunov dimension and hidden attractor of the Rabinovich system, *Nonlinear Dynamics* 92 (2) (2018) 267–285. doi:10.1007/s11071-018-4054-z.
- [5] D. Dudkowski, S. Jafari, T. Kapitaniak, N. Kuznetsov, G. Leonov, A. Prasad, Hidden attractors in dynamical systems, *Physics Reports* 637 (2016) 1–50. doi:10.1016/j.physrep.2016.05.002.

Analytical properties and numerical modelling of the coupled FitzHugh-Nagumo equations

S.F. Lavrova^{1,a)}, N.A. Kudryashov^{1,b)}, D.I. Sinelshchikov^{1,c)}

¹*National Research Nuclear University MEPhI*

Fitzhugh-Nagumo model describing propagation of impulses between neurons is considered. We analyze a pair of electrically coupled FitzHugh-Nagumo neurons. It is shown that the system of equations describing this model doesn't pass the Painleve test. The stability of system's stationary points is analyzed. Dynamics of non-stationary solutions is studied.

^{a)}Email: infuriatedot@gmail.com

^{b)}Email: nakudryashov@mephi.ru

^{c)}Email: disinelshchikov@mephi.ru

The FitzHugh-Nagumo model is used to describe propagation of impulses between neurons [1, 2]. In this work we consider a model of two FitzHugh-Nagumo neurons coupled via the flow of ions through the gap junctions between them [3]. The equations for this model are

$$\begin{aligned}\frac{dv_1}{dt} &= v_1(v_1 - a)(1 - v_1) - R_1 + g(v_1 - v_2), \\ \frac{dR_1}{dt} &= \epsilon(v_1 - \beta R_1), \\ \frac{dv_2}{dt} &= v_2(v_2 - a)(1 - v_2) - R_2 + g(v_2 - v_1), \\ \frac{dR_2}{dt} &= \epsilon(v_2 - \beta R_2),\end{aligned}\tag{1}$$

where (v_1, R_1) and (v_2, R_2) represent membrane potentials and recovery variables of the coupled neurons, a, β and ϵ are constant positive parameters and g describes the coupling strength.

We obtain that the system of equations (1) doesn't pass the Painleve test because one of the Fuchs indices is not integer. It means that the considered system of equations doesn't have any meromorphic solutions. After applying the third step of the Painleve test to (1) we find out that there exist an expansion of the general solution in the Puiseux series with two arbitrary constants.

Then, we study the stability of system's stationary points $O = (0, 0, 0, 0)$. We find that for some parameter regions rest state O is not stable.

Finally, we plot bifurcational diagrams and compute Lyapunov exponents for the studied system to see that considered non-stationary solutions are stable limit cycles.

References

- [1] FitzHugh, R. (1961). Impulses and physiological states in theoretical models of nerve membrane. *Biophysical journal*, 1(6), 445-466.
- [2] Fitzhugh, R. (1965). A kinetic model of the conductance changes in nerve membrane. *Journal of Cellular Physiology*, 66(S2), 111-117.
- [3] Skinner, F. K., Zhang, L., Velazquez, J. P., & Carlen, P. L. (1999). Bursting in inhibitory interneuronal networks: a role for gap-junctional coupling. *Journal of neurophysiology*, 81(3), 1274-1283.

Semiclassical asymptotics of the solution of the Helmholtz equation in a three-dimensional layer of variable thickness with a localized right-hand side

P.N. Petrov^{1,2,a)}, S.Y. Dobrokhotov^{1,2,b)}

¹*Moscow Institute of Physics and Technology (State University), 9 Institutskiy per., Dolgoprudny, Moscow Region, 141701, Russian Federation*

²*Ishlinsky Institute for Problems in Mechanics of the Russian Academy of Sciences, Prospekt Vernadskogo 101-1, Moscow, 119526, Russia*

^{a)}Email: petr.petrov@phystech.edu

^{b)}Email: dobr@ipmnet.ru

We construct the semiclassical asymptotics of the solution of the Helmholtz equation in a three-dimensional layer of variable thickness with a localized right-hand side.

$$(h^2\Delta + n^2(x, y))u = F\left(\frac{x - \xi_1}{\mu}, \frac{y - \xi_2}{\mu}\right)g\left(\frac{z - z_0}{\mu}\right),$$
$$u|_{z=hd_1(x,y)} = 0, \quad u|_{z=hd_2(x,y)} = 0.$$

Here coefficient a $n^2(x, y)$, and functions $d_1(x, y)$, $d_2(x, y)$, $F(x, y)$, $g(z)$ are smooth functions of their arguments. Functions $d_1(x, y) < d_2(x, y)$ define the boundary of the layer. We suppose that functions $F(x, y)$, $g(z)$ rapidly decay at infinity. Numbers (ξ_1, ξ_2, z_0) define coordinates of the point in the neighborhood of which the source is localized. The positive parameters h and μ are assumed to be small.

Using method of adiabatic reduction in operator form [1] and recently developed approach [2], assuming the absence of "trap" states and the fulfillment of the condition $1 \gg \mu \geq h$ we construct an asymptotic solution of the formulated problem satisfying the (asymptotic) limit absorption principle. The asymptotic solution can be represented as an decomposition into a finite number of modes, each mode is connected with pair of Lagrangian manifolds. One of the corresponding manifolds defines a localized ("singular") part of the solution in the neighborhood of the point $(x = \xi_1, y = \xi_2)$. The second manifold defines the oscillating (" wave ") part of the solution over the entire layer (taking into account the possible appearance of caustics and focal points). The obtained formula allows to describe influence of the source shape on the wave part of the solution quite explicitly. We consider several examples of functions $F(x, y)$, $g(z)$.

The research was carried out within the state assignment (theme No. AAAA-A17-117021310377-1), supported in part by RFBR (project No. 17-01-00644).

References

- [1] Belov, V. V., Dobrokhotov, S. Y., Tudorovskii, T. Y. (2004). Asymptotic solutions of nonrelativistic equations of quantum mechanics in curved nanotubes: I. Reduction to spatially one-dimensional equations. *Theoretical and mathematical physics*, 141(2), 1562-1592.
- [2] Anikin, A. Yu, et al. "The Maslov canonical operator on a pair of Lagrangian manifolds and asymptotic solutions of stationary equations with localized right-hand sides." *Doklady Mathematics*. Vol. 96. No. 1. Pleiades Publishing, 2017.

The method of nonlocal transformations: Applications to singularly perturbed boundary-value problems with a small parameter

A.D. Polyanin^{1,2,3,a)}, I.K. Shingareva^{4,b)}

¹*Ishlinsky Institute for Problems in Mechanics, Russian Academy of Sciences, 101 Vernadsky Avenue, bldg. 1, 119526 Moscow, Russia*

²*National Research Nuclear University MEPhI, 31 Kashirskoe Shosse, 115409 Moscow, Russia*

³*Bauman Moscow State Technical University, 5 Second Baumanskaya Street, 105005 Moscow, Russia*

⁴*University of Sonora, Blvd. Luis Encinas y Rosales S/N, Hermosillo C.P. 83000, Sonora, Mexico*

Singularly perturbed boundary-value problems for second-order ODEs of the form $\varepsilon y''_{xx} = F(x, y, y'_x)$ with the Dirichlet boundary conditions are considered. For $\varepsilon \rightarrow 0$, such problems are characterized by boundary layers with large gradients in narrow regions, and their solutions obtained by the standard fixed-step numerical methods can lead to significant errors. We propose a new method for numerical integration of similar problems, based on the introduction of a nonlocal independent variable ξ that is related to the original variables x and y by the auxiliary differential equation $\xi'_x = g(x, y, y'_x)$. With a suitable choice of the regularizing function g , the proposed method leads to more appropriate problems that allow the application of standard methods with a fixed stepsize in ξ .

1 Introduction

An important qualitative feature of singularly perturbed boundary-value problems is that for the zero value of a small parameter the order of the differential equation under consideration decreases and some parts of the boundary conditions cannot be satisfied. Solutions of singularly perturbed boundary-value problems with a small parameter have large gradients in the region of boundary layers, which leads to a loss of convergence of classical finite-difference schemes and makes them of little use or unsuitable for solving problems of this type.

2 Solution method based on nonlocal transformations

We consider two-point problems for second-order ODEs of the form

$$y''_{xx} = f(x, y, y'_x) \quad (0 < x < 1); \quad y(0) = a, \quad y(1) = b, \quad (1)$$

where $f(x, y, z) = \varepsilon^{-1}F(x, y, z)$ and $\varepsilon > 0$ is a small parameter.

We introduce a new nonlocal independent variable ξ by means of the first-order differential equation and the initial condition:

$$\xi'_x = g(x, y, y'_x), \quad \xi(0) = 0. \quad (2)$$

Here $g = g(x, y, y'_x)$ is a regularizing function that can vary.

^{a)}Email: polyanin@ipmnet.ru

^{b)}Email: inna@mat.uson.mx

We represent the second-order equation (1) in the form of an equivalent system of two equations of the first order

$$y'_x = z, \quad z'_x = f(x, y, z). \quad (3)$$

By using (2), we pass from x to the new independent variable ξ in (3). As a result, the boundary-value problem (1) is transformed to the following problem for the system of three equations:

$$\begin{aligned} x'_\xi = \frac{1}{g(x, y, z)}, \quad y'_\xi = \frac{z}{g(x, y, z)}, \quad z'_\xi = \frac{f(x, y, z)}{g(x, y, z)} \quad (0 < \xi < \xi_*); \\ x(0) = 0, \quad y(0) = a, \quad y(\xi_*) = b, \end{aligned} \quad (4)$$

where the value ξ_* is determined in the process of calculations according to the condition $x(\xi_*) = 1$.

Remark. The method of non-local transformations was used in [1, 2, 3] for numerical integration of Cauchy problems having monotonic and non-monotonic blow-up solutions. A comparison of the exact and numerical solutions of a number of test problems for differential equations of the first, second, third, and fourth orders showed the high efficiency of this method for numerical integration of blow-up problems.

3 Conditions to be satisfied by regularizing functions

For numerical solution of boundary-value problems, as well as for solving Cauchy problems, it is reasonable to use regularizing functions of the form

$$g = G(|z|, |f|) \equiv G(|y'_x|, |y''_{xx}|), \quad (5)$$

where $f = f(x, y, z)$ is the right-hand side of the equation (1) and $z = y'_x$. The following conditions are imposed on the function $G = G(u, v)$:

$$G > 0; \quad G_u \geq 0, \quad G_v \geq 0; \quad G \rightarrow \infty \text{ as } u + v \rightarrow \infty; \quad G(0, 0) = 1, \quad (6)$$

where $u \geq 0, v \geq 0$. The last relation in (6) is the normalization condition.

For singularly perturbed boundary-value problems with a small parameter at the highest derivative, for which the right-hand side of the equation (1) has the form $f = \varepsilon^{-1}F(x, y, z, \varepsilon)$, where $F(x, y, z, 0)$ is a smooth function that does not have singularities, when choosing regularizing functions, in addition to the conditions (5)–(6), some other considerations should be taken into account. For $g = 1$ (in this particular case, non-local transformations are not applied) and $\varepsilon \rightarrow 0$ in the boundary-layer region, the right-hand sides of the last two equations of the system (4) will tend to infinity since $|z| \rightarrow \infty$ and $|f| \rightarrow \infty$; moreover, the order relation $|f| \sim z^2$ is valid). This circumstance considerably complicates numerical integration of the problem under consideration and leads to the need to proportionally refine the grid spacing as ε decreases.

It is possible to avoid refining the grid as $\varepsilon \rightarrow 0$ and to work with a fixed stepsize with respect to the non-local variable ξ by using regularizing functions satisfying the condition

$$|z|/g = O(1) \quad \text{as } \varepsilon \rightarrow 0 \quad (7)$$

(in this case, the right-hand side of the second equation of the system (4) will not have singularities for small ε , and the third equation of this system in the boundary-layer region will have a substantially smaller singularity than for $g = 1$).

4 Brief conclusions

Comparison of exact and numerical solutions of a number singularly perturbed boundary-value problems has shown a high efficiency of the method of nonlocal transformations. For all the test problems considered, it is established that very good results are given, for example, by regularizing functions $g = (1 + |y'_x| + |y''_{xx}|)^{1/2}$ and $g = (1 + |y'_x|^2 + |y''_{xx}|)^{1/2}$, where y''_{xx} can be replaced by $\varepsilon^{-1}F(x, y, y'_x)$.

5 Acknowledgments

The work was supported by the Federal Agency for Scientific Organizations (State Registration Number AAAA-A17-117021310385-6) and was partially supported by the Russian Foundation for Basic Research (project No. 16-08-01252).

References

- [1] A. D. Polyinin, I. K. Shingareva, *Int. J. Non-Linear Mech.* 94 (2017) 178–184.
- [2] A. D. Polyinin, I. K. Shingareva, *Appl. Math. Letters* 76 (2018) 123–129.
- [3] A. D. Polyinin, I. K. Shingareva, *Int. J. Non-Linear Mech.* 99 (2018) 258–272.

Exact Polynomial Solutions for the Navier-Stokes Equations

E.Y. Prosviryakov^{1,2,a)}

¹*Institute of Engineering Science, Ural Branch of the Russian Academy of Science*

²*B. N. Yeltsin Ural Federal University*

One of the most famous and frequently used classes of exact solutions for the Navier-Stokes and Oberbeck-Boussinesq equations is the Lin-Sidorov-Aristov family. In the Lin-Sidorov-Aristov class, the velocities depend linearly on a part of the coordinates (horizontal and longitudinal) with coefficients depending on the transverse coordinate and time, and pressure and temperature are a quadratic form. Recently, this family of exact solutions has been generalized for the thermodiffusion equations, taking into account the cross dissipative effects of Soret and Dufour. The question of the possibility of constructing new exact solutions for the Navier-Stokes equations and its non-isothermal analogs for polynomial forms that generalize the class of exact Lin-Sidorov-Aristov solutions whose degree is at least two is completely natural. The report will give relevant generalizations of the known family of the exact solution for isothermal and convective flows of a viscous incompressible fluid.

^{a)}Email: evgen_pros@mail.ru

Modeling of laser-induced acoustic signals in layered nanostructures

O. Romanov^{1,2,a)}

¹*Belarusian State University, 4, Nezavisimosti av., 220030 Minsk, BELARUS*

²*The National Research Nuclear University "MEPhI", 31 Kashirskoe av., 115409 Moscow, RUSSIA*

The model and the results of numerical modeling of excitation of high-frequency acoustic signals in layered heterogeneous nanostructures due to absorption of the energy of ultrashort laser pulses are presented. Heating of metal films is described in terms of two-temperature model for the electron gas and the ionic lattice. Spatio-temporal dynamics of excitation and propagation of acoustic waves is investigated by numerical solution of the equations of motion of continuous media in the Lagrange form. Regularities in the propagation of acoustic signals in periodic and quasi-periodic multilayer nanostructures such as phononic crystals, acoustic nanocavities and plasmonic gratings are investigated, and possibilities of the use of such structures in the development of new devices for nanophotonics and nanoacoustics are discussed.

Nonlinear waves in the Hall magnetohydrodynamics in isothermal approximation

V.V. Savelyev^{1,a)}, I.V. Shutov^{2,b)}

¹*Keldysh Institute of Applied Mathematics of Russian Academy of Sciences*

²*National Research Nuclear University MEPhI*

In this work we consider the nonlinear waves in the Hall magnetohydrodynamics (HMHD) in the isothermal approximation.

In the course of the work the next expression for the wave velocity is obtained for one-dimensional differential equations of the HMHD (where q_0 – temperature parameter, B_y, B_x – components of magnetic field; B_m, Q, Π – constants)

$$V_{x1,2} = \frac{1}{4\Pi} \left((B_m^2 - B_y^2 - B_z^2) \pm \sqrt{(B_y^2 + B_z^2 - B_m^2)^2 - 16q_0\Pi^2} \right) \quad (1)$$

That mean, that system have two branches of solutions (for $q_0 = 0$ it merges into one): a branch with the plus sign will be called the first branch, with the minus – the second branch. Also was shown that for a set of parameters there is a restriction on the values that the components of the magnetic field strength can take.

The system of nonlinear ordinary differential equations was obtained and the system is solved numerically.

^{a)}Email: romanov@bsu.by

^{a)}Email: ssvvvv@rambler.ru

^{b)}Email: schutov.ilya@yandex.ru

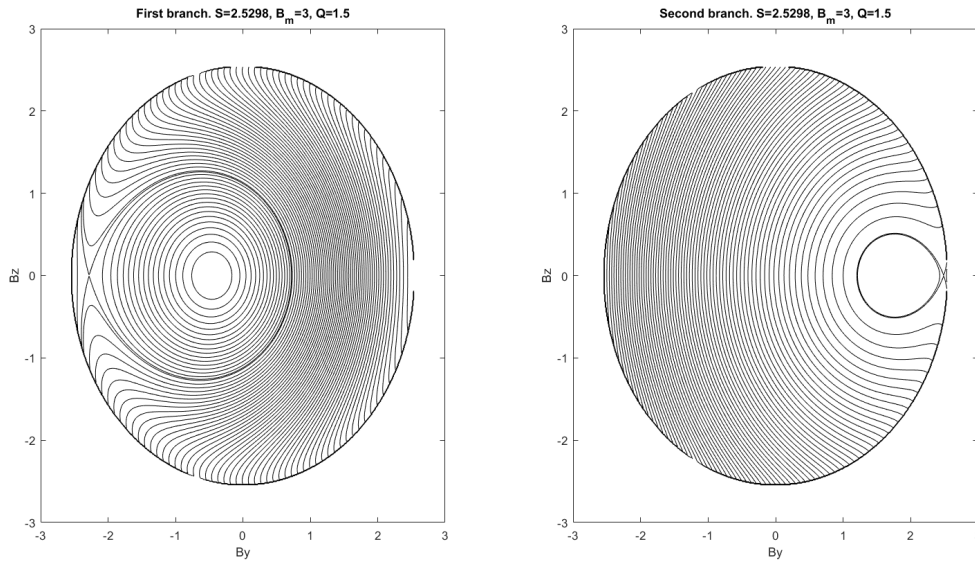


Fig. 1: The example of a phase portrait constructed with the aid of the level lines of the Hamiltonian. It is seen that on both branches there is a separatrix

$$\frac{dB_z}{dt} = \left(\frac{1}{4} \left(B_m^2 - B_y^2 - B_z^2 \pm \sqrt{(B_y^2 + B_z^2 - B_m^2)^2 - 16q_0\Pi^2} \right) - 1 \right) B_y + Q \quad (2)$$

$$\frac{dB_y}{dt} = - \left(\frac{1}{4} \left(B_m^2 - B_y^2 - B_z^2 \pm \sqrt{(B_y^2 + B_z^2 - B_m^2)^2 - 16q_0\Pi^2} \right) - 1 \right) B_z \quad (3)$$

This system proved to be a Hamiltonian system.

$$H(y, z) = \frac{B_y^2 + B_z^2}{2} \left(\frac{1}{4} B_m^2 - 1 \right) - \frac{B_z^2 B_y^2}{8} - \frac{B_y^4 + B_z^4}{16} + Q B_y \pm \left(\frac{B_y^2 + B_z^2 - B_m^2}{16} \sqrt{(B_y^2 + B_z^2 - B_m^2)^2 - 16q_0\Pi^2} - q_0\Pi^2 \ln \left| B_z^2 + B_y^2 - B_m^2 + \sqrt{(B_y^2 + B_z^2 - B_m^2)^2 - 16q_0\Pi^2} \right| \right) \quad (4)$$

Both branches were examined and analyzed: stable points of the given system were found (solutions were found numerically). Both branches have a stable point: the center. A consequence of this is the existence of periodic solutions for this system in both branches of the given system. They will exist with all the parameters of the system. These periodic systems were reviewed and analyzed.

Also, at low temperatures, there is another center and saddle point on the first branch. As a result, they form a separatrix, which we can observe on the lines of the level of the Hamiltonian. This separatrix is answered by a solitary wave.

The second branch of the separatrix appears only in a definite interval of temperature, depending on the parameters of the system. These temperature segments

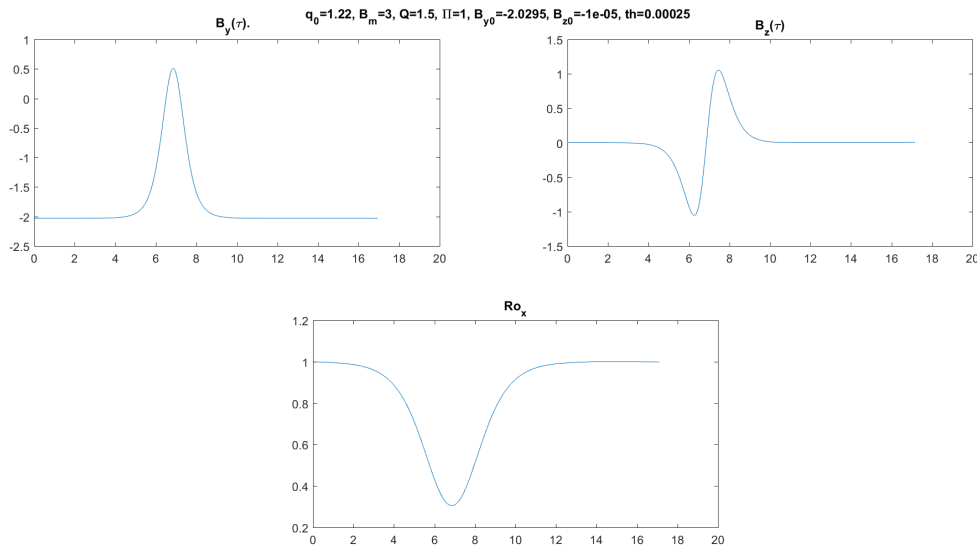


Fig. 2: The example of solitary plane wave in the first branch

intersect, and that indicates that at the same time there can be two solitary waves corresponding to the given system.

The boundaries of existence of a solitary wave on both branches and parameters of this wave, depending on the parameters of the system (wave amplitude, phase velocity) were found.

Comparison of tsunami heights calculated by asymptotic formulas with known numerical results for the transoceanic tsunami propagation.

S.Y. Sekerzh-Zen'kovich^{1,a)}, A.A. Tolchennikov^{1,2,b)}

¹*Ishlinsky Institute for Problems in Mechanics of the Russian Academy of Sciences*

²*Moscow Institute of Physics and Technology*

It is known from observations (for example, for Shikotan tsunami 1994) that modelling of transoceanic tsunami propagation claims to take into account the frequency dispersion. In order to estimate the height of the leading wave of transoceanic tsunami we use asymptotic formulas for the solution of the Cauchy problem for the linear Boussinesq equation. It allows us to take into considerations the effect of the dispersion. In our considerations we consider the cases of uniform and slowly varying depth. The research was supported by the Russian Science Foundation, grant 16-11-10282.

^{a)}Email: sekerzh@gmail.com

^{b)}Email: tolchennikovaa@gmail.com

Simulation of the propagation of acoustic pulse signal propagation in a shallow sea with penetrable bottom with the Maslov's canonical operator

S.A. Sergeev^{1,2,a)}, A.A. Tolchennikov^{1,2}, P.S. Petrov^{3,4}

¹*Institute for Problems in Mechanics of the Russian Academy of Sciences, Moscow, Russia*

²*Moscow Institute for Physics and Technology (State University), Dolgoprudny, Russia*

³*V.I. Il'ichev Pacific Oceanological Institute, Vladivostok, Russia*

⁴*Far Eastern Federal University, Vladivostok, Russia*

Recent work [1] was devoted to the modelling of the pulse acoustic signals in the deep ocean with the help of the Maslov's canonical operator [2]. Our current research is focused on the construction of the time series of pulse acoustic signal in the shallow sea [3].

In the mathematical terms this problem can be formulated as the Cauchy problem for the inhomogeneous wave equation with zero initial functions.

$$\frac{1}{c_0^2} p_{tt} - \Delta_x p = Q(x, t), \quad x = (x_1, x_2, x_3) \in B, \quad (1)$$
$$B = \{(x_1, x_2) \in \mathbb{R}^2, x_3 \in [0, H]\}, \quad c_0 = \text{const}, \quad H = \text{const}.$$

with the zero initial conditions

$$p|_{t=0} = p_t|_{t=0} = 0.$$

The variable x_3 describes the depth of the sea near the shore and the equation $x_3 = 0$ describes the surface of the sea. On the surface we posed the standard Dirichle boundary condition. The bottom is described by $x_3 = H$ and we assume it is penetrable for sound waves and at the bottom some part of the sound wave transmitted into the bottom. Therefore we pose the special reflection conditions [3].

The right-hand function $Q(x, t)$ depends on parameters λ, l :

$$Q(x, t) = \lambda^2 g'_0(\lambda t) \frac{1}{l^3} V\left(\frac{x - x^0}{l}\right)$$

with some fast decaying at infinity real functions $V(x), g_0(\tau)$ and parameters $l \ll 1, \omega = \frac{c_0}{\lambda l} < \omega_0$. While the parameter $\lambda \rightarrow \infty$ function $\lambda^2 g'_0(\lambda t)$ tends to δ' -function, and we pose in our calculations λ is sufficiently big. Parameter l describes radius of the source function and we seek the asymptotic solution of the posed problem (1) while $l \rightarrow 0$.

Using [2, 1] we describe the procedure based on the modified Maslov's canonical operator for the asymptotic solution. We simulate with this procedure the propagation of the acoustic waves in the shallow sea near the shore. The asymptotic solution is built in the point where located the receiver.

This work was supported by grant RFBR-18-31-00148 mol_a.

^{a)}Email: sergeevse1@yandex.ru

References

- [1] P. S. Petrov, S. A. Sergeev, A. A. Tolchennikov. *Doklady Akademii Nauk*, **473**, N. 2, 142–145 (2017) (in Russian)
- [2] S. Yu. Dobrokhotov, D. A. Minenkov, V. E. Nazaikinskii, B. Tirozzi, *Oper. Theory Adv. Appl.*, **228**, 95–125 (2013).
- [3] L. M. Brekhovskikh, *Waves in stratified media*, Moscow, Nauka, (1973) (In Russian).

Stability of phase transition evaporation interfaces in the form of travelling fronts

V.A. Shargatov^{1,2,a)}, A. Il'ichev³, S.V. Gorkunov^{1,2}, I.A. Artamonov^{1,2}

¹*National Research Nuclear University "MePhI", Kashirskoye shosse 31, 115409 Moscow, Russia*

²*Ishlinsky Institute for Problems in Mechanics RAS, Vernadskogo pr., 101 119526 Moscow, Russia*

³*Steklov Mathematical Institute, Russian Ac. Sci., Gubkina Str. 8, 119991 Moscow, Russia*

The paper is devoted to validity of the model KPP-Fisher equation in description of phase transition evaporation interfaces in the form of travelling fronts in horizontally extended domains of porous layers where the water is located over the vapor. It was indicated that for the case of close planar phase transition fronts the dynamics of the system is described by the KPP equation. We have shown, that even in case when the plane interfaces are not close and formally we can not use the KPP equation for description of fronts, the maximum deviation of the dimensionless traveling front amplitude from the corresponding (travelling with the same speed) KPP front is small enough. Moreover, the asymptotics of the front at infinity is always described by the KPP equation. The properties of the front solutions with monotonous structure of KPP equation is extensively studied in the literature, though as far as we understand, the existing still description is restricted to the domain between two states: 0 (which is unstable) and 1 (which is stable). In our problem we have not any more such a restriction and therefore, fronts with the oscillating structure also have to be considered. These fronts correspond to heteroclinic interfaces travelling with the travelling speed smaller than 2. The front solutions for this case (i. e. when the unstable state 0 is a focus) are absolutely unstable. Depending on the perturbation it evolves to growing non-stationary state or to the stable front of permanent form propagating with the speed 2, which serves in this case as an attractor. This work was supported by the Russian Science Foundation, project no. 16-11-10195.

^{a)}Email: shargatov@mail.ru

Integrable non–autonomous Liénard–type equations

D.I. Sinelshchikov^{1,a)}, N.A. Kudryashov^{1,b)}

¹*National Research Nuclear University MEPhI*

In this talk we consider the following family of nonlinear differential equations

$$y_{zz} + f(y)y_z^2 + g(z, y)y_z + h(z, y) = 0, \quad (1)$$

where f , g and h are arbitrary locally smooth functions and g and h do not vanish. Family of equations (1) contains the classical Liénard equation ($f = g_z = h_z = 0$), the quadratic Liénard equation ($g = h_z = 0$) and the mixed Liénard equation ($g_z = h_z = 0$) as particular cases. Equations from family (1) are used in various applications such as physics, biology and chemistry and also appear as symmetry reductions of certain nonlinear partial differential equations.

Here we consider the equivalence problem between family of equations (1) and type I Painlevé–Gambier equations via the generalized Sundman transformations. While this problem for the autonomous case has already been studied, non–autonomous one (i.e. $g_z, h_z \neq 0$ in (1)) has yet not been considered. Thus, we study connections given by the generalized Sundman transformations between equations from family (1) and type I Painlevé–Gambier equations. As a result, we find four new classes of integrable equations of type (1). We demonstrate several examples of integrable equations from family (1), some of them are traveling or stationary reductions of diffusion–convection equations.

Nonlinear delay partial differential equations: Linear and nonlinear instability of solutions and numerical integration

V.G. Sorokin^{1,2,a)}, A.D. Polyaniin^{1,2,3,b)}

¹*Ishlinsky Institute for Problems in Mechanics, Russian Academy of Sciences*

²*Bauman Moscow State Technical University*

³*National Research Nuclear University MEPhI*

Conditions for the linear and nonlinear instability of solutions to some reaction–diffusion systems with delay have been derived. Qualitative features of numerical integration by the method of lines of initial–boundary value problems for partial differential equations with delay have been described. The method is based on the approximation of spatial derivatives by corresponding finite differences. As a result, the original delay PDE is replaced by the approximate system of ordinary differential equations with delay. An extensive comparison of numerical and exact solutions of test problems has been given.

^{a)}Email: disine@gmail.com

^{b)}Email: nakudr@gmail.com

^{a)}Email: vsesor@gmail.com

^{b)}Email: polyaniin@ipmnet.ru

1 Analysis of linear stability/instability of solutions

The solution of the delay differential equation may be unstable and/or nonsmooth, which should be taken into account when developing and using the corresponding numerical methods.

Let us investigate the question of stability (or instability) of stationary solutions of initial-boundary value problems of the following class of nonlinear equations with delay:

$$u_t = au_{xx} + f(u, w), \quad w = u(x, t - \tau), \quad (1)$$

where $\tau > 0$ is the delay time and $a > 0$.

Let the constant $u = u_0$ be a solution of equation (1), i.e. we have the equality

$$f(u_0, u_0) = 0. \quad (2)$$

The constant u_0 is also the solution of the problem on the interval $0 \leq x \leq 1$ for equation (1) with the Dirichlet boundary conditions and the initial data

$$u(0, t) = u(1, t) = u_0, \quad t > 0; \quad u(x, t) = u_0, \quad -\tau \leq t \leq 0. \quad (3)$$

Let us analyze the linear stability of problem (1)–(3). To do this, we consider perturbed solutions of the following form:

$$u = u_0 + \epsilon e^{-\lambda t} \sin(\pi n x), \quad n = 1, 2, \dots, \quad (4)$$

where ϵ is a small parameter and λ is the spectral parameter. On the boundaries of the domain under consideration, solutions (4) satisfy the boundary conditions, $u|_{x=0} = u|_{x=1} = u_0$.

We substitute (4) into equation (1). Taking into account equality (2) and discarding terms of order ϵ^2 and higher, we obtain the dispersion equation for the spectral parameter λ :

$$\lambda - a(\pi n)^2 + f_u(u_0, u_0) + e^{\lambda \tau} f_w(u_0, u_0) = 0, \quad (5)$$

where $n = 1, 2, \dots$. If the real parts of all the roots of the transcendental equation (5) are positive, then the solution of problem (1)–(3) is considered stable (in the linear approximation). If the real part of at least one root of the transcendental equation (5) is negative, then the solution of problem (1)–(3) is considered unstable.

The above remains valid also for a wide class of more complicated initial-boundary value problems described by equation (1), whose solutions have the asymptotic property $\lim_{t \rightarrow \infty} u = u_0 = \text{const}$. Examples of similar problems that admit exact stable and unstable solutions are considered.

2 Nonlinear instability of solutions. Ill-posed problems

Let us consider a class of generalized equations of reaction-diffusion type with delay

$$\varepsilon u_{tt} + \sigma u_t = au_{xx} + bu - b \frac{u - kw}{1 - k} + f\left(\frac{u - kw}{1 - k}\right), \quad w = u(x, t - \tau), \quad (6)$$

where $f(z)$ is an arbitrary function (different from a constant), $k > 0$ and b are free parameters. At $\varepsilon = 0$, $\sigma = 1$ and in the absence of delay, which corresponds to the values $\tau = 0$ or $k = 0$, equation (6) becomes the standard heat equation with a nonlinear source $u_t = au_{xx} + f(u)$.

Let $u_0 = u_0(x, t)$ be a solution of equation (6). Then the function

$$u_1 = u_0 + \delta e^{ct} \sin(\gamma x), \quad (7)$$

$$c = (\ln k)/\tau, \quad \gamma = \sqrt{(b - \sigma c - \varepsilon c^2)/a}, \quad b - \sigma c - \varepsilon c^2 > 0,$$

where δ is an arbitrary constant, is also a solution of equation (6) (verified by substitution).

Let the following conditions be satisfied:

$$k > 1, \quad b > 0, \quad \tau > \tau_* = \frac{\ln k}{2b}(\sigma + \sqrt{\sigma^2 + 4\epsilon b}). \quad (8)$$

Then it follows from (7) that $|u_1 - u_0| \leq \delta$ and $|(u_1)_t - (u_0)_t| \leq c\delta$ for $-\tau \leq t \leq 0$. Therefore, for sufficiently small $\delta > 0$, the initial data for the solutions u_0 and u_1 differ from each other arbitrarily little, but for $t \rightarrow \infty$ these solutions at the points $x = \pi(2n + 1)/(2\gamma)$ ($n = 0, 1, \dots$) will unboundedly "diverge" due to the exponential factor e^{ct} in formula (7). It can be shown that if conditions (8) are satisfied, some initial-boundary value problems for equation (6) with boundary conditions of the first, second or third kind are ill-posed in the Hadamard sense for any kinetic function $f(u)$ (global instability).

3 Numerical integration based on the method of lines

We give a brief description of the method of lines. We consider a one-dimensional initial-boundary value problem for a nonlinear equation of the reaction-diffusion type with delay of sufficiently general form:

$$\begin{aligned} u_t &= [p(x, u, w)u_x]_x + q(x, u, w)u_x + f(x, u, w), \quad t > 0, \quad 0 \leq x \leq 1; \\ u(x, t) &= \varphi(x, t), \quad -\tau \leq t \leq 0; \quad u(0, t) = \psi_0(t), \quad u(1, t) = \psi_1(t), \quad t > 0. \end{aligned} \quad (9)$$

We introduce the spatial mesh $x_m = mh$, where $m = 0, 1, \dots, M$ and $h = 1/M$ is the grid spacing. Approximating the derivatives with respect to x by difference analogues and writing the equation at the point x_m , we reduce problem (9) to the ODE system:

$$\begin{aligned} (u_m)'_t &= \delta_x [p_m \delta_x u_m] + q_m \delta_x u_m + f_m, \quad m = 1, \dots, M - 1, \quad 0 < t \leq T; \\ u_m &= \varphi_m(t), \quad -\tau \leq t \leq 0 \quad (m = 0, 1, \dots, M); \quad u_0 = \psi_0(t), \quad u_M = \psi_1(t), \quad 0 < t \leq T. \end{aligned} \quad (10)$$

Here $u_m = u(x_m, t)$, $p_m = p(x_m, u_m, w_m)$, $q_m = q(x_m, u_m, w_m)$, $f_m = f(x_m, u_m, w_m)$, $w_m = u(x_m, t - \tau)$, $\varphi_m(t) = \varphi(x_m, t)$, T is the time interval of calculations, δ_x is the difference operator, which is defined as follows:

$$\delta_x u_m = \frac{1}{h}(u_{m+1} - u_m), \quad \delta_x [p_m \delta_x u_m] = \frac{1}{h^2}[p_m(u_{m+1} - u_m) - p_{m-1}(u_m - u_{m-1})].$$

System (10) contains $M - 1$ unknown function $u_m(t)$ and the same number of equations, as well as three known functions $u_0(t)$, $u_M(t)$, $w_m(t)$. We note that the ODE system obtained is often rigid and its solution must be carried out by appropriate numerical methods.

Comparison of exact and numerical solutions of a number initial-boundary value problems with stable and unstable solutions has shown high efficiency of the method of lines.

4 Acknowledgments

The work was supported by the Federal Agency for Scientific Organizations (State Registration Number AAAA-A17-117021310385-6) and was partially supported by the Russian Foundation for Basic Research (project No. 16-08-01252a).

Lyapunov functions and asymptotics for near-Hamiltonian systems

O.A. Sultanov^{1,a)}

¹*Institute of Mathematics Ufa Federal Research Center RAS*

We consider a nonlinear non-autonomous system of two ordinary differential equations having a stable fixed point. It is assumed that the non-Hamiltonian part of the system tends to zero at infinity. The asymptotic behavior of a two-parameter family of solutions starting from a neighborhood of stable equilibrium is investigated. The proposed construction of asymptotic solutions is based on the averaging method and the transition in the original system to new dependent variables, one of which is played by the angle of the limiting Hamiltonian system and the other by the Lyapunov function for the complete system.

Modeling of a pulse detonation chamber

A.V. Teterev^{1,2,a)}, L.V. Rudak¹, P.A. Mandrik¹

¹*Belarusian State University, Belarus*

²*National Research Nuclear University «MEPhI»*

A simple 2D-3D model of a flow in a pulse detonation chamber is described with accounting of the transition of combustion of a two-component fuel to detonation. Heptane was used as the fuel, and the oxidizer was air enriched with oxygen. A separate supply of fuel components was carried out in the form of spatially separated gas jets with a specified stoichiometric coefficient. Numerical simulation of the multi-cycle mode operation of the chamber was carried out. The conditions for an ignition of a mixture, a transition of combustion to detonation, and a dynamics of thrust of a pulse detonation chamber were analyzed.

A pulse detonation chamber (PDC), developed at the A.V. Luikov Heat and Mass Transfer Institute [1], is a sectional tube with an attached prechamber. This design allows changing quickly the length of the chamber, which can be important if the operating frequency of the chamber changes significantly. A combustion model used earlier in calculating combustion in combustion chambers of liquid-fuel rocket engines [2] corresponded to the diffusion type of combustion when ignition and combustion occur simultaneously with mixing [3]. In this case, the processes of heat conduction and diffusion were not explicitly considered. An instantaneous energy release described combustion well, because the flows of matter through the boundaries of the calculated cells carried out by small portions, what the diffusion process is imitated. A different picture is observed in the pulse detonation engine. The long period of filling the working volume of the chamber to the moment of ignition of the mixture leads to the fact that the fuel and oxidizer can mix quite well and become a so-called chemically uniform system [3]. In this connection, it is necessary to approach the description of the rate of chemical reactions more realistically, because it in the general case depends on a temperature and concentration of the components.

The new combustion model was constructed on the basis of the following assumptions:

^{a)}Email: oasultanov@gmail.com

^{a)}Email: teterev_a.v@mail.ru

- a PDC works in a multi-cycle mode;
- the thermodynamic properties of air, oxygen, heptane, combustion products and nitrogen are based on equilibrium tabular data calculated by CEA NASA [4];
- an ignition of a fuel and oxidizer mixture is carried out by Joule heat, allocated by a spark plug;
- the transfer of energy from the combustion area to the area of the still cold prepared mixture of oxidizer with fuel occurs due to the thermal conductivity;
- a combustion process begins when a temperature of the mixture exceeds the ignition temperature and oxidizer and fuel concentrations exceed a certain threshold value;
- a temperature of mixture components in a calculated cell is instantaneously equalized.

The velocity of the most common bimolecular homogeneous reaction, also called the second order reaction, in which two molecules take part, can be written in the form [3]:

$$W(T, c) = c_a c_b k_o e^{-\frac{E}{RT}}. \quad (1)$$

where c_a and c_b - molar concentrations of substances, k_o - accumulation coefficient weakly dependent on temperature, and E - activation energy. A mathematical model describing the flow of gas streams of fuel, oxidant and combustion products in a PDC is a system of gas dynamic equations. The energy equation in this case has the form

$$\frac{\partial [\rho (\varepsilon + v^2/2)]}{\partial t} + \nabla [\rho \vec{v} (\varepsilon + v^2/2) + p \vec{v}] = \nabla \lambda \nabla T + Q(t_i, \Delta t). \quad (2)$$

where $Q(t_i, \Delta t)$ - a heat emission of the spark plug at time t_i over time Δt , ρ - the total density of a gas stream. To close the system, the expression for the pressure in the medium uses in the form

$$p = \sum_i p_i, \quad p_i = p_i(\rho_i, \varepsilon), \quad (3)$$

where the pressures of mixture components are determined from the equations of state indicated in the tabular form in an iterative manner from the condition that their temperatures are equal.

Several parametric calculations were made. The calculations were carried out in a two-dimensional approximation in a cylindrical coordinate system on a computational mesh with a uniform spatial step $\Delta z = \Delta r = 0.75$ mm. The size of the modeling area was 1.15 m in the z -direction and 0.12 m in the r -direction, which corresponded to a calculated grid of 1440×131 cells. On all open sides of the computational region, the boundary conditions for free flow were set, and on the side of the back wall of the mixing chamber and on all surfaces of the detonation engine, the conditions of non-flowing in the form of a rigid wall with slip were set. The air supply was through a slit nozzle with a velocity vector directed at an angle of 45° towards the back wall of the mixing chamber. The air consumption was 600 l/s, as in the test calculations, and was constant throughout the simulation. In the first cycle of the propulsion system, the beginning of air enrichment with oxygen corresponded to the moment of time ($t = 0$ c), while the oxygen consumption was 300 l/s. Both gases were mixed before entering the mixing chamber and had an overall temperature of 300 K, and the modulus of the velocity vector varied from 90 m/s to 230 m/s. The supply of heptane was carried out in a similar manner, and the time of the start of its injection coincided with the time of oxygen supply. The direction of the velocity vector of

the fuel was 90° , which corresponded to a flow perpendicular to the axis of the mixing chamber. The heptane consumption was $5 \cdot 10^{-3}$ kg/s, and in the case of a periodic feed, it is twice as high. The activation energy varied from 45 to 55 kcal. The operating frequency of the pulsed detonation chamber was 20 Hz. The cycle of her work was divided into two stages. The first stage lasting from 15 ms to 25 ms corresponded to the process of filling the device with heptane and enriched air. The duration of the second stage was 35 ms and 25 ms, respectively, and began with the operation of a spark plug, the duration of which was 1.5 ms, and the energy released was 40 mJ. After the successful ignition the combustion of the prepared mixture followed, which turned into detonation.

We note some features of the simulated phenomenon. In some cases, an ignition of the mixture for the first cycle did not occur, which was due to the small concentration of fuel in spark plug area. Sometimes this happened in other working cycles. At certain ratios of the times of the first and second stages of the operating cycle, a temperature in the prechamber did not have time to fall below the ignition threshold, and the fuel supply led to the combustion of the mixture before the beginning work of spark plug. Detonation in such cases was not observed. At high values of the activation energy it was observed that the mixture burns along the tube without transition to detonation, and the flame did not have time to reach the lateral surface of the tube, since the flame propagation velocity in the radial direction in the heptane mixture with oxygen is less than 1 m/s, and along the axis reaches several hundred m/s due to the gasdynamic flow. At small values of the activation energy, the combustion transition to detonation is observed in the first half of the tube, and sometimes directly in the prechamber. Another feature of the working cycles of PDC is the non-stationary nature of thrust. At modeling till now it was not possible to leave on a constant mode. It is necessary to continue research on the causes of significant pulsations in the magnitude of the PDC thrust.

References

- [1] Assad M.S., Penyazkov O.G., Sevruk K.L. *Preliminary results of investigation of liquid fuel pulse detonation combustor* // Goren. Vzryv (Mosk.) - Combustion and Explosion, 2014, Vol. 7. P. 230-233. (In Russian).
- [2] Alhussan K.A., Teterev A.V. *Simulation of combustion products flow in the Laval nozzle in the software package SIFIN* // AIP Conference Proceedings 1863, 380010 (2017); doi: 10.1063/1.4992565.
- [3] Bartlmä F. *Gasdynamik der verbrennung* // Wien: Springer-Verlag, 1975. 534 p.
- [4] Gordon S., McBride B.J. *Computer Program for Calculation of Complex Chemical Equilibrium Compositions and Applications* // NASA Reference Publication 1311. 1996. 177 p.

Qualitative and analytical properties of solutions belonging to a family of three-dimensional four-component conservative dynamical systems with two quadratic nonlinearities

V. Tsegel'nik^{1,a)}

¹*Belarusian State University of Informatics and Radioelectronics, P. Brovka Str., 6, Minsk, 220013, Belarus*

It was investigated analytical and qualitative properties of solutions belonging to a family of three-dimensional conservative dynamical systems, the right-hand parts of which contain four components with two quadratic nonlinearities. It is proved, that only one of the 15 systems is of the Painlevé-type system. At the same time, one of the components of the two systems, which are not Painlevé-type systems, has no movable singular points at all. It is proved, that all systems of this family have no chaotic behavior.

1. The aim of this paper is to study the analytical and qualitative properties of solutions of systems of differential equations

$$\dot{x} = y^2 + yz, \quad \dot{y} = x, \quad \dot{z} = y. \tag{1}$$

$$\dot{x} = y^2 + yz, \quad \dot{y} = z, \quad \dot{z} = x. \tag{2}$$

$$\dot{x} = y^2 - z^2, \quad \dot{y} = x, \quad \dot{z} = y. \tag{3}$$

$$\dot{x} = 2xy + z, \quad \dot{y} = -y^2, \quad \dot{z} = x. \tag{4}$$

$$\dot{x} = y^2 - x, \quad \dot{y} = xz, \quad \dot{z} = z. \tag{5}$$

$$\dot{x} = xz + y, \quad \dot{y} = -yz, \quad \dot{z} = x. \tag{6}$$

$$\dot{x} = x^2 + z, \quad \dot{y} = -2xy, \quad \dot{z} = y. \tag{7}$$

$$\dot{x} = y^2 + y, \quad \dot{y} = xz, \quad \dot{z} = \varepsilon y. \tag{8}$$

$$\dot{x} = y^2 + y, \quad \dot{y} = z^2, \quad \dot{z} = x. \tag{9}$$

$$\dot{x} = y^2 + z, \quad \dot{y} = x^2, \quad \dot{z} = \varepsilon x. \tag{10}$$

$$\dot{x} = y^2 + z, \quad \dot{y} = x^2, \quad \dot{z} = \varepsilon y. \tag{11}$$

$$\dot{x} = y^2 + z, \quad \dot{y} = \varepsilon xz, \quad \dot{z} = y. \tag{12}$$

$$\dot{x} = y^2 + z, \quad \dot{y} = z^2, \quad \dot{z} = \varepsilon x. \tag{13}$$

$$\dot{x} = yz + x, \quad \dot{y} = x^2, \quad \dot{z} = -z. \tag{14}$$

$$\dot{x} = y^2 + z^2, \quad \dot{y} = x, \quad \dot{z} = y \tag{15}$$

with unknown functions x, y, z of the independent variable t ; $\varepsilon^2 = 1$.

In [1], it is proved, that none of the systems (1)–(14) had chaotic behavior.

2. Assuming the independent variable t to be complex, the following statements are proved

Theorem 1. The system (4) is the Painlevé-type system.

Theorem 2. None of the systems (1)–(3), (5)–(15) is of the Painlevé-type. At the same time, a component z of the systems (5), (14) has no movable singular points at all.

Theorem 3. Systems (3), (15) are invariant under transformation $t \rightarrow -t, x \rightarrow -x, y \rightarrow y, z \rightarrow -z$. The system (3) with the help of convert $t \rightarrow it, x \rightarrow ix, y \rightarrow -y, z \rightarrow iz, i^2 + 1 = 0$ is reduced to the system (15).

Theorem 4. The system (15) has no chaotic behavior.

^{a)}Email: tsegvv@bsuir.by

References

- [1] Heidel J and Zhang Fu 1999 *Nonchaotic behaviour in three-dimensional quadratic systems II. The conservative case* *Nonlinearity* **12**. pp 617 - 633.

On a pair of Lagrangian manifolds connected with the asymptotics of Hermite polynomials

A.V. Tsvetkova^{1,2,a)}

¹*Ishlinsky Institute for Problems in Mechanics RAS*

²*Moscow Institute of Physics and Technology (State University)*

We discuss two approaches to constructing the well-known asymptotics of Hermite polynomials $H_n(y)$ as $n \rightarrow \infty$. These approaches are related to the Maslov canonical operator.

The first approach is based on the presentation of Hermite functions $\psi_n(y) = (2^n n! \sqrt{\pi})^{-\frac{1}{2}} e^{-\frac{y^2}{2}} H_n(y)$ as solutions of the Schrödinger equation for a harmonic oscillator

$$-\frac{1}{2} \frac{d^2 \psi_n}{dy^2} + \frac{y^2}{2} \psi_n = \left(\frac{1}{2} + n \right) \psi_n, \|\psi_n\|_{L_2(\mathbb{R}_y)} = 1.$$

The second approach is based on the fact, that Hermite polynomials can be obtained from the recurrence relation with initial conditions

$$H_{n+1}(y) = 2yH_n(y) - 2nH_{n-1}(y), H_0(y) = 1, H_1(y) = 2y.$$

To construct the asymptotics we use the Maslov canonical operator. This operator is connected with the Lagrangian manifolds which are defined by trajectories of the corresponding Hamiltonian systems. In the first case the Lagrangian manifold is a circle, in the second case the Lagrangian manifolds are a family of "distorted" horizontal parabolas.

Described approaches give the uniform asymptotics of the Hermite polynomials in terms of the Airy function Ai . And it seems to us that such approaches can also be useful in constructing the asymptotics of other polynomials.

The research was supported by the Russian Science Foundation (project 16-11-10282).

^{a)}Email: annatsvetkova25@gmail.com

Using Machine Learning to predict survival in patients with brain metastases after Gamma Knife radiosurgery.

G.A. Vazhenin¹, S.M. Banov², A.V. Dalechina²

¹*NRNU MEPhI Department of Applied Mathematics (31)*

²*Moscow Gamma Knife center (Burdenko Neurosurgical Institute)*

In this research we developed methodology for estimating survival time for patients with brain metastases who had received the SRS in the Moscow Gamma Knife center. The main tool of our research became machine learning algorithms. We received the total data of 916 patients with 23 different features and predicts the time interval from the onset of disease to death. The initial data was restructured and converted into clean data, on which predictions were made with the median error of 0.88 months. It was founded that the most important factor which affects the survival time is the time interval from the onset of the disease to the date of Gamma Knife radiosurgery.

key words: radiosurgery, brain metastases, machine learning

Objective:

The quantity of detected cases of oncology diseases is being on arise all over the world. Brain metastases are one one of the most severe complications of oncological disease, accounting for significant mortality in oncology patients. Traditionally medical therapy includes surgical rejection, systemic corticosteroids fractionated whole brain radiation therapy (WBRT) . At the moment the most efficient and secure method in case of limited brain metastases is considered to be stereotactic radiosurgery (SRS) [1]. It is extremely important for cancer research to predict outcomes after a given therapy and detect the key features from complex datasets and identify the prognostic factors affecting patients survival.

The Machine Learning (ML) is a powerful tool to achieve all these goals. ML enables computers to learn from previous data to make accurate predictions on new data. The purpose of this study is to apply the ML to predict survival in patients with brain metastases (BS) after Gamma Knife radiosurgery .

Materials and methods:

We retrospectively evaluated the total data of 916 patients with 23 different patient characteristics who had received the SRS in the Moscow Gamma Knife center (Burdenko Neurosurgical Institute) in the period from 2009 to 2016.

All this patients with 23 features (5 - real, 7 - categorical, 10 - date) were included into analysis. We predicted survival time from the onset of disease to death taking into account the various factors: clinical, molecular - genetic, previous treatments, etc. Data were divided into two sets: "train" set and "test" set. Train set contains 479 patients with information about the date of death. In turn, "test" set does not include any information about the date of death for these patients or they have been being alive.

This research was based on the use of machine learning algorithms.

Algorithms and metrics:

RandomForestRegressor (RF) - Meta estimator that fits a number of classifying decision trees on various sub-samples of the dataset and use averaging to improve the predictive accuracy and control over-fitting.

Gradient boosting (GB) is a machine learning technique for regression and classification problems, which produces a prediction model in the form of an ensemble of weak prediction models. It builds the model in a stage-wise fashion like other boosting methods do, and it generalizes them by allowing optimization of an arbitrary differentiable loss function.

Cross-validation (CV) - Validation technique which is mainly used in settings where the goal is prediction, and one wants to estimate how accurately a predictive model will perform in practice. It involves partitioning a sample of data into complementary subsets, performing the analysis on one subset (called the training set), and validating the analysis on the other subset (called the validation set or testing set). Usually, validation scores averaged.

Metric Accuracy - The proportion of correctly predicted results relative to all. (In our research - the proportion of predicted results that fell within a month's ambit from reality). The metric is unstable to large deflection, but in order to increase development speed were decided to choose it.

72 additional attributes were generated during the data-engineering process. Categorical attributes were converted into binary. Because if we convert all distinct statements in numbers, model will certainly interpret it as sorted in a priority order attributes. Difference between every date pairs were converted into time intervals in case that dates don't bear semantic loading, otherwise, time intervals do.

The **RF** method in the conjunction with the "greedy" selection defines 20 most suitable features for the **GB+RF** model training. It was decided to use stack (the average predictions) of two models based on the GradientBoosting and RandomForest algorithms to determine the survival time interval.

The methods were implemented using open-source Python libraries: sklearn, catboost, pandas, numpy, scipy, pylab. To verify the correctness of the model, metric accuracy was used in conjunction with cross-validation.

Results:

The model (**GB+RF**) was trained within the 20 selected most-suitable features. For the training set of data, the discrepancies between the predicted results and the known ones were calculated. The absolute errors were measured in months.

- **GB+RF** accuracy: 0.95 (Cross-Validation)
- Mean absolute error: 1.26
- Median absolute error: 0.88
- Max absolute error: 12.52

The five most significant features were identified from 20 features. The most important feature in constructing the model is the time interval from the onset of the disease to the date of Gamma Knife radiosurgery. Further in descending order of importance: The time interval from Gamma Knife radiosurgery to the last observation of the patient, the time interval from the onset of the disease (diagnosing of the disease) to the last observation, the time interval from whole brain radiation treatment (WBRT) to the first radiosurgery. The importance of the factor is the weight that model defines to a factor in the final function.

Conclusion:

For 479 patients (train part) a prediction was made with a median error of 0, 88 months. It was revealed that the most significant feature is the time from the onset of the disease to

the radiosurgery. The data given were too raw to make good estimations by the reason of its incompleteness, we get good results on predictions for the patients with adverse forecast.

To make predictions more reliable, we should enlarge the sample train data, as well as increase its completeness. We see that machine learning methods demonstrate great potential in the analysis of medical data.

The next stage of our research will be determining the most favorable treatment option in terms of survival.

References

- [1] Bashir A. Impact of the number of metastatic brain lesions on survival after Gamma Knife radiosurgery

The chemical kinetics and the connection between the hydrodynamic and kinetic descriptions

B.V. Vedenyapin^{1,a)}, S.Z. Adzhiev^{2,b)}, V.V. Kazantseva^{1,c)}, I.V. Melikhov^{2,d)}

¹*Keldysh Institute of Applied Mathematics of Russian Academy of Sciences*

²*Lomonosov Moscow State University*

We consider the fundamental kinetic equations: the Boltzmann equation, which describes the short-range interactions, and its basic application – the theorem of entropy increase (the H-theorem). The H-theorem was considered for the first time by Boltzmann [1]. This theorem substantiates the convergence of solutions of the Boltzmann type equations to the Maxwell distribution. Latterly, Boltzmann associated the H-theorem with the law of entropy increase [2]-[21]. We investigate the generalizations of the equations of chemical kinetics, including classical and quantum chemical kinetics with continuous and discrete time [3], [14]-[21]. We discuss the Vlasov equation, which describes any long-range interaction with its major applications for plasma description [7]-[9]. We consider the Liouville equation or the continuity equation with applications to the statistical mechanics [3]-[5] and in the Hamilton–Jacobi method [6], [7], [12], [13], as well as in the ergodic theory [3], [4], [14]-[16].

References

- [1] Boltzmann L. Weitere Studien über das Wärmegleichgewicht unter Gasmolekülen. Wien. Ber., 1872, 66, 275–370; Wissenschaftliche Abhandlungen, Barth, Leipzig, 1909, 1, 316–402.
- [2] Boltzmann L. Über die Beziehung zwischen dem zweiten Hauptsatze der Mechanischen Wärmetheorie und der Wahrscheinlichkeitsrechnung, respektive den Sätzen über das Wärmegleichgewicht. Wien: Akad. Sitzungsber, 1878. Bd. 76, S. 373-435.

^{a)}Email: vicveden@yahoo.com

^{b)}Email: sergeyadzhiev@yandex.ru

^{c)}Email: vladastar@inbox.ru

^{d)}Email: melikhov@radio.chem.msu.ru

- [3] V. V. Vedenyapin, S. Z. Adzhiev, Entropy in the sense of Boltzmann and Poincare, *Uspekhi Mat. Nauk*, 69:6(420) (2014), 45–80; *Russian Math. Surveys*, 69:6 (2014), 995–1029.
- [4] H. Poincare, *Reflections sur la theorie cinetique des gaz*, *J. Phys. Theoret. Appl.* 5 (1906), 369–403; *OEuvres*, vol. IX, Gauthier-Villars, Paris 1954, pp. 587–619.
- [5] V. V. Kozlov and D. V. Treschev, “Weak convergence of solutions of then Liouville equation for nonlinear Hamiltonian systems”, *Theoret. and Math. Phys.* 134:3 (2003), 339–350.
- [6] V.V. Kozlov, *General Theory of Vortices*. Moscow–Izhevsk, 2013.
- [7] V. V. Vedenyapin, M. A. Negmatov, N. N. Fimin, “Vlasov-type and Liouville-type equations, their microscopic, energetic and hydrodynamical consequences”, *Izv. RAN. Ser. Mat.*, 81:3 (2017), 45–82; *Izv. Math.*, 81:3 (2017), 505–541.
- [8] V. V. Vedenyapin, “Boundary value problems for the steady-state Vlasov equation”, *Dokl. Akad. Nauk SSSR* 290:4 (1986), 777–780; English transl., *Soviet Math. Dokl.* 34:2 (1987), 335–338.
- [9] V. V. Vedenyapin, “On the classification of steady-state solutions of Vlasov’s equation on the torus, and a boundary value problem”, *Dokl. Akad. Nauk SSSR* 323:6 (1992), 1004–1006; English transl., *Russian Acad. Sci. Dokl. Math.* 45:2 (1992), 459–462.
- [10] V. V. Vedenyapin, "Time averages and Boltzmann extremals", *Dokl. Akad. Nauk*, 2008, 422:2, 161–163; English transl. *Dokl. Math.*, 2008, 78:2, 686–688.
- [11] Adzhiev S.Z., Vedenyapin V.V. Time averages and Boltzmann extremals for Markov chains, discrete Liouville equations, and the Kac circular model. *Comput. Math. Math. Phys.*, 2011, 51 (11), 1942–1952.
- [12] V. V. Vedenyapin and N. N. Fimin, "The Liouville equation, the hydrodynamic substitution, and the Hamilton–Jacobi equation", *Dokl. Akad. Nauk*, 2012, 446:2, 142–144; English transl. *Dokl. Math.*, 2012, 86:2, 697–699.
- [13] V. V. Vedenyapin and M. A. Negmatov, "On the topology of steady-state solutions of hydrodynamic and vortex consequences of the Vlasov equation and the Hamilton–Jacobi method", *Dokl. Akad. Nauk*, 2013, 449:5, 521–526; English transl. *Dokl. Math.*, 2013, 87:2, 240–244.
- [14] V.V. Vedenyapin, *Boltzmann’s and Vlasov’s kinetic equations*, Fizmatlit, Moscow 2001.
- [15] S. Z. Adzhiev, S. A. Amosov, V. V. Vedenyapin, “One-dimensional discrete models of kinetic equations for mixtures”, *Zh. Vychisl. Mat. Mat. Fiz.*, 44:3 (2004), 553–558; *Comput. Math. Math. Phys.*, 44:3 (2004), 523–528.
- [16] Vedenyapin V., Sinitsyn A., Dulov E. *Kinetic Boltzmann, Vlasov and Related Equations*, Amsterdam, 2011.
- [17] Adzhiev S.Z., Vedenyapin V.V., Volkov Yu.A., Melikhov I.V. *Generalized Boltzmann-Type Equations for Aggregation in Gases*. *Computational Mathematics and Mathematical Physics*, 2017, 57 (12), 2017–2029.
- [18] S. Z. Adzhiev, V. V. Vedenyapin, “On the sizes of discrete velocity models of the Boltzmann equation for mixtures”, *Zh. Vychisl. Mat. Mat. Fiz.*, 47:6 (2007), 1045–1054; *Comput. Math. Math. Phys.*, 47:6 (2007), 998–1006.

- [19] Adzhiev S.Z., Melikhov I.V., Vedenyapin V.V. The H-theorem for the physico-chemical kinetic equations with discrete time and for their generalizations. *Physica A: Statistical Mechanics and its Applications*, 2017, 480, 39–50.
- [20] Adzhiev S.Z., Melikhov I.V., Vedenyapin V.V. The H-theorem for the physico-chemical kinetic equations with explicit time discretization. *Physica A: Statistical Mechanics and its Applications*, 2017, 481, 60–69.
- [21] Adzhiev S., Melikhov I., Vedenyapin V. The H-theorem for the chemical kinetic equations with discrete time and for their generalizations // *Journal of Physics: Conference Series*. 2017. Vol. 788, № 1. P. 012001.

Section “Mathematical modelling”

On the application of systems of functions of special kind in mathematical physics

A. Barmenkov^{1,a)}, N. Barmenkov^{1,b)}

¹*National research nuclear university "MEPhI"*

The report considered the application of functional sequences of special kind for the study of some boundary value problems of equations mathematical physics. This sequences may be used in modelling physical processes.

Consider of functional sequences of special kind

$$\left\{ \operatorname{Re}[W(x)]^n; \operatorname{Im}[W(x)]^n \right\}_{n=0}^{\infty}, \quad (1)$$

where $W(x)$ continuous complex-valued function of $x \in [a, b]$. In [1, 2], the basic properties such sequences are proved. In [3] Minzonii A.A. proved completeness in $L_2[0; 2\pi]$ system of functions of special kind

$$\left\{ e^{-np(x)} \cos(nt); e^{-np(x)} \sin(nt) \right\}_{n=0}^{\infty} \quad (2)$$

where $p(x)$ real function $p(x) \in C^{1,\alpha}$. The proof is based on the fact that this sequence is applied to the solution of the following problem of Coshi (see [4] Vequa)

$$\Delta w(x, y) = 0, \quad (3)$$

$$w(x, p(x)) = f(x)$$

$$w(0, y) = w(2\pi, y)$$

$$w(x, y) \rightarrow 0,$$

as $y \rightarrow 0$. The solution of this problem is given in the form of a series

$$w(x, y) = \sum_{n=0}^{\infty} (A_n e^{-ny} \cos(nx) + B_n e^{-ny} \sin(nx)),$$

where the coefficients satisfy the relation

$$w(x, p(x)) = \sum_{n=0}^{\infty} (A_n e^{-np(x)} \cos(nx) + B_n e^{-np(x)} \sin(nx))$$

Moreover, the function $p(x)$ is subject to rather rigid conditions $p(x) \in C^{1,\alpha}[0; 2\pi]$. In fact, the sequence (2)(see [3]) is a system of the form (1) for

$$w(x) = e^{-p(x)+ix}, \text{ i.e. } \{e^{-p(x)} \cos(nx); e^{-p(x)} \sin(nx)\}_{n=0}^{\infty}, x \in [0; 2\pi]$$

In fact, this result follows from the works of [1, 2], proved in a different way earlier than [3] and under more general conditions for the $p(x)$ function. The completeness of the system of

^{a)}Email: anbarmenkov@mail.ru

^{b)}Email: nikkibarm@mail.ru

functions (1) in different spaces is proved in [1], and the minimality in [2]. In [2], the minimality is proved and the sequence biorthogonally conjugate to (1) is given explicitly. From the results of [2] it follows that the image of the segment $[0; 2\pi]$ when $w(x) = e^{-p(x)+ix}$, $x \in [0; 2\pi]$ displayed is the curve $\Gamma = w[0; 2\pi]$.

If $p(0) \neq p(2\pi)$, then the contour Γ is open and the sequence (2) is dense complete in different spaces. If $p(0) = p(2\pi)$, then the contour Γ is closed, and the point 0 (origin) lies in the finite region bounded by this contour Γ , then this sequence (2) is complete and minimal in various functional spaces depending on the values of the angles at the angular points of the contour Γ (see [2]). At least for a smooth closed contour $\Gamma = w[0; 2\pi]$ the sequence (2) is complete and minimal in space $L_2[0; 2\pi]$.

Hence, the statement of Minzoni [3] is a special case of the results [1, 2].

The following properties of the boundary value problem (3) of differential equations of mathematical physics are shown.

Boundary condition $p(0) \neq p(2\pi)$ of the problem (3) means the dense completeness of the sequence (2) in $L_2[0; 2\pi]$.

Boundary condition $p(0) = p(2\pi)$ of the problem (3) means the completeness and minimality of the sequence (2) in $L_2[0; 2\pi]$.

References

- [1] Kazmin J. A., Closure of the linear shell of one system of functions, Siberian mathematical journal, v 18, №4, 799-805, 1977.
- [2] Barmenkov A. N., Minimality and orthogonality one system of functions, Siberian mathematical journal, v 22, №1, 8-26, 1981.
- [3] Minzonii A.A., On completeness of one system of functions properties $\left\{ e^{-np(x)} \cos(nx); e^{-np(x)} \sin(nx) \right\}_{n=0}^{\infty}$ Studies in Applied Mathematic, v75, №3, 265-266, 1986.
- [4] Vequa I.N., Common analytical functions, M. Fizmatgiz, 1959.

Refinement of the Reactor Dynamics Mathematical Model

A.V. Baskakov¹, N.P. Volkov^{1,a)}

¹*National Research Nuclear University MEPhI (Moscow)*

The report is devoted to the problems of improvement of the mathematical model of reactor dynamics. Physical processes of reactor dynamics are studied, which are described by a system of non-stationary integral-differential equations: a non-stationary anisotropic multi-speed kinetic transfer equation and a delayed neutrons balance equation. Sufficient conditions of existence and singularity of generalized solutions of the examined observation problems were obtained.

^{a)}Email: npvolkov@mephi.ru

The mathematical model of reactor dynamics is considered herein without accounting for temperature feedback [1] and described by a system of non-stationary integral-differential equations:

1) by the non-stationary anisotropic multi-speed kinetic transport equation

$$\begin{aligned} \frac{\partial u}{\partial t}(\mathbf{x}, \mathbf{v}, t) + (\mathbf{v}, \nabla_{\mathbf{x}})u(\mathbf{x}, \mathbf{v}, t) + \Sigma(\mathbf{x}, \mathbf{v}, t)u(\mathbf{x}, \mathbf{v}, t) = \\ = \int_V J(\mathbf{x}, \mathbf{v}, \mathbf{v}', t)u(\mathbf{x}, \mathbf{v}', t)d\mathbf{v}' + \sum_{k=1}^N z_k R_k(\mathbf{x}, \mathbf{v}, t) + F(\mathbf{x}, \mathbf{v}, t), \end{aligned} \quad (1)$$

2) by the delayed neutrons balance equation

$$\frac{\partial R_k}{\partial t}(\mathbf{x}, \mathbf{v}, t) = -z_k R_k(\mathbf{x}, \mathbf{v}, t) + \int_V J_k(\mathbf{x}, \mathbf{v}, \mathbf{v}', t)u(\mathbf{x}, \mathbf{v}', t)d\mathbf{v}', \quad \forall k = \overline{1, N}, \quad (2)$$

$$(\mathbf{x}, \mathbf{v}, t) \in D = G \times V \times (0, T).$$

Whereas the following initial conditions for the functions $u(\mathbf{x}, \mathbf{v}, t)$ and $R_k(\mathbf{x}, \mathbf{v}, t)$ are set

$$u(\mathbf{x}, \mathbf{v}, 0) = \varphi(\mathbf{x}, \mathbf{v}), \quad (\mathbf{x}, \mathbf{v}, t) \in \overline{G} \times V, \quad (3)$$

$$R_k(\mathbf{x}, \mathbf{v}, 0) = R_{k0}(\mathbf{x}, \mathbf{v}), \quad \forall k = \overline{1, N}, \quad (\mathbf{x}, \mathbf{v}, t) \in \overline{G} \times V. \quad (4)$$

and boundary conditions (lack of external sources, i.e. the reactor walls do not let external radiation pass)

$$u(\mathbf{x}, \mathbf{v}, t) = 0, \quad (\mathbf{x}, \mathbf{v}, t) \in \gamma_- \times [0, T], \quad (5)$$

where $\gamma_- = \{(\mathbf{x}, \mathbf{v}) \in \partial G \times V : (\mathbf{v}, n_x < 0)\}$, and n_x is an outward normal to a boundary ∂G of G at a point \mathbf{x} .

We will consider the redefinition condition (internal measurement)

$$\int_G \omega_{\mathbf{x}^0}(\mathbf{x})u(\mathbf{x}, \mathbf{v}, t)d\mathbf{x} = \chi(\mathbf{v}, t), \in \overline{G} \times [0, T], \quad (6)$$

which, in physical terms, describes the measurement of neutron density in a certain vicinity of point $\mathbf{x}^0 \in G$. The finite function $\omega_{\mathbf{x}^0} \in L_2(G)$ which is referred to as an instrument function and characterizes parameters of the instrument the measurements are performed with, has the pronounced maximum in point \mathbf{x}^0 , and the carrier $\text{supp}(\omega_{\mathbf{x}^0}) \subset G$.

The problems of finding of one of the sources, absorption factor or scattering indicatrix functions were examined and are set out as follows:

$$F(\mathbf{x}, \mathbf{v}, t) = f(\mathbf{v}, t)g_1(\mathbf{x}, \mathbf{v}, t), \quad (7)$$

$$\Sigma(\mathbf{x}, \mathbf{v}, t) = \sigma(\mathbf{v}, t)g_2(\mathbf{x}, \mathbf{v}, t), \quad (8)$$

$$J(\mathbf{x}, \mathbf{v}, \mathbf{v}', t, t) = j(\mathbf{v}, t)g_3(\mathbf{x}, \mathbf{v}, \mathbf{v}', t), \quad (9)$$

the correction functions g_1, g_2, g_3 are preset functions, while functions $f(\mathbf{v}, t), \sigma(\mathbf{v}, t)$ and $j(\mathbf{v}, t)$ are desired functions.

The assigned problems (1)-(7) or (1)-(6),(8) or (1)-(6),(9) are usually referred to as observation problems, wherein functions $F(\mathbf{x}, \mathbf{v}, t)$ or $\Sigma(\mathbf{x}, \mathbf{v}, t)$ or $J(\mathbf{x}, \mathbf{v}, \mathbf{v}', t, t)$ are improved on basis of the supplementary data (6), and thus the entire mathematical model of reactor dynamics is improved.

Sufficient conditions of existence and singularity of generalized solutions of the problems under study were obtained, i.e. problems of simultaneous definition of the function of neutron distribution density $u(\mathbf{x}, \mathbf{v}, t)$, the function of distribution density of the k th group delayed neutron carriers $R_k(\mathbf{x}, \mathbf{v}, t)$ and the required part of one of functions $F(\mathbf{x}, \mathbf{v}, t)$ - the density of internal sources of neutrons, $\Sigma(\mathbf{x}, \mathbf{v}, t)$ - the complete macroscopic neutronic section or $J(\mathbf{x}, \mathbf{v}, \mathbf{v}', t, t)$ - the scattering integral core which characterizes the distribution density of the secondary scattering, and macroscopic sections of resilient and non-resilient scattering.

Existence and uniqueness theorems of generalized solutions for the studied observation problems are proved.

References

- [1] Kryanev A.V., Shikhov S.B., Questions in the Mathematical Theory of Reactors: Nonlinear Analysis, Atomizdat, Moscow (1983) (Russian). 280 p.

A new look at the double sine-Gordon kink-antikink scattering

E.G. Belendryasova^{1,a)}, V.A. Gani^{1,2,b)}, A. Moradi Marjaneh^{3,c)}, A. Askari⁴, D. Saadatmand⁵

¹*National Research Nuclear University MEPhI (Moscow Engineering Physics Institute), Moscow, Russia*

²*National Research Center Kurchatov Institute, Institute for Theoretical and Experimental Physics, Moscow, Russia*

³*Young Researchers and Elite Club, Quchan Branch, Islamic Azad University, Quchan, Iran*

⁴*Department of Physics, Faculty of Science, University of Hormozgan, P.O.Box 3995, Bandar Abbas, Iran*

⁵*Department of Physics, University of Sistan and Baluchestan, Zahedan, Iran*

We study kink-antikink scattering withing the $(1 + 1)$ -dimensional double sine-Gordon (DSG) model. The dynamics of the real scalar field $\varphi(x, t)$ is described by the Lagrangian

$$\mathcal{L} = \frac{1}{2} \left(\frac{\partial \varphi}{\partial t} \right)^2 - \frac{1}{2} \left(\frac{\partial \varphi}{\partial x} \right)^2 - V(\varphi) \quad (1)$$

with the potential

$$V_R(\varphi) = \tanh^2 R (1 - \cos \varphi) + \frac{4}{\cosh^2 R} \left(1 + \cos \frac{\varphi}{2} \right), \quad R > 0. \quad (2)$$

The DSG kink (antikink)

$$\phi_{k(\bar{k})}(x) = 4\pi n \pm 4 \arctan \frac{\sinh x}{\cosh R} \quad (3)$$

^{a)}Email: 7.95@bk.ru

^{b)}Email: vagani@mephi.ru

^{c)}Email: moradimarjaneh@gmail.com

can be viewed as two subkinks separated by some distance. We use a parameter R which can be interpreted as the separation of the subkinks.

In the kink-antikink collisions we found a critical velocity v_{cr} , which separates two different regimes: at initial velocities above v_{cr} kinks reflect from each other and escape to infinities, while at velocities below v_{cr} kinks can either escape after (two or more) collisions or capture and form a bound state of the kinks — a bion. We show that the dependence v_{cr} on R has several local maxima.

In the kink-antikink collisions below v_{cr} we observed a phenomenon, which, to the best of our knowledge, has not been reported for the DSG model before. At some initial velocities of the colliding kinks we found final configuration in the form of two escaping oscillons. At the same time, at some initial velocities we observed formation of the configuration, which can be classified as a bound state of two oscillons. Formation of the bound state of oscillons and the escape of oscillons are extremely sensitive to changes of the initial velocity of the colliding kinks.

This research was supported by the MEPhI Academic Excellence Project (contract No. 02.a03.21.0005, 27.08.2013).

The influence of potential parameters of a binary mixture components on the calculation accuracy by the Monte Carlo simulations

Y.A. Bogdanova^{1,a)}, Z. Mamedov¹, A.V. Kudinov¹

¹*National Research Nuclear University MEPhI (Moscow Engineering Physics Institute)*

The effect of potential parameters of the components of a binary mixture on the accuracy of calculations of thermodynamic properties using an effective one-fluid model based on the Monte Carlo simulation was investigated. It is shown that the well depth ratio has the most significant effect. With increasing value of the well depth ratio, the deviation of the pressure values from the model vdW1f from the exact simulation of the binary mixture increases linearly.

1

In practical problems aimed at studying physical and chemical processes at high pressures and temperatures, complex chemical systems are considered in which the gas (fluid) phase is multicomponent. To model complex multicomponent mixtures the effective one-fluid model (vdW1f) is widely used [1, 2]. In this model a multicomponent mixture of fluids is considered as a hypothetical (effective) pure fluid. Potential parameters of the effective fluid are determined through the parameters of the intermolecular interaction of the potentials of a multicomponent mixture and depend on its composition. In [3] it was shown that it is necessary to determine the area of applicability of the vdW1f model as a function of the potential parameters of the mixture components. Therefore, in this paper, we investigate the influence of potential parameters of the

^{a)}Email: yabogdanova@mephi.ru

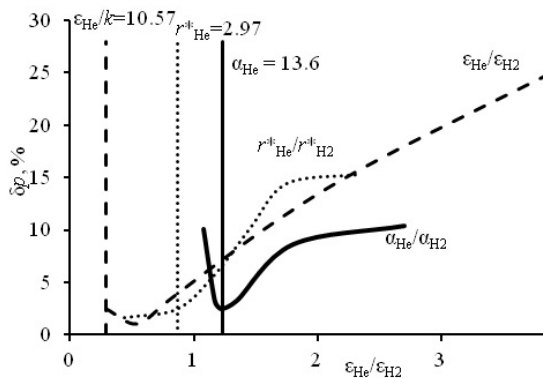


Fig. 1: Dependence of pressure error on potential parameters

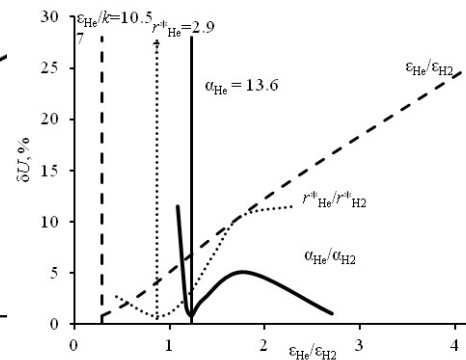


Fig. 2: Dependence of internal energy error on potential parameters

components of a binary mixture on the calculations accuracy in comparison with the exact model of a two-component system based on Monte Carlo simulation results. For the studies, a model mixture of hydrogen molecules and helium atoms with different compositions was chosen. The interaction of the particles of this binary mixture is described by the paired spherically symmetric potential Exp-6, applied in the region of high pressures and temperatures. Potential parameters of hydrogen are taken from [1] and the helium parameters were varied to study the accuracy of the model vdW1f in comparison with the results of calculations of the binary mixture. The parameters of the unlike potential were assumed to be additive and calculated according to the Lorentz-Berthelott rule [4]. Calculations in this work were carried out using the software code MCCC (The Monte Carlo for Complex Chemical Systems) Towhee [5]–[10]. This is a software package that implements the Monte Carlo method with the required accuracy. Calculations were performed on the cluster of the National Research Nuclear University MEPhI.

The results of the calculations are shown in Figures 1 and 2 in the form of the dependence of the relative pressure deviations (figure 1) and internal energy (figure 2) calculated according to the vdW1f model from the results of the exact simulation of the binary mixture. The solid lines show the dependencies on the ratios stiffness parameters α_{He}/α_{H2} , the dashed lines show the dependence on the ratio r_{He}^*/r_{H2}^* , the dashed lines depend on the ratio of the well depth $\varepsilon_{He}/\varepsilon_{H2}$. The vertical asymptotes correspond to the values of the potential parameters of helium He [3].

It can be seen from the figures that the difference of the well depth of the components has the most significant effect on the accuracy of the calculated quantities using the effective one-fluid model. With an increase in the ratio of the well depth of the components of the binary mixture, the deviation of the results of calculations by the vdW1f model from the results of the exact simulation of the binary mixture increases. Thus, the use of the vdW1f model for thermodynamic modeling of multicomponent systems can lead to absolutely unrealistic results. Therefore, additional studies are needed on the applicability region of the vdW1f model.

The work was supported by the Russian Science Foundation (project No. 16-19-00188).

References

- [1] Ree F.H. // J. Chem. Phys. 1983. Vol. 78. No. 1. P. 409.
- [2] Victorov S.B., El-Rabii H., Gubin S.A., Maklashova I.V., Bogdanova Yu.A. // Journal of Energetic Materials. 2010. V. 28. P. 35.

- [3] Bogdanova Yu.A., Gubin S.A., Anikeev A.A., Victorov S.B. // Russian Journal of Physical Chemistry A. 2015. Vol. 89. No. 5. P. 741.
- [4] Dodge Barnett F. Chemical Engineering Thermodynamics. NY: McGraw-Hill Book Company, Inc. 1944. 709 p.
- [5] MCCCSTowhee. <http://towhee.sourceforge.net>.
- [6] Metropolis N., Rosenbluth A.W., Rosenbluth M.N., Teller A.H., Teller E. // J. Chem. Phys. 1953. V. 21. P. 1087.
- [7] Martin M.G., Frischknecht A.L. // Mol. Phys. 2006. V. 104. P. 2439.
- [8] Luscher M. // Comp. Phys. Comm. 1994. V. 79. P. 100.
- [9] James F. // Comp. Phys. Comm. 1990. V. 60. P. 329.
- [10] James F. // Comp. Phys. Comm. 1994. V. 79. P. 111

On Inverse Problem of Determination of the Coefficient in Strongly Degenerate Parabolic Equation

T.I. Bukharova^{1,a)}, V.L. Kamynin^{1,b)}, A.P. Tonkikh^{2,c)}

¹*National Research Nuclear University MEPHI*

²*Bryansk State Academician I.G.Petrovski University*

We investigate the unique solvability of the inverse problem of determination of the lower term in the strongly degenerate parabolic equation with two independent variables.

We consider the inverse problem of determination of the pair of functions $\{u(t, x), \gamma(t)\}$ satisfying in the rectangle $Q \equiv [0, T] \times [0, l]$ the equation

$$u_t - a(t, x)u_{xx} + b(t, x)u_x + \gamma(t)u = f(t, x), \quad (1)$$

with initial and boundary conditions

$$u(0, x) = u_0(x), \quad x \in [0, l], \quad u(t, l) = 0, \quad t \in [0, T], \quad (2)$$

and additional condition of integral observation

$$\int_0^l u(t, x)\omega(x)dx = \varphi(t), \quad t \in [0, T]. \quad (3)$$

^{a)}Email: vlkamynin@mephi.ru

^{b)}Email: bukharova_t@mail.ru

^{c)}Email: a_tonkih@mail.ru

We suppose that the input data functions of the problem (10)–(3) are measurable and satisfy the conditions

$$x^2 a_1 \leq a(t, x) \leq a_2, (t, x) \in Q; \quad a_1, a_2 = \text{const} > 0;$$

$$a_x(t, x), \frac{a_x^2(t, x)}{a(t, x)} \in L_\infty(Q); \quad a(t, 0) = 0, t \in [0, T]; \quad (A)$$

$$\frac{b^2(t, x)}{a(t, x)} \in L_\infty(Q), \frac{f^2(t, x)}{a(t, x)} \in L_1(Q), f(t, x) \in L_\infty(0, T; L_1(0, l)); \quad (B)$$

$$\omega(x) \in W_2^1(0, l), \omega(l) = 0, (a\omega)_x, (a\omega)_{xx}, (b\omega)_x \in L_\infty(0, T; L_2(0, l)); \quad (C)$$

$$\varphi(t) \in W_\infty^1(0, T), |\varphi(t)| \geq \varphi_0 > 0, t \in [0, T]; \quad (D)$$

$$u_0(x) \in W_2^1(0, l), \varphi(0) = \int_0^l u_0(x)\omega(x)dx. \quad (E)$$

We note that, in view of the assumption (A) we can consider as an equation (1) the well-known Black-Scholes equation which is widely used in financial mathematics.

Definition. Generalized solution of the inverse problem (1)–(3) is a pair of functions $\{u(t, x), \gamma(t)\}$ such that

- 1) $u(t, x) \in L_\infty(0, T; W_2^1(0, l)) \cap C^{0,\beta}(Q), \beta = \text{const} \in (0, 1), u_t \in L_2(Q),$
 $au_{xx} \in L_1(Q), u_{xx} \in L_2(Q^\delta) \forall \delta > 0, \text{ where } Q^\delta = [0, T] \times [\delta, l]; \gamma(t) \in L_\infty(0, T);$
- 2) this pair satisfies the equation (1) a.e. in Q ;
- 3) the function $u(t, x)$ satisfies the conditions (2),(3) in classical sense.

Theorem 1. Let the conditions (A) – (E) hold. Then there are no two different generalized solutions of the inverse problem (1)–(3).

Theorem 2. Let the conditions (A) – (E) hold. Suppose that T is less than the constant which is written explicitly through the input data functions. Then there exists a generalized solution $\{u(t, x), \gamma(t)\}$ of the problem (1)–(3) and function $u(t, x)$ satisfies the boundary condition $u(0, x) = 0$.

The first and second authors were partially supported by the Programm of Competitiveness Increase of the National Research Nuclear University MEPhI (Moscow Engineering Physics Institute); contract No 02.a03.21.0005,27.08.2013.

Dependence of micromobility of dental implants on its thread geometry

I.N. Dashevskiy^{1,a)}

¹*Ishlinsky Institute for Problems in Mechanics of the Russian Academy of Sciences*

The effect of the profile, pitch and depth of thread on the primary stability of dental implants was studied. With the same occlusal load values and observed macromobility of the implant the thread characteristics can change micromobility on the implant-bone interface by times. Minimal local displacements were obtained for the square and dovetail profiles. Maximum of local displacements was observed at the apex thread turn.

^{a)}Email: dash@ipmnet.ru

One of the key factors in the success of dental implantation is osseointegration [1] – intergrowth of the implant with the bone. Excessive micromobility on the implant-bone interface at loading violates the osseointegration. A natural question arises: is it possible to minimize micromobility by controlling the structural characteristics of the implant, in particular, of the threads?

The effect of the thread characteristics (and conditions on the interface implant-bone) on the stability of dental implants was studied in a number of papers [2-4]. In this paper, the emphasis is on studying the effect of thread characteristics (profile, depth and thread pitch) on the stability of dental implants under immediate loading (primary stability), when osseointegration has not yet occurred and there is no complete adhesion at the implant-bone interface. Implant was modeled by a ribbed cylinder flush with the half-space surface, the slip condition was set on the implant-bone interface, typical values for the load, geometric and mechanical characteristics of the bone and implant were taken. Calculations were carried out in ANSYS.

The change in the thread profile was modeled by the variation in the slope angle of the profile sides with a successive transition from the triangular through the trapezoidal and square threads to the dovetail thread. With this, the implant subsidence (global mobility) varied little (a fraction of a percent). At the same time, the maximums of local displacements (that is of relative displacements of mutual points on the implant-bone interface) – and namely they affect osseointegration – could vary at times (with a general tendency to fall) with this change in the profile of the thread (Fig. 1). Apparently, this is due to the increase in the engagement and, consequently, in constraint of movements on the faces of the thread. Minima of maximum displacements were obtained for the square and dovetail profiles. Their values were microns, which corresponds to the results of other authors. In this case, the displacements values grew monotonically from the last thread turn to the first (apex) one and the maximum was invariably observed at the first (apex) thread turn.

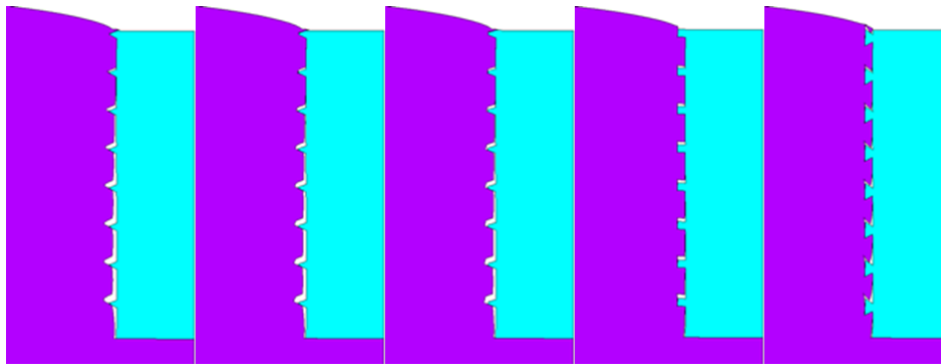


Fig. 1: Evolution of the displacements pattern at the interface of a dental implant and bone versus thread profile under vertical loading

The effect of the thread depth and pitch was studied on a square profile. It turned out that an increase in the thread depth from 0.1 to 0.4 mm (as well as reducing the thread pitch from 2.0 to 0.4 mm) led to a decrease in the implant sediment by 3-6

The study was carried out together with PS Shushpannikov on the theme of the state assignment (state registration number AAAA-A17-117021310386-3) and with partial support of RFBR grants No. 17-08-01579 and No. 17-08-01312.

References

- [1] Misch CE, Perel ML, Wang HL, et al., Implant success, survival, and failure: the International Congress of Oral Implantologists (ICOI) Pisa Consensus Conference // *Implant Dent.*, 2008 Mar, Vol. 17. № 1. P. 5-15.
- [2] Rajiv. S. Jadhav, Prof. P. N. Dhattrak, Dr. S. Y. Gajjal, A review: Mechanical Design of Dental Implants to Reduce Stresses around Implant-Bone Interface // *International Journal of New Technologies in Science and Engineering*, Vol. 2, Issue 2, Aug 2015, 142-146
- [3] Huang HL, Hsu JT, Fuh LJ, Tu MG, Ko CC, Shen YW. Bone stress and interfacial sliding analysis of implant designs on an immediately loaded maxillary implant: a non-linear finite element study. *J Dent* 2008;36:409–17.
- [4] Satoshi Horita, Tsutomu Sugiura, Kazuhiko Yamamoto, Kazuhiro Murakami, Yuichiro Imai, Tadaaki Kirita. Biomechanical analysis of immediately loaded implants according to the “All-on-Four” concept. *journal of prosthodontic research* 61 (2017) 123–132.

On personification of the evaluation of stress-strain state in a mandible according to CT data for different dental implantation schemes

I.N. Dashevskiy^{1,a)}, D.A. Gribov^{1,b)}

¹*Ishlinsky Institute for Problems in Mechanics of the Russian Academy of Sciences*

A computer simulation of orthopedic rehabilitation planning for a patient 67 years old with implants placement onto the edentulous mandible was carried out. The material of implants and dentures (titanium or zirconium dioxide) had little effect on the stress-strain state of bone tissue. Increased osseointegration (modeled by increasing friction from full slip to full adhesion) led to a decrease in the concentration of both stresses and displacements. Oblique loads were more dangerous than vertical ones, loading in the lateral part of the artificial dentition – more dangerous than in the frontal compartment. Comparison of different implantation schemes showed that an increase in the number of implants somewhat smoothed the concentration of both stresses and displacements in bone tissues.

Individualization of medical treat is one of the hot points of today’s medicine including implant dentistry [1]. A computer simulation of orthopedic rehabilitation planning [2] for a patient 67 years old with implants placement onto the edentulous mandible was carried out.

In order to optimize the distribution of functional stresses in the bone tissue around the implants, as well as in prosthetic structures, several implantation schemes were considered with different number of implants. Implants computer models were created according to the data given in the accompanying documentation, as well as from the results of direct measurements. To personalize the diagnostic data, mandible cone-beam computerized tomography was done with the dental tomograph Galileos (Sirona). Image processing, including segmentation, creation of

^{a)}Email: dash@ipmnet.ru

^{b)}Email: denis4@inbox.ru

a three-dimensional triangulated surface model and a tetrahedral grid, was carried out in the MIMICS program complex [3] (Fig. 1). The model obtained was supplemented with implants models and passed on to the finite-element complex ANSYS, where numerical simulation was carried out.

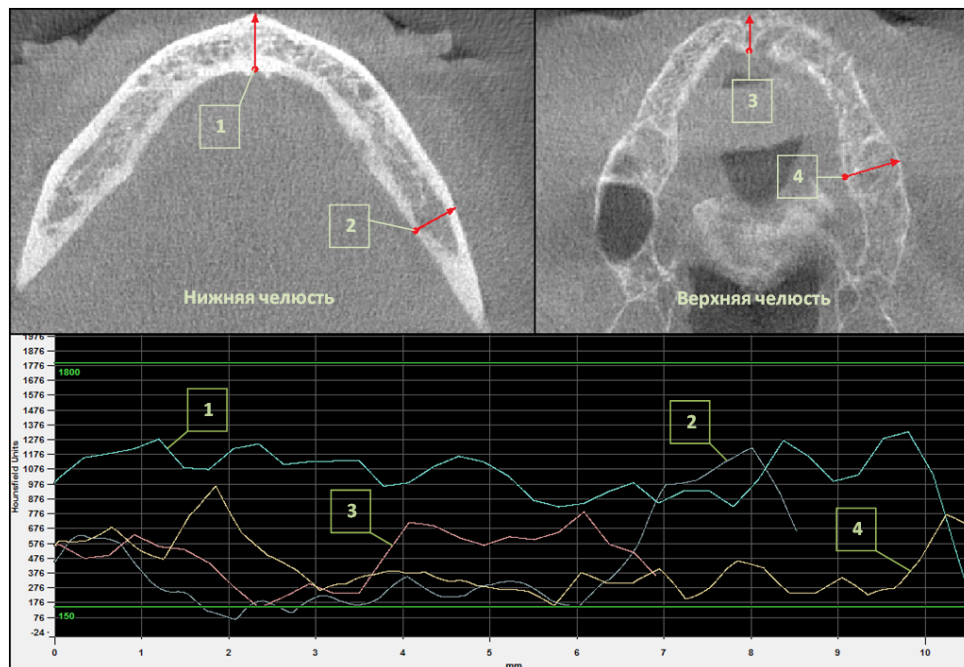


Fig. 1: Determination of the x-ray density of the mandible

Titanium and zirconium dioxide implants 10-11 mm long and 3.5 mm in diameter were taken. For removable dentures schemes were studied on a beam with a semi labile fixation and with rigid locking fastening to the beam, fixed dentures were provided with small cantilevers. Different loading schemes were considered, corresponding to central (nibble) and one-sided (chewing) occlusion. Central occlusion was modeled by applying vertical or oblique loads to two central implants. There were cases of complete (adhesion on the implant-bone interface) and incomplete (sliding or friction on the interface) osseointegration.

Areas of stress concentration in the bone in all cases arose at the thread tops and carvings, and especially in the vicinity of the implant neck (platform). Micromotions (relative displacement of corresponding points on the implant-bone interface) in the case of complete osseointegration were absent, while for incomplete osseointegration (primary stability) the maximum micromotions appeared on the first (apex) thread. The material of implants and dentures (titanium or zirconium dioxide) had little effect on the stress-strain state of bone tissue. Increased osseointegration (modeled by increasing friction from full slip to full adhesion) led to a decrease in the concentration of both stresses and displacements. Oblique loads were more dangerous than vertical ones, loading in the lateral part of the artificial dentition – more dangerous than in the frontal compartment. Comparison of different implantation schemes showed that an increase in the number of implants somewhat smoothed the concentration of both stresses and displacements in bone tissues.

The study was carried out on the theme of the state assignment (state registration number AAAA-A17-117021310386-3) and with partial support of RFBR grants No. 17-08-01579 and No. 17-08-01312.

References

- [1] Misch C.E. Contemporary Implant Dentistry. 3rd Edition, Elsevier MOSBY, 2007, 1120 p.
- [2] Elnaz Moslehifard (2011). Computer Aided Techniques Developed for Diagnosis and Treatment Planning in Implantology, Implant Dentistry - The Most Promising Discipline of Dentistry, Prof. Ilser Turkyilmaz (Ed.), ISBN: 978-953-307-481-8, InTech, Available from: <http://www.intechopen.com/books/implant-dentistry-the-most-promising-discipline-of-dentistry/computer-aided-techniques-developed-for-diagnosis-and-treatment-planning-in-implantology>
- [3] <http://www.materialise.com/en/medical/software/mimics>

Governing Equations of the Thermoelastoplasticity in Toroidal Coordinates

E.P. Dats^{1,a)}, E.V. Murashkin^{2,3,b)}

¹*Vladivostok State University of Economics and Service*

²*Ishlinskiy Institute for Problems in Mechanics RAS*

³*National Research Nuclear University MEPhI*

A governing system of equations for the theory of thermal stresses in a toroidal coordinate system is obtained. The boundary value problems for thermoelasticplastic solids with toroidal symmetry properties are considered. A solution is presented for the problem of thermoelastic toroid deformation under conditions of uniform thermal expansion.

The toroidal coordinate system is widely used for mathematical simulations of processes occurring in solids with geometrical properties possessing the toroidal symmetry. For example in astrophysics, toroidal coordinates naturally define the geometry of spiralling galaxies and allow us to investigate their dynamics and evolution. For another hand in thermonuclear physics, toroidal chambers with magnetic coils are the main objects for studying the processes of thermonuclear fusion. The magnetohydrodynamics governing equations simulating the behavior of the plasma are often written in toroidal coordinates [1]. The toroidal coordinates can be used in the study of the magnetic accelerators exploitation [2]. The calculation of the stress–strain state characteristics of the solids having a toroidal shape is the actual problem of applied science and technology [3].

One of the sections of solid mechanics that attract the attention of scientists and engineers is the theory of thermoelastoplasticity, which makes it possible to simulate the processes of deformation in a solid material subject to the influence of a thermal gradient. The analytical solutions of a number of boundary value problems in the frameworks of thermal stresses theory and under conditions of axisymmetric thermal action were early obtained taking into account the plastic properties of the material. In depth studies of the problems of the residual strains and stresses under conditions of spherical symmetry for an elastoplastic material under nonstationary thermal action are carried out in [4, 5]. The solutions for stresses and displacements fields in

^{a)}Email: dats@dvo.ru

^{b)}Email: evmurashkin@gmail.com

elastoplastic material under conditions of axial symmetry in cylindrical coordinates are obtained in [6, 7, 8, 9, 10, 11]. Specific features of the stress–strain state calculation in the case of a plane stress of plane strain hypotheses were found for materials with the yield stress depending on temperature. Investigation of the stress–strain state of the material under toroidal symmetry conditions promotes the further development of the theory of temperature stresses and can generalize the early results.

The system of equilibrium equations can be furnished in the following form

$$\begin{aligned} \sigma_{rr,r} + \frac{\sigma_{r\theta,\theta}}{r} + \frac{\sigma_{r\varphi,\varphi}}{R_0 + r \sin(\theta)} + \frac{\sigma_{rr} - \sigma_{\theta\theta}}{r} + \frac{\sin(\theta)}{R_0 + r \sin(\theta)}(\sigma_{rr} - \sigma_{\varphi\varphi} + ctg(\sigma_{r\theta})) &= 0, \\ \sigma_{r\theta,r} + \frac{\sigma_{\theta\theta,\theta}}{r} + \frac{\sigma_{\theta\varphi,\varphi}}{(R_0 + r \sin(\theta))} + \frac{2\sigma_{r\theta}}{r} + \frac{\sin(\theta)}{R_0 + r \sin(\theta)}(\sigma_{r\theta} + ctg(\theta)(\sigma_{\theta\theta} - \sigma_{\varphi\varphi})) &= 0, \quad (1) \\ \sigma_{r\varphi,r} + \frac{\sigma_{\theta\varphi,\theta}}{r} + \frac{\sigma_{\varphi\varphi,\varphi}}{R_0 + r \sin(\theta)} + \frac{\sigma_{r\varphi}}{r} + \frac{2 \sin(\theta)}{R_0 + r \sin(\theta)}(\sigma_{r\varphi} + ctg(\theta)\sigma_{\theta\varphi}) &= 0 \end{aligned}$$

It is assumed that the effect of deformation processes on the variation of the temperature field is negligible in the framework of the theory of thermal stresses. Thus the stress-strain state is determined by a prescribed temperature distribution. The stationary heat conduct equation in toroidal coordinates reads by

$$T_{,rr} + \frac{(R_0 + 2r \sin(\theta))T_{,r}}{r(R_0 + r \sin(\theta))} + \frac{T_{,\theta\theta}}{r^2} + \frac{\cos(\theta)T_{,\theta}}{r(R_0 + r \sin(\theta))} + \frac{T_{,\varphi\varphi}}{(R_0 + r \sin(\theta))^2} = 0 \quad (2)$$

Among the methods for the reduced system of equations solving one can chose the expansion in a series on the parameter $\epsilon = r_0/R_0$ [12]. In many calculations this parameter can be considered as small. Value ϵ arises in the presented system of equations with the dimensionless radial coordinate $r = r/r_0$. As an example, we give the simplest solution for a torus with a uniform heating to a temperature T_m . This solution implies that even in the trivial case the solution is two-dimensional with following stress–strain state parameters

$$\begin{aligned} u_r(r, \theta) = \alpha(T_m - T_0)(r + R_0 \sin(\theta)), \quad u_\theta = \alpha(T_m - T_0)R_0 \cos(\theta), \quad u_\varphi = 0, \\ \sigma_{rr} = \sigma_{\varphi\varphi} = \sigma_{\theta\theta} = 0, \quad e_{rr} = e_{\varphi\varphi} = e_{\theta\theta} = \alpha(T_m - T_0) \end{aligned} \quad (3)$$

The nondiagonal components of stress and strain tensors are vanished. T_0 is the referential temperature of the torus at which no deformations are assumed, α is the linear thermal expansion coefficient. Numerical analysis of displacements in the hollow torus occupying domain $r_1 < r < r_2$ under the nonuniform thermal expansion of ($T(r_1) \neq T(r_2)$) shows that the angular displacement can be approximated for the parameter $\epsilon > 5$ by an expression obtained in (3) if we use for the temperature T_m the value of the mean temperature of the torus determined by the following equation

$$\bar{T} = \frac{1}{\pi R_0(r_2^2 - r_1^2)} \int_0^{2\pi} \int_{r_1}^{r_2} T(\rho, \theta) \rho (R_0 + \rho \sin(\theta)) d\rho d\theta \quad (4)$$

The present study is supported by the Federal Agency for Scientific Organizations (State Registration Number AAAA-A17-117021310381-8) and by the Russian Foundation for Basic Research financially (project No. 18-51-05012, 18-01-00844, 17-51-45054, 17-01-00712).

References

- [1] Dini F, Baghdadi R, Amrollahi R and Khorasani S, An Overview of Plasma Confinement in Toroidal Systems //Glow Discharges and Tokamaks. №4. 2010. pp. 159-279.

- [2] Schnizer P, Fischer E and Schnizer B, Cylindrical Circular and Elliptical, Toroidal Circular and Elliptical Multipoles Fields, Potentials and their Measurement for Accelerator Magnets // arXiv:1410.8090 [physics.acc-ph]. 2014.
- [3] Sun B, Closed-Form Solution of Axisymmetric Slender Elastic Toroidal Shells // Journal of Engineering Mechanics. № 136. 2010 pp. 1281 -1288
- [4] Dats E, Murashkin E and Velmurugan R, Calculation of irreversible deformations in a hollow elasto-plastic ball under unsteady thermal action // Bulletin of Yakovlev Chuvash State Pedagogical University. Series: Mechanics of Limit State . 2015. № 25. pp. 168–175. [in Russian]
- [5] Dats E and Murashkin E, Thermoelastoplastic Deformation of a Multilayer Ball // Mechanics of Solids. 2017. № 52. pp. 187–193. 187–193
- [6] Dats E, Mokrin S and Murashkin E, Calculation of the residual stresses of hollow cylinder under unsteady thermal action // Lecture Notes in Engineering and Computer Science. 2015. № 2218. pp. 1043–1046.
- [7] Dats E, Mokrin S and Murashkin E, Calculation of the residual stress field of the thin circular plate under unsteady thermal action // Key Engineering Materials. 2016. № 685. pp. 37–41
- [8] Dats E, Murashkin E and Stadnik N, On a Multi-Physics Modelling Framework for Thermo-elastic-plastic Materials Processing // Procedia Manufacturing. 2017 №7. pp. 427–434.
- [9] Dats E and Murashkin E, On unsteady heat effect in center of the elastic-plastic disk // Lecture Notes in Engineering and Computer Science. 2016. № 2223. pp. 69–72.
- [10] Dats E, Murashkin E and Stadnik N , On Heating of Thin Circular Elastic-plastic Plate with the Yield Stress Depending on Temperature // Procedia Engineering . 2017 . №173. pp. 891–896.
- [11] Burenin A, Dats E and Murashkin E, Formation of the residual stress field under local thermal actions // Mechanics of Solids . 2014. № 49. pp. 218–224.
- [12] G. Kutsenko, Axisymmetric Deformation of a Thick-Walled Toroidal Shell // Prikladnaya Mehanika. 1964. pp 27-30.

Computation of potential of a single layer for Helmholtz equation in three-dimensional case by quadrature formulas of increased accuracy

A.D. Fedotova^{1,a)}, V.V. Kolybasova^{1,b)}, P.A. Krutitskii^{2,c)}

¹*Lomonosov Moscow State University*

²*Keldysh Institute of Applied Mathematics*

^{a)}Email: nyonk@mail.ru

^{b)}Email: kolybasova@physics.msu.ru

^{c)}Email: krutitsk@mail.ru

In this paper we present algorithm for calculating the potential of a single layer with increased accuracy on the basis of the quadrature formulas obtained in the course work of B.E. Gonochenko. Also the accuracy is estimated.

As is known, when solving boundary value problems for the Laplace and Helmholtz equations the method of reducing them to integral equations along the boundary of the region is used [1]. For this, the solution is sought in the form of a single or double layer potential or in the form of a linear combination of them (also sometimes the angular potential in the two-dimensional case and the bulk potential are used). The density of the potential is found from the integral equation at the boundary of the region.

In particular, let us consider the potential of a single layer. For the Laplace equation $\Delta w = 0$ in the three-dimensional case, it has the form

$$V(x) = \frac{1}{4\pi} \iint_{\Phi} \frac{\sigma(y) dS_y}{R_{xy}},$$

where Φ is a smooth closed surface, x is a point not lying on the surface Φ , y is point lying on the surface Φ , R_{xy} is the distance between points x and y , $\sigma(y)$ is the density of the potential.

For the Helmholtz equation $\Delta w + k^2 w = 0$ in the three-dimensional case the potential of a single layer has the form

$$V(x) = \frac{1}{4\pi} \iint_{\Phi} \frac{\sigma(y) e^{ikR_{xy}} dS_y}{R_{xy}}.$$

With the approximate calculation of the potential of a single layer the following problem arises. The kernel of the potential of a single layer is a singular function, i.e. tends to infinity with $x \rightarrow y$. At the same time, the potential of a single layer $V(x)$ is continuous when passing through the surface Φ . Hence, if one calculates the potential of a single layer by discretizing the surface and using standard quadrature formulas the error will increase sharply if the observation point x is near the surface Φ (the approximate solution will tend to infinity when the exact solution is finite).

To avoid this problem and obtain a uniform approximation in the region D of the single layer potential is possible if one singles out the main (singular) part of the single-layer potential and calculates the integral for it exactly at each part of the discretization of the surface Φ . In this case the main parts of the single-layer potential for the Laplace equation and for the Helmholtz equation are equal and therefore the results can be used both for solving boundary value problems for the Laplace equation and for solving boundary value problems for the Helmholtz equation. We note that the same approach is also suitable for approximate calculation of the potential of a double layer and for an approximate solution of integral equations on the boundary of a region into which direct values of potential on the surface Φ are included.

In the two-dimensional case, this approach was implemented in [2] where exact quadrature formulas for solving the skew-derivative problem for the Laplace equation in the exterior of an open arc were constructed. Examples of numerical calculations in [2] show that these formulas really make it possible to achieve high accuracy uniformly throughout the region.

In this paper we calculated the potential for the Laplace equation and the Helmholtz equation by the quadrature formulas of increased accuracy for the cases when the surface is a sphere, an ellipsoid of rotation and a rectangle. Dependences of the potential from different coordinates and equipotential contours for the Laplace equation were plotted. In the case of a spherical surface these dependencies were compared with theoretical ones. It was found that the deviation from the theoretical values is proportional to the square of the step of the discretization. A table of relative errors for different discretizations and distances from the center of the sphere was made.

References

- [1] *A.N. Tikhonov, A.A. Samarskii. Equations of Mathematical Physics. — M.: MSU, 2004. — p. 798.*
- [2] *P. A. Krutitskii, D. Y. Kwak, Y. K. Hyon. Numerical treatment of a skew-derivative problem for the Laplace equation in the exterior of an open arc. Journal of Engineering Mathematics. (2007) v. 59, p. 25-60.*

An approximate analytical solution for the shock wave structure in a duct with a pseudo-perforated wall

S.V. Gorkunov^{1,a)}, Y.A. Bogdanova^{1,b)}, A.V. Karabulin^{1,c)}

¹*National Research Nuclear University MEPhI (Moscow Engineering Physics Institute)*

An approximate analytical solution is obtained for the shock tube problem in a rectangular duct with an array of rectangular grooves in the lower wall. The analytical solution is based on the approximate quasi-1D shock adiabat for a shock wave that propagates in a channel with periodically located barriers. This problem is also studied numerically. It is found that the approximate analytical solution correctly predicts the propagation velocity of the leading discontinuity and the flow parameters at this discontinuity. The leading gas-dynamic discontinuity is followed by a relaxation zone in which there are long-wave and short-wave flow oscillations. These oscillations are caused by waves arising from the interaction of the flow behind the leading shock wave with the side and bottom walls of the grooves. An approximate analytical solution allows one to obtain the values of the flow parameters at the end of the relaxation zone. These values are in good agreement with the numerical calculation.

The present work is devoted to the study of the propagation of shock waves in a duct with grooves (a pseudo-perforated wall). The computational model is shown in Figure 1. The channel consists of two sections. On the right side of the channel there are grooves in the lower channel wall. The wall is smooth in the left part of the channel.

At the initial instant of time, for $x < 0$, the gas has parameters P_3 , $v_3 = 0$ and ρ_3 and the parameters P_0 , $v_0 = 0$, ρ_0 for $x \geq 0$. Here P is the pressure, v is the velocity, and ρ is the gas density. The normal component of the velocity of the gas is zero at the gas-channel-wall and gas-groove-wall boundaries. Adhesion on the walls is absent. The basic equations governing the propagation of a shock wave along a pseudo-perforated tube are as follows

$$\frac{\partial}{\partial t} \begin{bmatrix} \rho \\ \rho v_i \\ \rho E \end{bmatrix} + \frac{\partial}{\partial x_j} \begin{bmatrix} \rho v_j \\ \rho v_i v_j \\ (\rho E + P)v_j \end{bmatrix} = 0, \quad E = e + \frac{|v|^2}{2}, \quad e = \frac{P}{(\gamma - 1)\rho}, \quad (1)$$

^{a)}Email: gorkunov.ser@gmail.com

^{b)}Email: yabogdanova@mephi.ru

^{c)}Email: avkarabulin@mephi.ru

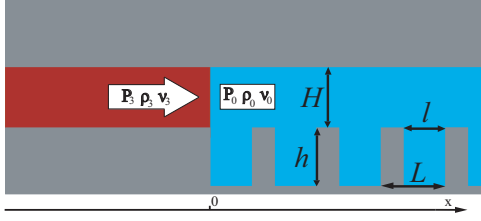


Fig. 1: Geometry of the problem.

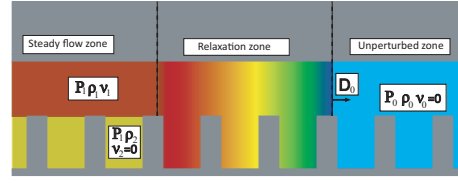


Fig. 2: Division of the flow into zones used to obtain approximate formulas for the discontinuity structure.

where E is the total specific energy of the gas and e is the specific internal energy.

It was found in [6] that, from the point of view of large spatial scales, a complex consisting of a leading gas-dynamic discontinuity and a relaxation zone can be considered as a discontinuity with the structure, and an effective shock adiabat for such a discontinuity is obtained. The presence of a relatively narrow zone in which a nonmonotonic change in the flow parameters occurs to a certain constant value is characteristic of the structure of discontinuities in the presence of dispersion and dissipation [1, 2, 3, 4, 5].

According to [6], behind the leading gas-dynamic discontinuity there is a relaxation zone in which the flow parameters change rapidly and nonmonotonically. Behind the zone of relaxation is a zone in which flow parameters change slowly. A diagram of the simplifying separation of the flow into zones and regions is shown in Fig. 2. For the average values of the gas parameters at the end of the relaxation zone, we use the index 1 if the gas is outside the groove and the index is 2 if the gas is inside the groove. It is assumed that $P_1 = P_2$, $v_2 = 0$, $\rho_1 \neq \rho_2$.

The approximate relations for the shock parameters was obtained in [6]. These relations have the form

$$\begin{cases} \rho_0 D_0 + \alpha \rho_0 D_0 + v_1 \rho_1 - \rho_1 D_0 - \alpha \rho_2 D_0 = 0, & \rho_1 v_1 D_0 + \alpha v_1 (\rho_2 - \rho_0) D_0 + P_0 - \rho_1 v_1^2 - P_1 = 0 \\ \frac{(1+\alpha)(P_1 - P_0)}{\gamma - 1} D_0 - \frac{\rho_1 v_1^2}{2} (v_1 - D_0) - \frac{\gamma P_1 v_1}{\gamma - 1} = 0, & \rho_2 = \rho_0 + (1 - \frac{\rho_0}{\rho_1}) P_1 \left(\frac{P_1}{\rho_1} + \frac{(\gamma - 1) v_1^2}{2} \right)^{-1} \end{cases} \quad (2)$$

where $\alpha = hl/(HL)$. The system (2) implicitly determines the dependence of P_1 on v_1 .

For $H = 10$ m, $L = 2$ m, $h = 10$ m, $l = 0.8$ m, $P_0 = 100$ kPa, $\rho_0 = 1.17$ kg/m³, $P_3 = 1$ MPa and $\rho_3 = 11.7$ kg/m³ the system of equations (2) has the solution $P_1 = 235$ kPa, $v_1 = 290$ m/s, $\rho_1 = 2.23$ kg/m³, $\rho_2 = 2.10$ kg/m³ and $D = 451$ m/s.

The pressure profiles at the time $t = 0.96$ s are shown in Figure 3 by lines 4 and 5. The presence of the grooves leads to a decrease in the average velocity of the shock wave by 19% and the overpressure decreases by 17%.

The system of equations (1) was solved by the Godunov-Kolgan method. Figure 3 shows the distribution of the average pressure \bar{P} as a function of the coordinate x .

The flow parameters averaged over the channel cross section have long-wave and short-wave oscillations. These oscillations are not introduced numerically, but are inherent in the solution of the system (1). The amplitude of the oscillations decays with distance from the leading gas-dynamic discontinuity. In the relaxation zone, long-wave pressure oscillations occur near the mean value, which agrees well with the value of P_1 (line 5, in Figure 3) obtained using the analytical approach described above. The appearance of long-wavelength and short-wave oscillations of the flow parameters in the relaxation zone is associated with reflection of the waves from the lower and lateral walls of the groove (Figure 4).

This work was supported by the Russian Science Foundation, project no. 16-19-00188.

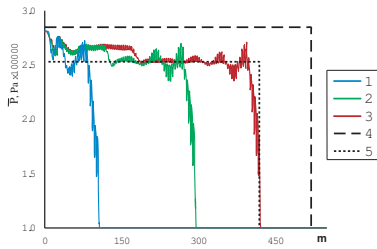


Fig. 3: Numerical (1-3) and analytical (4,5) average pressure distributions at time $t = 0.28$ s (1), 0.69 s (2) and 0.96 s (3,4,5). Line 4 - the duct without grooves, line 5 - the duct with a pseudo-perforated wall.

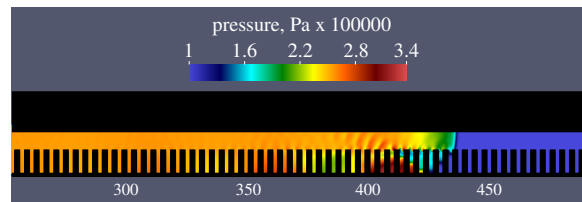


Fig. 4: Pressure field at time $t = 0.96$ s.

References

- [1] Chugainova A.P., Shargatov V.A. // Comput. Math. Math. Phys. 5. 2015.V.55. P.251-263.
- [2] Il'ichev A.T., Chugainova A.P., Shargatov V.A. // Doklady Mathematics. 2015. V.91. P.347-351.
- [3] Chugainova A.P., Shargatov V.A. // Comput. Math. Math. Phys. 5. 2016. V.56. P.263-277
- [4] Kulikovskii A.G., Chugainova A.P., Shargatov V. A. // Comput. Math. Math. Phys. 5. 2016. V.56. P.1355-1362.
- [5] Chugainova A.P., Il'ichev A.T., Kulikovskii A.G. and Shargatov V.A. // J. Appl. Math. 2017. V.82. P.496-525.
- [6] Shargatov V.A., Chugainova A.P., Gorkunov S. V. and. Sumskoi S. I. // Proceedings of the Steklov Institute of Mathematics. 2018.V.300. P.206-218.

The accuracy of the theories based on statistical physics for the thermodynamic modeling of state parameters of dense pure gases (fluids).

S.A. Gubin^{1,a)}, S.B. Victorov²

¹National Research Nuclear University MEPhI (Moscow Engineering Physics Institute), Russia

²OpenSearchServer, Paris, France

The current level of development of statistical mechanics allows to obtain equations of state for pure substances based on the intermolecular interaction potentials. There are three theories that provide the highest accuracy of calculation of the thermodynamic properties of pure fluid (liquid or gas at the supercritical state) in a wide range of pressures and temperatures. Comparison of the accuracy of calculations of the state parameters of substances is performed on the basis of these theories.

^{a)}Email: sagubin@mephi.ru

To date, experimental determination of composition and thermodynamic parameters of complex chemical systems at high pressures and temperatures is extremely difficult and often even impossible. Therefore, a realistic thermodynamic simulation quasi-equilibrium processes in this range of thermodynamic conditions is of considerable scientific and practical interest including problems of detonation and shock waves, geophysics, astrophysics, etc.

Today there are three theories that provide the highest accuracy of calculation of thermodynamic properties of one-component fluid (liquid or gas in the supercritical state), molecules which interact with a given spherically symmetric potential, in a wide range of pressures and temperatures, including the range of high densities. These are variational perturbation theory MCRSR[1], HMSA integral equation[2] and the KLRR perturbation theory[3]. These theories were developed on the basis of statistical physics and have a deep physical basis. The equations of state models (EOS), developed on the basis of these theories are theoretically substantiated too. The application of the potential theories allows to get a much more reliable EOS for fluids, compared with empirical equations.

These theories allow to calculate the thermodynamic properties of substances in different phase state (gas, liquid and solid) in agreement with the Monte Carlo (MC) data a hundred times faster MC calculations and molecular modeling (MD). Therefore, computer codes based on these theories are developed for thermodynamic calculations in a wide region of pressures and temperatures.

These theories calculations are consistent with a direct computer Monte Carlo simulation (computer experiment) that allows to accurately calculate thermodynamic properties of systems of molecules with interacting with each other with a given intermolecular potential and to assess the accuracy of the considered theories.

Nowadays, we have developed models of the EOS of the fluid phase on the basis of improved KLRR perturbation theory[4] and integral equations HSMA/C [2]. In this work the variational theory was developed in two ways using the function proposed in [1] to correct for excess Helmholtz energy in such a way that the pressure and internal energy are in good agreement with the results of computer simulation Monte Carlo and without this function. Now it is possible to compare the statistics of the deviations of calculations of the thermodynamic properties of one-component fluid from the MC data on the best three theories and determine the most accurate theory. There are assumed that the interaction of molecules is described by spherically symmetric potential, Exp-6 in all three theories.

In the variational theories of the perturbations of the excess Helmholtz energy is minimized by variation of the diameter of hard spheres at fixed temperature T , specific volume V and number of particles N . The value of the hard-sphere diameter d is determined by minimization of the excess Helmholtz energy with the use of assumptions made in [1].

In the developed theory MCRSR multiple numerical integration and differentiation leads to significant costs in computer time in the developed theory. But of course, these costs are not comparable with the required time for MC and MD.

The computer program calculation of thermodynamic properties of one component fluids has been developed based on the methodology MCRSR. The results of calculations were compared with the MC data (see table 1).

MCRSR theory provides a satisfactory agreement with calculations of Monte Carlo for a wide class of intermolecular potentials, especially, for the interesting us potential of Exp-6. This theory has been implemented in the computer code CHEQ [5], which was developed at Lawrence Livermore lab in the U.S. and in the French code CARTE [6].

Calculations show that the semiempirical term Ross significantly improves the agreement between theory MCRSR and MC simulation data. Even using this semi-empirical term Ross theory MCRSR is less accurate compared to an improved version of the KLRR[1]. Comparison

Table 1: The statistics of the relative deviations calculated in this work values of the dimensionless pressure, Z and the dimensionless excess internal energy U^* , on the base theories MCRSR, HMSA/C and an improved version of the KLRR [4] of fluid with the potential Exp-6 from the MC results [2].

Method	Phver 55 MC points:		Over 19 MC points for $\alpha = 11.5$		Over 18 MC points for $\alpha = 13.5$		Over 18 MC points for $\alpha = 15.5$	
	$\delta Z, \%$	$\delta U^*, \%$	$\delta Z, \%$	$\delta U^*, \%$	$\delta Z, \%$	$\delta U^*, \%$	$\delta Z, \%$	$\delta U^*, \%$
Relative average deviation, %								
KLRR	0.60	0.87	0.55	0.60	0.50	0.75	0.75	1.26
MCRSR	2.07	2.46	2.92	1.87	1.78	2.29	1.52	3.24
HMSA/P \ddot{Y}	0.72	1.89	0.46	1.19	0.72	1.69	0.98	2.85
Relative rms deviation, %								
KLRR	0.90	1.44	0.62	0.76	0.56	0.99	1.32	2.16
MCRSR	2.33	3.29	3.10	2.14	1.86	2.85	1.79	4.45
HMSA/C	0.84	3.64	0.54	1.32	0.80	2.28	1.10	5.78
Relative maximum deviation, %								
KLRR	5.30	7.00	1.48	1.72	1.05	2.96	5.30	7.00
MCRSR	5.06	11.56	4.11	3.87	2.40	4.82	5.06	11.56
HMSA/C	2.43	23.42	1.08	2.20	1.63	7.62	2.43	23.42

of calculations of dimensionless deviations of pressure and internal energy from MC data on these three theories give similar results (table 1).

However, the improved version of the calculations on the base of the KLRR perturbation theory[4] are more accurate than the integral equations HMSA/C [2] and variational theory MCRSR [1] calculations. It follows from the table 1. This conclusion is confirmed by [7]

This work is supported by the Russian Science Foundation under grant 16-19-00188.

References

- [1] Ross M. // J. Chem. Phys. 1979. V. 71. No. 4. P. 1567.
- [2] Fried L.E., Howard W.M. // J. Chem. Phys. 1998. V. 109. No. 17. P. 7338.
- [3] Kang H.S., Lee C.S., Ree T., Ree F.H. // J. Chem. Phys. 1985. V. 82. No. 1. P. 414.
- [4] Victorov S.B., Gubin S.A. // Proc. 13th Int. Detonation Symp. 2006. P. 13.1118.
- [5] Ree F.H. // J. Chem. Phys. 1984. V. 81. No. 3. P. 1251.
- [6] Dubois V., Desbiens N., Auroux E. // Chemical Physics Letters. 2010. V. 494. P. 306.
- [7] Desbiens N. and Dubois V. // EPJ Web of Conferences. 2010. V. 10. P. 00013.

Axial closed form texture component approximating the canonical normal distribution

T.M. Ivanova^{1,a)}

¹*National Research Nuclear University MEPhI*

Easily calculated texture components are necessary for solving problems of quantitative texture analysis. In the present work we obtain closed form approximation for the axial component of the canonical normal distribution on $SO(3)$ with central and non-central scattering.

Modeling and interpreting the texture of polycrystalline materials by the method of texture components is based on the use of standard functions [1]. The latter describe the shape, position in the orientation space and the scattering of texture components. The texture components in the form of the canonical normal distribution on the rotation group $SO(3)$ are widely used [2]-[4].

The peak component of the canonical normal distribution is represented by the series

$$f^{peak}(g, g_0, \varepsilon^2) = \sum_{l=0}^{\infty} (2l+1) \exp(-l(l+1)\varepsilon^2) \frac{\sin(2l+1)\frac{\omega}{2}}{\sin\frac{\omega}{2}}, \quad \cos\omega = 0.5 (\text{Sp}(g_0^{-1}g) - 1), \quad (1)$$

while the axial component with the axis \vec{n}_A has the form

$$f^{axial}(g, g_0, \varepsilon^2, \vec{n}_A) = \sum_{l=0}^{\infty} (2l+1) \exp(-l(l+1)\varepsilon^2) P_l((g_0\vec{n}_A, g\vec{n}_A)). \quad (2)$$

The use of texture components of the form (1),(2) is associated with the high complexity of calculations and the need to truncate the series depending on the sharpness of the texture.

Closed form approximation for the distribution (1) was proposed in [5]. In the present work we obtain closed form approximation for the distribution (2). For the central canonical normal distribution it has the form

$$f_{approx}^{axial}(g, g_0, \varepsilon^2, \vec{n}_A) = \frac{\frac{1}{\varepsilon^2} + \frac{1}{2} \left(1 - [\vec{n}_A, \vec{n}]^2 \sin^2 \frac{\omega}{2}\right)}{\left(1 - [\vec{n}_A, \vec{n}]^2 \sin^2 \frac{\omega}{2}\right)^{3/2}} \exp\left\{-\frac{1}{\varepsilon^2} \frac{[\vec{n}_A, \vec{n}]^2 \sin^2 \frac{\omega}{2}}{1 - [\vec{n}_A, \vec{n}]^2 \sin^2 \frac{\omega}{2}}\right\},$$

$$g_0^{-1}g = [\vec{n}, \omega], \quad \cos\omega = 0.5 (\text{Sp}(g_0^{-1}g) - 1).$$

In particular, if $\vec{n}_A = \{001\}$ then

$$f_{approx}^{axial}(g, g_0, \varepsilon^2) = \frac{\frac{1}{\varepsilon^2} + \frac{1}{2} \cos^2 \frac{\beta}{2}}{\cos^3 \frac{\beta}{2}} \exp\left\{-\frac{1}{\varepsilon^2} \tan^2 \frac{\beta}{2}\right\}, \quad \beta = \beta(g_0^{-1}g).$$

It should be noted that the closed form approximation for the axial component is constructed not only for the central normal distribution (2), but also for the normal distribution with non-central scattering, which coefficients can be found only numerically.

References

- [1] Bunge H J 1982 *Texture Analysis in Material Science* (Butterworths:London)

^{a)}Email: ivatatiana@gmail.com

- [2] Ivanova T M and Savelova T I 2006 Robust method of approximating the orientation distribution function by canonical normal distributions *Phys. Met. Metallog.* 101 N2 114–118
- [3] Ivanova T M and Serebryany V N 2017 Methods of recovering orientation distribution function using texture components with a circular normal distribution *Indust. Lab.* 83 I-1 43–47
- [4] Ivanova T M Savyolova T I and Sypchenko M V 2010 The modified component method for calculation of orientation distribution function from pole figures *Inverse Problems in Science and Engineering* 18 N1 163–171
- [5] Ivanova T M and Nikolayev D I 2001 New Standard Function for Quantitative Texture Analysis *Physica Status Solidi* 228 N3 825–836

Determination of the right-hand term in degenerate parabolic equation with two independent variables

V.L. Kamynin^{1,a)}, A.B. Kostin^{1,b)}

¹*National Research Nuclear University MEPhI (Moscow Engineering Physics Institute)*

We find two type conditions sufficient for unique solvability of inverse problem of source determination for degenerate parabolic equation with two independent variables.

Let us give a formulation of the problem. We consider the inverse problem of determination of a pair of functions $\{u(x, t); p(x)\}$, satisfying in $Q \equiv [0, T] \times [0, l]$ the parabolic equation

$$u_t - a(x, t)u_{xx} - b(x, t)u_x - d(x, t)u = p(x)g(x, t) + r(x, t), \quad (1)$$

the initial and boundary conditions

$$u(x, 0) = u_0(x), \quad x \in [0, l], \quad u(0, t) = u(l, t) = 0, \quad t \in [0, T], \quad (2)$$

and additional condition of integral observation

$$\int_0^T u(x, t)\chi(t) dt = \varphi(x), \quad x \in [0, l]. \quad (3)$$

Here $T > 0$, $l > 0$ are some fixed numbers. The main feature of our study is that the leading coefficient $a(x, t)$ of the equation (1) is bounded but only nonnegative, and satisfy the condition

$$1/a(x, t) \in L_q(Q), \quad q > 1. \quad (4)$$

Thus the equation (1) is a degenerate parabolic equation.

^{a)}Email: vlkamynin2008@yandex.ru

^{b)}Email: abkostin@yandex.ru

Definition. By the generalized solution of the problem (1)–(3) we mean the pair of functions $\{u(x, t); p(x)\}$,

$$u \in C^{0,\sigma}(Q) \cap L_\infty(0, T; \overset{\circ}{W}_2^1(0, l)) \cap W_s^{2,1}(Q), \quad s > 1, \quad \sigma \in (0, 1), \quad p \in L_\infty(0, l)$$

such that this pair satisfies the equation (1) almost everywhere in Q and the function $u(x, t)$ satisfies the conditions (2), (3) in classical sense.

We note that the inverse problem (1)–(3) with $a(x, t)$ strictly positive ($a(x, t) \geq a_0 > 0$) but unbounded were investigated in [1]. Inverse problem for higher order degenerate parabolic equation without lower terms and with additional condition (3) was investigated in [2]. Let us also mention that the close inverse problem of determination of the source term in degenerate parabolic equation with the leading coefficient satisfied the condition (4) were studied in [3, 4] in the case when additional condition has the form

$$\int_0^l u(x, t)\omega(x) dx = \psi(t), \quad t \in [0, T].$$

The inverse problems for degenerate parabolic equations are important in applications in engineering and financial mathematics.

In our study we give two types of conditions sufficient for unique solvability of inverse problem (1)–(3). This results are based on the investigation of corresponding direct problem (1)–(2) (where the function $p(x)$ is known) and on estimates of it generalized solution. The obtained results for direct problem are also new and of independent interest.

The authors were partially supported by the program of competitiveness increase of the National Research Nuclear University MEPhI (Moscow Engineering Physics Institute) contract no 02.a03.21.0005.27.08.2013.

References

- [1] Prilepko A. I., Kamynin V. L., Kostin A. B. Inverse source problem for parabolic equation with the condition of integral observation in time // Journal Inverse and Ill-Posed problems. 2017. doi:10.1515/jiip-2017-0049.
- [2] Kamynin V. L., Bukharova T. I. On inverse problem of determination the right-hand side term in higher order degenerate parabolic equation with integral observation in time // Journal of Physics, Conf. Series. V. 937 (2017): 012018. doi:10.1088/1742-6596/937/1/012018
- [3] Kamynin V. L. On the solvability of the inverse problem for determining the right-hand side of a degenerate parabolic equation with integral observation // Mathematical Notes. V. 98 (2015), 765-777.
- [4] Kamynin V. L. Inverse problem of determining the right-hand side in a degenerating parabolic equation with unbounded coefficients // Comp. Math. Math. Phys. V. 57 (2017), 832-841.

Plane contact problem for foundation with multilayer nonuniform coating

K.E. Kazakov^{1,2,a)}, A.V. Manzhurov^{1,2,3,b)}

¹*Ishlinsky Institute for Problems in Mechanics of the Russian Academy of Sciences*

²*Bauman Moscow State Technical University*

³*National Research Nuclear University MEPhI*

Plane contact problem for a viscoelastic foundation with multilayer coating and a rigid punch is considered. It is assumed that thin coating consist of several different elastic layers. The rigidity of each layer depend on longitudinal coordinate and can be described by own rapidly changing function. We obtain basic integral equation and additional conditions for this problem. The analytic solution of the problem is constructed.

1 Statement of the Problem

We assume that a viscoelastic layer with a multilayer coating lies on a rigid basis. At time τ_0 , the force $P(t)$ with eccentricity $e(t)$ starts to indent a smooth rigid punch of width $2a$ into the surface of such a foundation. A specific characteristic of this contact interaction is the fact that the rigidity of each layer in coating depend on longitudinal coordinate and can be described by rapidly changing function. The coating is assumed to be thin compared with the contact area, i.e., its total thickness (sum of layers thicknesses) satisfies the condition $h = h_1 + h_2 + \dots + h_n \ll 2a$. (Here h_i is thickness of i th layer in coating, n is number of layers.) The lower viscoelastic layer has arbitrary thickness H . We denote the moment of its production τ_{lower} . We assume that the coating maximum rigidity is less than the rigidity of the lower layer or they are of the same order of magnitude. We consider the case of plane strain and the case of smooth layer-layer and layer-basis contact.

The integral equation of the problem has a form [1]:

$$\sum_{i=1}^n \frac{q(x, t) h_i}{R_i(x)} + \frac{2(1 - \nu_2^2)}{\pi} (\mathbf{I} - \mathbf{V}) \int_{-a}^a k_{\text{pl}}\left(\frac{x - \xi}{H}\right) \frac{q(\xi, t)}{E_{\text{lower}}(t - \tau_{\text{lower}})} d\xi = \delta(t) + \alpha(t)x - g(x), \quad (1)$$

$$\mathbf{V}f(x, t) = \int_{\tau_0}^t K(t - \tau_{\text{lower}}, \tau - \tau_{\text{lower}}) f(x, \tau) d\tau, \quad K(t, \tau) = E_{\text{lower}}(\tau) \frac{\partial}{\partial \tau} \left[\frac{1}{E_{\text{lower}}(\tau)} + C^{\text{lower}}(t, \tau) \right],$$

where $R_i(t)$ are contact rigidities of the coating layers depend on Young moduli and Poisson's ratios of this layers; E_{lower} and ν_{lower} are the Young modulus and Poisson's ratio of lower layer; $\delta(t)$ and $\alpha(t)$ are punch settlement and tilt angle; $g(x)$ is punch base form; \mathbf{I} is the identity operator; \mathbf{V} is the Volterra integral operators with tensile creep kernels $K(t, \tau)$; $C^{\text{lower}}(t, \tau)$ is the tensile creep functions; $k_{\text{pl}}[(x - \xi)/H]$ is known kernel of the plane contact problem, which has the form

$$k_{\text{pl}}(s) = \int_0^\infty \frac{L(u)}{u} \cos(su) du, \quad L(u) = \frac{\cosh 2u - 1}{\sinh 2u + 2u}.$$

The additional conditions has a form

$$\int_{-a}^a q(\xi, t) d\xi = P(t), \quad \int_{-a}^a q(\xi, t) \xi d\xi = P(t)e(t). \quad (2)$$

^{a)}Email: kazakov-ke@yandex.ru

^{b)}Email: manzh@inbox.ru

There are exist 4 different versions of the problem: 1) the settlement and tilt angle of the punch are given (i.e., the right-hand side of the equation is given); 2) the punch settlement and the moment of the load application are given; 3) the tilt angle of the punch and the force of the load application are given; 4) the force and the moment of the load application are given.

2 Final Solution

If we introduce into (1) new function

$$m(x) = \sum_{i=1}^n \frac{h_i}{R_i(x)},$$

we obtain the problem, described in [2].

The solution of such a problem for the case of known force and eccentricity can be constructed by using special basis and generalized projection method [3]. We note that earlier no solutions of the problem with incomplete information about the right-hand side and additional conditions (cases 2)–4)) have been obtained even in the case of an elastic material. This could be done only by using the generalized projection method. Moreover, this methods allowed us to construct a new effective solution of the classical problem for the Fredholm integral equation of second kind with the Schmidt kernel fora given right-hand side, which differs from theclassical solution presented in Goursat’s book [4].

The final solution for this case has a form:

$$q(x, t) = \frac{1}{m(x)} [z_0(t)p_0(x) + z_1(t)p_1(x) + \dots] = \left[\sum_{i=1}^n \frac{h_i}{R_i(x)} \right]^{-1} [z_0(t)p_0(x) + z_1(t)p_1(x) + \dots],$$

where $p_k(x)$ is polynomial of degree k , $z_k(t)$ is known function depend on time. This form of solution allows one to perform computations for actual nonuniformities of layers in coating, which are described by different rapidly changing functions $R_i(x)$. The use of other known methods for constructing the analytic solution of the basic integral equation leads to major errors in the numerical implementation.

We can obtain the explicit formulas for the punch settlement and the tilt angle also.

Acknowledgments

This work was financially supported by the Russian Foundation for Basic Research (project No. 18-01-00770) and the Federal Agency for Scientific Organizations (State Registration Number AAAA-A17-117021310381-8).

References

- [1] N. Kh. Arutyunyan and A. V. Manzhurov, Contact Problems in Creep Theory (Izdat. NAN RA, Erevan, 1999).
- [2] K. E. Kazakov, “Modeling of contract interaction of solids with inhomogeneous coatings,” *Journal of Physics: Conference Series* **181**, 012013 (2009).
- [3] A. V. Manzhurov, “A mixed integral equation of mechanics and a generalized projection method of its solution,” *Doklady Physics* **61**(10), 489–493 (2016).

- [4] E. Goursat, Cours d'Analyse Mathématique, Tome III. Intégrales Infiniment Voisines; Équations aux Dérivées Partielles du Second Ordre; Équations Intégrales; Calcul des Variations (Gauthier–Villars, Paris, 1927; GTTI, Moscow–Leningrad, 1934).

Basic operators method extension for 3D stationary problems on unstructured tetrahedral meshes

I.A. Kondratyev^{1,2,a)}, S.G. Moiseenko^{1,b)}

¹*Space Research Institute RAS*

²*National Research Nuclear University MEPhI*

Support operator method (Samarskii's method, operator-difference method) has proven itself well in 2D numerical simulations of astrophysical problems. We extended this method for three dimensional case. 3D grid analogues for continuous differential operators using a cell-node approximation were derived. A test problem for calculation of spatial Newtonian gravitational potential was solved. The stationary heat transfer equation in spherical layer with Dirichlet boundary condition on the inner surface and third type boundary condition on the outer one was calculated. It is planned to continue developing the method and apply it to different astrophysical problems.

The idea of operator approach [1] was developed by Samarskii and his disciples for partial differential equations. It consists of inclusion of boundary conditions in finite difference form into the grid analogue of solving problem and formulation of the finite difference problem as operator equation. Basic operators method consists of construction of grid analogues of vector operators. The finite difference operators are constructed in the way to fulfill corresponding relations between continuous operators (for instance, $\text{div}(\text{rot})=0$, div is conjugated to $-\text{grad}$; $\text{div}(\text{grad})$ is self-conjugated etc.). The method allows obtaining completely conservative finite difference schemes. The matrix which corresponds to the self-conjugated operator is symmetrical and can be inversed efficiently by modern iteration methods. 2D basic operators approach on the triangular grid was suggested by Ardelyan [2, 3]. It was successfully applied for numerical solution of different plasma physics [4] and astrophysical problems such as collapse of magnetized rotating cloud [5], magnetorotational core-collapse supernovae [6] and etc. We derived 3D analogues of corresponding differential operators on the unstructured tetrahedral grid (Fig. 1). Operator-difference technique, developed by Ardelyan, includes also formulation of boundary conditions of different types in operator form a consequent its inclusion into operator equation. For testing of the 3D extension of the operator method we calculated gravitational potential of the star (Fig. 2). It was found that the method allows calculating the gravitational potential for the case when the density of the star is changing by many orders (neutron star) on grid with moderate grid dimension. The second test was the calculation of the heat transfer in spherical layer with the first type boundary condition on the inner surface of the layer and third order boundary condition on the outer surface of the layer.

^{a)}Email: mrkondratyev95@gmail.com

^{b)}Email: moiseenko@iki.rssi.ru

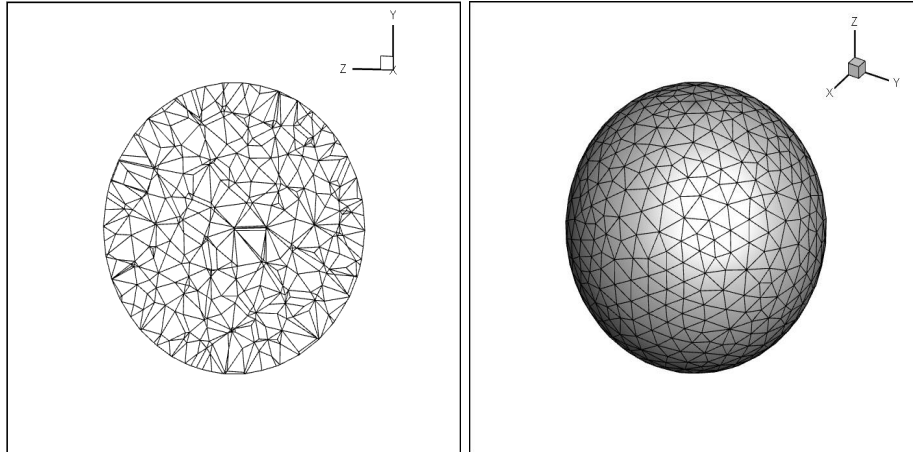


Fig. 1: Tetrahedral mesh cross section in $Y - Z$ plane (left) and boundary surface of the mesh (right)

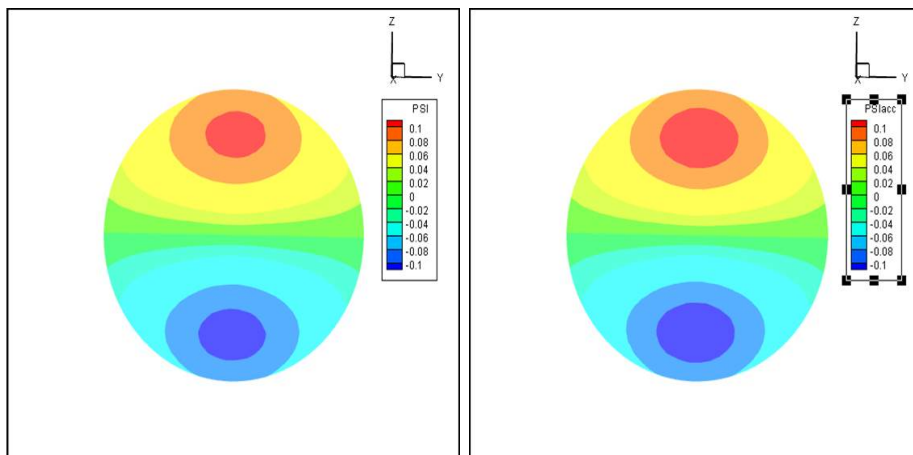


Fig. 2: Solution for the gravitational potential (cross section in $Y - Z$ plane) for the given mass density $\rho = \frac{1}{4\pi} \frac{z}{\sqrt{x^2+y^2+z^2}}$ (left - numerical, right - accurate)

Acknowledgements

We thank RFBR grant 18-02-00619 for partial support.

References

- [1] *Samarskii A. A.* Finite difference schemes theory (in Russian) // Moscow: Nauka, 1989, 616p.
- [2] *Ardelyan N.V.* About mesh analogues of basic differential operators on nonregular triangular mesh (in Russian) // Difference methods for mathematical physics M.: MSU, 1981. p.49-58.
- [3] *Ardelyan N.V., Gush'in I. S.* About one approach for construction completely conservative difference schemes (in Russian) // Vestnik MSU, 1982, Ser. 15., No. 3, p.3-20.
- [4] *N. Ardelyan, V. Bychkov, A. Belousov, K. Kosmachevskii* Processes of electron attachment and detachment in near breakdown conditions in air plasma. Journal of Physics: Conference Series. — 2017. — Vol. 927, no. 1. — P. 1–8.
- [5] *Ardeljan N.V., Bisnovatyi-Kogan G.S., Moiseenko S.G.* Collapse of a magnetized rotating cloud. 2D numerical simulations. Astrophysics and Space Science, 2000, v.274, 389-397.
- [6] *G.S. Bisnovatyi-Kogan, N.V. Ardeljan, S.G. Moiseenko* Magnetorotational explosions: supernovae and jet formation. Mem.Soc. Astron. Ital., 2002, v.73, 1134-1143.

Calculation of sums of Rayleigh type by zeros of equation containing Bessel function and its derivative

A.B. Kostin^{1,a)}, V.B. Sherstyukov^{1,b)}

¹*National Research Nuclear University MEPhI (Moscow Engineering Physics Institute)*

In the paper equations of view $azJ'_\nu(z) + bJ_\nu(z) = 0$ with complex parameters ν, a, b and the Bessel function $J_\nu(z)$ are studied. Special summation relations for zeros of the equation are proved. The obtained results are consistent with well-known formulas for classical Rayleigh sums calculated by zeros of the Bessel function.

The paper is a continuation of researches published in [1, 2]. We consider the equation

$$azJ'_\nu(z) + bJ_\nu(z) = 0, \quad z \in \mathbb{C}, \quad (1)$$

with parameters $\nu, a, b \in \mathbb{C}$ that $|a| + |b| > 0$. We are interested in non-trivial, i. e. other than $z = 0$, zeros of the equation (1). There are infinitely many zeros and all ones are located in some horizontal strip symmetrically with respect to the point $z = 0$. We denote the zeros $\pm z_{\nu,k}(a, b) \equiv \pm z_{\nu,k}$, $k \in \mathbb{N}$, where $z_{\nu,k}$ are zeros of (1) belonging to the set $\{\operatorname{Re} z > 0\} \cup \{\operatorname{Re} z = 0, \operatorname{Im} z > 0\}$

^{a)}Email: abkostin@yandex.ru

^{b)}Email: shervb73@gmail.com

and numbered in order of increasing the module taking into account the multiplicity. Any zero $z \neq 0$ has multiplicity ≤ 2 and its multiplicity is equal to two only in the case $a^2 z^2 = a^2 \nu^2 - b^2$. Thus, all non-trivial zeros of the equation (1) are simple with the possible exception of one pair of symmetric zeros. Similarly with the classical Rayleigh sums [3, 4] we define the sums of Rayleigh type

$$\eta^{(2m)}(\nu, a, b) = \sum_{k=1}^{\infty} \frac{1}{z_{\nu, k}^{2m}(a, b)}, \quad m \in \mathbb{N}. \quad (2)$$

Similar sums were studied in articles [5]–[8]. Our main result gives recurrent formulas for calculating sums of (2). The relations

$$\begin{aligned} \eta^{(2)}(\nu, a, b) &= \frac{b + a\nu + 2a}{4(\nu + 1)(b + a\nu)}, \\ \eta^{(4)}(\nu, a, b) &= \frac{a^2}{4(b^2 - a^2\nu^2)(\nu + 2)} + \frac{1}{\nu + 2} \left[\eta^{(2)}(\nu, a, b) \right]^2 - \frac{a^2\nu}{(b^2 - a^2\nu^2)(\nu + 2)} \eta^{(2)}(\nu, a, b), \\ \eta^{(2m+2)}(\nu, a, b) &= \frac{a^2}{(b^2 - a^2\nu^2)(\nu + m + 1)} \sum_{p=1}^{m-1} \eta^{(2m-2p)}(\nu, a, b) \eta^{(2p)}(\nu, a, b) + \\ &+ \frac{1}{\nu + m + 1} \sum_{p=1}^m \eta^{(2m+2-2p)}(\nu, a, b) \eta^{(2p)}(\nu, a, b) - \frac{a^2(\nu + m - 1)}{(b^2 - a^2\nu^2)(\nu + m + 1)} \eta^{(2m)}(\nu, a, b), \end{aligned}$$

where $m = 2, 3, \dots$, $a, b \in \mathbb{C}$, $\nu \in \mathbb{C} \setminus \{-1, -2, \dots\}$, $b^2 - a^2\nu^2 \neq 0$ are taken place. Special cases not covered by these formulas are separately analyzed.

The authors were partially supported by the program of competitiveness increase of the National Research Nuclear University MEPhI (Moscow Engineering Physics Institute) contract no 02.a03.21.0005.27.08.2013. The second author also was supported by RFBR under Grant 18-01-00236.

References

- [1] Kostin A. B. and Sherstyukov V. B. On complex roots of an equation arising in the oblique derivative problem // IOP Conf. Series: Journal of Physics: Conf. Series 788 (2017) 012052 doi:10.1088/1742-6596/788/1/012052. P. 1–7.
- [2] Kostin A. B. and Sherstyukov V. B. Calculation of Rayleigh type sums for zeros of the equation arising in spectral problem // IOP Conf. Series: Journal of Physics: Conf. Series 937 (2017) 012022 doi:10.1088/1742-6596/937/1/012022. P. 1–9.
- [3] Rayleigh 1874 Note on the Numerical Calculation of the Roots of Fluctuating Functions // Proc. London Math. Soc. V. 5, 119–124.
- [4] Watson G. N. 1944 A Treatise on the Theory of Bessel Functions (Cambridge: Cambridge University Press).
- [5] Kapitsa P. L. 1951 Computation of Negative Even Power Sums of the Zeros of Bessel Functions // Dokl. Akad. Nauk SSSR. V. 77, 561–564.
- [6] Meiman N. N. 1956 On Recurrence Formulas for Power Sums of the Zeros of Bessel Functions // Dokl. Akad. Nauk SSSR. V. 108, 190–193.

- [7] Kishore N. 1963 The Rayleigh Function // Proc. Amer. Math. Soc. V. 14, 527–533.
[8] Kerimov M. K. 2008 Overview Some New Results Concerning the Theory and Applications of the Rayleigh Special Function // Comput. Math. Math. Phys. V. 48, 1454–1507.

Modeling of acetylene detonation in a shock tube by the large particle method with TVD correction

I.M. Kozlov^{1,a)}, N.I. Misuchenko¹, A.V. Teterev^{1,2}

¹*Belarusian State University, Belarus*

²*National Research Nuclear University «MEPhI»*

A one-dimensional TVD correction scheme is described, which can be successfully applied not only in 1D calculations, but also in 2D-3D modeling [1],[2]. The advantage of the proposed scheme is the lack of solving matrix equations. The implementation of the scheme in conjunction with the large particle method was tested on the problems of arbitrary discontinuity breakup and strong point explosion. The modeling of acetylene combustion in a shock tube and its transition to detonation was performed depending on the conditions set on the surface of the tube, and the parameters of the problem.

In the difference scheme of the large particle method [3], all the principal independent hydrodynamic variables - density, velocity and specific energy of the substance are determined in the center of cells. To obtain the flows of these quantities in this scheme, they are interpolated first to the cell edges, and then the corresponding flows of mass, momentum and energy are formed. In the classical TVD schemes the basic value flows are first calculated in the cell center, where these variables are defined, and then the resulting flows are interpolated to the cell edge. This circumstance causes the necessity of verification of the joint operation of the large particle scheme and the TVD correction one. The problem of the decay of an arbitrary discontinuity and the problem of a strong point explosion were chosen as test problems.

Nowadays, the use of detailed chemical kinetics in modeling two-dimensional and, moreover, three-dimensional problems of gas dynamics to describe combustion and detonation processes is extremely expensive and ineffective. Therefore, the proposed physical-chemical model uses tabular descriptions of the thermodynamic state for each component of the gas mixture separately, but they may not be in a state of chemical equilibrium and may participate in mutual chemical transformation. In addition, each component can be a given mixture of simpler elements with a fixed composition, which is not changed either as a result of the chemical reactions included in the model, or due to convective transfer or other processes. For example, oxygen-enriched air mixture can be represented as one component having a given volume fraction of oxygen and nitrogen molecules $2.5\text{O}_2+5.2\text{N}_2$.

To calculate the correcting TVD flows in the modified method of large particle, it is necessary to know not only the equation for the mixture pressure $p = p(\rho, \varepsilon, Y)$, but also its derivatives:

$$\chi = \left(\frac{\partial p}{\partial \rho} \right)_{\rho\varepsilon, Y}, \quad k = \left(\frac{\partial p}{\partial \rho\varepsilon} \right)_{\rho, Y}, \quad \eta_i = \left(\frac{\partial p}{\partial Y_i} \right)_{\rho, \rho\varepsilon}, \quad \varepsilon = E - \frac{u^2 + v^2}{2}. \quad (1)$$

^{a)}Email: kim.kozlov@yandex.by

Here we can find: ρ - density, ε - specific internal energy and the p - pressure of the mixture, and $Y_i = \rho_i/\rho$ - mass fraction of the i -th component of the mixture ($i = 1, \dots, N$).

The temperature used to calculate the partial pressure and the energy of the mixture components is determined based on the energy conservation equation for the mixture in a given calculation cell:

$$\varepsilon = \sum_i^N Y_i \varepsilon_i(T, Y_i \rho), \quad (2)$$

that is solved iteratively by Newton's method under the assumption of equal temperatures for all components of the mixture:

$$T_{s+1} = T_s + \left(\varepsilon - \sum_i^N Y_i \varepsilon_i(T_s, Y_i \rho) \right) / \sum_i^N \frac{\partial \varepsilon_i(T_s, Y_i \rho)}{\partial T}. \quad (3)$$

The numerical simulation uses the functions $\varepsilon_i = \varepsilon_i(T, \rho)$ and $p_i = p_i(T, \rho)$ obtained in the form of tables, calculated with a given grid on the parameters of temperature and density. For these calculations, a uniform temperature scale ranging from 200 K to 6000 K in increments of 50 K and a logarithmic scale in densities ranging from 10^{-8} kg/m³ to 102.5 kg/m³ with a uniform logarithmic step of 0.25 is used.

For a realistic description of the thermodynamic properties of the substance, equilibrium tables calculated by CEA NASA for specific components of the burning mixture considered in the simulation were used. Calculations were made for a long pipe with a diameter of about 0.04 m and a length of 1 m to 6 m, sealed on one side. Initially, the pipe was filled with the rest stoichiometric acetylene-air mixture enriched with oxygen at a temperature of about 300 K, with a reduced density of 0.18 kg/m³ and a pressure of 0.142 Pa. Initiation of combustion was carried out by modeling Joule heat release from the electric spark of the spark plug. The energy of the spark plug stood out in a gas mixture with 0.04 J in the period of 1.5 ms in a small volume at the axis adjacent to the end face of the closed pipe end.

Numerical simulation was performed by a modified method of large particles with TVD correction of flows in a two-dimensional setting in the axisymmetric coordinate system. The symmetric spatial scheme of the large particle method of the 2nd order on space and the 1st order of approximation on time without artificial viscosity was used. To account for heat transfer by thermal conductivity, a scheme of the 2nd order of approximation was also used. A homogeneous difference grid with a cell size in both directions (axial and radial) equal to $9.77 \cdot 10^4$ m was applied. The mesh size was 24×6140 cells. On the face ends of the pipe conditions of non-flow of gas were placed, on the side walls conditions of non-flow were also put with the choice of either sliding or partial adhesion to the surface of the pipe. This possibility was envisaged, since it is known that wall phenomena such as boundary viscous layer or heat loss of the mixture on the wall can affect the shape and length of the combustion wave and, therefore, the rate of its spread. To compare the influence of the wall layer on the formation of the combustion wave, we calculated the variants with both conditions.

Simulation results for several variants of calculations are considered. The variants differed in setting the conditions for the interaction of the flow with the side walls of the pipe, as well as the value of the activation energy for the combustion reaction rate. The first option was considered at rather low activation energy of 53 kcal, which allows the combustion wave to maintain a high speed due to the heat released as a result of the reaction. Two variants with the given activation energy, differing by a condition of adhesion on a pipe wall, are calculated. In these variants, the combustion wave that occurs after the spark is initiated from the spark plug is accelerated quite quickly and at a distance of about 9 cm passes into a classic detonation wave propagating at

a constant speed and having a fairly stable detonation front. However, the differences are still there. In variant with adhesion, the temperature of the front is about 35 degrees lower and is equal to 3075 K; the speed of the front is lower by 80 m/s and is 1810 m/s. In addition, the front temperature on the axis of symmetry in the version with adhesion experiences small oscillations with constant amplitude of 5 degrees and a frequency of 1.25 kHz. This suggests that the surface of the detonation wave front is not flat and stationary.

Another value of the activation energy with which the calculations were performed was 63.7 kcal. It represents a certain critical value, above which combustion was not spread. Note that for the slip case, the critical value of the activation energy is significantly lower than the given value. Moreover, in a slip-on model with its critical value of activation energy, combustion can propagate at subsonic speed, but not go into detonation. In contrast, in a model with adhesion, combustion either does not propagate at all or necessarily enters detonation mode. This is due to the fact that the combustion front in terms of adhesion stretches along the axis faster than it reaches the walls, spreading along the radius of the pipe. In this case, the surface area of the flame increases, and at the same time increases the rate of combustion. The flame speed increases until the detonation conditions are met. As soon as combustion enters the detonation mode, the velocity of its propagation is stabilized.

References

- [1] Moon J., Yee H.C. *Numerical simulation by TVD schemes of complex shock reflections from airfoils at high angle of attack.* // AIAA Paper, No. 350, 1987. 1-17 pp.
- [2] Yee H. C. *Linearized form of implicit TVD schemes for multidimensional Euler and Navier-Stokes equations* // Int. J. Comp. Math. Appl. , Vol. 12A. No. 4/5, 1986. 413-432 pp.
- [3] Belotserkovsky O.M., Davydov Yu.M. *Coarse particle (large particle) method in hydrodynamics* // Moscow: Nauka, 1982. 392 pp.

On the mechanism of electroplasticity of a metal under the action of a pulsed high-energy electromagnetic field

K.V. Kukudzhanov^{1,a)}, A.L. Levitin^{1,b)}

¹*Ishlinsky Institute for Problems in Mechanics RAS*

Electroplastic effect is reduction of the yield strength of the material or an increase in the ultimate plastic deformation up to failure. Electroplastic effect is observed if the electromagnetic field induces a current in the material with a current density of 10^8 to 10^{11} A/m² for a sufficiently short time interval of up to several 100 μ s. The specific electromagnetic energy dissipated during the specified time interval in the material is found to be in the range $10^6 \leq e \leq 10^{10}$ J/m³. In this case, we will refer to the field as a pulsed high-energy electromagnetic field (HEEMP), if, under such action, the scattered specific electromagnetic energy in the material is in the range $10^8 \leq e \leq 10^{10}$ J/m³.

^{a)}Email: kconstantin@mail.ru

^{b)}Email: alex_lev@ipmnet.ru

When a current flows in a metal, free electrons are scattered by crystal lattice ions, during which thermal energy (Joule heat) is released. At the same time, there is no doubt that this heat release in regions with defects in the structure of the material (dislocations, microcracks, inclusions) and in regions where such defects are absent occurs in different ways. It is known that dislocations possess "easy" mobility, i.e. A relatively small shear stress is required to, for example, the edge dislocation begin to move in the crystallite (grain). The situation is different in the case of more "large" defects, such as microcracks and micropores, which were formed during the preliminary plastic deformation of a polycrystalline metal. Simulation shows that inhomogeneous heat release in the vicinity of microdefects is the reason for their healing. In this process, healing takes place in the form of restoring the continuity of the material by "welding" the shores of microcracks (in contrast to the earlier models that showed only the appearance of compressive stresses in the tops of microcracks or a slight convergence of the mesocrack shores). This is confirmed by experiments.

On the basis of the developed mathematical model, it is shown that in order to move the boundaries of microdefects, it is required to disperse electromagnetic energy in the material volume unit by two orders of magnitude greater than for initiating the electron-dislocation interaction and driving dislocations. At the same time, the value of the "threshold" scattered specific energy required for the defects to begin to heal is in good agreement with the value of the scattered specific energy needed to initiate the process of electroplastic deformation obtained in experiments on the effect of HEEMP on materials.

It is shown that to initiate the processes of healing defects and a significant increase in the ultimate plastic deformation prior to failure in the process of electroplastic deformation, it is precisely the impulsive HEEMP that is required.

Based on the micromodel analysis carried out for intergranular and intragranular microcracks, macroparameters for the healing and damage of the material were introduced, a macroscopic dependence of the change in the metal damage on the specific electromagnetic energy of the pulsed HEEMP scattered in it and the "length" of the microcrack was obtained.

This work was supported by the Russian Foundation for Basic Research (RFBR) under Grant No. 18-08-00958.

References

- [1] Kukudzhanov K.V., Levitin A.L. Healing of damaged metal by a pulsed high-energy electromagnetic field // *Journal of Physics: Conference Series*. Vol. 991 (2018) 012049 DOI: 10.1088/1742-6596/991/1/012049
- [2] Kukudzhanov K.V., Levitin A.L. Phase Transformations in Metals Stimulated by a Pulsed High-Energy Electromagnetic Field // *Procedia IUTAM*. Vol. 23. P.84-100 (2017) DOI: 10.1016/j.piutam.2017.06.008
- [3] Kukudzhanov K.V., Levitin A.L. Modeling the Healing of Microcracks in Metal Stimulated by a Pulsed High-Energy Electromagnetic Field. Part I // *Nanomechanics Science and Technology: An International Journal*. 2015. Vol. 6. Issue 3. P.233-249. DOI: 10.1615/NanomechanicsSciTechnolIntJ.v6.i3.60
- [4] Kukudzhanov K.V., Levitin A.L. Modeling the Healing of Microcracks in Metal Stimulated by a Pulsed High-Energy Electromagnetic Field. Part II // *Nanomechanics Sci-*

Application of M.Riesz potentials for solving a 3D inverse problem of acoustic sounding

A.S. Leonov^{1,a)}

¹*National Research Nuclear University 'MEPhI'*

An inverse coefficient problem for time-dependent 3D wave equation is under consideration. We recover a spatially varying coefficient of this equation knowing special time integrals of the wave field in an observation domain. The inverse problem has applications to the acoustic sounding, medical imaging, etc. We reduce the inverse problem to a new linear 3D Fredholm integral equation of the first kind in which the integral operator has the form of well-known M.Riesz potentials. The equation has a unique solution for a considered class of acoustic inhomogeneities. Assuming a special scheme for recording the data of the inverse problem, we present and substantiate a numerical algorithm of solving this integral equation. The algorithm does not require significant computational resources and a long solution time. It is based on the use of fast Fourier transform. Typical results of solving 3D inverse problem in question on a personal computer for simulated data demonstrate high capabilities of the proposed algorithm.

1. We consider the wave equation $\frac{1}{c^2(\mathbf{x})}u_{tt}(\mathbf{x}, t) = \Delta u(\mathbf{x}, t) - g(t)\varphi(\mathbf{x})$, $\mathbf{x} = (x, y, z) \in \mathbb{R}^3$, $t > 0$, with homogeneous initial conditions. For this equation, the coefficient inverse problem is usually formulated as follows: knowing the wave field $u(\mathbf{x}, t)$ in a domain $Y \subset \mathbb{R}^3$ and the source functions $g(t)$, $\varphi(\mathbf{x})$, $\mathbf{x} \in S$, to find the function $c(\mathbf{x})$ in a known domain X , $X \cap Y = \emptyset$, $X \cap S = \emptyset$, if $c(\mathbf{x})$ is a known constant c_0 outside the region X . A detailed statement of the inverse problem with an indication of the spaces used is given in the report. Such a task, as established in a number of works, requires for its solution significant computing resources (supercomputer, long calculation time, etc.). However, there are alternative statements of such a problem, where special integral functionals of the function $u(\mathbf{x}, t)$ are used as data. For example, in [1], a three-dimensional linear integral equation of the first kind was obtained for finding the function $\xi(\mathbf{x}) = \frac{1}{c_0^2} - \frac{1}{c^2(\mathbf{x})}$ associated with $c(\mathbf{x})$. The right-hand side of this equation contains the function $V_2(\mathbf{x}) = \int_0^\infty t^2 u(\mathbf{x}, t) dt$, $\mathbf{x} \in Y$, which can be calculated from the scattered wave field or directly measured. However, the solution of the integral equation may not be unique, and it was suggested in [1] to seek the normal solution. In the present report, the uniqueness problem is eliminated by considering a new integral equation.

2. Suppose that we have at our disposal two functions, $V_2(\mathbf{x})$ and $V_2^{(0)}(\mathbf{x})$. The function $V_2^{(0)}(\mathbf{x})$ is an analog of the function $V_2(\mathbf{x})$, which is measured or calculated from the wave field $u^{(0)}(\mathbf{x}, t)$, $\mathbf{x} \in Y$, in the case when there are no scatterers in the region X . Introducing the auxiliary functions

$$V_0(\mathbf{x}) = -\frac{A_0}{4\pi} \int_S \frac{\varphi(\mathbf{x}') d\mathbf{x}'}{|\mathbf{x} - \mathbf{x}'|}, \zeta(\mathbf{x}) = \left(\frac{1}{c_0^2} - \frac{1}{c^2(\mathbf{x})} \right) V_0(\mathbf{x}); A_0 = \int_0^\infty g(t) dt,$$

^{a)}Email: asleonov@mephi.ru

we can obtain under assumptions that will be detailed in the report the equation for finding $\zeta(\mathbf{x})$,

$$\int_X \frac{\zeta(\mathbf{x}')d\mathbf{x}'}{|\mathbf{x} - \mathbf{x}'|^\lambda} = w(\mathbf{x}), \quad \mathbf{x} \in Y; \quad w(\mathbf{x}) = \frac{1}{2}b(\lambda) \left\{ (-\Delta)^{\frac{\lambda-1}{2}} (V_2(\mathbf{x}) - V_2^{(0)}(\mathbf{x})) \right\} \quad (1)$$

with $b(\lambda) = 2^{3-\lambda}\pi^{3/2}\Gamma\left(\frac{3-\lambda}{2}\right)\Gamma^{-1}\left(\frac{\lambda}{2}\right)$. For $1 < \lambda < 3$, Eq.(1) can have only a unique solution (see [2]). It turned out that the most convenient case is $\lambda = 2$, in which

$$\int_X \frac{\zeta(\mathbf{x}')d\mathbf{x}'}{|\mathbf{x} - \mathbf{x}'|^2} = w(\mathbf{x}), \quad \mathbf{x} \in Y; \quad w(\mathbf{x}) = \pi^2(-\Delta)^{\frac{1}{2}}[V_2(\mathbf{x}) - V_2^{(0)}(\mathbf{x})]. \quad (2)$$

3. The solution of Eq.(2) requires preliminary preparation of its data, i.e. calculation of the function $w(\mathbf{x}) = \pi^2(-\Delta)^{\frac{1}{2}}[V_2(\mathbf{x}) - V_2^{(0)}(\mathbf{x})]$. It can be proved under certain assumptions on the data $U(\mathbf{x}) = V_2(\mathbf{x}) - V_2^{(0)}(\mathbf{x})$ that the function $w(\mathbf{x})$ is a unique solution of the integral equation

$$\int_{\mathbb{R}^3} \frac{w(\mathbf{x}')d\mathbf{x}'}{|\mathbf{x} - \mathbf{x}'|^2} = 2\pi^4 U(\mathbf{x}), \quad \mathbf{x} \in Y. \quad (3)$$

Eqs.(2) and (3) can be solved in the same manner by the use of regularization methods. In what follows, we describe the corresponding solution procedure.

4. We consider schematically the algorithm for solving Eqs.(2) and (3) in the case when the wave field is measured in a «plane layer» $Y = \mathbb{R}_{xy}^2 \times [h, H]$ while the scatterers are located in $X = \mathbb{R}_{xy}^2 \times [l, L]$. First of all, we represent the equation (3), from which it is necessary to find $w(x)$, in the form

$$\int_{-\infty}^{\infty} dz' \iint_{\mathbb{R}_{xy}^2} K(x - x', y - y', z - z')w(x', y', z')dx'dy' = 2\pi^4 U(x, y, z),$$

with $(x, y) \in \mathbb{R}_{xy}^2, z \in [h, H]$ and $K(x, y, z) = (x^2 + y^2 + z^2)^{-1}$. From here, using two-dimensional Fourier transforms $\tilde{K}(\omega_1, \omega_2, z), \tilde{w}(\omega_1, \omega_2, z), \tilde{U}(\omega_1, \omega_2, z)$ of the functions K, w, U with respect to (x, y) and applying the convolution theorem we obtain a family of one-dimensional integral equations of the first kind

$$\int_{-\infty}^{\infty} \tilde{K}(\omega_1, \omega_2, z - z')\tilde{w}(\omega_1, \omega_2, z')dz' = \tilde{U}(\omega_1, \omega_2, z), \quad z \in [h, H],$$

which depend on the parameters $(\omega_1, \omega_2) \in \mathbb{R}_{\omega_1\omega_2}^2$. These equations can be approximately solved using the well-known TSVD method, and as a result we obtain the approximation of the function $\tilde{w}(\omega_1, \omega_2, z'), z \in \mathbb{R}^1$. Similarly, we can reduce the equation (2) to the set of integral equations

$$\int_l^L \tilde{K}(\omega_1, \omega_2, z - z')\tilde{\zeta}(\omega_1, \omega_2, z')dz' = \tilde{w}(\omega_1, \omega_2, z), \quad z \in [h, H], \quad (4)$$

where $\tilde{\zeta}(\omega_1, \omega_2, z')$ is the Fourier transform of the function $\zeta(\mathbf{x})$. Solving Eqs.(4) by the TSVD method we can find the family $\tilde{\zeta}(\omega_1, \omega_2, z')$, and then restore the functions $\zeta(\mathbf{x}), \xi(\mathbf{x}) = \zeta(\mathbf{x})/V_0(\mathbf{x})$ and $c(\mathbf{x})$. In the report we give a justification for this algorithm and its discretized form. Results of solving the inverse problem (2) on a personal computer for typical model solutions are also presented.

This work was supported by the Russian Foundation for Basic Research (project no.16-01-00039a) and the Programm of Competitiveness Increase of the National Research Nuclear University MEPhI (Moscow Engineering Physics Institute); contract no. 02.a03.21.0005, 27.08.2013.

References

- [1] Bakushinsky A.B. and Leonov A.S. Fast numerical method of solving 3D coefficient inverse problem for wave equation with integral data. *J. Inverse Ill-Posed Probl.* 2017, aop (DOI: 10.1515/jiip-2017-0041)
- [2] Riesz M. *Intégrales de Riemann–Liouville et potentiels.* Acta Litt. Acad. Sci. Szeged, 1938. V.9. PP.1–42.

Description of liquid-vapor equilibria in binary associated of nonelectrolyte systems

M.S. Mitrofanov^{1,a)}, O.A. Nagovitsyna^{1,b)}, V.V. Sergievskii^{1,c)}

¹*National Research Nuclear University "MEPhI"*

Liquid-vapor equilibrium research is widely used to optimize various physical and chemical processes for components separation in liquid mixtures, for example, rectification, extraction, etc. We propose a model for describing the equilibrium in binary mixtures of nonelectrolytes that show positive deviations from Raoult's law due to association of one of the components in this paper. The description adequacy for the experimental data by model equations is checked using as example systems with alcohols solution.

Keywords: cluster model, vapor-liquid equilibria, aliphatic alcohol - chlorobutane.

Theoretical part

Earlier [1], the model of associated nonelectrolyte solutions, whose parameter is the number of solute stoichiometric association (A_1) in the standard state was substantiated. The model is applicable to binary solutions of nonelectrolytes exhibiting positive deviations from Raoult's law, whose nonideality is mainly contributed by the association of one of the components. The concentration dependence of the mean number of association A is described by equation $A = A_1 x^r$, where $r = D_1/A_1$, $D_1 = D(x=1)$, $A_1 = A(x=1)$ are the dispersion and distribution of the association mean number in the standard state with solute molar fraction $x = 1$. The corresponding expressions for the activity coefficients of the components (f) are obtained. Taking into account the solution nonideality, the expression for vapor pressure P dependence of the system composition has the form:

$$P = P^0_a + P_s^0 a_s \tag{1}$$

where P^0 and P_s^0 are vapor pressure over the pure substance and solvent, $a = fx$ and $a_s = f_s x_s$ are the activity of the solute and the solvent.

It is of interest to take into account the contribution of one of the components association not by the association numbers, but by the association equilibrium constants. For systems in

^{a)}Email: mitrofanov_mephi@mail.ru

^{b)}Email: alija212@mail.ru

^{c)}Email: vsereg0776@gmail.com

which the association of one of the components is limited by associates formation with small association numbers i in [2], the following relationships are obtained:

$$\begin{aligned} \ln f_s &= x^2 \frac{\sum_i i k_i x^{i-1}}{\sum_i k_i x^i} \\ \ln f &= \ln \frac{\sum_i k_i}{\sum_i k_i x^i} - x_s \frac{\sum_i i k_i x^i}{\sum_i k_i x^i} \end{aligned} \tag{2}$$

which relate the concentration dependences of components activity coefficients directly to the thermodynamic equilibrium association constants.

In the present work some mixtures of aliphatic alcohols with alkanes were analyzed. For such systems, the literature has reliably established that their nonideality is primarily connected with alcohols association. With reference to the equations of models considered in this paper, the standard deviation is used as an optimization criterion:

$$\sigma = \sqrt{\frac{\sum_{j=1}^v (Y_{j,exp} - Y(\theta)_{j,mod})^2}{v - b - 1}} \tag{3}$$

where $Y_{j,exp}$ and $Y(\theta)_{j,mod}$ are the experimental and calculated values for certain thermodynamic property at the j th point, v is the number of experimental points, b is the number of empirical parameters θ in the model equation.

Results and discussion

Table 1 shows the errors in identifying model parameters, (constants), describing the vapor pressures above the solution.

Table 1. Results of modeling vapor pressure in system 1-chlorobutane - 2 butanol [3] in the temperature range within the framework of the model (constants). It is proposed to associate alcohol with the formation of di-, tri-, and tetramers.

T, K	k₂	k₃	k₄	σ, kPa	δ, %	k₂	k₃	k₄	σ, kPa	δ, %
Alcohol is associated						Chlorobutane is associated				
278.15	9.35	0	3.40	0.04	0.8	0.69	0	1.89	0.19	3.3
288.15	7.25	0	2.38	0.06	0.7	0.72	0	1.69	0.26	2.7
293.15	6.51	0	1.99	0.07	0.6	0.71	0	1.59	0.30	2.4
298.15	5.92	0	1.75	0.08	0.5	0.73	0	1.52	0.34	2.2
303.15	5.20	0	1.42	0.09	0.4	0.74	0	1.40	0.37	1.9
313.15	4.47	0	1.07	0.11	0.4	0.72	0	1.24	0.47	1.5
318.15	4.14	0	0.91	0.13	0.3	0.71	0	1.16	0.52	1.4
323.15	3.85	0	0.77	0.13	0.3	0.69	0	1.08	0.57	1.2

The symmetry of the model equation is observed. It is clear that the errors in the choice of alcohol as associated component is significantly lower than choosing alkylhalide as associated component. The results of estimations of the parameters of the considered models are close (Table 2).

Table 2. Results of parameters calculating of the cluster model equations in some systems of hydrocarbon-aliphatic alcohol type [4] at 298.15 K. It is proposed to associate alcohol with the formation of di-, tri-, and tetramers.

Conclusions

Binary mixtures of completely miscible non-electrolytes are considered, the non-ideality of which is determined by the association of one of the components. It is established that the

Chemical system	k_2	k_3	k_4	A_1	D_1	r_1	A_1	D_1	r_1
Model parameters using the association constant						Cluster model			
1-bromobutane + 2-methyl-2-propanol	6.28	0	1.96	1.33	0.89	0.67	1.28	0.65	0.51
1-butanol + 1-bromobutane	7.56	1.07	1.73	1.31	0.69	0.53	1.29	0.58	0.45
1-chlorobutane + 2-methyl-1-propanol	8.59	0.01	2.41	1.32	0.79	0.6	1.29	0.58	0.45
1-chlorobutane + 2 butanol	5.92	0	1.75	1.29	0.84	0.65	1.25	0.65	0.52

model with association constants describes with good accuracy the vapor pressure over solutions of alcohols in alkanes. The simulation results are consistent with the literature data on the state of the components with respect to molecular association.

References

- [1] Rudakov A.M., Sergievskii V.V. J. Phys. Chem. 2010. 84. 10. 1876-1881.
- [2] Rudakov A.M., Mitrofanov M.S., Sergievskii V.V. // Condensed matter and interphases. 2012. 14. 3. 377-383.
- [3] Garriga R. et al. Thermodynamic excess properties for binary mixtures of 1-chlorobutane with 2-butanol or 2-methyl-1-propanol // Fluid phase equilibria. - 2001. 181. 1-2. 203-214
- [4] Garriga R. et al. Vapor Pressures at Several Temperatures between 278.15 and 323.15 K and Excess Functions at T= 298.15 K for 1-Bromobutane with 1-Butanol or 2-Methyl-2-propanol //Journal of Chemical & Engineering Data. 2002. 47. 2. 322-328.

Heat transport modelling in hemitropic micropolar continuum

E.V. Murashkin^{1,a)}, Y.N. Radayev^{1,b)}

¹*Ishlinsky Institute for Problems in Mechanics of the Russian Academy of Sciences*

The present study is devoted to problems of heat transport modelling in hemitropic micropolar continuum. The notion of hemitropic micropolar continua and irreversible thermodynamics formalism are applied to extent existing continuum thermomechanical models to hemitropic micropolar thermoelastic media. Constitutive laws of heat propagation as of type-III thermoelasticity complying with the principle of thermomechanical orthogonality are proposed and discussed. The energy and entropy balance equations specific for hemitropic micropolar thermoelasticity are considered. The special form of the Helmholtz free energy is given providing fully coupling of the equations of motion and heat conduction for hemitropic thermoelastic micropolar media. The resulting system of differential equations is obtained and discussed.

^{a)}Email: evmurashkin@gmail.com

^{b)}Email: radayev@ipmnet.ru

The most challenge problems in modern biomechanics are the modelling of soft biological tissues behaviour and their response on thermomechanical treatments. Biomaterials being composed of chiral molecules often expose chiral properties. Such solids are isotropic with respect to coordinate frame rotations but not with respect to coordinate inversions and are called non-centrosymmetric, acentric, hemitropic, or chiral. Structural noncentrosymmetry is an intrinsic characteristic of bone tissues, wood, foams, chiral sculptured thin films. It is also true for fibers, auxetics, granular, fibrous, lattice materials and other artificial materials.

Chiral effects cannot be modelled within conventional elasticity since the 4-rank constitutive tensor is unchanged under a coordinates inversion. The effects of chirality in elastic materials can be described by a generalized continuum theories, for example, the Cosserat elasticity [1, 2]. The early study on hemitropic micropolar materials modelling has been presented by Aero and Kuvshinskii in 1961 [3].

The present study is devoted to problems of heat transport in hemitropic micropolar continua. The irreversible thermodynamics formalism is applied to develop a continuum thermomechanical model of hemitropic micropolar thermoelastic media. There are different mechanisms of the heat conduction in solids such as thermal diffusion based on the Fourier's law and thermal wave propagation characterized by the finite velocity of the heat transport. The generalized type-III thermoelasticity can be reduced to the distinguished limit cases of conventional thermoelasticity (CTE/GNI) [4] and type-II hyperbolic thermoelasticity (GNII) [5] implying no dissipation of thermal energy in the course of heat transfer. The type-II thermoelasticity constitutive laws can be naturally formulated as a physical field theory starting from the variational action integral and the least action principle and permits the heat flow as thermal waves. Numerous discussions have been devoted to GN thermomechanical model. we would like to attract attention to the following papers [6–15]. Constitutive laws of heat propagation as of type-III thermoelasticity complying with the principle of thermomechanical orthogonality are proposed and discussed. The energy and entropy balance equations specific for hemitropic micropolar thermoelasticity are considered. The special form of the Helmholtz free energy is given providing fully coupling of the equations of motion and heat conduction for hemitropic thermoelastic micropolar media. The problems related to propagation of surfaces of weak and strong discontinuities of translational displacements, microrotations and temperature are investigated by the aid of the geometrical and kinematical compatibility conditions akin to Hadamard and Thomas.

The resulting differential system of linear hemitropic micropolar type-I thermoelastic continuum can be furnished in terms of translational displacements \mathbf{u} and microrotations ϕ as follows

$$\left\{ \begin{array}{l} (\mu + \alpha)\nabla\nabla \cdot \mathbf{u} + (\lambda + \mu - \alpha)\nabla \cdot \nabla\mathbf{u} + 2\alpha\nabla \times \phi + \\ + (\chi + \nu)\nabla\nabla\phi + (\chi - \nu + \kappa)\nabla \cdot \nabla\phi - \eta\nabla\theta = \rho\ddot{\mathbf{u}}, \\ (\gamma + \varepsilon)\nabla\nabla \cdot \phi - 4\alpha\phi + (\beta + \gamma - \varepsilon)\nabla \cdot \nabla\phi + 2\alpha\nabla \times \mathbf{u} + 2\nu\nabla \times \phi \\ + (\chi + \nu)\nabla\nabla\mathbf{u} + (\chi - \nu + \kappa)\nabla \cdot \nabla\mathbf{u} - \varsigma\nabla\theta = J\ddot{\phi}, \\ \nabla^2\theta - \frac{C}{\Lambda_*}\dot{\theta} - \frac{\eta}{\Lambda_*}\nabla \cdot \dot{\mathbf{u}} - \frac{\varsigma}{\Lambda_*}\nabla \cdot \dot{\phi} = 0. \end{array} \right.$$

where ∇ is the three-dimensional Hamiltonian differential operator (the nabla symbol); ρ is the mass density; J is a scalar dynamic characteristic of continuum (the rotational inertia); superimposed dot denotes partial differentiation with respect to time at fixed spatial coordinates; C is the heat capacity (per unit volume) at constant (zero) strains; θ denotes the temperature increment over the referential temperature; $\alpha, \beta, \gamma, \lambda, \mu, \chi, \varepsilon$ are isothermal constitutive constants of micropolar thermoelastic continuum; η, ς are constitutive constants providing coupling of equations of motion and heat conduction. The differential system given above is considered as the limit case of the generalized hemitropic micropolar type-III thermoelasticity.

The present study is supported by the Federal Agency for Scientific Organizations (State Registration Number AAAA-A17-117021310381-8) and by the Russian Foundation for Basic Research financially (project No. 18-01-00844).

References

- [1] Cosserat E. et F. *Theorie des corps Deformables*. Paris: Librairie Scientifique A. Hermann et Fils. 1909. 226 p.
- [2] Nowacki W. *Theory of Asymmetric Elasticity*. Oxford: Pergamon Press. 1986. 384 p.
- [3] Aero E. L. and Kuvshinskii E. V. *Fundamental Equations of the Theory of Elastic Media with Rotationally Interacting Particles // Fizika Tverdogo Tela*. 1960. Vol. 2. Pp. 1399–1409.
- [4] Green A. E., Naghdi P. M. *On Undamped Heat Waves in an Elastic Solid // J. Therm. Stress*. 1992. Vol. 15. Pp. 253–264.
- [5] Green A. E., Naghdi P. M. *Thermoelasticity without Energy Dissipation // J. Elasticity*. 1993. Vol. 31. Pp. 189–208.
- [6] Kovalev V. A. and Radaev Yu. N. *On Wavenumbers of Plane Harmonic Type III Thermoelastic Waves // Izv. Saratov Univ. (N.S.), Ser. Math. Mech. Inform.* 2010. Vol. 10. Iss. 3. pp. 46–53.
- [7] Kovalev V.A. and Radayev Yu.N. *Wave Problems of the Field Theory and Thermomechanics*. Saratov University Press, Saratov. 2010. (in Russian)
- [8] Kovalev V. A. and Radayev Yu. N. *Thermomechanical orthogonality in nonlinear type-III thermoelasticity (GNIII) // Izv. Saratov Univ. (N.S.), Ser. Math. Mech. Inform.* 2012. Vol. 12. Iss. 3. Pp. 72–82 .
- [9] Murashkin E. V. and Radayev Y. N. *On a Classification of Weak Discontinuities in Micropolar Thermoelasticity // Materials Physics and Mechanics*. 2015. Vol. 23. Pp. 10–13.
- [10] Kovalev V. A., Murashkin E. V. and Radayev Yu. N. *On a Physical Field Theory of Micropolar Thermoelasticity // Journal of Physics: Conference Series*. 2017. Vol. 788. No. 1. Pp. 012043.
- [11] Murashkin E. V. and Radaev Y. N. *On Thermodynamics of Wave Processes of Heat Transport, In: Mechanics for Materials and Technologies. Volume 46 of the series Advanced Structured Materials*. Cham. Springer. 2017. Pp. 3–58.
- [12] Murashkin E. V. and Radayev Y. N. *Full Thermomechanical Coupling in Modelling of Micropolar Thermoelasticity // Journal of Physics: Conference Series*. 2018. Vol. 991. No. 1. Pp. 012061.
- [13] Kovalev V. A., Murashkin E.V. and Radayev Y.N. *Wave Propagation Problem for a Micropolar Elastic Waveguide // Journal of Physics: Conference Series*. 2018. Vol. 991. No. 1. Pp. 070018.
- [14] Murashkin E. V. and Radayev Y. N. *Divergent Conservation Laws in Hyperbolic Thermoelasticity // AIP Conference Proceedings*. 2018. Vol. 1959. No. 1. Pp. 070025.

- [15] Kovalev V. A., Murashkin E. V. and Radayev Y. N. On Deformation of Complex Continuum Immersed in a Plane Space // AIP Conference Proceedings. 2018. Vol. 1959. No. 1. Pp. 070018.

Cooling effect for evaporating of drops situated at high-conductivity substrate

O.V. Nagornov^{1,a)}, S.Z. Dunin^{1,b)}

¹*National Research Nuclear University MEPhI*

Evaporation of liquid drops at the solid substrates have been studied in numerous papers. As a rule it is studied by numerical methods. In this paper we obtain the solution in quadrature. It allows us to analyze various physical features.

Evaporation of drops is studied during more than hundred years. However, even spherically symmetric solution for sphere have many uncertainties [1]. The problem is significantly complicated for sessile drops [2, 3] due to additional factors connected with the evaporation processes.

Important effect of the drop evaporation results in the cooling effect at the surface. In majority of papers this effect is taken into account numerically with correction on experimental data.

We obtained the solution in quadratures. The temperature depends on the heat conductivity k_L , and the evaporative number Γ . If the heat conductivity of substrate k_s is high comparing with ones for drop k_L , then the bottom part of the drop is isothermal. The convective terms and the gravitational effects can be neglected because the Pecle number $Pe \ll 1$, and $B_0 \ll 1$. The evaporation of the drop is assumed to be quasi-steady. Then we can use the Laplace equations $\Delta T_L = 0$, $\Delta c = 0$ for temperature T_L and concentration c together with the boundary equations $T_L(\alpha, \theta = 0) = T_{tr}$, and $dc(\alpha, \theta = \pi)/d\theta = 0$. The solution of this problem in toroidal coordinates (α, θ) under condition $(1 - \Gamma)(T_L(\alpha, \theta_c) - T_{tr}) \ll \Gamma \frac{\Delta c_{tr}}{c_{tr}}$ is derived analytically:

$$\begin{aligned} T_L(\alpha, \theta) - T_{tr} &= \{2(\cosh \alpha + \cos \theta)\}^{\frac{1}{2}} \cdot \\ &\cdot \int_0^\infty d\tau P_{-\frac{1}{2}+i\tau}(\cosh \alpha) \frac{\cosh \tau \theta_s}{\cosh \tau \pi} A_L \frac{\sinh \tau \theta}{\sinh \tau \theta_c}, \\ T_L(\alpha, 0) &= T_{tr}, \\ c(\alpha, \theta) - c_\infty &= \{2(\cosh \alpha + \cos \theta)\}^{\frac{1}{2}} \cdot \\ &\cdot \int_0^\infty d\tau P_{-\frac{1}{2}+i\tau}(\cosh \alpha) B \frac{\cosh \tau \theta_s}{\cosh \tau \pi} \frac{\cosh \tau(\pi - \theta)}{\cosh \tau(\pi + \theta_c)}. \end{aligned}$$

Nuclei of integrals are found out from the following conditions: the Claiperon-Clausius equation and the energy ballance equation. We calculated the temperature inside the drop and the local mass flux at the drop surface. It is derived that maximum and minimum temperatures are at the drop edge and the drop top, respectively.

^{a)}Email: nagornov@yandex.ru

^{b)}Email: szdunin@mephi.ru

References

- [1] S. Farshid Chinia, A. Amirfazlia, Understanding the evaporation of spherical drops in quiescent environment. *Colloids and Surfaces A: Physicochem. Eng. Aspects* 432, 82–88 (2013).
- [2] R.G. Larson, Transport and deposition patterns in drying sessile droplets. *AIChE J.* 60(5), 1538 (2014).
- [3] S.Z. Dunin, O.V. Nagornov and V.P. Trifonenkov, Model of spontaneous evaporating droplet on solid horizontal substrate. *Journal of Physics: Conference Series* 788, 012048 (2017).

Determination of paleotemperature for the Elbrus glacier based on the inverse problem solution

O.V. Nagornov^{1,a)}, S.A. Tyuffin^{1,b)}, V.N. Mikhailenko², G.A. Chernyakov²

¹*National Research Nuclear University MEPhI*

²*Institute of Geography, Russian Academy of Sciences*

The surface temperature reconstruction for the Elbrus Plato is built. It takes into account new data on the annual layers in glacier. The dendrochronological data are used as an additional information that allows us to improve accuracy of calculations and stability of the solution.

Previous surface temperature reconstructions for the Elbrus Plato had big discrepancies between each other [1]. It was connected with absence of data on the advection rate in glacier. The new dating of the annual glacier layers [2] allows us to find out the proper solution.

The underground temperature distribution is mainly determined by two types of processes [3]. The first is the surface temperature changes and the second is the heat flux from the Earth that is subjected to the long-time geological processes. The mathematical statement of the inverse problem consists of the thermal conductivity equation that takes into account the vertical advection term, the initial condition, the boundary condition at the bottom of glacier and the re-determination condition. The measured-temperature-depth profile is used as the re-determination condition, $\chi(z)$, where z is vertical coordinate. Then the inverse problem to find the temperature in the past is the solution of the following one-dimensional problem:

$$\begin{aligned}
 \rho(z)C(z)T_t &= (k(z)T_z)_z - \rho(z)C(z)w(z)T_z, & (t, z) \in Q \equiv [0, t_f] \times [0, H], \\
 T(z, 0) &= U(z), & z \in [0, H], \\
 T(0, t) &= U_s + \mu(t), & t \in [0, t_f], \\
 -k(H)T_z(H, t) &= q, & t \in [0, t_f], \\
 T(z, t_f) &= \chi(z), & z \in [0, H],
 \end{aligned} \tag{1}$$

where H is the ice sheet thickness, $\rho(z)$, $C(z)$, and $k(z)$ are the density, specific heat, and thermal conductivity of ice, $w(z)$ is the vertical ice velocity, q is the geothermal heat flux, $U(z)$ is the

^{a)}Email: nagornov@yandex.ru

^{b)}Email: satyuffin@mephi.ru

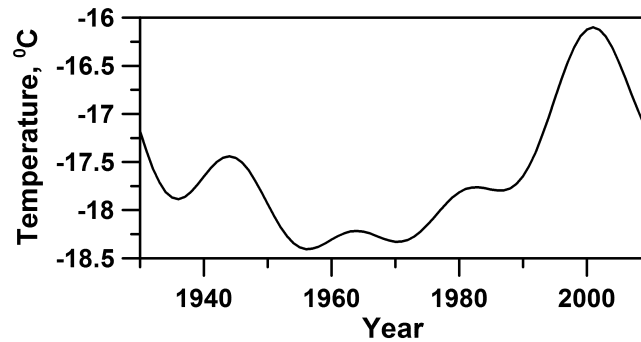


Fig. 1: Past surface temperature reconstruction.

steady-state temperature profile associated with this flux. U_s – is the initial temperature on the surface, which characterizes the average temperature that was on the surface in the past before the beginning of sharp temperature variations on the surface. $\mu(t)$ is temperature variations on the surface in time with respect to its initial value U_s from the moment $t = 0$ ($\mu(0) = 0$) to the time of measurements of the borehole temperature profile t_f .

Physical parameters of glacier are taken from [1]. We assume that the reconstructed temperature corresponds to the temperature at the depth of the activity layer equal approximately to 10 m. The temperature changes at this depth arise due to long-term temperature changes at the surface. The seasonal temperature variations do not penetrate at this depth. We decompose the temperature in the finite Fourier's series where each term corresponds to the characteristic climatic signal at the surface. It provides the uniqueness and stability of the reconstructed temperature [4]. We used the signal periods of the following duration: 264, 165, 78, 41, 27 and 19 years. These periods were obtained by the wavelet analysis of the chronology data of the tree-rings situated in this region. The tree-ring data have high resolution that improves the accuracy of the reconstruction.

The solution is shown in Fig. 1. It correlates enough well with the data based on the Kulkhor meteo-station. The correlation coefficient is 0.65.

References

- [1] Mikhalenko et al., Stratigraphic structure and thermal regime of the infiltration layer at the Elbrus west plate, in *Extreme natural phenomena and disasters, vol. 2: Uranium geology, geo-ecology, glaciology*, Moscow: IFZ RAN, 180–188 (2011)
- [2] Mikhalenko et al., Investigation of a deep ice core from the Elbrus western plateau, the Caucasus, Russia. *The Cryosphere* 9, 2253–2270 (2015)
- [3] V.M. Kotlyakov et al., Deep drilling of glaciers in Eurasian Arctic as a source of paleoclimatic records. *Quaternary Science Reviews* 23, 1371–1390 (2004)
- [4] O.V. Nagornov and S.A. Tyuffin, Inverse Problem for Paleo-Temperature Reconstruction Based on the Tree-Ring Width and Glacier-Borehole Data. *Lecture Notes in Computer Science* 10187, 508–516 (2017)

Application of eigenvalue problems for tensor and tensor-block matrices for mathematical modeling of micropolar thin bodies

M. Nikabadze^{1,2,a)}

¹*Lomonosov Moscow State University*

²*Bauman Moscow State Technical University*

The eigenvalue problems of any even rank tensor and tensor-block matrix which consists of the identical even rank tensors are considered. Formulas are obtained that express the classical invariants of the tensor $\mathbf{A} \in \mathbb{R}_{2p}(\Omega)$ through the first invariants of the degrees of this tensor. The relations that are inverse to these formulas are also given.

The complete orthonormal system of eigentensors of the symmetric tensor of the module $\mathbb{R}_{2p}(\Omega)$, as well as the complete orthonormal system of eigentensor-columns of the symmetric tensor-block matrix of the module $\mathbb{R}_{2p}^4(\Omega)$ are constructed in an explicit form. These eigentensor-columns are, of course, the elements of the module $\mathbb{R}_p^2(\Omega)$.

Some applications to mechanics are given. In particular, the representations of the elastic deformation energy and the constitutive equations (Hooke's law) of the micropolar theory are given using the introduced tensor columns and the tensor-block matrix. The definition of a positive definite tensor-block matrix is given and the positive definiteness of the tensor-block matrix of the elastic modulus tensor is shown. The definitions of the eigenvalue and the eigentensor-column of the tensor-block matrix are introduced and the problem of finding the eigenvalues and the eigentensor-column of the tensor-block matrix is considered. The characteristic equation of the tensor-block matrix has the 18th degree in the micropolar theory and according to the positive definiteness of the tensor-block matrix it has 18 positive roots. Each root should be taken as many times as its multiplicity. Consequently, each eigenvalue has the corresponding eigentensor-column. The complete orthonormal system of tensor columns of the tensor-block matrix consists of 18 tensor columns. A canonical representation of the tensor-block matrix is given. Based on this representation the canonical forms of the specific strain energy and constitutive relations are given. The concept of the structure symbols (the symbol of anisotropy) of the tensor and the tensor-block matrix are introduced.

Classification of the tensor-block matrices of the elastic modulus tensor of the micropolar linear theory of elasticity of anisotropic bodies without a center of symmetry is given. All linear anisotropic micropolar elastic materials that do not have a center of symmetry in the sense of elastic properties are divided into 18 classes which equals to the number of different eigenvalues. At the same time these classes, depending on the multiplicities of eigenvalues, are subdivided into subclasses.

The complete orthonormal system of eigentensor-column of the tensor-block-matrix of the elastic modulus tensor using 153 independent parameters, and the complete orthonormal system of eigentensor-columns of the tensor-block-diagonal matrix of the elastic modulus tensor using 72 independent parameters as well as the complete orthonormal system of eigentensors for the positive definite symmetric elastic modulus tensor of the micropolar elasticity theory by means of 36 independent parameters were constructed in an explicit form.

^{a)}Email: munikabadze@yandex.ru

Applying the canonical representations of the tensor and the tensor-block matrix, we formulated the initial-boundary value problems for the micropolar theory of some anisotropic thin bodies, and also we considered the problems of waves propagation in some continuum.

Acknowledgements: this work was supported by the Shota Rustaveli National Science Foundation (project no. DI-2016-41).

To mathematical modeling of deformation of micropolar thin bodies with two small sizes

M. Nikabadze^{1,a)}, A. Ulukhanyan^{2,b)}, G. Sakhvadze^{3,c)}

¹*Lomonosov Moscow State University*

²*Bauman Moscow State Technical University*

³*Blagonravov Mechanical Engineering Research Institute of the Russian Academy of Sciences*

A set of variety thin bodies used in engineering and construction is increasing at the present time. There were chosen some subsets of elements from this set with similar properties for which the corresponding versions of the thin body theories were developed. We note some of them: 1) the thin rods theory; 2) the single-layered thin shells theory; 3) the ribbed shells theory; 4) the single-layer thick shells theory; 5) the theory of multilayer structures and others. We can refer to several versions of each theories that differ both in the original assumptions and in the final equations.

Thus, we can conclude that the modern theory of thin bodies is a deeply developed part of the solids mechanics. However, the development the thin bodies theories is not complete, since new structures are continuously arising in the engineering. But it turns out it is impossible to make calculations of these constructions using existing versions of the theories. In this regard, we should expect the appearance of new versions of refined theories and improved methods for their calculation. Therefore, the construction of the refined theories of thin bodies and the development of effective methods for their calculation are an important and actual.

Here we consider some problems of modeling the deformation of micropolar thin bodies with two small sizes. For this purpose, the parametrization of the thin body domain with respect of arbitrary point is considered. In particular, the vector parametric equation of the thin body domain is given. There are introduced the geometric characteristics that appear under this parametrization. Different families of basis (frames) are considered and expressions for the components of the second-rank identity tensor are obtained. The representations of the gradient and the divergence of the tensor under the parametrization of the thin body domain are obtained. Based on the three-dimensional equations of motion, the constitutive relations and the boundary conditions of the micropolar elasticity theory, we got the equations

^{a)}Email: nikabadze@mail.ru

^{b)}Email: armine_msu@mail.ru

^{c)}Email: sakhvadze@mail.ru

of motion, the constitutive relations and the boundary conditions of the micropolar theory of thin bodies under the offered parametrization.

Based on the main recurrence formulas several recurrence formulas for Legendre polynomials playing an important role in the construction of various versions of the thin bodies theories are obtained. Definitions of the (m,n)-th order moment of some quantity with respect to an arbitrary system of orthogonal polynomials and the Legendre system of polynomials are given. The expressions for the moments of partial derivatives and some relations with respect to the system of Legendre polynomials, as well as the boundary conditions and various representations of the system of equations of motion and the constitutive relations of physical content in moments are obtained.

It should be noted that using this method of construction the thin bodies theory with two small sizes, we get an infinite system of ordinary differential equations. This system contains quantities which depends on one variable, namely, depends on the parameter of the base line. Thus, decreasing the number of independent variables from three to one we increase the number of equations to infinity, which, of course, has its obvious practical inconveniences. In this regard, the next necessary step is made to simplify the problem. We reduce an infinite system to the finite system. A simplified method of reduction an infinite system of equations to a finite one is presented. The initial-boundary value problems are formulated. To satisfy the boundary conditions on the front surfaces we constructed correcting terms. As a special case, we considered a prismatic body. In particular, the equations with respect to displacement and rotation vectors in moments with respect to arbitrary systems of orthogonal polynomials, including the system of Legendre polynomials, have been derived. Several equations of the first approximation were obtained. We used the tensor calculus to do this research.

Acknowledgements: this work was supported by the Shota Rustaveli National Science Foundation (project no. DI-2016-41).

Optical radiation sensor signal distortion model in the computer microscopy system

V.G. Nikitaev^{1,a)}, O.V. Nagornov^{1,b)}, A.N. Pronichev^{1,c)}, E.V. Polyakov^{1,d)}, V.V. Dmitrieva^{1,e)}

¹*National Research Nuclear University MEPhI (Moscow Engineering Physics Institute)*

The article is devoted to the analysis of the possibilities of improving the accuracy of the microscopic analysis of low contrast objects images in the optical radiation range. The factors influencing the distortion of the recorded image in the computer light

^{a)}Email: vgnikitayev@mephi.ru

^{b)}Email: ovnagornov@mephi.ru

^{c)}Email: anpronichev@mephi.ru

^{d)}Email: evpolyakov@mephi.ru

^{e)}Email: vvdmitriyeva@mephi.ru

microscopy systems, in which sensor is based on the CCD matrix, are considered. The generalized model of distortions reflecting various influencing factors is offered. Experimental evaluation of the model parameters allows you to make necessary corrections to the recorded signal. It provides an increase in the accuracy of automated analysis of microscopic images of low contrast objects in the optical radiation range.

The microscopic research method in the optical range is widely used in various fields of science, industry, medicine [1, 2]. The image analysis basis in such a microscopic study is the identification of structural elements based on their color or brightness contrast with the surrounding background. In a number of tasks this contrast is visually hardly noticeable [3, 4, 5]. Electronic means of image registration based on optical radiation sensors can be used to enhance the contrast of the image. The formation of a digital image in the computer microscopy system allows you to automate the analysis of images, highlight objects of interest and measure their characteristics. Automatic detection of low-contrast objects is limited by the capabilities of the optical radiation sensors.

Next, we consider the features of signal formation in optical radiation sensors based on charge-coupled devices (CCD). The formation of the image in the computer microscopy system is as follows (the passing light mode is considered in the example): the light flux from the light source is directed by an optical condenser to the sample under study, part of the light is absorbed and dissipated by the structural elements of the sample, the light transmitted is projected onto the light-sensitive matrix of the CCD by the lens of microscope. Light energy trapped in the CCD cell is converted into charge packet, which in a certain sequence is transmitted to the capacitor, forming a proportional charge voltage at the input of the amplifier. The amplifier performs the necessary transformation for further processing of the signal, which is subjected to analog-digital conversion, the resulting digital code is written in computer memory.

The formation of the image in the computer microscopy system along with the light flux is influenced by side factors. The set of factors determining the distortion of the signal formed by the optical radiation sensor based on the CCD matrix for each cell can be represented by the model:

$$\langle Er, Kr, T, Tr, P, Pr, Ur \rangle$$

Here Er is a random component of the light energy trapped in the CCD cell (due to the fluctuation of the light flux density at a constant brightness of the light source). Kr is the deviation of the quantum yield characteristic of a single CCD cell from the mean value of the quantum yield for all cells of the CCD matrix (different CCD cells have different quantum yield). T, Tr is a constant and a random component of the dark current (dark current fluctuation) - parasitic charge generation is in each CCD cell, even in the absence of illumination. It is dark current. P, Pr - a constant and random component of the characteristics of the charge transfer efficiency in the CCD matrix, given to the CCD cell under consideration (part of the charge packet is lost in the process of transfer of charge packets when reading the image signal); Ur - the noise of reset and reading, due to the processes of conversion of the charge package into voltage and its amplification to the level necessary for further processing.

By separating the target signal registration function and side factors, it is possible to present the generated image signal $I(x,y,t)$ by the following model:

$$I(x, y, t) = K * G(x,y) + S(x,y,t).$$

Here $G(x,y)$ is a function that determines the distribution of the light transmitted through the sample for corresponding area of the light-sensitive CCD cell. (x, y) - integer spatial coordinates in the plane of the sample (the numbers x and y correspond to the row and column numbers of the CCD cell). K - the light-signal conversion factor (it is a constant value for an ideal system). t - the time at which the image registration occurred. $S(x,y,t)$ is a function of the distortion

associated with the imperfection of the image registration system. The function $G(x, y)$ is time-independent under constant lighting conditions and a stationary sample. The dependence of the function $S(x, y, t)$ on time reflects the time-random nature of the distortion.

Deterministic and random components of the signal can be identified in these side factors that affect the formation of the image. Summarizing the impact of these factors, we can present the function of distortion in the form of:

$$S(x, y, t) = C(x, y, G(x, y)) + V(x, y, t, G(x, y)).$$

The first term in the formula determines the time-independent constant component of the distortion for each cell with coordinates (x, y) . The second term corresponds to the time-random changes in the signal under constant lighting conditions of a stationary sample. The estimation of the distortion component $C(x, y, G(x, y))$ is made according to the results of experimental studies. This allows to make a correction to the signal registered in the system. Such correction improves the accuracy of measurements performed in the computer microscopy system and increases the efficiency of automated analysis of low-contrast objects.

The reported study was funded by RFBR according to the research project № 18-07-01456.

References

- [1] Nikitaev V G, Nagornov O V, Pronichev A N, Polyakov E V, Sel'chuk V Y, Chistov K S, Blyndar V N, Dmitrieva V V, Zaytsev S M, Gordeev V V 2015 *Measurement Techniques* 57(10) 1203
- [2] Nikitaev V G, Nagornov O V, Pronichev A N, Polyakov E V, Sel'chuk V Y, Chistov K S, Blyndar V N, Dmitrieva V V, Gordeev V V 2015 *Measurement Techniques* 57(5) 560
- [3] Nikitaev V G, Nagornov O V, Pronichev A N, Polyakov E V, Dmitrieva V V 2015 *WSEAS TRANSACTIONS on BIOLOGY and BIOMEDICINE* 12 16
- [4] Nikitaev V G, Pronichev A N, Polyakov E V, Dmitrieva V V, Tupitsyn N N, Frenkel M A, Mozhenkova A V *Journal of Physics: Conference Series* vol 784, no 1, p 012042 2017.
- [5] Nikitaev V G, Nagornov O V, Pronichev A N, Dmitrieva V V, Polyakov E V *Journal of Physics: Conference Series* Volume 788 Issue 1, 2 February 2017 Article number 012056

Inverse Problem for a Differential Equation with Caputo fractional derivative in a Hilbert Space

D.G. Orlovsky^{1,a)}

¹*Mephi*

The Cauchy problem for a equation with fractional derivative and self-adjoint operator in a Hilbert space is considered. The problem of parameter determination in equation by the value of the solution at a fixed point is presented. Theorems of existence and uniqueness of the solution are proved.

^{a)}Email: odg@bk.ru

Consider the following inverse Cauchy problem

$$\begin{cases} D^\alpha u(t) = Au(t) + \varphi(t)p, & 0 \leq t \leq T, \\ u(0) = x, \\ u(T) = y, \end{cases} \quad (1)$$

where A is self-adjoint operator in a Hilbert space H , $\varphi(t)$ is a scalar non zero function and $x, y \in H$, $p \in H$ is unknown element, $0 < \alpha < 1$ and D^α is the Caputo fractional derivative

$$(D^\alpha u)(t) = \frac{1}{\Gamma(1-\alpha)} \frac{d}{dt} \left(\int_0^t \frac{u(s)}{(t-s)^\alpha} ds - u(0) \right)$$

(Γ is the Gamma function).

Solution $u(t)$ of (1) is a function which satisfies the conditions

$$u \in C([0; T], D(A)) \cap C([0; T], H),$$

$$\int_0^t \frac{u(s)}{(t-s)^\alpha} ds - u(0) \in C^1([0; T], H).$$

We need to find the function $u(t)$ and the element $p \in H$ from the system (1). The key point in the study of the inverse problem is the behavior of the characteristic function

$$F(z) = \int_0^T (T-s)^{\alpha-1} E_{\alpha,\alpha}(z(T-s)^\alpha) \varphi(s) ds, \quad (2)$$

where

$$E_{\alpha,\beta}(z) = \sum_{n=0}^{\infty} \frac{z^n}{\Gamma(\alpha n + \beta)}$$

is Mittag-Leffler function.

Theorem 1. Let us assume that operator A is self-adjoint and non-positive, function $\varphi \in C^1[0; T]$, it is not identically equal to zero and the elements $x, y \in H$. The solution of problem (1) is unique if and only if point spectrum of the operator A does not contain zeros of the characteristic function (2). The solution of problem (1) exists if and only if

$$\int_{-\infty}^0 |F(\lambda)|^{-2} d(E_\lambda h, h) < \infty,$$

where E_λ is a spectral resolution of the operator A , and the element

$$h = y - E_{\alpha,1}(T^\alpha A)x.$$

Theorem 2. Let us assume that operator A is self-adjoint and non-positive, function $\varphi \in C^1[0; T]$, everywhere either $\varphi(t) \geq 0$ or $\varphi(t) \leq 0$, $\varphi(T) \neq 0$, $x, y \in D(A)$. Then solution of problem (1) exists and it is unique.

Theorem 3. Let us assume that operator A is self-adjoint and non-positive, function $\varphi(t) = t^\beta$, where $\beta \geq 0$, the elements $x, y \in D(A)$. Then the solution of problem (1) exists, it is unique and has the form

$$p = \frac{1}{\Gamma(\beta+1)T^{\alpha+\beta}} E_{\alpha,\alpha+\beta+1}^{-1}(T^\alpha A)(y - E_{\alpha,1}(T^\alpha A)x),$$

$$u(t) = E_{\alpha,1}(t^\alpha A)x + \Gamma(\beta + 1)t^{\alpha+\beta}E_{\alpha,\alpha+\beta+1}(t^\alpha A)p.$$

Corollary 1. Let us assume that operator A is self-adjoint and non-positive, function $\varphi(t) \equiv 1$. Then the solution of problem (1) exists, it is unique and has the form

$$p = \frac{1}{T^\alpha}E_{\alpha,\alpha+1}^{-1}(T^\alpha A)(y - E_{\alpha,1}(T^\alpha A)x),$$
$$u(t) = E_{\alpha,1}(t^\alpha A)x + t^\alpha E_{\alpha,\alpha+1}(t^\alpha A)p.$$

Mathematical model of additively formed solids for the mechanical analysis of layer-by-layer manufacturing viscoelastic materials on rotating cylindrical substrates

D.A. Parshin^{1,2,a)}, A.V. Manzhirov^{1,2,3,b)}

¹*Ishlinsky Institute for Problems in Mechanics of the Russian Academy of Sciences*

²*Bauman Moscow State Technical University*

³*National Research Nuclear University MEPhI (Moscow Engineering Physics Institute)*

Additive technological processes of layer-by-layer manufacturing of material on the inner surface of an axisymmetric cylindrical substrate rotating around its axis are investigated. The obtained material exhibits properties of viscoelasticity and aging. The compliance of the substrate is not taken into account. A mechanical model of the processes is proposed. The model is based on the general approaches of the mathematical theory of accreted solids developed by the authors. The corresponding nonclassical boundary value problem for the velocity characteristics of the deformation process of the formed material layer under the action of centrifugal forces is stated. The closed analytical solution of the stated problem is obtained. By means of this solution the evolution of the stress state of the layer during and after the process of its additive manufacturing is described. The found technological stresses in the obtained layer, caused by the action of centrifugal forces in the process of its manufacturing, depend on the history of the process in determining wise. The distributions of these stresses essentially differ from the classical stresses distributions in a similar rotating material layer that did not undergo straining factors during the manufacturing process. This difference is explained by the fundamental mechanical features of the accreting process itself and causes the inevitable occurrence of residual stresses in the obtained layer after stopping its rotation and, if the simulated technological process implies it, after detaching the completed material layer from the substrate. The distributions of these residual stresses can be found by means of the dependences constructed in the presented work.

This work is devoted to modeling the processes of gradual depositing the uniform in thickness layers of additional material on the inner surface of a axisymmetric cylindrical substrate rotating around its axis at the angular velocity $\Omega(t)$ arbitrarily changing in time t . It is assumed that when

^{a)}Email: parshin@ipmnet.ru

^{b)}Email: manzh@inbox.ru

deposing the material the velocity of its inflow in the circumferential direction is incomparably higher than the velocity of its inflow in the radial direction. This assumption makes it possible to simulate the considered process of depositing the material as axisymmetric process of depositing the layer being formed simultaneously throughout its whole inner surface. In addition, this depositing process is considered as continuous, in which each infinitely small period of time an infinitely thin additional layer joins the accreting solid. Thus, the time dependence of the inner radius of the generated layer $a(t)$ is a continuous function.

It is stated the task to trace the evolution of the stress-strain state of the layer being deposited under the influence of the inertia forces of its rotational motion together with the substrate. A sufficiently slow time variation of the substrate rotational speed is assumed, $|\dot{\Omega}(t)| \ll \Omega^2(t)$, so that the tangential inertia forces of rotation are negligible if comparing to centrifugal forces. It is supposed that the potentially possible dynamic effects from the attaching the additional material to the surface of the accreted layer are insignificant, and therefore the forces of inertia of its deformation can also be neglected in comparison with the centrifugal forces of inertia and the problem can be considered in a quasi-static statement.

The problem is solved in the approximation of the plane strain state under small strain condition. In view of the latter, it makes no sense to take into account the depending on the time strain component of the inner radius of the formed layer $a(t)$ decreasing due to the inflow of additional material. This dependence can be considered a prescribed program of attaching material, which is implemented in the simulated process. Thus, in the considered problem the dependence $a(t)$ is a given continuous function, strictly decreasing at those time intervals at which the material is deposited, and constant at those time intervals at which the inflow of additional material to the formed layer is temporarily or finally stopped.

It is obvious that if the additional material joins a certain solid that is already in the process of deformation under the exposure of certain impact, then the entire newly joined material is inevitably involved in the process of deformation. One of the objectives of the present study is a refined demonstration of the mechanical effects that arise due to building-up the solid under simultaneous acting on it centrifugal forces regardless of the influence of deformation processes, occurring in the part of the solid under consideration existing before start of accreting (initial). Therefore, in the proposed model the possible compliance of the substrate on which the layer is being built is not taken into consideration (although its consideration does not represent a fundamental difficulty), and the substrate is considered to be absolutely rigid. The inner radius of the substrate let us denote by a_0 .

Elements of the additional material to be attached to the solid in the process of accreting, can for some reasons — mechanical, physical, chemical — undergo pre-deforming when joining. This will cause some initial stresses in them. In this case, stress and strain fields will be formed in the accreted solid even in the absence of an external load. Taking into account the initial stresses in the elements of any accreted solid is an integral part of the formulation of boundary conditions on the surface of its growth. In this paper, these stresses are considered to be zero, that is, when setting the problem of the considered accreted layer deformation, it is considered that the processes and effects accompanying the continuous inclusion of the additional substance in its composition does not lead to the appearance of nonzero stresses in it near the growth surface. It is important to note that this assumption in the studied problem, where the deforming of the accreted solid occurs in the field of mass forces action, from the mathematical point of view, does not simplify the formulation and solution of the problem in comparison with the case of action of some nonzero initial stresses in the attached material. Consideration of zero initial stress in the proposed model only allows to focus on the effect of exclusively centrifugal forces on the development of stress-strain state of the formed layer and convincingly show the fundamental differences of this condition from the state of the layer of similar size and material properties,

firstly formed entirely on the surface of a rigid substrate without any residual stresses, and only then forced to rotate. The latter state can be obviously determined from the solution of the corresponding classical problem of mechanics, which does not take into account the process of the considered solid formation and involves the applying the load to the solid already in its final composition.

If the elastic solid is formed by deposition, the rate of change of its stress-strain state is obviously determined only by instantaneous characteristics of the processes of its depositing and loading. After depositing is completed and the loading and kinematic constraints are fixed, the state of the solid no longer changes. This is not the case when the deformation response of the material to the mechanical loads applied to it depends on the duration of these loads acting and on the age of the material in which these loads were applied. Extended in time the processes of accreting solids with the use of such materials are quite difficult to simulate as in this case the process of changing the stress-strain state of accreted solid is affected at any given time by the entire previous history of deforming its every material element, in particular those that were in the part of the solid existed prior to the increase. However, the study of this very kind of processes is relevant from the point of view of various engineering applications since many materials used in practice exhibit conspicuous rheological properties and their mechanical characteristics are often significantly changed with age regardless of acting loads.

In the model proposed, we consider a linear viscoelastic uniformly aging isotropic material with the same constant (independent of either the material age or the time elapsed since the application of loads to it) Poisson's ratio $\nu = \text{const}$ for instantaneous elastic strain and creep strain developing over time. For the given material the relation between the stress tensor \mathbf{T} and the small strain tensor \mathbf{E} at each point \mathbf{r} of the solid at any time moment t has the form: $\mathcal{H}_{\tau_0(\mathbf{r})}\mathbf{T}(\mathbf{r}, t) = 2\mathbf{E}(\mathbf{r}, t) + (\varkappa - 1)\mathbf{1}\text{tr}\mathbf{E}(\mathbf{r}, t)$. Here $\mathbf{1}$ is the unit tensor of the second rank, $\varkappa = (1 - 2\nu)^{-1}$, \mathcal{H}_s is the linear viscoelasticity integral operator acting under the rule $\mathcal{H}_s f(t) = f(t)/G(t) - \int_s^t f(\tau)/G(\tau)K(t, \tau) d\tau$, where $G(t)$ is the elastic shear modulus of the material at its age t , and $K(t, \tau)$ is the creep kernel. Since the accreted solid is increased with new material elements already during the process of its deformation, the moment of occurrence of stresses at the points \mathbf{r} of such a solid will change from point to point and be set by a certain function $\tau_0(\mathbf{r})$, which is taken into account in the constitutive relation. In the additive processes modeled in the presented work we assume that the elementary layers of the additional material join to the inner cylindrical surface of the formed solid in the initially non-stressed state and thus begin to deform only as a part of this solid. In this case, the value $\tau_0(\mathbf{r}) \equiv \tau_0(\rho)$ should be considered as the moment of joining to the growing solid of the material layer with the radius $\rho < a_0$.

This work was financially supported by the Federal Agency for Scientific Organizations (State Registration No. AAAA-A17-117021310381-8) and in part by the Russian Foundation for Basic Research (under grant No. 17-01-00712-a).

Relativistic length contraction and time dilation as dynamical phenomena

D.V. Peregoudov^{1,a)}

¹*Geophysical Center RAS*

It is commonly accepted that the rod being accelerated and then left free contracts in accordance to Lorentz factor $\sqrt{1 - v^2/c^2}$, and also that the clock being accelerated and then returned to rest demonstrates time dilation in accordance to proper time formula $\int \sqrt{1 - v^2/c^2} dt$. Although both issues were debated numerous times, no models were proposed to trace dynamical nature of these phenomena. The purpose of present paper is to propose simple relativistic elastic rod model, which allows exact analytical solutions for a number of problems. The solutions of two problems are presented: 1) acceleration of rod with constant force applied at one of its ends during finite time interval, the result is Lorentz contraction, 2) acceleration and deceleration of Einstein clock, the result is time dilation.

A number of issues in special relativity among those Lorentz contraction [1], Ehrenfest paradox [2], Bell's spaceships paradox [3, 4] and even (implicitly, via the construction of clock) twin paradox [5] involve extended bodies. However systematic relativistic consideration is mostly suited for point particles and becomes extremely complicated in the case of extended bodies. This is the main reason why numerous times debated during more than a century issues still have no clear dynamical explanation and all attempts of such an explanation remain handwaving and mere wishes [6, 7, 8].

In this situation even simplified and purely phenomenological relativistic elastic model would be appropriate. The aim of present paper is to develop such a model. We restrict ourselves to one-dimensional case and isoentropic motion, then one can use well-known Euler and continuity equations

$$nu^\mu \partial_\mu (\tilde{w}u^\nu) - \partial^\nu p = 0, \quad \partial_\mu (nu^\mu) = 0,$$

where $u^\mu = (1/\sqrt{1 - v^2}, v/\sqrt{1 - v^2})$ stands for 4-velocity (v is ordinary velocity, natural units are used, velocity of light equals unity), n stands for 4-concentration (ordinary concentration equals $n/\sqrt{1 - v^2}$), $\tilde{w}(n)$ and $p(n)$ stand for enthalpy per particle and pressure, these are related by thermodynamical law $d\tilde{w} = \frac{1}{n} dp$. The particular choice of $\tilde{w}(n)$ defines elastic properties of the body.

The equations of motion can be rewritten in the form

$$\left(\frac{\partial}{\partial t} + \frac{v \pm c}{1 \pm vc} \frac{\partial}{\partial x} \right) J_\pm = 0, \quad J_\pm = \text{arth } v \pm \int \frac{c dn}{n},$$

where $c^2(n) = p'/\tilde{w}$ — elastic wave velocity. Equations are simplified drastically, if we choose $\tilde{w} = n$. Then $p = (n^2 - 1)/2$ (we assume $n = 1$ corresponds to the absence of stress), $c = 1$, $J_\pm = \text{arth } v \pm \ln n$, equations are reduced to

$$\left(\frac{\partial}{\partial t} \pm \frac{\partial}{\partial x} \right) J_\pm = 0,$$

thus general solution is

$$\text{arth } v + \ln n = \ln g(t - x), \quad \text{arth } v - \ln n = \ln f(t - x),$$

^{a)}Email: peregoudov@gcras.ru

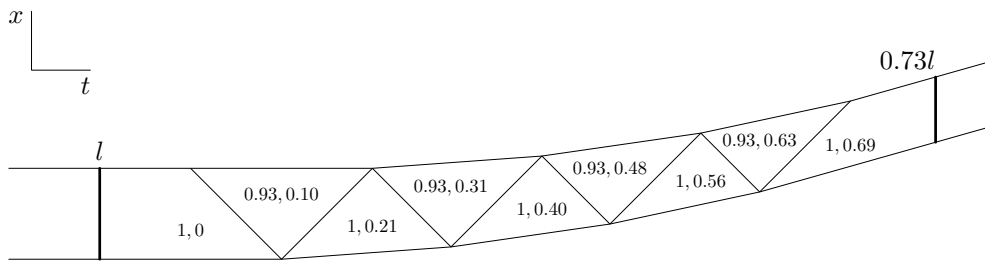


Fig. 1: Space-time diagram for the rod, accelerated with constant force applied at its front end. The correspondent pressure at the front end equals $p(0.93)$ and correspondent 4-concentration equals 0.93. Upper and lower polylines are world line of rod's ends, zigzag line is shock wave world line, numbers denote 4-concentration n and velocity v on corresponding spacetime areas. The force is applied during four shock wave trips forth and back over the rod. Rod's length contraction from l to $0.73l$ is shown.

f and g are determined by initial and boundary conditions.

The figures below demonstrate the solutions of two particular problems: acceleration of rod and acceleration and deceleration of Einstein clock.

This work was conducted in the framework of budgetary funding of GC RAS adopted by FASO Russia.

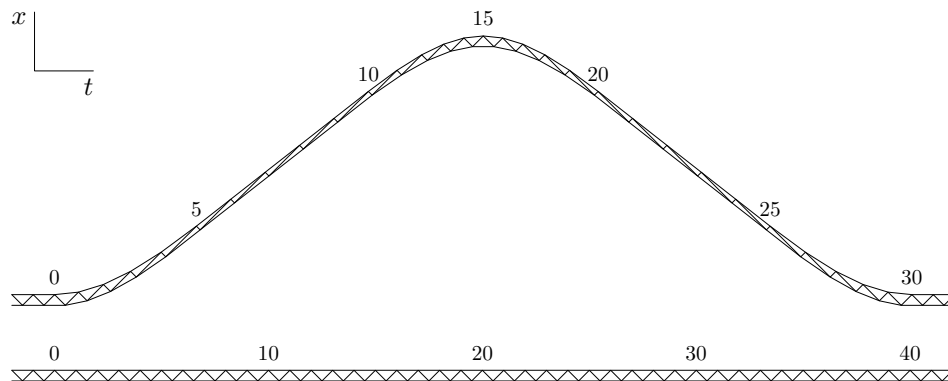


Fig. 2: Space-time diagram for two Einstein clock (the rod with two mirrors at its ends and a light pulse between them) the first one accelerated and decelerated with piecewise constant force applied at its front end and the second one at rest. The corresponding 4-concentration equals 1 (no force), 0.9 (acceleration) and $1/0.9$ (deceleration). Upper and lower polylines are world lines of mirrors, zigzag lines are the world lines of light pulses. The labels show the number of tic-tacs starting with the beginning of the first clock acceleration. The clock is accelerated during 0–5th and 25–30th and decelerated during 10–20th tic-tacs. Finally the clock undergone acceleration is ten tic-tacs behind the clock at rest.

References

- [1] H. A. Lorentz. Versuch einer Theorie der electrischen und optischen Erscheinungen in bewegten Körpern. (1895), E. J. Brill, Leiden
- [2] P. Ehrenfest. Gleichförmige Rotation starrer Körper und Relativitätstheorie. Phys. Zeit. 10 (1909), 918
- [3] E. Dewan and M. Beran. Note on Stress Effects due to Relativistic Contraction. Amer. J. Phys. 27 (1959), 517–518
- [4] J. S. Bell How to teach special relativity. Prog. Sci. Cult. 1 (1976), no. 2, 1–13
- [5] A. Einstein. Elektrodynamik bewegter Körper. Ann. d. Phys. 17 (1905), 891–921
- [6] S. S. Gerstein, A. A. Logunov. J. S. Bell’s problem. Physics of Particles and Nuclei 29 (1998), no. 5, 463–468
- [7] E. L. Feinberg. Can the relativistic change in the scales of length and time be considered the result of the action of certain forces? Sov. Phys. Usp. 18 (1975), 624–635; Special theory of relativity: how good-faith delusions come about. Phys. Usp. 40 (1997), 433–435
- [8] Brian Coleman. Minkowski spacetime does not apply to a homogeneously accelerating medium. Results in Physics 6 (2016), 31–38

Boundary integral equations for stress analysis of technical structures (from jet blades to tooth implants)

M.N. Perelmuter^{1,a)}

¹*Ishlinsky Institute for Problems in Mechanics RAS*

For solution of stress concentration and fracture mechanics problems the direct boundary integral equation (BIE) method is used. For elasticity problem without body forces the direct BIE for homogeneous structure is given by [1]:

$$c_{ij}(p) u_i(p) = \int_{\Gamma} [G_{ij}(q,p) t_i(q) - F_{ij}(q,p) u_i(q)] d\Gamma(q), \quad i, j = 1..m \quad (1)$$

where $c_{ij}(p)$ depends on the local geometry of the boundary Γ (for a smooth boundary $c_{ij}(p) = 0.5\delta_{ij}$), $G_{ij}(q,p)$ and $F_{ij}(q,p)$ are fundamental solutions of the equilibrium equations for displacements and stresses, respectively, $t_i(q)$ and $u_i(q)$ are the boundary tractions and the boundary displacements on the structure surface and the location of source and field points belonging to the boundary are defined by the coordinates of points q and p , $m = 2$ for two-dimensional and axisymmetric problems, $m = 3$ for three dimensional problems.

The multi-domain formulation of the BIE is applied for the composite structures modelling. The equations (1) are considered for each of homogeneous sub-region of the structure with the additional boundary conditions between sub-regions.

^{a)}Email: perelm@ipmnet.ru

The fundamental solutions in the equation (1) for an isotropic material are well-known [1]. When 3D problems with an arbitrary anisotropy are considered, only numerical methods can be used for representation of the fundamental solutions. For this purpose we use the method based on the multipole decomposition into the series of spherical harmonics [2].

The numerical procedure including the computation of the fundamental solutions for a body with an arbitrary elastic anisotropy was incorporated into the boundary element package for the analysis of 2D and 3D thermo-elastic multi-region problems with body forces [3, 4].

Plates with holes of different shapes and orientations are wide used in the modern technology. In the neighborhood of holes the stress state is often triaxial in nature and the problem should be considered as the three-dimensional one.

The computational analysis of the stresses concentration for some flat plates with oblique and conical holes under in-plane tensile and thermal loading for different angles of the obliquity was performed.

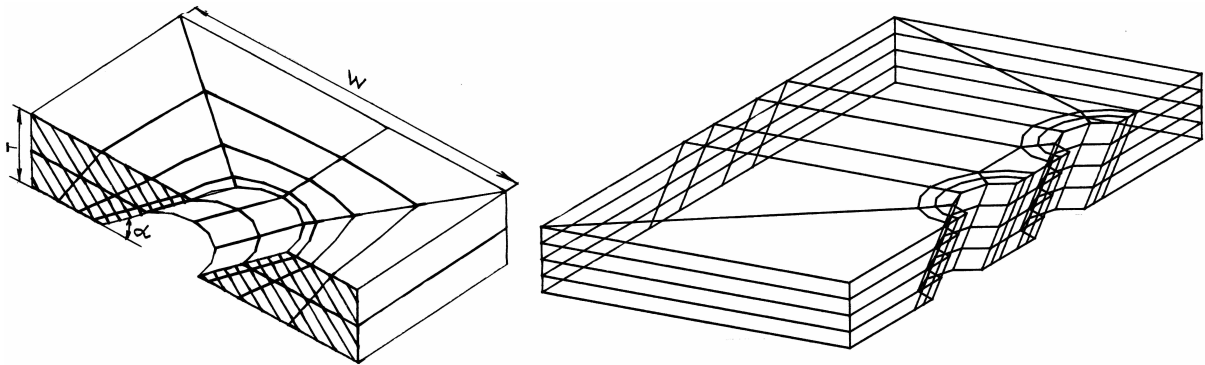


Fig. 1: Plates with one (left) and two oblique holes - models of turbine blades cooling system

Stresses concentration analysis in dental implants consists of the two stages:

- 1) analysis of the structure whole with smoothed screw in the junction between an implant and a bone;
- 2) analysis of the stresses concentration in the screwed junction at the contact boundary between the implant and bone.

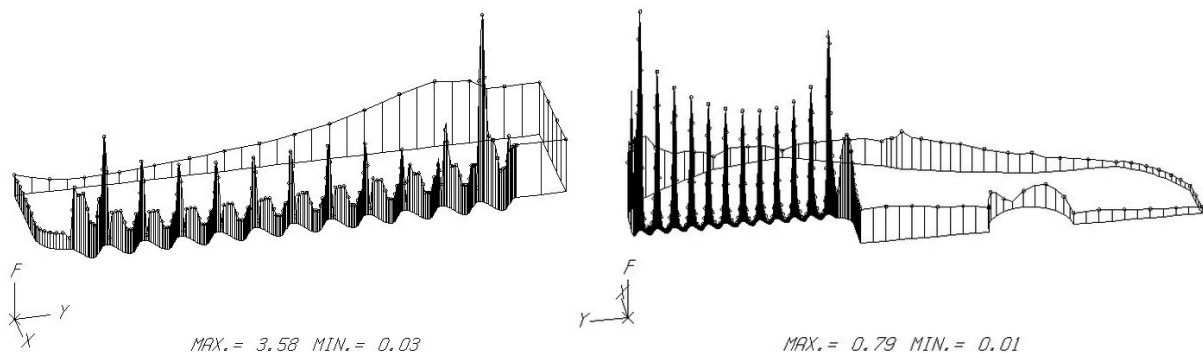


Fig. 2: Relative stresses along the boundary of the ceramic implant (left) and spongy bone

The computational model of the first stage contain of 7 sub-domains which are conforming to various parts of the implant. On all boundaries between sub-domains of the implant model were imposed the ideal contact conditions.

Analysis of the stresses concentration at the screw and bone junction was performed at the second stage of the research. It was assumed, that hollows in the spongy bone, formed in a bone after an implant penetration, are conformed to the screw thread on the implant. The following parameters of models were investigated: mechanical properties of implants and surrounding bones; shape of screw thread; the quality of junction conditions between implants and bones - from full sliding to full osseointegration. In the latter case the boundary between the implant screw thread and the bone was considered on the basis of weak interface model.

This work was partly supported by the RFBR (the Projects 17-08-01312 and 17-08-01579).

References

- [1] Banerjee P.K., Butterfield R. (1981). *Boundary Element Methods in Engineering Science*, London, McGraw Hill.
- [2] Kuznetsov S. V. (1995). Direct boundary integral equation method in the theory of elasticity, *Quart. Appl. Math.*, Vol. 53, 1-8.
- [3] Genna F., Perelmuter M. (2010) Speeding-up Finite Element analyses by replacing the linear equation solver with a Boundary Element code. Part 1: 2D linear elasticity, *Computers and Structures*, Vol. 88, 845–858
- [4] Perelmuter M. (2013). Boundary element analysis of structures with bridged interfacial cracks. *Computational Mechanics*, Vol. 51, Issue 4, 523-534

An Example of a None-zero Walsh Series with Riesz-spaces' Coefficients and Vanishing Partial Sums S_{2^k}

S.V. Petrov¹, V.M. Prostokishin^{1,a)}

¹*National Research Nuclear University MEPhI (Moscow Engineering Physics Institute), 31 Kashirskoe shosse, 115409 Moscow, Russia*

A none-zero Walsh series with coefficients from a Riesz-space and partial sums S_{2^k} (o)-converging to 0 is presented.

In this work we consider an example of a Walsh series [1] with coefficients belonging to a Riesz-space [2]. The partial sums S_{2^k} of this series (o)-converge to the element 0 of the Riesz-space [3, 4]. Nevertheless, the series is not the null series. Thus, we can not recover coefficients of the series using (o)-convergence. It is an additional argument for introduction of (u)-convergence (see [4]). There are some results of using it in [4, 5].

Theorem 1. There exist a series in the Walsh system with coefficients belonging to a Riesz-space R such that it (o)-converges to $0 \in R$ with respect to the subsequence of the natural numbers $n_k = 2^k$, $k = 0, 1, \dots$ but this series is not a null series.

^{a)}Email: vmprostokishin@mephi.ru

Let f be a function $f: \mathbb{R} \rightarrow \mathbb{L}^0([0, 1])$. By definition, put (see [3], p.300)

$$f(t) = 1_{]t-1/8, t+1/8[\cap]0, 1[}, \quad t \in \mathbb{R}.$$

Notice that the space $\mathbb{L}^0([0, 1])$ is a (super) Dedekind complete Riesz-space (see [3], p.300).

Lemma 1. Let $t, t_0 \in \mathbb{R}$ be points such that $0 \leq t_0 < t < t_0 + 1/8 \leq 1$, and $s \in \mathbb{R}$; then

$$\frac{f(t) - f(t_0)}{t - t_0}(s) = \begin{cases} -\frac{1}{t-t_0}, & \text{if } s \in]t_0 - 1/8, t - 1/8[, \\ \frac{1}{t-t_0}, & \text{if } s \in]t_0 + 1/8, t + 1/8[, \\ 0, & \text{otherwise.} \end{cases}$$

We now recall some definitions. Here we use the notions and conceptions of Walsh systems, a Riesz-space, (o) -convergence and ets. from [1, 2, 3, 3].

Definition 1. A function $F: [a, b] \rightarrow R$ is said to be differentiable at x_0 if

$$(o)\text{-}\lim_{x \rightarrow x_0} \frac{F(x) - F(x_0)}{x - x_0}, \quad \text{exists in } R.$$

Half-bounded intervals $\Delta_m^{(k)} = [\frac{m}{2^k}, \frac{m+1}{2^k})$, $0 \leq m \leq 2^k - 1$, $k = 0, 1, \dots$ are called binary-intervals (or intervals) of the rank $k \geq 0$.

The set of all intervals of the rank k is called the binary-net \mathfrak{M}_k of the rank k . Let $\Delta_x^{(k)}$ be a interval of the rank k such that the point x belongs to it. By $\{\Delta_x^{(k)}\} = \{[\alpha_k, \beta_k]_{k=0}^\infty\}$ denote a sequence of the intervals such that $x \in \Delta_x^{(k)}$ for any $k \geq 0$. There exists a nest of intervals $\{\Delta_x^{(k)}\}$ for any point $x \in [0, 1]$.

Definition 2. Suppose that for a function $F: [a, b] \rightarrow R$, there exists a limit

$$(o)\text{-}\lim_{k \rightarrow \infty} \frac{F(\beta_k) - F(\alpha_k)}{\beta_k - \alpha_k}.$$

This limit is called the (o) -derivative with respect to the binary sequence of nets $\{\mathfrak{M}_k\}$ or $(o)\{\mathfrak{M}_k\}$ -derivative and is denoted by $(o)D_{\{\mathfrak{M}_k\}}F(x)$.

Lemma 2. The limit of the right of the function f at any point $t_0 \in [0, 1]$ equals 0: $(o)f'_+(t_0) = 0 \in R$. (In fact, it means that $f'_+(t_0)(s) = 0$ is true almost everywhere on $[0, 1]$.)

Likewise, we have $(o)f'_-(t_0) = 0 \in R$. It follows that $(o)f'(t_0) = 0 \in R$.

Hereafter we suppose that ϕ is a Riesz-space-valued function defined on the set of dyadic-rational points. We use the Henstock-Kurzweil type integral over $J = [0, 1]$ with respect to the basis \mathfrak{B} for Riesz-Space-valued functions (see [4]). In our case, the basis \mathfrak{B} is a dyadic basis \mathfrak{D} . The elements of the set \mathfrak{D} are pairs (I, x) such that $x \in I$ and I is any interval of the rank $k \in \mathbb{N}$.

By definition, put

$$\phi_k(x) = \frac{\phi(\frac{m+1}{2^k}) - \phi(\frac{m}{2^k})}{|\Delta_m^{(k)}|}, \quad \text{where } x \in \Delta_m^{(k)}, \quad 0 \leq m \leq 2^k - 1, \quad k = 0, 1, \dots$$

Proposition 1.

$$\int_{\Delta_m^{(k)}} \phi_k(x) dx = \int_{\Delta_{2m}^{(k+1)}} \phi_k(x) dx + \int_{\Delta_{2m+1}^{(k+1)}} \phi_k(x) dx = \int_{\Delta_m^{(k+1)}} \phi_k(x) dx.$$

Let $S_n = \sum_{j=0}^{n-1} a_j w_j$ be the partial sum of a series in the Walsh system $\{w_j\}_j$, where coefficients a_j belong to a Riesz-space R .

The following theorem is needed for the sequel. This theorem can be proved similarly to proposition 3.1.1. from [1] for Riesz-space-valued functions.

Theorem 2. Let $\{k_j\}_j$ be an increasing sequence of natural numbers and $\{\phi_k\}_j$ be a sequence of functions such that $\{\phi_k\}$ is a constant on any interval $\Delta_m^{(k_j)}$ and for any interval $\Delta_m^{(k_j)}$ the following condition holds

$$\int_{\Delta_m^{(k)}} \phi_k(x) dx = \int_{\Delta_m^{(k+1)}} \phi_k(x) dx.$$

Then, there exists a Walsh series such that sums $S_{2^{k_j}}(x)$ are equal to the functions $\{\phi_j\}$.

Take the function f as ϕ . The application of Theorem 2 yields that the sequence $\{f_k(x)\}$ defines a unique series with partial sums $S_{2^{k_j}}(x) = f_k(x)$ (where $k_j = j$), and for any $x \in \Delta_m^k$ the following condition holds

$$S_{2^k}(x) = \frac{f(\frac{m+1}{2^k}) - f(\frac{m}{2^k})}{|\Delta_m^{(k)}|}. \quad (\text{I})$$

The limit as $k \rightarrow \infty$ for the fraction of the right side of equality (I) equals the $(o)\{\mathfrak{M}_k\}$ -derivative of the function f . Thus we have $(o)\text{-}\lim_{k \rightarrow \infty} S_{2^k}(x) = (o)D_{\{\mathfrak{M}_k\}}f(x)$.

To complete the example, we need the following proposition:

Proposition 2. If a function Y has the (o) -derivative $(o)Y'(x) = y(x)$ at some point x , then there exists a unique (o) -derivative with respect to the binary sequence of nets and $(o)D_{\{\mathfrak{M}_k\}}f(x) = y(x)$ at this point x .

Finally, we obtain $(o)\text{-}\lim_{k \rightarrow \infty} S_{2^k}(x) = (o)D_{\{\mathfrak{M}_k\}}f(x) = (o)f'(x) \equiv 0$ for any $x \in [0, 1]$.

We claim that our series is not a null series. Indeed,

$$S_1(x) = a_0 + w_1(x) = S_{2^0}(x) = \frac{f(1) - f(0)}{\Delta_0^{(0)}} = 1_{]7/8, 1[} - 1_{]0, 1/8[} \neq 0.$$

Hence it is clear that $a_0 \neq 0 \in \mathcal{R}$. Thus Theorem 1 is proved.

References

- [1] Golubov B., Efimov A., Skvortsov V. Walsh Series and Transforms: Theory and Applications (Mathematics and its Applications, Book 64), Springer, 1991, 368 p.
- [2] Vulih B. Z. An Introduction to Functional Analysis [in Russian]. M.: Nauka, 1967. 415 p.
- [3] Boccuto A. Differential and integral calculus in Riesz space. Tatra Mt. Math. Publ. 14. (1998), P. 419–438.
- [4] Boccuto A., Skvortsov V. A. Henstock-Kurzweil type integration of Riesz-space-valued functions and applications to Walsh series//Real Anal. Exch. – 2003/04. – Vol. 29, N 1. – P. 419–438.
- [5] Petrov S. V., Prostokishin V. M. On Representation of Riesz-space-valued Functions by Fourier Series on Multiplicative Systems. 2017 J. Phys.: Conf. Ser. 937 012040.

On Simulation of Blood Vessels Growth

N.E. Stadnik^{1,a)}, V.V. Klindukhov^{2,b)}

¹*Ishlinsky Institute for Problems in Mechanics of the Russian Academy of Sciences*

²*National Research Nuclear University MEPhI*

The present study is devoted to the problem of the human blood vessel growth simulation. The vessels are modelled by the thin-walled circular cylinder. The boundary value problem of the surface growth of such cylinder is solved. The analytical solution is obtained in terms of velocities of stress and strain tensors. The condition of thinness allows us to study growth processes by means of infinitesimal deformations. The stress-strain state characteristics are numerically computed and graphically analysed for various mechanical parameters of the growth processes.

The organs in the human body and animals morphologically are discriminated in two types: tubular and stromal. The first type is characterized by a cavity with walls such as vessels, bronchial tubes, bile ducts, gastrointestinal tract, etc. The most of pathological processes leading to obturation of the lumen of tubular organs due to the surface deposition of particles. The present study is devoted to the two pathological processes modelling such as atherosclerotic lesions of the arteries and thrombosis of the veins. First one is characterized by infiltration of proteins and lipids into a thin layer of the artery. Second one occurs due to the subsidence of blood and plasma proteins on the wall of the vessel.

The wall of a large vessel, both arteries and veins, structurally consists of three shells: outer, middle and inner. The outer shell is a loose connective tissue rich in blood vessels. The middle shell is represented by smooth muscle cells and the arteries also have elastic membranes. The inner membrane is thin and is represented by a flat single-layered epithelium lying on the basal membrane [1, 2]. Infiltration of the inner membrane with lipids, proteins and blood cells (macrophages, leukocytes) occurs during atherosclerotic lesions of the artery resulting in the deposition of atherosclerotic masses in the thin layer, which gradually accumulate form an atherosclerotic plaque that grows predominantly in the lumen of the vessel in virtue of elastic forces acting at the muscular membrane [3, 4]. The outer diameter of the vessel during an atherosclerotic lesion does not generally increase.

The thrombus formation is caused by a change in the vascular wall in response to which the platelets adhere to the site of injury. Further, the formation of fibrin with the participation of platelets and consolidation of the protein content of the growing thrombus. At the next stage, there is a seizure and adherence of leukocytes, erythrocytes. The final formation of the thrombus is completed by the settling of the plasma proteins of the blood on the formed convolution and its compaction [5]. As a result of the above-described processes, the thrombus has a non-uniform layered structure. The above processes are characterized mainly by surface growth of the artery wall in a thin layer. On vessels with an atherosclerotic lesion for the resumption of normal blood flow stenting is performed. A stent is a thin metal tube, consisting of wire cells, inflated with a special balloon [6, 7]. It is introduced into the affected vessel and is pressed by expansion into the walls of the vessel increasing its lumen.

Another pathological process is the remodeling of the vessel wall as a result of which a volumetric thickening of the wall occurs. With persistent high blood pressure in the arteries of large and medium diameter elastosis and elastofibrosis is revealed. Elastosis and elastofibrosis are sequential stages of the process and represent hyperplasia and cleavage of the internal elastic

^{a)}Email: nik-122@mail.ru

^{b)}Email: vklindukhov@yandex.ru

membrane, which develops compensatory in response to a persistent increase in blood pressure. In the future, the destruction of elastic fibers occurs and their replacement by collagen fibers, i.e. sclerosis. Thus, the wall of the vessels thickens, the lumen tapers [8, 9]. On Figure 1 changes in the vessel wall (thickness, outer and inner radius) are shown in the first approximation for various pathological processes.

The pathological growth of blood vessel wall can be described in some cases by surface growth mechanics technique. At present study we will focused on the processes of surface growth of thin-walled vessels. We use the ideas of the mechanics of growing solids [10, 11, 12]. Some problems concerning the residual stresses computation in frameworks of the thermoelastoplasticity and circular symmetry conditions are early studied in many papers [13, 14, 15, 16]. The principal variables of the boundary value problem for a growing body are the stress rate tensor, the strain rate tensor and the velocity vector. On the surface of growth we set a specific boundary condition depending on the curvature tensor of the growth surface and the tension and inflow rates of the incremented elements.

Some problems for an elastic thin-walled surface-growing circular cylinder are considered at present work. The condition of thinness allows us to simulate finite displacements of cylinder points under the condition of small deformations. This, in particular, makes it possible to solve the problem with exact boundary conditions on a moving surface. The behaviour features of the strain–stress state characteristics depending on the pressure on the inner and outer surfaces of the cylinder are observed and analysed.

The present study is supported by the Federal Agency for Scientific Organizations (State Registration Number AAAA-A17-117021310381-8) and by the Russian Foundation for Basic Research financially (project No. 18-01-00844, 17-01-00712, 17-51-45054).

References

- [1] M. Tennant and J. K. McGeachie, “Blood vessel structure and function: a brief update on recent advances,” *ANZ Journal of Surgery*, vol. 60, no. 10, pp. 747–753, 1990.
- [2] J. Folkman, “Angiogenesis,” *Annu. Rev. Med.*, vol. 57, pp. 1–18, 2006.
- [3] R. Kahlon, J. Shapero, and A. Gotlieb, “Angiogenesis in atherosclerosis,” *The Canadian journal of cardiology*, vol. 8, no. 1, pp. 60–64, 1992.
- [4] V. Zeev and J. E. Edwards, “Pathology of coronary atherosclerosis,” *Progress in cardiovascular diseases*, vol. 14, no. 3, pp. 256–274, 1971.
- [5] B. Furie and B. C. Furie, “Mechanisms of thrombus formation,” *New England Journal of Medicine*, vol. 359, no. 9, pp. 938–949, 2008.
- [6] C.C. Phatouros et al., “Carotid artery stent placement for atherosclerotic disease: rationale, technique, and current status,” *Radiology*, vol. 217, no. 1, pp. 26–41, 2000.
- [7] J.A. Rodriguez-Lopez et al., “Stenting for atherosclerotic occlusive disease of the subclavian artery,” *Annals of vascular surgery*, vol. 13, no. 3, pp. 254–260, 1999.
- [8] M. J. Mulvany, “Resistance vessel structure and the pathogenesis of hypertension.” *Journal of hypertension. Supplement: official journal of the International Society of Hypertension*, vol. 11, no. 5, pp. S7–12, 1993.
- [9] W. Risau, “Mechanisms of angiogenesis,” *Nature*, vol. 386, no. 6626, p. 671, 1997.

- [10] A. V. Manzhirov, M. N. Mikhin, and E. V. Murashkin, “Torsion of a growing shaft,” *Vestnik Samarskogo Gosudarstvennogo Tekhnicheskogo Universiteta. Seriya Fiziko-Matematicheskie Nauki*, vol. 221, no. 4, pp. 684–698, 2017.
- [11] A. Manzhirov, “Some problems in mechanics of growing solids with applications to am technologies,” in *Journal of Physics: Conference Series*, vol. 991, no. 1. IOP Publishing, 2018, p. 012056.
- [12] N. Stadnik and E. Dats, “Continuum mathematical modelling of pathological growth of blood vessels,” in *Journal of Physics: Conference Series*, vol. 991, no. 1. IOP Publishing, 2018, p. 012075.
- [13] E. Dats, E. Murashkin, and N. Stadnik, “On a multi-physics modelling framework for thermo-elastic-plastic materials processing,” *Procedia Manufacturing*, vol. 7, pp. 427–434, 2017.
- [14] E. P. Dats, E. V. Murashkin, and N. K. Gupta, “On yield criterion choice in thermoelasto-plastic problems,” *Procedia IUTAM*, vol. 23, pp. 187–200, 2017.
- [15] E. Murashkin, E. Dats, and V. Klindukhov, “Numerical analysis of the elastic-plastic boundaries in the thermal stresses theory frameworks,” in *Journal of Physics: Conference Series*, vol. 937, no. 1. IOP Publishing, 2017, p. 012030.
- [16] E. Murashkin and E. Dats, “Coupled thermal stresses analysis in the composite elastic-plastic cylinder,” in *Journal of Physics: Conference Series*, vol. 991, no. 1. IOP Publishing, 2018, p. 012060.

Steady trans-Alfvenic and sub-Alfvenic MHD flows in coaxial channels with longitudinal magnetic field

E.V. Stepin^{1,a)}

¹*Keldysh Institute of Applied Mathematics, Russian Academy of Sciences, Miusskaya sq. 4, 125047, Moscow, Russia*

Theoretical and numerical researches of plasma flows in coaxial channels in the presence of a longitudinal magnetic field are presented. The process of flow transition through the Alfvenic velocity corresponding to the longitudinal magnetic field in narrow channels of an arbitrary geometry is considered. Features of the relaxation process and characteristics of the transonic sub-Alfvenic flow type with acceleration in a narrow channel with a constant mean radius are studied. The main results are obtained in the quasi-one-dimensional (hydraulic) approach.

The study of processes in plasma accelerators is one of the most important theoretical and practical problems in plasma physics [1]. In the accelerator output, plasma fluxes with high velocity and energy values are formed, thus these devices have a number of actual and perspective applications. Two coaxial electrodes connected to an electric current source form a nozzle

^{a)}Email: eugene.v.stepin@gmail.com

accelerator channel (fig. 1). Plasma acceleration in the axial direction comes at the expense of the Ampere force of the interaction between the azimuthal (i.e., transverse with respect to the flow) magnetic field generated by the current in the central electrode and the electric current flowing between the electrodes. The further development of the flow acceleration mechanism in plasma accelerators channels implies the introduction of the longitudinal magnetic field induced by external conductors.

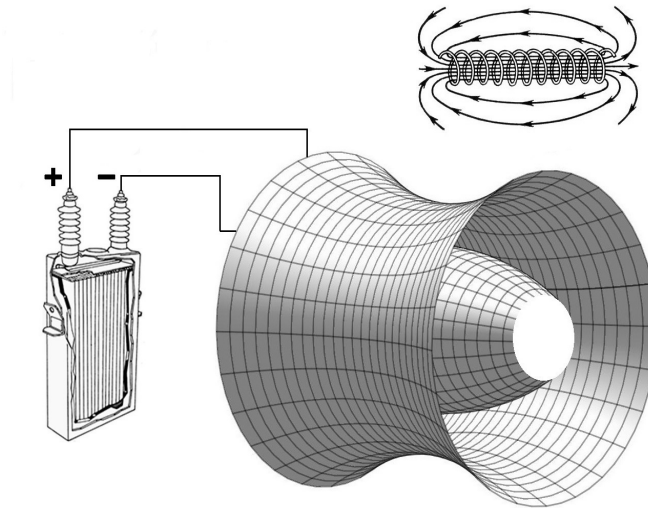


Fig. 1: Schematic view of coaxial plasma accelerator with longitudinal magnetic field.

An important role in the development of plasma accelerators is played by their mathematical models and by theoretical and numerical studies of their plasma dynamic processes. Plasma is considered as a continuous medium that moves in narrow tubes, therefore its behavior can be described by the equations of magnetic hydrodynamics (MHD) in the quasi-one-dimensional approach.

As is known [2], in the presence of a longitudinal magnetic field, plasma flows are subdivided into the two fundamentally different classes: super-Alfvénic and sub-Alfvénic (relative to the Alfvén velocity corresponding to the longitudinal magnetic field). The most important in terms of applications super-Alfvénic accelerated flows, which exist in a weak longitudinal field or in its absence (i.e., in the transverse magnetic field), have been studied in detail in the previous works [3, 4].

The sub-Alfvénic class is much less studied. In [5], in particular, the classification of all steady flow types in narrow channels with a constant mean radius is presented and the properties of the Alfvénic flow in which plasma velocity coincides with the Alfvénic velocity along the entire length of the channel are highlighted. In [6], features of the relaxation and characteristics of near-Alfvénic flow types in the channels of the same geometry have been determined.

Developing previous researches, trans-Alfvénic flows in which plasma velocity passes through the Alfvénic velocity are considered in the present paper. This transition, in contrast to narrow channels with a constant mean radius, is possible in channels with a curvilinear configuration. The calculations of this process in the narrow curved tubes with two opposite variants of geometry are provided. Some of its features are obtained by the theoretical analysis of the first integrals of the steady system of equations. It has been determined that a geometric place of the transition under consideration in a channel is directly related to its configuration.

The part of the present researches concerns the transonic sub-Alfvénic flow type with accel-

eration. In the narrow channel with a constant mean radius, its relaxation process is studied and the dependence of plasma parameters on the value of the longitudinal magnetic field is determined. It has been noted that this flow type has a mechanism of energy transformation different from its super-Alfvénic analogue. Moreover, unlike super-Alfvénic flows, there are entire families of transonic sub-Alfvénic accelerated flows at the same value of a longitudinal magnetic field.

The reported study was funded by RFBR according to the research project № 18-31-00351.

References

- [1] Morozov A.I. *Introduction to Plasma Dynamics*. Boca Raton: CRC, 2012.
- [2] Morozov A.I., Solov'ev L.S. In: M.A. Leontovich (Ed.), *Reviews of Plasma Physics*. NY: Consultants Bureau, 1980, Vol. 8, pp. 1-103.
- [3] Brushlinskii K.V., Styopin E.V. *J. Phys.: Conf. Ser.*, 2017, **788**, 012009.
- [4] Brushlinskii K.V., Zhdanova N.S., Stepin E.V. *Comp. Math. and Math. Phys.*, 2018, **58(1)**, 593-603.
- [5] Brushlinskii K.V. *Mathematical and Computational Problems in Magnetohydrodynamics*. Moscow: Binom, 2009. (in Russian)
- [6] Styopin E.V. *J. of Plasma Phys.*, 2015, **81**, 905810309.

Simulation of gas release from trunk pipelines using a new numerical method based on the Godunov approach

S.I. Sumskoi^{1,a)}

¹*National Research Nuclear University "MEPhI" (Moscow Engineering Physics Institute)*

The paper proposes a new numerical method for solving problems of pipeline transport of natural gas (methane), including the problems of modeling the gas release when accidental rupture of gas pipeline takes place.

At present, simple algebraic relations are used to calculate the release rate for disrupted gas pipeline - the Bell formula. This formula allows to calculate the release rate for a single-pipe pipeline when the valve closest to the accident site is closed. However, this approach also has disadvantages: it does not allow us to calculate, for example, a such parameter as the release temperature, which is extremely important for subsequent calculations: the temperature will significantly affect the buoyancy of the release, and hence the process of methane dispersion. It also does not allow to calculate the flow pattern for a complex pipeline scheme. Therefore, it is of interest to develop new numerical methods that make it possible to describe in more detail the process of the gas release from a destroyed gas pipeline. In this paper, it is proposed to use the standard system of gas dynamics equations describing the nonstationary one-dimensional motion of an ideal gas in a pipe of constant cross section to describe the gas flow through a gas pipeline

^{a)}Email: sumskoi@mail.ru

(including the case of its full rupture). A distinctive feature of the equations used is that in the energy balance not only the kinetic energy of motion with an average flow velocity is considered, but also internal pulsational motions with respect to the averaged flow. Also in the energy conservation equation, in addition to the standard terms, a special term is included to describe heat exchange with the environment, the intensity of this heat exchange is proportional to the difference in gas and ambient temperatures: To solve the system of equations of gas dynamics, a numerical method was proposed on the basis of the splitting of the calculation procedure according to physical processes. The calculation was carried out in two stages. At the first stage, the usual system of gas dynamics equations is solved - without taking into account such processes as the gravity, friction and heat transfer. In fact, this means rejecting the source terms from the main system and considering only such gas dynamic factors as convective transfer and the action of pressure forces. At this stage the numerical Godunov type method in Kolgan's modification is applied. Its additional modification in the framework of this paper is that the total kinetic energy took into account the pulsating component of the flow velocity. Also, to solve the Riemann problem, a solver was developed, taking into account the presence of the gas compressibility factor in the ideal gas equation. At the second stage, only the processes of gravity, friction on the walls and heat exchange through the walls of the pipeline were modeled numerically. To model the guillotine rupture, boundary conditions were considered with constant pressures at the inlet of the pipeline (the pressure was assumed equal to the pressure of the compressor station) and at the release point (the pressure was assumed to be equal to atmospheric pressure). Using the proposed numerical method, a computational program was developed. Test calculations of the release problem at a complete rupture of the pipeline were performed. The rupture was considered in the middle of a gas pipeline 120 km long and 1420 mm in diameter. The inlet pressure is equal to 150 atm, the flow rate is equal to 200 million cubic meter per day. Calculations showed that, depending on time, the release intensity remains extremely high for a long time interval. The flow rate of 5 tons per second can exist up to 20 minutes. This work is supported by the Russian Science Foundation under grant 16-19-00188

On the Holomorphy of Functions that Define Mappings with Asymptotically Constant Stretching

D.S. Telyakovskii^{1,a)}

¹*National Research Nuclear University MEPhI (Moscow Engineering Physics Institute)*

The following theorem is proved: *Let $f(z)$, $z \in G \subset \mathbb{C}$ be a function that defines the mapping $w = f(z)$, which is direct and has asymptotically constant stretching at each point of G , and the function $\log^+ |f(z)|$ is locally integrable in G , then $f(z)$ is holomorphic in G .*

We obtain a sufficient condition for the holomorphy of functions $f(z)$, $z \in G \subset \mathbb{C}$. Existence of a nonzero derivative of $f(z)$ at the point ζ is equivalent to the conformality of the mapping $w = f(z)$ at that point, that is emitting from ζ infinitely small vectors dz stretched with the same non-zero coefficient (the condition of a constant stretching) and are rotated by the same angle (the condition of preserving the angles by magnitude and direction).

^{a)}Email: dtelyakov@mail.ru

Thus, the conformality of the mapping $w = f(z)$ at each point of the domain G is a sufficient condition for the function $f(z)$ to be holomorphic in G . Conditions of the constancy of stretchings and preservation of angles under the mapping $w = f(z)$, taken separately, also give sufficient conditions for holomorphy. Menchoff [1] showed that a continuous univalent function, setting an angle-preserving mapping at all the points of G is holomorphic in G , and if the constancy of stretchings condition satisfies in G , then holomorphic is either $f(z)$, or $\overline{f(z)}$. Then Menchoff proved [2] that for continuous univalent functions, the conditions of angle preservation and the constancy of the stretchings is sufficient to assume only along three mutually noncollinear rays emitting from each point $\zeta \in G$; moreover, the directions of these rays depends on ζ .

Then Trokhimchuk [3] removed the assumption of univalence of $f(z)$ in these Menchoff's theorems. The Bohr's examples shows that the condition of univalence is essential to prove holomorphy of functions setting mappings with constant stretchings. Trokhimchuk replaced condition of univalence with the assumption that the mapping $w = f(z)$ is direct at each point $\zeta \in G$ ([3], p. 107).

Different conditions of complex differentiability set different conditions of preservation angles and constancy of stretchings. In this paper, we consider the constant-stretching condition for asymptotically monogenic functions. The function $f(z)$ is said to be asymptotically monogenic at ζ , if there exists the finite limit

$$\lim \frac{f(z) - f(\zeta)}{z - \zeta} \quad \text{as } z \rightarrow \zeta, \quad z \in E_\zeta,$$

where E_ζ is measurable set (with respect to planar Lebesgue measure) and ζ is its point of density. Accordingly we can say that the mapping $w = f(z)$ obtains asymptotically constant stretching at ζ , if there exists a finite limit

$$\lim \left| \frac{f(z) - f(\zeta)}{z - \zeta} \right| \quad \text{as } z \rightarrow \zeta, \quad z \in E_\zeta.$$

Menchoff [4] proved holomorphy of continuous asymptotically monogenic functions. In the same paper Menchoff gave an example, going back to Luzin, of a function that is asymptotically monogenic in a domain but not holomorphic there. Thus the assumption of continuity can't be removed completely but it can be sufficiently weakened. The author [5] replaced it by condition of integrability of $\log^+ |f(z)|$. For functions, setting transformations with asymptotically constant stretching, the following theorem is proved.

Theorem. *Let $f(z)$, $z \in G \subset \mathbb{C}$ be a function that defines the mapping $w = f(z)$, which is direct and has asymptotically constant stretching at each point of G , and the function $\log^+ |f(z)|$ is locally integrable in G , then $f(z)$ is holomorphic in G .*

References

- [1] *Menchoff D.* Sur les representation conforme des domaines plane, *Math. Ann.*, 1926, 95, 641–670.
- [2] *Menchoff D.* Les conditions de monogenité, *Actualités Sci. Indust.*, no 329, Hermann, Paris, 1936.
- [3] *Trokhimchuk Yu. Yu.* Continuous Mappings and Conditions of Monogeneity [in Russian], Fizmatgiz, Moscow, 1963.
- [4] *Menchoff D.* Sur la monogenité asymptotique, *Mat. sb.*, 1936, 1(43), 189–210, [in Russian; French summary].

- [5] *Telyakovskii D. S.* On asymptotically monogenic functions, *Trudy MIRAN*, 1992, 198, 186–193; English transl. in *Proc. of the Steklov Inst. of Math.* 1994, Issue 1, 177–182.

Global uniqueness of the compact support source identification problem

D.S. Tkachenko^{1,a)}, V.V. Soloviev¹

¹*National Research Nuclear University MEPhI*

An inverse problem of reconstructing the source of a special kind for parabolic equations in a bounded region with smooth boundary is considered. Solutions are sought in the Hölder classes. The source is considered to have an unknown term with a compact support on a segment inside the main domain. We prove an uniqueness theorem for the solution of the problem.

Let $T > 0$, $0 < \alpha < 1$ - fixed numbers, and on a plane with Cartesian coordinates $x = (x_1, x_2)$ there is a bounded domain Ω with a smooth boundary of $C^{2,\alpha}$ class. In the point space (x, t) we define the cylinder $\Omega_T = \Omega \times [0, T]$ with the side boundary $\Gamma_T = \partial\Omega \times [0, T]$. Let the numbers $a, b \in \mathbb{R}$ and the domain Ω be such that the interval $\omega = (a, b) \times \{0\} \subset \Omega$ and, moreover, $\bar{\omega} = [a, b] \times \{0\} \subset \Omega$. Consider the inverse problem to determine in the cylinder $\bar{\Omega}_T$ the pair of functions $u : \bar{\Omega}_T \rightarrow \mathbb{R}$, $f : \mathbb{R} \rightarrow \mathbb{R}$, $u \in C^{2+\alpha, 1+\frac{\alpha}{2}}(\Omega_T) \cap C(\bar{\Omega}_T)$, $f \in C[a, b]$ from given conditions:

$$u_t(x, t) - \Delta u(x, t) = f(x_1)h(x, t) + g(x, t), \quad (x, t) \in \Omega_T, \quad (1)$$

$$u(x, t) = \mu(x, t), \quad (x, t) \in \Gamma_T, \quad u(x, 0) = \phi(x), \quad x \in \bar{\Omega}, \quad (2)$$

$$u(x_1, 0, T) = \chi(x_1), \quad x_1 \in [a, b]. \quad (3)$$

We further assume that the f function has a compact support on the interval $[a, b]$, i.e. $f(x_1) = 0$ at $x_1 < a$, $x_1 > b$. In addition, we further assume that domain Ω is symmetric with respect to the $x_2 = 0$ axis. Denote $\tilde{h}(x, t) = \frac{h(x_1, x_2, t) + h(x_1, -x_2, t)}{2}$. For the inverse problem (1) – (3), the uniqueness theorem holds.

Theorem *Let domain Ω is symmetric with respect to the line $x_2 = 0$ and function h satisfies conditions $h, h_t, h_{x_2} \in C^{\alpha, \frac{\alpha}{2}}(\bar{\Omega}_T)$, $h(x_1, 0, T) \geq h_T > 0$, $h(x, t) \geq 0$, $h_t(x, t) \geq 0$, $x_1 \in [a, b]$, $\tilde{h}_{x_2}(x, t) \geq 0$, $x_1 \in [a, b]$, $x_2 < 0$. Then the inverse problem (1) - (3) cannot have two different solutions.*

^{a)}Email: dstkachenko@mephi.ru

Tikhonov-type Cauchy problem for Relativistic Schrodinger Equation

S.A. Vasilyev^{1,a)}, I.S. Kolosova^{1,b)}

¹*Peoples' Friendship University of Russia (RUDN University)*

Tikhonov-type Cauchy problem on the interval $[0, r_0]$ for relativistic Schrodinger equation which is an infinite order singularly perturbed differential equation is considered. The runcated equation for relativistic Schrodinger equation is build. For solving the runcated relativistic Schrodinger equation with some quasipotentials numerical methods is used. The numerical schemes on an irregular grid is applied for the solution analysis.

In the papers [1]-[4] it was investigated the relativistic Schrodinger difference equation with the quasipotential (Logunov–Tavkhelidze–Kadyshevsky equation, LTK equation) in the relativistic configurational space for the radial wave functions of bound states for two identical elementary particles without spin

$$[H_0^{rad} + V(r) - 2c\sqrt{q^2 + m^2c^2}]\psi(r, l) = 0,$$

$$H_0^{rad} = 2mc^2 ch \left(\frac{i\hbar}{mc} D \right) + \frac{\hbar^2 l(l+1)}{mr(r + \frac{i\hbar}{mc})} \exp \left(\frac{i\hbar}{mc} D \right)$$

where m is the mass, q is the momentum, l is the angular momentum of each elementary particles and $V(r)$ is the quasipotential (a piecewise continuous function).

If in this equation we let the velocity of light to infinity ($c \rightarrow \infty$) formaly it is possible to get the nonrelativistic Schrodinger equation [4].

Asymptotic solutions of boundary value problems for LTK equation was presented in [1]. For this equation were studied boundary value problems with the quasipotential on an interval and on a positive half-line. Using asymptotic methods were obtained solutions in the form of regular and boundary layer parts, and investigated the question of the asymptotic behavior of the solutions when a small parameter $\varepsilon \rightarrow 0$. Also in [1] for LTK equation was made the transition from equations of infinite order equation to finite order $2m$. For this "cutting" equation (Logunov–Tavkhelidze–Kadyshevsky cutting equation, LTKC equation) have also been formulated boundary value problems on an interval and on a positive half-line, it is were built asymptotic solution for these problems and studied their behavior when the order LTKC equation $2m \rightarrow \infty$.

If in this equation we assume that $\hbar = 1, m = 1, l = 0$ (S -wave function),

$$\varepsilon = \frac{1}{c}, \lambda_{\varepsilon, \infty} = 2q^2 / \sqrt{1 + \varepsilon^2 q^2} + 1, v = V(r), q^2 = (1 + 0.25\varepsilon^2 \lambda_{\varepsilon, \infty}) \lambda_{\varepsilon, \infty},$$

then the equation has the form:

$$[\tilde{L}_\infty^\varepsilon - \lambda_{\varepsilon, \infty}] \psi_{\varepsilon, \infty}(r) = 0,$$

$$\tilde{L}_\infty^\varepsilon = L_2 + \varepsilon^2 L_\infty^\varepsilon = \sum_{p=1}^{\infty} \varepsilon^{2p-2} \hat{L}_{2p} + v(r), \quad \hat{L}_{2p} = \frac{2(-1)^p}{(2p)!!} D^{2p}, \quad D^p = d^p / dr^p,$$

$$L_2 = \hat{L}_2 + v(r) = -D^2 + v(r), \quad L_\infty^\varepsilon = \sum_{p=1}^{\infty} \varepsilon^{2p-2} \hat{L}_{2p+2} = \sum_{p=1}^{\infty} \frac{2(-1)^{p+1}}{(2p+2)!!} \varepsilon^{2p-2} D^{2p+2}.$$

^{a)}Email: vasilyev_sa@rudn.university

^{b)}Email: i.se.kolosova@gmail.com

This differential equation of infinite order with a small parameter ($\varepsilon \ll 1$) belongs to the class of singularly perturbed equations.

For this differential equation we can build truncated equation in the form:

$$\begin{aligned} & [\tilde{L}_{2m}^\varepsilon - \lambda_{\varepsilon, \infty}] \psi_{\varepsilon, 2m}(r) = 0, \\ \tilde{L}_{2m}^\varepsilon &= L_2 + \varepsilon^2 L_{2m}^\varepsilon = \sum_{p=1}^{2m} \varepsilon^{2p-2} \hat{L}_{2p} + v(r), \quad \hat{L}_{2p} = \frac{2(-1)^p}{(2p)!!} D^{2p}, \quad D^p = d^p / dr^p, \\ L_2 &= \hat{L}_2 + v(r) = -D^2 + v(r), \quad L_{2m}^\varepsilon = \sum_{p=1}^{2m} \varepsilon^{2p-2} \hat{L}_{2p+2} = \sum_{p=1}^{2m} \frac{2(-1)^{p+1}}{(2p+2)!!} \varepsilon^{2p-2} D^{2p+2}. \end{aligned}$$

For this differential equation we can formulate Tikhonov-type Cauchy problem $A_{TCI, \varepsilon}^{2m}$ on the interval $[0, r_0]$

$$\begin{aligned} & [\tilde{L}_{2m} - \lambda_{\varepsilon, 2m}] \psi_{\varepsilon, 2m}(r) = 0, \\ & D^i \psi_{\varepsilon, 2m}(0) = 0, \quad i = 0, 1, \dots, 2m - 1. \end{aligned}$$

If we assume that $\varepsilon = 0$ we can formulate degenerate Cauchy problems A_0

$$\begin{aligned} & [L_2 - \lambda_0] \psi_0(r) = 0, \\ & D^i \psi_0(0) = 0, \quad i = 0, 1. \end{aligned}$$

In this work Tikhonov-type Cauchy problem $A_{TCI, \varepsilon}^{2m}$ and Cauchy problems A_0 are investigated with some continuous quasipotentials. The numerical schemes on an irregular grid is applied for the solution analysis of problems $A_{TCI, \varepsilon}^{2m}$ and A_0 .

References

- [1] Amirkhanov I. V., Zhidkov E. P., Zhidkova I. E., Vasilyev S. A. *Mat. Model.* Vol. 15, N 9, pp. 3–16, 2003.
- [2] Kadyshevsky V.G. *Nucl.Phys.* Vol. B6, N1, pp. 125 – 148, 1968.
- [3] Logunov A.A., Tavkhelidze A.N. *Nuovo Cimento.* Vol. 29, pp. 380 – 399, 1963.
- [4] Zhidkov E.P., Kadyshevskii V.G., Katyshev Yu.V. *Teoreticheskaya i Matematicheskaya Fizika.* Vol.3, N2, pp. 191 – 195, 1970.

Mathematical modelling and optimization of High-Power Channel-Type Reactor's core charge

G. Zaluzhnaya^{1,a)}, A. Zagrebayev^{1,b)}

¹*NRNU MEPhI*

Optimizing the decommissioning of nuclear power units that have worked their resources out is now one of the most urgent tasks. In addition to technical problems related to safety, there is a problem of efficient use of fuel in a decommissioning reactor, particularly for reactors with continuous overload of RBMK-type fuel. During the operation of the reactor there are fuel assemblies with different energy-producing values in the core and there is a fundamental possibility of their rearrangement, forming accordingly the structure of the core, which in turn determines the efficiency of using the remaining fuel. To solve these problems, we provide a mathematical model of fuel assemblies' spectrum in this paper.

Let us note that the mathematical model of fuel assemblies spectrum dynamics by energy-producing was obtained by analogy with the mathematical model of the Fermi neutron slowdown spectrum. link1 Fuel assemblies' balance in interval dE of energy-producing is

$$\frac{\partial n(E, t)}{\partial t} = \frac{\partial q(E, t)}{\partial E} - S(E, t) + B(E, t) \quad (1)$$

where the first term on the right-hand side is the rate of decrease due to burning out, $S(E, t)$ is the rate of loss due to unloading from core, $B(E, t)$ is the rate of fuelling from another reactor.

The model was tested using data of the Kursk and Smolensk NPPs. For comparison, the average energy production by the zone was used and fuelling (in reality, it does not usually exceed 2 – 3 assemblies per day, taking into account replacement of defective fuel assemblies). The calculation results showed an error approximately 1% when calculating the average energy-producing in the core, and the values of fuelling correspond to the technically feasible ones.

First way to maintain reactor's criticality is to take out fuel out of the core — "collapse of reactor core". Maximum of energy-producing can be calculated and depends on effective multiplication factor.

Second way to maintain reactor's criticality is to form two-region core charge: fuel assemblies with less energy-producing have to stay in central region, and others have to stay in peripheral region. Effective multiplication factor depends on diapason of fuel assemblies energy-producing in central zone. It is shown that we can find a charge that provides maximum effective multiplication factor.

Mathematical modeling has shown that anyway there is a gain in the use of fuel from 40% to 50% in comparison with the normal mode of reactor decommission. All results were obtained using reactor's point model and linear approximation of fuel assembly's power and multiplication factor. The results just show the possibility of HPCTR's decommissioning optimization. Concrete values may be specified after full neutronic computation.

References

- [1] *J. Zeldovich (memories, letters, documents)* M., 2014

^{a)}Email: zaluzhnaya_galya@mail.ru

^{b)}Email: AMZagrebayev@mephi.ru

Section “Mathematical methods of processing and data analysis”

A Simple Model of Active Queue Management System According to the RED Algorithm

A.Y. Apreutesey^{1,a)}, A.V. Korolkova^{1,b)}

¹*Department of Applied Probability and Informatics*

Peoples' Friendship University of Russia (RUDN University)

6 Miklukho-Maklaya str., Moscow, 117198, Russian Federation

The Active Queue Management system with RED algorithm is used to control and prevent congestion in the queues of gateways [1]. When the average queue size exceeds a preset thresholds, the gateway marks each incoming packet with a certain probability, where the exact probability is a function of the average queue size and average TCP-window size. The algorithm randomly drops the packets with the marking, while reducing the traffic intensity from the source. As the queue grows, the statistical probability for dropping an arriving packet grows too. Consequently, in simulation modeling it is optimal to use a hybrid approach that might be implemented in the Modelica language. Modelica is an object-oriented physical modeling language that supports continuous and hybrid, as well as discrete paradigms. The main purpose of this work are to construct of the simplified model of the AQM system with RED algorithm and to demonstrate the behaviour of main system parameters depending on the preset thresholds.

The work is partially supported by RFBR grant No 16-07-00556. Also the publication was prepared with the support of the “RUDN University Program 5-100”.

A Simple Mathematician Model of the AQM system with RED algorithm [1] is presented in the following equations

$$\dot{W}(t) = \frac{1}{R} - \frac{W(t)W(t-R)}{2R(t-R)}KQ(t-R), \quad (1)$$

$$\dot{Q}(t) = \begin{cases} N\frac{W(t)}{R} - C, & Q(t) > 0, \\ \max\left\{N\frac{W(t)}{R} - C, 0\right\}, & Q(t) = 0, \end{cases} \quad (2)$$

$$\dot{\hat{q}}(t) = \frac{\ln(1-\alpha)}{\delta}\hat{q}(t) - \frac{\ln(1-\alpha)}{\delta}Q(t), \quad (3)$$

describing the behaviour of the three main functions: $W(t)$ – average TCP-window size (packets); $Q(t)$ – average queue size (packets); $\hat{q}(t)$ – an estimate of the average queue length at the router.

The packet discard function takes the form:

$$p = \begin{cases} 0, & 0 \leq \hat{q} < Q_{\min}, \\ \frac{\hat{q} - Q_{\min}}{Q_{\max} - Q_{\min}} p_{\max}, & Q_{\min} \leq \hat{q} \leq Q_{\max}, \\ 1, & \hat{q} > Q_{\max}, \end{cases} \quad (4)$$

where Q_{\max} , Q_{\min} are the queue size thresholds, p_{\max} shows part of dropped packets.

^{a)}Email: 1032152610@pfur.ru

^{b)}Email: akorolkova@sci.pfu.edu.ru

We consider a system in which there is a single congested router with a transmission capacity of C , amount of the TCP-session N and round trip time R (sec). The equation (1) describes the behavior of the TCP window size. This models the additive-increase multiplicative-decrease behavior of TCP. In the equation (2) the behaviour of the queue size is showed. The first term corresponds to the increase in the queue length due to the arrival of packets, the second term models the decrease in the queue length. The equation (3) describes an exponentially weighted moving average of queue size based on samples taken every δ seconds using a weight α , $\delta = 1/C$, $\alpha = 1 - e^{-1/C}$. Full model is presented in [2].

In the OpenModelica the program might have the following form:

```

model TCPRED
parameter Real Qmin(start=20),Qmax(start=60),pmax(start=0.1),N(start=1),
C(start=11),R(start=1);
Real p(start=0.1), alfa, qcap(start=1), Q(start=1), W(start=0.1);
equation
p = if((qcap>=0)and(qcap<Qmin)) then 0 else (if((qcap>=Qmin) and
(qcap<=Qmax)) then((qcap - Qmin)*pmax/(Qmax-Qmin)) else 1);
der(W)=(1/R)-(W*delay(W,R)*delay(p,R)/(2*R));
der(Q)= if Q>0 then ((N*W*(1-p)/R)-C) else max(((N*W*(1-p))/R)-C,0);
alfa=1-exp(-1/C);
der(qcap)=(log(1-alfa)*qcap/(1/C))-(log(1-alfa)*Q/(1/C));
end TCPRED;
    
```

At initial threshold values $Q_{\min} = 20$ and $Q_{\max} = 60$ the phase portrait (fig. 1) has the form of a limiting cycle, that indicates the presence of an self-oscillation [3]. When using other threshold values $Q_{\min} = 10$, $Q_{\max} = 85$, the phase portrait (fig. 2) has the focus form, which indicates the absence of self-oscillations.

In conclusion, the work demonstrates the application of the Modelica language to simulate a hybrid simple system with control by the algorithm type RED. It is shown that there is an auto oscillatory mode for certain specified parameters of the system.

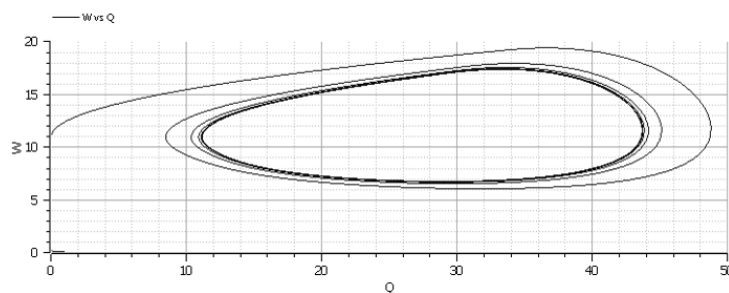


Fig. 1: Phase portrait (W, Q) , $Q_{\min} = 20$, $Q_{\max} = 60$

References

- [1] Floyd S., Jacobson V. Random Early Detection Gateways for Congestion Avoidance // IEEE/ACM Transactions on Networking. — 1993. —Vol. 1, Issue 4. — P. 397–413.
- [2] Misra V., Gong W.-B., Towsley D. Fluid-Based Analysis of a Network of AQM Routers Supporting TCP Flows with an Application to RED // ACM SIGCOMM Computer Communication Review. — Volume 30, Issue 4, October 2000. — P. 151–160.

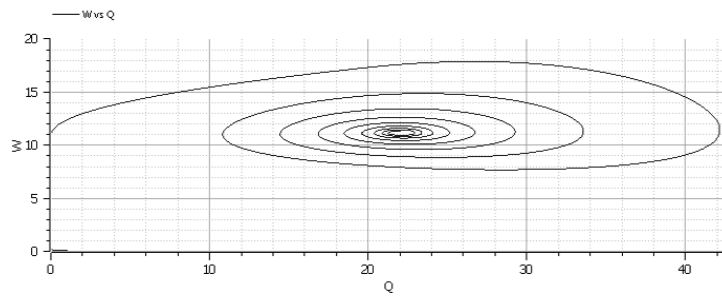


Fig. 2: Phase portrait (W, Q) , $Q_{\min} = 10$, $Q_{\max} = 85$

- [3] Korolkova A. V. Defining the Areas of Self-Oscillation in RED-Like Systems // Bulletin of Peoples' Friendship University of Russia. Series "Mathematics. Information Sciences. Physics". — 2010. — № 1. — P. 103–105.

Mathematical model for predicting the resource allocation within a system in the course of a transition process

E. Bychovets¹, S.G. Klimanov¹, V.V. Klimov¹, A.V. Kryanev^{1,a)}, D.E. Sliva¹

¹*National Research Nuclear University "MEPhI"*

The problems of dynamic change of shares of distributed resources are considered. A mathematical model for predicting the dynamics of shares for a transition process from one equilibrium state of the system to another equilibrium state is proposed. The case of the presence of a noise chaotic component in such a model is considered. Practical examples implementing the proposed model applicable to investments are given.

1 Introduction

In the formulation of many applied problems, the unknown time-varying functions are the shares of a resource distributed among the objects of a considered system. Examples of such problems are the problems of restructuring the composition of effective investment portfolios [1, 2, 3, 4] or the dynamics of the distribution of the priority coefficients of performance parameters of a complex economic or technical system [5, 6, 7]. Often when solving this type of problem, the distribution of shares at a future fixed time point is known, sometimes with some degree of uncertainty. The paper considers the problem of determining the transition process from the initial distribution of shares to their final distribution.

2 The scheme for calculating the dynamics of the transition process for the shares of resource allocation in the system

The predicted dynamics of the transition process for the shares of the distributed resource is described by the following compound system of equations

^{a)}Email: avkryanev@mephi.ru

$$\frac{\partial x_i(t)}{\partial t} = a_i - a \cdot x_i, 0 < t < t^*, i = 1, \dots, n \tag{1}$$

with the initial condition

$$x_i(t) = x_{i0} \geq 0, i = 1, \dots, n, \sum_{i=1}^n x_i = 1. \tag{2}$$

In system (1) the parameters $a_i, i = 1, \dots, n$ are unknown and are to be determined. Consider the following inverse problem for the system of differential equations (1). It is required to find parameters $a_i, i = 1, \dots, n$ such that the normalization conditions $\sum_{i=1}^n x_i(t) = 1, 0 < t < t^*, x_i(t) \geq 0, i = 1, \dots, n$, are fulfilled, and the solution of the Cauchy problem (1) - (2) must satisfy the terminal condition

$$x_i(t^*) = x_i^* \geq 0, i = 1, \dots, n, \sum_{i=1}^n x_i^* = 1. \tag{3}$$

The solution of the inverse problem (1) - (3) is given by

$$x_i(t) = x_i^* + (x_{i0} - x_i^*) \cdot \exp(-\alpha \cdot t), i = 1, \dots, n. \tag{4}$$

If there is an additive chaotic component $\epsilon(t), M\epsilon(t) = 0$ on the right-hand side of the original system (1), (4) is also the unbiased estimate of the solution of the inverse problem (1) - (3), and the estimate of the parameter α can be found using samples of the dynamics of the changes in $x_i(t), i = 1, \dots, n$ by means of the ordinary least squares method. Below is a numerical example of the dynamics of the shares of a distributed resource for a system of objects into which these resources are allocated. Table 1 presents the results of forecasting the shares of the distributed resource using the above scheme (the shares in Table 1 are given in percentages). Here the initial shares are defined by the equalities: $x_{10} = 0.04, x_{20} = 0.21, x_{30} = 0.75, x_{40} = 0.00$, and the shares of the final state by the equalities $x_1^* = 0.01, x_2^* = 0.03, x_3^* = 0.21, x_4^* = 0.75$. Table 1 contains samples of resource allocation shares at regular time intervals for four objects (the projected values of shares are given in parentheses).

Table 1: Sample resource shares dynamics

4%	21%	75%	0%
3% (3%)	15% (15%)	61% (58%)	21% (24%)
3% (2.8%)	12% (12.2%)	50% (51%)	35% (34%)
2% (2%)	10% (10%)	43% (42%)	45% (46%)
2% (2%)	7% (7%)	35% (32%)	56% (59%)
2% (1.5%)	6% (6.5%)	29% (30%)	63% (62%)
1% (1.5%)	5% (5.5%)	25% (28%)	69% (65%)
2% (1%)	4% (4%)	24% (24%)	70% (71%)
1% (1%)	4% (4%)	22% (22%)	73% (73%)
1% (1%)	3% (3%)	21% (21%)	75% (75%)
1% (1%)	3% (3%)	21% (21%)	75% (75%)

3 Conclusion

The report presents a mathematical model for predicting the dynamic process of resource allocation in the transition from one equilibrium state to another equilibrium state. The mathematical model is based on the inverse problem for a system of ordinary differential equations with allowance for the normalization and non-negativity of the fractions for the entire considered period of time. An explicit solution of the inverse problem is obtained. It is noted that the obtained solution can be used as an estimate of the forecast in a dynamic mode in the presence of an unbiased chaotic component.

References

- [1] H.M. Markowitz. Mean Variance Analysis in Portfolio Choice and Capital Markets. Basil: Blackwell, 1990.
- [2] U.F. Sharpe, G.Dg. Alexander, D.V. Baily. Investment. Moscow: Infra-M, 2001.
- [3] Rockafellar, R.T., Uryasev, S. Optimization of conditional value-at-risk. *J. Risk*, 2(3), 2000.
- [4] Lim Churlzu, Sherali Hanif D., Uryasev Stan. Portfolio optimization by minimizing conditional value-at-risk via non-differentiable optimization. *Computational Optimization and Applications*, 46(3), 2010.
- [5] S.S. Semenov, E.M. Voronov, A.V. Poltavskii, A.V. Kryanev. Methods of decision-making in problems assessing the quality and technical level of complex technical systems. Moscow: URSS, 2015 (in Russian).
- [6] F.F. Urlov, E.I. Shapkin, Selecting effective strategic decisions on the basis of multi-level and multi-criteria approach. N. Novgorod: Tutorial, 2007 (in Russian).
- [7] V.D. Nogin. Decision-making in many criteria. SPb.: Publisher UTAS, 2007 (in Russian).

Study of the dynamics of a system with delay that described of the operation of a nuclear reactor

N.D. Bykova^{1,a)}

¹*P.G. Demidov Yaroslavl State University*

The dynamics of a system of differential-difference equations

$$\begin{aligned}\dot{N}(t) &= [a(N(t) - N_0) + bT(t - \tau)]N(t) \\ \dot{T}(t) &= r[N(t) - N_0 - T(t)].\end{aligned}$$

was studied using asymptotic methods.

This system of differential-difference equations is used for the description of the operation of a nuclear reactor. In this case $N(t)$ is reactor power, $N_0 > 0$ is stable

^{a)}Email: n.bykova90@gmail.com

value of reactor power, $T(t)$ is temperature variation, a and b are values was proportional to the power coefficient of reactivity and proportional coefficient of reactivity, $r > 0$ is value that describes total thermal capacity, $\tau > 0$ is delay, t is time.

We assumed that the parameter $|b|$ or the delay τ is sufficiently large. The results about the existence, stability and asymptotics of periodic solutions of this system were obtained.

Stochastic modeling of spreading of computer viruses

A.V. Demidova^{1,a)}, T.S. Demidova¹, A.A. Sobolev¹

¹*Peoples' Friendship University of Russia (RUDN University)*

In this paper we consider the simplest SIR model, which is used to describe the dynamics of the propagation of network worms. Taking into account probabilistic phenomena in modeling complex systems can potentially improve the mathematical model of the system under study. The aim of this work is to apply stochastic epidemiological models to the modeling computer viruses spreading in the local network.

Network worms are one of the varieties of network malware, capable of independent search for new nodes to infect and use them to spread over local and global computer networks, creating copies of themselves. Modern protection tools are not always able to respond quickly to the epidemic of network worms, so the urgent task is to simulate the dynamics of the malware spreading, which will create more effective protection tools that can prevent or contain epidemics in the early stages. Numerous studies have shown that the use of mathematical theory of biological epidemics can be helpful for viruses spreading modeling. The aim of this work is to apply stochastic epidemiological models to the simulation of computer viruses spreading dynamics in the local network.

1 The SIR model of an epidemic

The SIR model can be used to describe the attenuation of network epidemics. In this system, there are three states of computers: S -susceptible, I - infected, R – recovered (or immune). The system is closed, i.e. the nodes do not appear and do not exit it. For this model, the statement is true $S+I+R=N$. To describe the relative numbers of nodes, we introduce variables $s=S/N$, $i=I/N$, $r=R / N$. All nodes are assumed to be infected equally. The following ODE system describes this model:

$$\begin{cases} \frac{ds}{dt} = -\beta is \\ \frac{di}{dt} = \beta is - \gamma i \\ \frac{dr}{dt} = \gamma i \end{cases} \quad (1)$$

In the system (1) the β is computer infection rate and γ is computer recovery rate.

^{a)}Email: demidova_av@pfur.ru

2 A stochastic model of network worms spreading

Classical epidemiological models are deterministic and represent a system of ordinary differential equations, so they can't take into account the stochastic properties of the environment such as instability of communication channels, a variable number of computers on the network, user actions, etc. One way to consider these phenomena is the transition from deterministic to stochastic equations. In papers [1, 2] stochastic models construction method is developed. This method allows one to construct consistent stochastic and deterministic parts of SDE. The method is based on combinatorial methodology described in [3, 4]. Consistency refers to the fact that stochastics is related to the structure of the system under study and is not a description of the external influence on it. The method consists in constructing an interaction scheme – a symbolic record of all interactions of the system elements. From the interaction scheme one can get the master equation of kinetic chemistry and approximate Fokker-Planck and Langevin equations. For the stochastic SIR model, we get the following interactions scheme:



In (2) the first line describes the interaction of infected host with the susceptible, with the result that in the system formed a new infected host. The second line describes the application of "medicine" to the infected node, as a result of which this node becomes immune to infection.

3 Numerical analysis of network worms propagation dynamics

Numerical analysis of the dynamics of distribution of network worms was carried out using the developed software package, implemented in Python 3 using NumPy and SciPy libraries, as well as Matplotlib for graphical representation of calculations [5, 6]. In addition, the possibility of interactive selection of model parameters using jupyter's ipywidgets library is implemented.

4 Conclusion

The paper deals with deterministic and stochastic models of network worms spreading. The structure of stochastic models is described, Fokker–Planck equation is written out, transition rule to stochastic differential equation in Langevin form is formulated. The comparative analysis of deterministic and stochastic models is carried out. Analysis of the simplest SIR model showed that this model does not take into account many factors affecting the dynamics of the spread of network worms. So, this model does not take into account the structure of the network, the stochastic aspects of the network and the departure of its nodes, as well as various probabilistic factors. Analysis of the stochastic model showed that the introduction of stochastic weakly affects the behavior of the system, so the deterministic model is decent approximation for stochastic one. Numerical experiments show consistency with analytical results for the studied deterministic model.

Acknowledgments

The work is partially supported by RFBR grants No 16-07-00556. Also the publication was prepared with the support of the “RUDN University Program 5-100”.

References

- [1] A.V. Demidova, D.S. Kulyabov, Introduction of Self-Consistent Term in Stochastic Population Model Equation, Bulletin of Peoples' Friendship University of Russia. Series Mathematics. Information Sciences. Physics (3) (2012) 69–78
- [2] A.V. Demidova, M.N. Gevorkyan, A.D. Egorov, A.V. Korolkova, D.S. Kulyabov, L.A. Sevastyanov, Influence of stochastization to one-step model. Bulletin of Peoples' Friendship University of Russia. Series Mathematics. Information Sciences. Physics (1) (2014) 71–85.
- [3] N.G. van Kampen, Stochastic Processes in Physics and Chemistry, Elsevier Science (1992).
- [4] C. W. Gardiner, Handbook of Stochastic Methods: for Physics, Chemistry and the Natural Sciences. Springer Series in Synergetics. Springer, Heidelberg, (1985).
- [5] M.N. Gevorkyan, T.R. Velieva, A.V. Korolkova, D.S. Kulyabov, L.A. Sevastyanov, Stochastic Runge-Kutta Software Package for Stochastic Differential Equations, in Dependability Engineering and Complex Systems, 70 (2016) 169-179.
- [6] E. G. Eferina, A. V. Korolkova, M. N. Gevorkyan, D. S. Kulyabov, L. A. Sevastyanov, One-Step Stochastic Processes Simulation Software Package, Bulletin of Peoples' Friendship University of Russia. Series "Mathematics. Information Sciences. Physics" (3) (2014) 46–59.

Method of anomaly recognition in time series of matrix data based on confidence interval systems and space-time filtering

M.N. Dobrovolsky^{1,a)}, V.G. Getmanov^{1,2,b)}, A.A. Soloviev^{1,3,c)}, E.Y. Butirskiy^{4,d)},
A.N. Dmitrieva^{2,e)}

¹*Geophysical Center RAS*

²*National Research Nuclear University MEPhI*

³*Schmidt Institute of Physics of the Earth RAS*

⁴*Saint Petersburg State University*

A method for anomaly recognition in time series of matrix data is proposed. The mathematical apparatus of confidence intervals and space-time filtering is applied. The reference and sliding matrix systems of confidence intervals are formed. The anomaly recognition is performed based on decision rules for comparing the reference and sliding systems of confidence intervals. An example of anomaly recognition in the matrix data of the URAGAN muon hodoscope is given.

The problem of anomaly recognition in time series of matrix data is considered. Time series of matrix data $Y(i, j, Tk)$, $i = 1, \dots, N_1$, $j = 1, \dots, N_2$, $k = 1, \dots, K$ are given, where T

^{a)}Email: m.dobrovolsky@gcras.ru

^{b)}Email: v.getmanov@gcras.ru

^{c)}Email: a.soloviev@gcras.ru

^{d)}Email: evgenira88@mail.ru

^{e)}Email: ANDmitriyeva@mephi.ru

is the time step. The goal is to recognize the anomalous areas $W_k \subset W = \{i, j: i = 1, \dots, N_1, j = 1, \dots, N_2\}$ for moments Tk . Anomalousness is understood as a sufficiently large change in the expectations and, possibly, dispersions of time series data at points of the area W_k . Time series of data in the elements of the matrix W are considered to be normally distributed.

Estimates of mathematical expectations and standard deviations are calculated for each element of the matrix at the reference interval of length k_0 :

$$m_0(i, j) = \frac{1}{k_0} \sum_{k=1}^{k_0} Y(i, j, Tk), \quad D_0(i, j) = \frac{1}{k_0 - 1} \sum_{k=1}^{k_0} (Y(i, j, Tk) - m_0(i, j))^2,$$

$$\sigma_0(i, j) = \sqrt{D_0(i, j)}.$$

Matrices of reference systems of confidence intervals are calculated based on the obtained estimates $m_0(i, j)$ and $\sigma_0(i, j)$:

$$T_{01}(i, j) = m_0(i, j) - c \frac{\sigma_0(i, j)}{\sqrt{k_0}}, \quad T_{02}(i, j) = m_0(i, j) + c \frac{\sigma_0(i, j)}{\sqrt{k_0}}.$$

Here $c = t_{p, k_0-1}$ is a $(1 - p)$ -quantile of the Student's distribution, p is the specified confidence level. After this, a system of sliding intervals of length k_0 is formed: $((k_{s1}, k_{s2}): s = 1, \dots, S, k_{s2} = k_{s1} + k_0 - 1, k_{11} \geq k_0 + 1)$. The procedure for constructing confidence intervals is repeated for each sliding interval:

$$T_{s1}(i, j) = m_s(i, j) - c \frac{\sigma_s(i, j)}{\sqrt{k_0}}, \quad T_{s2}(i, j) = m_s(i, j) + c \frac{\sigma_s(i, j)}{\sqrt{k_0}}.$$

Non-intersections of confidence intervals, constructed in a sliding window, with reference confidence intervals are determined: $T_{s1}(i, j) \geq T_{02}(i, j)$ or $T_{s2}(i, j) \leq T_{01}(i, j)$. The indicator matrices A_s for sliding intervals are calculated: for elements where confidence intervals do not intersect $A_s(i, j) = 1$, otherwise $A_s(i, j) = 0$. As a result, a sequence of sliding indicator matrices $A_s(i, j)$, $s = 1, \dots, S$, consisting of zeros and ones, is obtained.

Space-time filtering of the sequence of indicator matrices is performed [1]. Matrices are subdivided into equal matrices of smaller size $\Delta N_1 \times \Delta N_2$, and the values inside the indicated matrices are summed, a spatial filtration is performed:

$$B_s(i, j) = \sum_{i=(p-1)\Delta N_1+1}^{p\Delta N_1} \sum_{j=(q-1)\Delta N_2+1}^{q\Delta N_2} A_s(i, j),$$

$$i \in [(p-1)\Delta N_1 + 1, p\Delta N_1], \quad j \in [(q-1)\Delta N_2 + 1, q\Delta N_2].$$

The values of the indicator matrices are summed, a temporal filtration is performed:

$$C_n(i, j) = \sum_{s=(n-1)\Delta s+1}^{n\Delta s} B_s(i, j), \quad n = 1, \dots, [S/\Delta s].$$

The decision rule for determining the anomalous regions is the comparison with a certain threshold $C_n(i, j) \geq C_0$. The threshold C_0 is selected separately for each problem being solved.

The developed method for the anomaly recognition was applied to the time series of the matrix observational data of the URAGAN muon hodoscope [2]. An example of a hodoscope observation matrix for a fixed time is shown on Fig. 1a. An example of an indicator matrix constructed from the matrices of observations for the same instant of time is given in Fig. 1b. The dots denote ones in the indicator matrix. The concentrations of points near the bottom left and the bottom

right corners can be seen. An example of the resulting matrix obtained by filtering of indicator matrices is presented on Fig. 1c. On it, the elevated values near the bottom left and the bottom right corners can be seen also. This means that in these areas the time series of the hodoscope observations vary the most and can be considered anomalous.

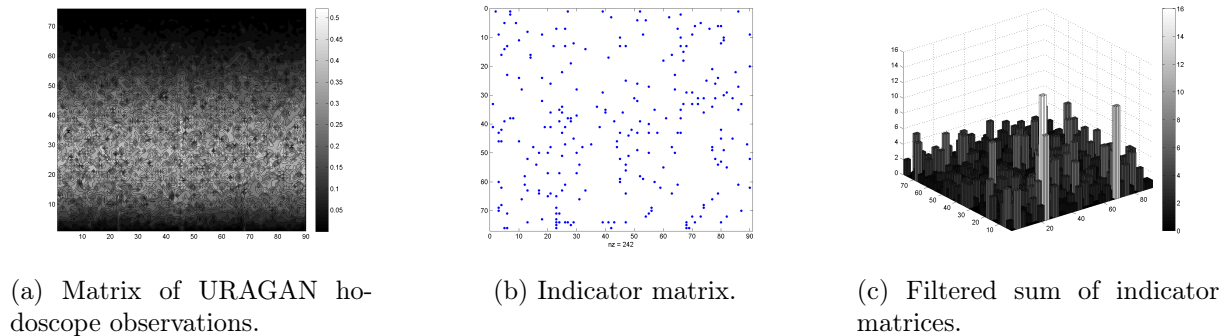


Fig. 1

A method for anomaly recognition in time series of matrix data based on confidence interval systems and space-time filtering is proposed. It made possible to recognize anomalies in the time series of the matrix data of the URAGAN muon hodoscope.

This research is supported by the Russian Science Foundation grant 17-17-01215.

References

- [1] M.I. Kurjachij, A.G. Kostevich, I.V. Gal'chuk. Space-time rank image processing in video information systems. Tomsk: TUSUR, 2013. (In Russian)
- [2] N.S. Barbashina, R.P. Kokoulin, K.G. Kompaniets, G. Mannocchi, A.A. Petrukhin, O. Saavedra, D.A. Timashkov, G. Trincherro, D.V. Chernov, V.V. Shutenko, I.I. Yashin. The URAGAN wide-aperture large-area muon hodoscope. *Instruments and Experimental Techniques*. 2008, Volume 51, Issue 2, pp. 180–186. DOI: 10.1134/S002044120802005X

Numerical analysis of Kurzanov bearing oscillation

O.V. Druzhinina^{1,a)}, L.A. Sevastianov^{2,b)}, S.A. Vasilyev^{2,c)}, D.G. Vasilyeva^{2,d)}

¹*Federal Research Center Computer "Science and Control" of Russian Academy of Sciences (FRC CSC RAS)*

²*Peoples' Friendship University of Russia (RUDN University)*

We consider Kurzanov bearing oscillation using numerical analysis. We show that this system is dynamically stable to the harmonic vertical and horizontal forced oscillations of the bearing with finite frequencies and amplitudes.

^{a)}Email: ovdruzh@gmail.com

^{b)}Email: sevastianov_la@rudn.university

^{c)}Email: vasilyev_sa@rudn.university

^{d)}Email: vasilyeva.darya@yandex.ru

The seismic isolation is based on some principles. The natural frequency of the system that protected object seismic isolation should be considerably lower than the major frequency of external influence which leads to a filtering of high frequencies. The contribution to the solution of the problem seismic isolation has made [1], [3]-[6]. In the work [2] Lyapunov stability analysis of the motion for this pendulum subjected to excitation of periodic driving forces and stochastic driving forces that act in the vertical and horizontal planes studied. The numerical study of the random motion for generalized Kapitza pendulum under stochastic driving forces made. It was shown the existence of stable quasi-periodic motion for this pendulum.

In this work numerical analysis of Kurzanov bearing [3] oscillation is provided. We show that this system is dynamically stable to the harmonic vertical and horizontal forced oscillations of the bearing with finite frequencies and amplitudes.

Each type seismic isolation kinematics bearings in the process of vibrations make a complex movement along a curved path due to the raising of structures when rotating the bearing. Taking into account the geometric parameters of a bearing and the nature of their surface have been obtained the equations of motion.

The equations of motion for Kurzanov bearing oscillation is presented in [6] and has a form

$$\ddot{\theta}(1 + \beta^2 + 4v(v + \cos \theta + \beta \sin \theta)) + (2v\dot{\theta}^2 + gR^{-1} \text{sign } \theta)(\beta \cos \theta - \sin \theta) = 0, \quad (1)$$

$$\beta = b - 2r/h, v = r/h,$$

where $\theta(t)$ is an angle of the inclination, h is a height, R, r are the external and internal radii of the bearing, g is the gravitational constant. The equations of the motion for Kurzanov bearing oscillation has two features that the presence of $\dot{\theta}^2$ and with the nonlinearity of two types. Kurzanov bearing is arranged in such a way that the center of the circle involute is located on the neutral axis of the structure, but higher in relation to the point of the application longitudinal force on of the value b .

The first there is the difference between the law of change of restoring force from linear in the continuous change of the angle θ and the second there is the jump of the restoring force in the neighborhood the justice of the point $\theta = 0$.

We can rewrite this equation in the form of the system differential equations first order

$$\begin{cases} \dot{\theta} = \varphi(t), \\ \dot{\varphi} = (2v\varphi^2(t) + gR^{-1} \text{sign } \theta)(\sin \theta - \beta \cos \theta)/(1 + \beta^2 + 4v(v + \cos \theta + \beta \sin \theta)), \end{cases} \quad (2)$$

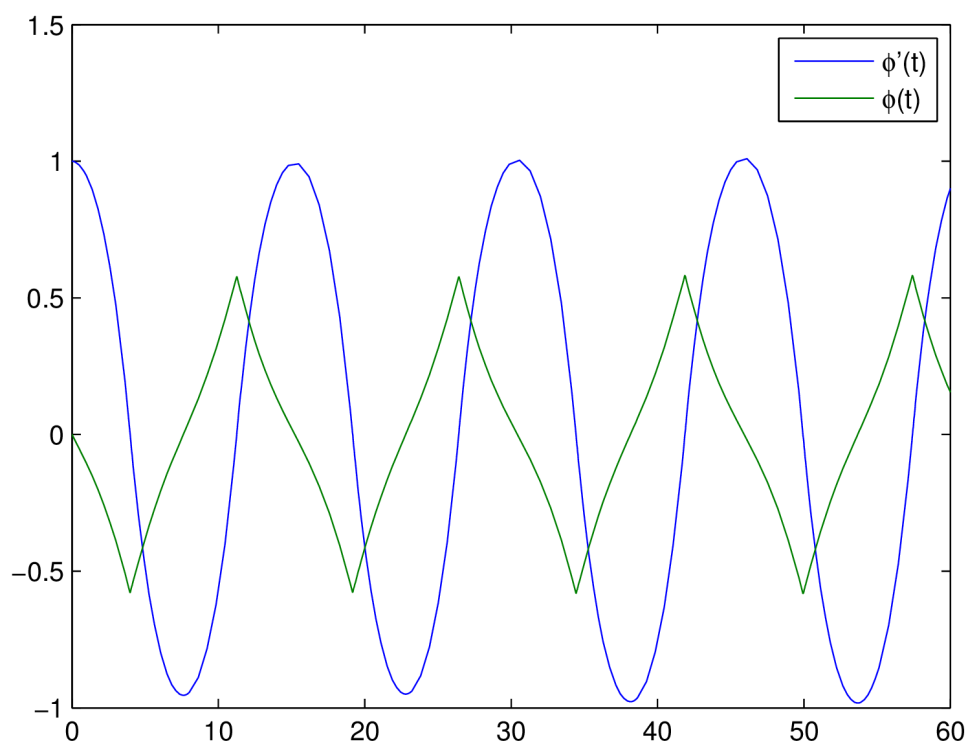
where φ is an auxiliary variable. For this system differential equations we can formulate problem

$$\begin{cases} \dot{\theta} = \varphi(t), \\ \dot{\varphi} = (2v\varphi^2(t) + gR^{-1} \text{sign } \theta)(\sin \theta - \beta \cos \theta)/(1 + \beta^2 + 4v(v + \cos \theta + \beta \sin \theta)), \\ \theta(0) = 0, \varphi(0) = \varphi_0, \\ \varphi(t_k) = -\varphi(t_k), \text{ if } \theta(t_k) = 0, k \in \mathbf{Z}_+. \end{cases} \quad (3)$$

Fig. 1: Kurzanov bearing oscillations.

The numerical example is presented in the figure (see Fig.1) where $\varphi_0 = 1 \text{ deg/sec.}$, $h = 1 \text{ m.}$, $R = 0.3 \text{ m.}$, $r = 0.25 \text{ m.}$, $b = 0.05 \text{ m.}$, $g = 10 \text{ m/sec.}$

In this numerical example it was shown the existence of steady state conditions for evolutions $\theta(t)$, $\varphi(t)$ with the quasi-periodic dynamics.



References

- [1] Chopra A. K. Dynamic of structures. Theory and Applications to Earthquake Engineering. New Jersey: Prentice-Hall, 2006. 794 p.
- [2] Druzhinina O.V., Sevastianov L.A., Vasilyev S.A., Vasilyeva D.G. Lyapunov stability analysis for the generalized Kapitza pendulum. VI International Conference Problems of Mathematical Physics and Mathematical Modelling 25–27 May 2017, Moscow, Russian Federation. IOP Conf. Series: Journal of Physics: Conf. Series Vol. 937, 012011, 2017. doi :10.1088/1742-6596/937/1/012011
- [3] Kurzanov A.M., Semenov S. Yu. Dynamic tests of a multi-storey monolithic house in Sochi. — Industrial and civil construction. — M.: Publishing House. PGS. — No. 3, P. 42-43, 2005.
- [4] Martelli A., Forny M. Seismic isolation: present application and perspectives. International Workshop On Base Isolated High-rise Buildings. Yerevan, Armenia: P. 1-26, 2006.
- [5] Masahiko Higashino, Shin Okamoto. Response Control and Seismic Isolation of Buildings. New York: Taylor& Francis, 2006.
- [6] Qouzah S.N. Using of the kinematic supports in the seismic system of buildings. — Ref. journal "Earthquake resistant construction". No 4, 1995.

Data Mining of Changing Rules in Time Series

N. Filipenkov^{1,a)}, M. Petrova^{2,b)}

¹*SAS Institute*

²*MEPhI*

The problem of forecasting multidimensional time series and mining rules in them has received much attention. The hypothesis that a rule may change in the course of time is also quite common. This paper is focused on mining rules that change slightly in the course of time. This means that a rule may be replaced only by a similar rule. In this paper a novel approach for mining slightly changing rules is introduced. The approach is based on a rule similarity measure, which is used as a weight of an arc on a rule graph. The process of mining slightly changing rules lies in optimizing the path in the rule graph.

The problem of mining rules in multidimensional time series has received much attention and is now a relatively mature field. The considerable part of research in the area is focused on mining rules in nonstationary time series. In the most general definition nonstationarity assumes that laws determining the series may vary from one time period to another. The hypothesis of nonstationarity can be amplified with the assumption that rules change slightly in the course of time. This means that a rule may be replaced only by similar rule. That is why the term “slightly changing rule” is based on the rule similarity measure. In this paper, a novel approach for mining rules in finite-valued multidimensional time series is introduced. This approach is based on the hypothesis that a rule may slightly change in the course of time. A term of rule similarity measure is defined and its implementation for discovering slightly changing rules is described. Several rule quality measures and algorithms using them are introduced.

Time series analysis is a wide area of knowledge that studies processes in their evolution. Classical research in the area tends to find global laws underlying the behaviour of time series. This means that a model defines a time series’ value at each point of time.

Contemporary knowledge discovery in time series mainly focuses on mining local rules. Local rules do not aim to define time series value at each point of time. They provide forecast for special conditions, e.g. “if Microsoft price goes up and IBM declines strongly then Intel stays about level next day”. Such rules are used by an expert or a decision support system only when the if-conditions are fulfilled. But plenty of real world problems such as stock price forecast need decisions on a regular basis, not occasional ones. An ability to make forecast in any case is reached either by large database of rules or by universality of rules. Universal rules define the arguments of a forecasted variable, i.e. “Today’s Intel price is defined by yesterday’s Microsoft price and the price of IBM two days before”. Such universal rule defines the Intel price trend for all (or most) combinations of Microsoft and IBM trends.

In this paper we discuss mining rules that are partial functions on a finite-valued domain. Both local rules and universal rules fit the introduced rule model. Local rule is a partial function which defines predicted time series only for one set of argument time series values. Universal rule defines predicted time series for all (or most) sets of argument time series values.

The paper focuses on mining rules in nonstationary time series. In the most general definition nonstationarity assumes that laws determining the series may vary from one time period to another. The hypothesis of nonstationarity can be amplified with the assumption that rules change slightly in the course of time. This means that a rule may be replaced only by similar

^{a)}Email: n.filipenkov@mail.ru

^{b)}Email: marina_petrova@mail.ru

rule. For example, the rule “if Microsoft price goes up and IBM *declines strongly* then Intel stays about level next day” transforms into similar rule “if Microsoft price goes up and IBM *stays about level* then Intel stays about level next day”. Sequence of these two rules is a slightly changing rule. Here we assume that time series are finite-valued. Actually, methods introduced below work with real time series after the preliminary discretization.

The algorithms introduced above were tested on modeled and real data. The algorithms were stable in finding artificially generated rules. They performed an accurate search of the randomly generated rules with various time lags, masks, functions and rule tracks. Main results on the modeled data are the following:

1. Previously generated rules were mined by the algorithm in 95% of the cases.
2. If the mask changed in half of its ones with 50% probability, the changing rule was found in 90% of the cases.
3. The generated rule was selected as the best rule in 93% of the cases.

The algorithms were also tested on the real data which included discretized stock prices for a period of two years. The results of the experiments compared to the results of exponential smoothing are introduced in the Table.

Table 1: Experimental results on the real data.

Target series	Exp. smoothing ($\alpha = 0, 1$)	Exp. smoothing ($\alpha = 0, 3$)	Inroduced algorithm
Adobe	$9,05 \cdot 10^{-2}$	$7,32 \cdot 10^{-2}$	$6,89 \cdot 10^{-2}$
BMC	$13,24 \cdot 10^{-3}$	$11,15 \cdot 10^{-3}$	$9,72 \cdot 10^{-3}$
Business Objects	$17,42 \cdot 10^{-2}$	$7,19 \cdot 10^{-2}$	$3,74 \cdot 10^{-2}$
Cognos	$6,73 \cdot 10^{-2}$	$3,08 \cdot 10^{-2}$	$2,39 \cdot 10^{-2}$
Computer Associate	$4,49 \cdot 10^{-2}$	$2,87 \cdot 10^{-2}$	$1,91 \cdot 10^{-2}$
Novell	$7,62 \cdot 10^{-3}$	$4,18 \cdot 10^{-3}$	$2,54 \cdot 10^{-3}$
Oracle	$8,61 \cdot 10^{-3}$	$6,77 \cdot 10^{-3}$	$5,45 \cdot 10^{-3}$
Peoplesoft	$3,24 \cdot 10^{-3}$	$2,94 \cdot 10^{-3}$	$1,26 \cdot 10^{-3}$
Rational	$5,19 \cdot 10^{-2}$	$3,43 \cdot 10^{-2}$	$2,06 \cdot 10^{-2}$

In this paper, a novel approach for mining slightly changing rules is proposed. The approach is based on the hypothesis that a rule may be replaced only by similar rule. The rule similarity measure is proposed to formalize the idea of slight changes. The measure depends on the mask resemblance and function resemblance.

The use of the rule similarity measure on the rule graph is illustrated. The rule graph is defined as a directed graph with weighted arcs. A weight of an arc connecting two rules is the similarity measure of the respective rules. The structure of the graph may change depending on the peculiarities of a problem solved.

Several quality measures for slightly changing rules are introduced. The representativeness and effectiveness of the changing rule are based on the average representativeness and effectiveness of permanent rules. The length of a changing rule is the length of the shortest path on the rule graph. The idea of mining a slightly changing rule lies in minimizing its length and finding the best chain of permanent rules in terms of representativeness and effectiveness.

References

- [1] Agrawal, R.; Imielinski, T.; Swami A. (1993) Mining association rules between sets of items in large databases, *Proc. of Conf. on Management of Data*, Washington, USA, 207-216.

- [2] Agrawal, R.; Srikant R. (1995) Mining sequential patterns, *Proc. 11th International Conf. on Data Engineering*, Taipei, Taiwan, 3-14.
- [3] Das, G et al. (1998) Rule discovery from time series, *Proc. 4th International Conf. on Knowledge Discovery and Data Mining*, New York, USA, 16-22.
- [4] Mannila, H.; Toivonen, H.; Verkamo, A.I. (1997) Discovery of frequent episodes in event sequences, *Data Mining and Knowledge Discovery*, 1(3), 259-289.
- [5] Mörchen, F.; Ultsch, A. (2005) Optimizing time series discretization for knowledge discovery, *Proc. 11th International Conf. on Knowledge Discovery and Data Mining*, Chicago, USA, 660-665.

About periodic solutions for certain functional equation

E.V. Gayduk^{1,a)}

¹*P.G. Demidov Yaroslavl State University*

Consider a functional equation for finding unknown periodic function $f(t)$

$$f(t) = g(t + f(t)),$$

where $g(t)$ is certain fixed function satisfying the condition $g'(t) > -1$. The main assumption is that $g(t)$ is T -periodic solution for some second-order nonlinear differential equation of the form

$$g'' = G(g, g').$$

The main result is that function $f(t)$ is T -periodic solution for second-order nonlinear differential equation

$$f'' = G(f, f'(1 + f')^{-1})(1 + f')^3$$

with initial conditions $f(0) = z$, $f'(0) = g'(z)(1 + g'(z))^{-1}$ and z is root of equation $z = g(z)$. There are some interesting examples.

^{a)}Email: elja5@yandex.ru

A method of two-dimensional filtering of modulated matrix data sequences

V.G. Getmanov^{1,2,a)}, R.V. Sidorov^{1,b)}

¹*Geophysical Center of RAS*

²*National Research Nuclear university MEPhI*

The method of two-dimensional filtering of modulated matrix data sequences is proposed. The structure of a two-dimensional filter based on operations of element-by-element matrix multiplications is developed. An example of a two-dimensional filtering of the daily modulation of the URAGAN muon hodoscope matrix data is analyzed.

The method of two-dimensional filtering is proposed for sequences of modulated matrix data consisting of the sums of the initial and modulated matrix components. The need for such filtering arises in many applications, for example, in the analysis of modulations of solar muon fluxes due to the rotation of the Sun [1], in data processing problems with modulations during aerial and satellite photography of the Earth surface etc. The method is based on the adaptation of standard one-dimensional digital filters to solutions of two-dimensional problems.

Let $Y_0(i, j, Tk)$ be the initial sequence of matrix data slowly changing in space and time variables i, j, Tk , $i = 1, \dots, N_1$, $j = 1, \dots, N_2$, T is a time sampling interval, $k = 1, 2, \dots$. The model of the data sequence with modulations $Y(i, j, Tk)$ is the following:

$$Y(i, j, Tk) = Y_0(i, j, Tk)[1 + \mu(i, j) \cdot Y_M(i, j, Tk, \Omega_0)],$$

where $\mu(i, j)$ is a modulation ratio; the $Y_M(i, j, Tk, \Omega_0)$ component for a fixed i, j and for indices k represents a set of narrow-band time functions with an average frequency Ω_0 .

The problem of elimination of the modulating component $Y_M(i, j, Tk, \Omega_0)$ in the observations $Y(i, j, Tk)$ is posed. Its possible solution can be made for each component of the discrete time function $Y_M(i, j, Tk, \Omega_0)$ with fixed i, j using a low-pass digital filter with cutoff frequencies $\omega_{c0} \leq \Omega_0$ based on standard one-dimensional low-pass digital filters using $N_1 N_2$ filtering operations. At the same time, there are problems of reducing the time spent filtering and selecting the cutoff frequency ω_{c0} . When the cutoff frequency is low, the original component is distorted, and when it is high, the modulation component is not completely eliminated.

A standard one-dimensional digital filter for the input $Y(i, j, Tk)$ and the output $Y_\Phi(i, j, Tk)$ time functions with fixed i, j is realized in the form of the following difference equation:

$$Y_\Phi(i, j, Tk) = -b_1 Y_\Phi(i, j, T(k-1)) - \dots - b_{\bar{r}} Y_\Phi(i, j, T(k-\bar{r})) + a_0 Y(i, j, T(k)) + \dots + a_{\bar{s}} Y(i, j, T(k-\bar{s})),$$

where $b_1, \dots, b_{\bar{s}}, a_0, \dots, a_{\bar{s}}$ are the filter parameters, $k = 1, 2, \dots$

Two-dimensional filtering is realized on the basis of the possibility of rapid element-by-element multiplication of matrices from [2]. The component matrices of the two-dimensional filter B_r, A_s consist of the elements $b_r(i, j) = b_r$, $r = 1, \dots, \bar{r}$, $a_s(i, j) = a_s$, $s = 0, \bar{s}$, $i = 1, \dots, N$, $j = 1, \dots, N_2$. The equation for the two-dimensional filter is the following:

$$Y_\Phi(i, j, Tk) = - \sum_{r=1}^{\bar{r}} B_r \circ Y_\Phi(T(k-r)) + \sum_{s=1}^{\bar{s}} A_s \circ Y(T(k-s)),$$

where "o" the the designation of element-by-element multiplication of matrices also known as entrywise product, $Y_\Phi(Tk), Y(Tk)$ are the sequences of output and input matrices.

^{a)}Email: v.getmanov@gcras.ru

^{b)}Email: r.sidorov@gcras.ru

The developed two-dimensional filter was used to eliminate the daily modulations of the muon fluxes intensity in the URAGAN muon hodoscope [3] hourly matrix data sequences $Y(i, j, Tk)$, $T = 1$ hour.

On Fig.1a, the functional connection $S_0(Tk)$ of the analyzed hourly matrix data averaged by i, j , corresponding to observations on 01-30.06.2015, is displayed. Spectral analysis for $S_0(Tk)$ showed the presence of a daily modulation component with a frequency $\Omega_0 = 2\pi/24 \cdot 3600$. This component was eliminated by a two-dimensional Butterworth filter with a cutoff frequency $\omega_{c0} = 0.8\Omega_0$ and the filter order $N_B = 10$, the parameters were calculated for the matrices B_r, A_s .

figure

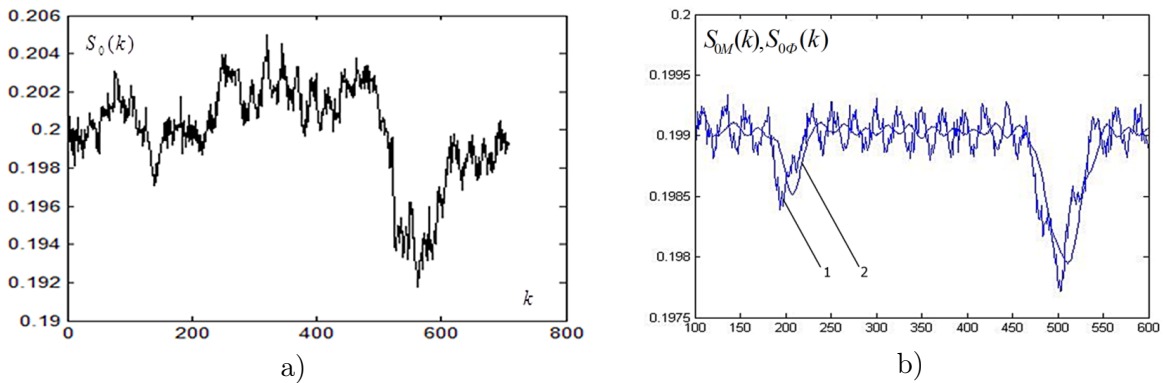


Fig. 1: a) The URAGAN hodoscope averaged hourly matrix data function; b) The averaged hourly model matrix data function : 1 – initial, 2 – filtered.

A sequence of modulated matrix data was modeled:

$$Y(i, j, Tk) = (A_0(i, j, Tk) + A_1(i, j))(1 + \mu \cos(\Omega_0 Tk)), \quad A_1(i, j) = A_1 \sin(2\pi f_{11}(i - i_0)) \sin(2\pi f_{12}(j - j_0)),$$

where $i = 1, \dots, N_1$, $j = 1, \dots, N_2$, $k = 1, \dots, k_{f0}$, $A_1 = 1$, $f_{11} = 0.006$, $f_{12} = 0.01$, $\mu = 0.02$, here $A_0(i, j, Tk)$ is a piecewise-linear function imitating the $S_0(Tk)$ trends.

On Fig.1b, line 1 depicts the model functional connection $S_{0M}(k)$ for the initial unfiltered matrix data, line 2 is for the filtered data function $S_{0\Phi}(k)$. The ω_{c0} selection for hodoscope matrix data filtering was carried out based on computational experiments.

It is seen that the proposed two-dimensional filter successfully performed the modulation component filtering in the matrix data sequence.

This research was conducted in the framework of the Russian Science Foundation project No. 17-17-01215.

References

- [1] Y. Okazaki, A. Fushishita, T. Narumi et al. *Drift Effects and the Cosmic Ray Density Gradient in Solar Rotation Period: First Observation with the Global Muon Detector Network.* // The Astrophysical Journal. 2008. Vol. 681. P. 693–707.
- [2] www.matlab.exponenta.ru
- [3] I.I. Yashin, I.I. Astapov, N.S. Barbashina, V.V. Borog, D.V. Chernov, A.N. Dmitrieva, R.P. Kokoulin, K.G. Kompaniets, Yu.N. Mishutina, A.A. Petrukhin, V.V. Shutenko, E.I. Yakovl-

eva. *Real-time data of muon hodoscope URAGAN.* // *Advances in Space Research.* 2015. Vol. 56. P. 2693–2703.

Statistically significant performance testing of Julia scientific programming language

M.N. Gevorkyan^{1,a)}, A.V. Demidova^{1,b)}, D.S. Kulyabov^{1,2,c)}, A.V. Korolkova^{1,d)}

¹*Peoples' Friendship University of Russia (RUDN University)*

²*Laboratory of Information Technologies Joint Institute for Nuclear Research, Dubna*

This paper we test the performance of Julia programming language for a number of common computational problems. We use statistical methods to obtain statistically significant results and to identify the optimal number of repetitions and levels of the experiment. The statistical methods are implemented in Julia itself and are organized as a separate Julia-module.

Nowadays, a large number of programming languages have been created and their number continues to increase. One of the new languages is Julia [1, 2]. Julia is language for scientific computing. It is currently under development and has version 0.6.2, but it already provides a lot of features. One of the features of Julia is the combination of simplicity of syntax of interpreted languages and performance of compiled languages..

A large number of languages creates the problem of choosing and comparing them with each other. The most obvious parameter for comparison is computation speed of created programs. However, the implementation of such a comparison faces a number of not always obvious problems.

- Different languages offer different syntax, built-in functions, and external functions. One can implement the same algorithm in multiple ways, using even the same language so that the execution time differs significantly. When comparing two different languages, the situation becomes even more complicated.
- Modern compilers, JIT-compilers and interpreters can use randomization in their work, which can give a performance difference between different executions of the same program.
- Modern processors use multiple levels of cache memory, and sophisticated speculative execution. This may cause the first few runs of the program to be significantly slower than the next ones. The program requires several starts to «warm-up».
- In general, the program execution time can be considered as a stochastic variable, the spread of it's values can be very large, depending on the complexity of the tested program.

Therefore, when testing performance, one must use statistical methods that take into account the above factors. Otherwise, a calculation error may completely offset the resulting performance

^{a)}Email: gevorkyan_mn@rudn.university

^{b)}Email: demidova_av@rudn.university

^{c)}Email: kulyabov_ds@rudn.university

^{d)}Email: korolkova_av@rudn.university

difference. In the papers [3, 4] authors describe a technique that allows to identify the number of initial runs required to warm-up the program, to determine the optimal number of runs and levels of the experiment and to build a trusted interval for the average time of program execution.

In this paper we use the method [3, 4] to estimate the performance of Julia language. Testing is performed on simple computational tasks (matrix actions, sorting algorithms, iterative and recursive procedures) and compared with results for Fortran language. Fortran is chosen because Julia claims to be as fast as compiled languages are. We also test Julia's capabilities of SIMD vectorization, as this capability improves performance of numerical methods for systems of differential equations [5].

The essence of the technique is described in the report on a specific example. We have also implemented a module for the Julia language, which allows one to test the functions (analogue functions of «magic» commands %time for iPython).

The publication was prepared with the support of the “RUDN University Program 5-100”

References

- [1] Julia: A Fresh Approach to Numerical Computing / Jeff Bezanson, Alan Edelman, Stefan Karpinski, Viral B. Shah // SIAM Review. — 2017. — Vol. 59, no. 1. — P. 65–98. — <https://doi.org/10.1137/141000671>.
- [2] Support for parallel computing in julia language / D.S. Kulyabov, M.N. Gevorkyan, A.V. Korolkova, L.A. Sevastianov // CEUR Workshop Proceedings. — Moscow : RUDN University, 2017. — P. 94–99.
- [3] Quantifying Performance Changes with Effect Size Confidence Intervals : Technical Report : 4–12 / University of Kent ; Executor: Tomas Kalibera, Richard E. Jones : 2012. — June. — Access mode: <http://www.cs.kent.ac.uk/pubs/2012/3233>.
- [4] Rigorous Benchmarking in Reasonable Time. — New York : ACM, 2013. — June. — Access mode: <http://kar.kent.ac.uk/33611/>.
- [5] Stochastic Runge–Kutta Software Package for Stochastic Differential Equations / M. N. Gevorkyan, T. R. Velieva, A. V. Korolkova et al. // Dependability Engineering and Complex Systems. — Springer International Publishing, 2016. — Vol. 470. — P. 169–179. — 1606.06604.

Information spaces: optimizing sequential and parallel processing for big data

P.V. Golubtsov^{1,a)}

¹*Lomonosov Moscow State University*

The process of Bayesian information update is essentially sequential: as a result of observation, a prior information is transformed to a posterior, which is later interpreted as a prior for the next observation, etc. It is shown that this procedure can be unified and parallelized by converting both the measurement results and the original prior information to a special form. Various forms of information representation

^{a)}Email: golubtsov@physics.msu.ru

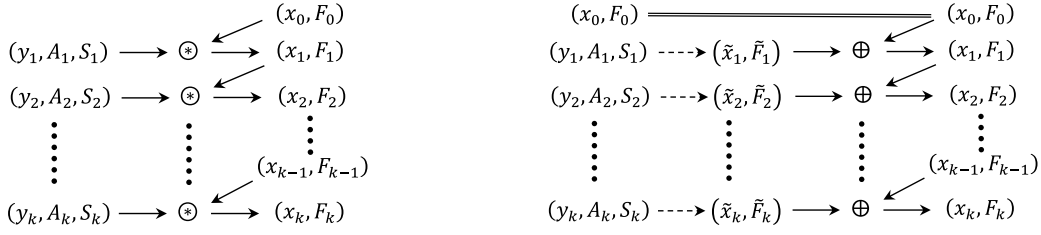


Fig. 1: Sequential information updating: traditional (left) and in explicit form (right).

and relations between them are studied. Rich algebraic properties of the introduced canonical information space allow to efficiently scale Bayesian procedure and adapt it to processing large amounts of distributed data.

Consider a series of independent linear measurements [1] $y_i = A_i x + \nu_i$ of a vector $x \in \mathcal{D}$. Here, $A_i : \mathcal{D} \rightarrow \mathcal{R}_i$ are linear mappings, $\nu_i \in \mathcal{R}_i$ are normal random vectors with $E\nu_i = 0$ and covariance operators $S_i > 0$, and $y_i \in \mathcal{R}_i$ are measurement results. All the information about each measurement is represented by a triplet of the form (y_i, A_i, S_i) . Also assume that there is a normal prior distribution of x , specified by its prior mean $Ex = x_0$ and covariance operator $F_0 > 0$.

When the measurement (y_1, A_1, S_1) arrives, the prior information (x_0, F_0) “transforms” to the posterior (x_1, F_1) , which then acts as the prior for the measurement (y_2, A_2, S_2) etc., see Fig. 1 left. The result (x_k, F_k) of the information update at the k -th step represents the posterior normal distribution of x with respect to the k -th observation [1] and has the form

$$(x_{k-1}, F_{k-1}) \otimes (y_k, A_k, S_k) = ((F_{k-1}^{-1} + A_k^* S_k^{-1} A_k)^{-1} (F_{k-1}^{-1} x_{k-1} + A_k^* S_k^{-1} y_k), (F_{k-1}^{-1} + A_k^* S_k^{-1} A_k)^{-1}).$$

This procedure of sequential updating of information is important for “big data streams” processing because it avoids storing the original data. However, it looks unnecessarily resource intensive since it involves repetitive operator inversions. Besides, it involves combining information in two different forms: explicit, (x_{k-1}, F_{k-1}) and raw (y_k, A_k, S_k) .

Information update can be made more homogeneous by first transforming the original raw information into explicit form and then adding it to the accumulated explicit information, Fig. 1 right. Here, $\tilde{F}_k = (A_k^* S_k^{-1} A_k)^{-1}$ and $\tilde{x}_k = F_k A_k^* S_k^{-1} y_k$ are the optimal linear estimate [2] of the vector x and its covariance operator, based on the measurement (y_k, A_k, S_k) . Then $F_k = (F_{k-1}^{-1} + \tilde{F}_k^{-1})^{-1}$ and $x_k = F_k (F_{k-1}^{-1} x_{k-1} + \tilde{F}_k^{-1} \tilde{x}_k)$. The use of explicit form as the main one is attractive, since such form has the obvious interpretation. However, this scheme is also too resource intensive. Besides, representing raw information (y_k, A_k, S_k) in explicit form is possible only if $A_k^* S_k^{-1} A_k$ is invertible. Thus, the explicit form can not be used as a universal and efficient form of information representation.

Let us now define and study various forms of information representation and relations between them.

Let $\mathfrak{R}_{\mathcal{R}} = \{(y, A, S) \mid y \in \mathcal{R}, A : \mathcal{D} \rightarrow \mathcal{R}, S : \mathcal{R} \rightarrow \mathcal{R}, S > 0\}$ be the set of all possible measurements in the space \mathcal{R} . Define the *initial information space* $\mathfrak{R} = \bigcup_{n=0}^{\infty} \mathfrak{R}_{\mathbb{R}^n}$ and the composition \oplus on \mathfrak{R} as

$$(y_1, A_1, S_1) \oplus (y_2, A_2, S_2) = \left(\begin{pmatrix} y_1 \\ y_2 \end{pmatrix}, \begin{pmatrix} A_1 \\ A_2 \end{pmatrix}, \begin{pmatrix} S_1 & 0 \\ 0 & S_2 \end{pmatrix} \right).$$

The *explicit information space* is defined as $\mathfrak{E} = \{(x, F) \mid x \in \mathcal{D}, F : \mathcal{D} \rightarrow \mathcal{D}, F > 0\}$ with the composition operation $(x_1, F_1) \oplus (x_2, F_2) = ((F_1^{-1} + F_2^{-1})^{-1} (F_1^{-1} x_1 + F_2^{-1} x_2), (F_1^{-1} + F_2^{-1})^{-1})$.

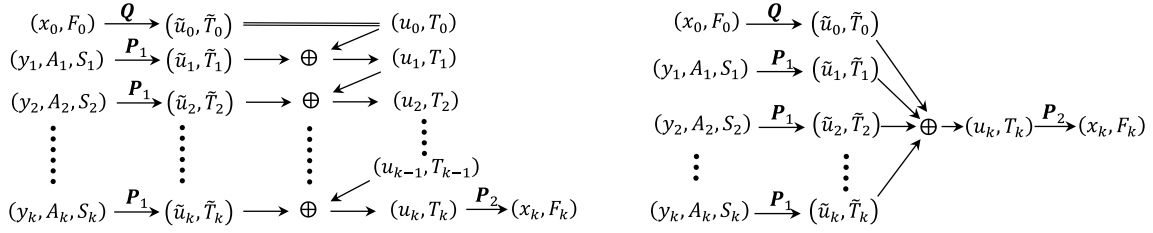


Fig. 2: Sequential (left) and parallel (right) information processing.

In [2] it was shown that the canonical form $(u, T) = (A^*S^{-1}y, A^*S^{-1}A)$ is a convenient form to represent a measurement $(y, A, S) \in \mathfrak{R}$. Define the *canonical information space* $\mathfrak{I} = \{(u, T) \mid T : \mathcal{D} \rightarrow \mathcal{D}, T \geq 0, u \in \mathcal{R}(T)\}$ with the composition operation $(u_1, T_1) \oplus (u_2, T_2) = (u_1 + u_2, T_1 + T_2)$.

Proposition 1. *The initial information space $(\mathfrak{R}, \oplus, 0)$ is a (noncommutative) monoid.*

*The subsemigroup $\mathfrak{R}^+ = \{(y, A, S) \in \mathfrak{R} \mid A^*S^{-1}A > 0\}$ is a two-sided ideal in \mathfrak{R} , i.e., if $a \in \mathfrak{R}^+$ and $b \in \mathfrak{R}$, then $a \oplus b \in \mathfrak{R}^+$ and $b \oplus a \in \mathfrak{R}^+$.*

The space \mathfrak{E} does not have a neutral element and is a commutative cancellative semigroup.

The space \mathfrak{I} is a commutative cancellative monoid, i.e., for all $a, b, c \in \mathfrak{I}$ the following relations hold: $a \oplus b = b \oplus a$, $(a \oplus b) \oplus c = a \oplus (b \oplus c)$, $a \oplus 0 = a$, $a \oplus b = a \oplus c \implies b = c$.

The commutative subsemigroup $\mathfrak{I}^+ = \{(u, T) \in \mathfrak{I} \mid T > 0\}$ is an ideal in \mathfrak{I} , i.e., if $a \in \mathfrak{I}^+$ and $b \in \mathfrak{I}$, then $a \oplus b \in \mathfrak{I}^+$.

Proposition 2. *The transformation of raw information into explicit $\mathbf{P} : (y, A, S) \mapsto ((A^*S^{-1}A)^{-1}A^*S^{-1}y, (A^*S^{-1}A)^{-1})\mathbf{P}$ is defined only on the subsemigroup $\mathfrak{R}^+ \subset \mathfrak{R}$, i.e., $\mathbf{P} : \mathfrak{R}^+ \rightarrow \mathfrak{E}$. On its domain of definition \mathfrak{R}^+ the mapping \mathbf{P} is a homomorphism of semigroups.*

*The transformation of raw information to canonical $\mathbf{P}_1 : (y, A, S) \mapsto (u, T) = (A^*S^{-1}y, A^*S^{-1}A)$ is a monoid homomorphism $\mathbf{P}_1 : \mathfrak{R} \rightarrow \mathfrak{I}$.*

The transformation of canonical information to explicit, $\mathbf{P}_2 : (u, T) \mapsto (x_0, F) = (T^{-1}u, T^{-1})$ is defined on the subsemigroup $\mathfrak{I}^+ \subset \mathfrak{I}$, i.e., $\mathbf{P}_2 : \mathfrak{I}^+ \rightarrow \mathfrak{E}$ and is a homomorphism of commutative semigroups.

The transformation $\mathbf{Q} : \mathfrak{E} \rightarrow \mathfrak{I}$ of explicit information to canonical: $\mathbf{Q} : (x_0, F) \mapsto (u, T) = (F^{-1}x_0, F^{-1})$ is a homomorphism of commutative semigroups.

The transformation \mathbf{P} realizes the complete solution of the optimal estimation problem (with no prior information) [2]. The mappings \mathbf{P}_1 and \mathbf{P}_2 split the data processing \mathbf{P} into two phases: extracting canonical information and constructing the processing result from it, i.e., $\mathbf{P} = \mathbf{P}_2 \circ \mathbf{P}_1$. The mapping \mathbf{Q} allows to represent any explicit (and, in particular, prior) information in canonical form.

The canonical form is the most rich and universal form of information representation. Choosing it as the main one, allows to transform the sequential updating schemes to the form on Fig. 2 left or even to a completely parallel one, Fig. 2 right. These schemes surpass the previous ones. All forms of information can be transformed to canonical. Canonical information (in contrast to explicit) is defined for any raw information. Composition of information in canonical form is most efficient. Construction of the final information (x_k, F_k) can be made only after canonical information is collected from all available data. Besides, in the parallel version, various pieces of data and the prior information can be transformed to canonical form independently and in parallel on different computers. The cancellation property and commutativity in the space \mathfrak{I} makes it possible to “subtract” any previously included information.

Thanks to rich algebraic properties of the canonical information space, the sequential Bayesian procedure allows various parallelization options that are ideally suited for distributed data processing platforms, such as Hadoop MapReduce. This opens up the possibility of a flexible

and efficient scaling of information accumulation in distributed data processing systems.

References

- [1] Pyt'ev Yu. P. Methods of mathematical modeling of measurement-computer systems. Moscow: Fizmatlit, 2012.(in Russian)
- [2] Golubtsov P.V., The Linear Estimation Problem and Information in Big-Data Systems. Automatic Documentation and Mathematical Linguistics, 2018, Vol. 52, No. 2, 73-79.

On the Identification of the Objects Shape Invariant to Projective Transformation

I. Gostev^{2,a)}, M. Malykh^{1,b)}, L. Sevastianov^{1,3,c)}

¹*Department of Applied Probability and Informatics, Peoples' Friendship University of Russia (RUDN University), Moscow, Russia*

²*Higher School of Economics, Moscow, Russia*

³*Bogoliubov Laboratory of Theoretical Physics of the Joint Institute for Nuclear Research, Dubna, Russia*

The problem of pattern recognition arose with the development of aerophotography, and at the present stage it is required to quickly, maybe even in real time, identify objects often very small, in a photo made by a rapidly flying copter or, say, from space. The characteristic difficulty of this class of object recognition problems consists in the fact that when photographing an object, the shape of the object is distorted. If we neglect the three-dimensionality of the object (in some cases it is very reasonable, because, for example, the aircraft will hardly be visible from the side when viewed from space) and assume that the operation of the camera lens can be described in the framework of Gaussian optics, the form of the object undergoes a projective transformation. Thus, the actual mathematical problem is the pattern recognition by attributes that are invariant under projective transformations.

Apparently the problems of the theory of pattern recognition, in full accordance with the Erlangen program of Felix Klein, should be divided into classes, depending on the invariants with respect to which group of transformations it uses. It is clear that, for example, when recognizing typewritten text, there is no need to apply projective methods, but it is necessary to take into account the "topology" of letters.

The projective transformation of a plane is a birational transformation that translates straight lines into straight lines (collineation) and, therefore, preserves the orders of algebraic curves. This transformation does not preserve lengths and angles, which is the main difficulty in recognition. Its main invariant is the anharmonic ratio of four points lying on one line, or, by the small principle of duality, of four lines passing through one point. The simplest object that you can try to recognize is pentagon. We can associate with each of its vertices the four straight lines passing

^{a)}Email: igostev@hse.ru

^{b)}Email: malykh_md@rudn.university

^{c)}Email: sevastianov_la@rudn.university

through the remaining vertices and count the anharmonic ratio for this bunch of lines. Since the order of the points is not given to us, in this way we obtain not 5 but 10 numbers. If we knew the coordinates of the points exactly, then by coincidence of all these numbers it would be possible to recognize the object.

However, when making a photograph, some mistake is made. Since lengths in the projective theory can not play an independent role, there is no way to assume that the coordinates of points are known with some additive error. In our opinion, errors should be estimated for dimensionless anharmonic relations. We express this idea mathematically by introducing a new metric. In this metric, two pentagons are close in the case when matrices composed of all the above-mentioned anharmonic relations are close.

The report will show that this approach allows to recognize figures in practice. Particularly a difficult case will be discussed when points lying on one line, due to errors, turn into a polygon, and vice versa, when the polygon degenerates into an almost straight line.

Comparison of piston, vane and perspective scroll air motors performance

V.I. Ivlev^{1,a)}, S.Y. Misyurin^{1,2,b)}, N.Y. Nosova^{1,2,c)}

¹*Mechanical Engineering Research Institute RAS*

²*National Research Nuclear University MEPhI (Moscow Engineering Physics Institute)*

The experimental results of testing scroll machine in air motor mode, such as mechanical and flow performance, leakage coefficient, specific volume and weight power are presented. This results analysed and compared with the same properties of radial – piston and vane air motors with equal power.

Nowadays the scroll machines have been widely used as air or refrigeration compressors and also vacuum pumps. As compared with piston compressors, scroll compressors with the same capacity, have more energy efficiency (about 10-15%), smaller dimension and weight (accordingly 25-40% and 15-20%), a low level of noise and vibrations. The volumetric rotary scroll machine is reversible and can function in air motor (expander) mode without any significant contraction modification and with preservation all advantages to piston air motors.

The investigation of the scroll machine in air motor mode began quite a lone time ago [1, 2]. But at the present time, in technical literature there are no data allowing to compare the characteristics of scroll air motor with the corresponding indices of the other types of air motors commercially produced by industry. These data are usually given in the catalogues of manufacturers in the form of mechanical and air consumption characteristics, weight and dimensions.

^{a)}Email: 6805158@mail.ru

^{b)}Email: symisyurin@mephi.ru

^{c)}Email: nynosova@mephi.ru

Table 1: Main indicators of air motors and scroll air motor

Model	Power <i>kW</i>	Supply pressure <i>MPa</i>	Specific flow rate <i>m³/min</i> <i>kW</i>	Specific weight power <i>kW/kg</i>	Specific volume power <i>kW/l³</i>	Leakage coefficient
Atlas Copco LZB54A180	1,2	0,63	1,13	0,51	2,12	0,22
Atlas Copco LZL05S	1,3	0,63	1,7	0,33	2,2	0,2
Globe RM-110	1,15	0,60	1,3	0,09	0,46	0,12
Gardner- Denver A6 series	1,42	0,62	1,24	0,12	0,45	–
Scroll airmotor	1,25	0,6	0,78	0,29	0,94	0,16

The most interesting is the comparison with the characteristics of such mass-produced types of air motors as vane (up to 75 – 80% of the market of air motors) and radial piston. Carrying out such a comparative analysis is the purpose of this paper.

To measure the mechanical and flow consumption characteristics of scroll air motor a test rig was assembled. As a scroll air motor was used the converted compressor «Mitsubishi» model MSC90CAS. It is necessary to compare the characteristics of different types of air motors with their approximately equal power developed at the same supply pressure because for air motors of one type, but different power, the specific characteristics may differ significantly. For comparison, samples of air motors, which in our opinion have the best performance (except cost) were selected. Table 1 shows the main indicators of this air motors, as well as the performance of our scroll air motor.

It should be noted that our scroll air motor has a rather high energy efficiency. This is due to the following factors: very small «dead» volume; the leakages from central chamber pass other chambers before come to atmosphere and take part in forming moving torque. Also scroll air motor have a low level of noise and vibration; small pulse of moving torque.

For the most part scroll air motor performance is better (or equal) than traditional types, except cost. If this limitation will be removed, it will find a wide industrial application in the near future.

References

- [1] Zanelli R., Favrat D. Experimental Investigation of a Hermetic Scroll Expander – Generator. // Proc. 12-th International Compressor Engineering Conf. 1994. Perdue. P. 459–464.
- [2] Yanagisawa T., Fukuta M., Ogi Y. Performance of an oil-free scroll – type air expander. // Proc. of the ImahE Conference on Compressors and their systems. 2001. P. 167–174.

Mathematical method for search of a multi alignment of DNA sequences with weak similarity

E.V. Korotkov^{2,a)}, M.A. Korotkova^{1,b)}

¹*National Research Nuclear University MEPhI (Moscow Engineering Physics Institute)*

²*Institute of Bioengineering, Research Center of Biotechnology of the Russian Academy of Sciences*

A new mathematical method is proposed for calculation of a multiple alignment of weakly similar amino acid or nucleotide sequences. The method uses a multiple alignment representation in the form of position-weight matrices (PWM) and global dynamic programming. An optimization procedure for PWM has been developed with the aim of finding a multiple alignment with maximum of a statistical significance. The method allows to find multiple alignment of sequences with the number of nucleotide or amino acid substitutions more than 2.5. The developed approach is applied to obtain multiple alignment of promoter sequences that have a length of 600 bases.

At present, a large number of DNA sequences from various species are known. Therefore, the problem of determining the functional value of accumulated sequences, that is, their annotation, is topical. The problem is put in this way: it is necessary to find some statistical regularities (SR) in sequences (Seq), which perform the same biological function (we denote it as F), show the specificity of SR only to Seq, and then develop a mathematical method for finding the SR in new sequences. If SR are found somewhere, then we can say that with a certain probability we found a sequence that has a biological function F. Usually in the role of SR appears a statistically significant multiple alignment of sequences that have the same biological function F. After constructing the multiple alignment, a hidden Markov model could be developed, which then analyses the new sequences for SR detection. It turns out that the effectiveness of the SR search depends on the quality of multiple alignment, ie, the efficiency of the annotation of sequences of different genomes depends on quality of multiple alignment. At present, methods for constructing of a multiple alignment based on pair comparison of sequences are applied. These methods work fine if there is a statistically significant pair similarity of compared sequences. However, cases exist when sequences do not have statistically significant pair alignment but they have the same biological function. It is impossible to construct multiple alignments for these sequences and therefore it is impossible to annotate their biological function. Promoter sequences are the examples of these sequences. Promoter sequences are at the beginning of each gene and control its activity. These sequences have a length equals to about 600 bases. Multiple alignment for all promoters from one genome was not built. However, it is possible to have multiple alignment in the absence of pair alignment of sequences. In this case a statistically significant alignment becomes group property, which could be found only for a certain set of sequences with the number sequences in set more than two. In this case, all previously developed methods for constructing multiple alignment can not find it at a statistically significant level. In our work, we tried to fill this gap. To build multiple alignment, we used PWM, a genetic algorithm, and two-dimensional dynamic programming. The method was applied to align promoter sequences from *A.thaliana* genome. We were able to obtain a statistically significant alignment of about 75 percent of the promoter sequences (more than 15 thousand sequences) from this genome. The

^{a)}Email: bioinf@yandex.ru

^{b)}Email: bioinf@rambler.ru

constructed multiple alignment is divided into approximately 5 groups. The results obtained can be applied to search of promoter sequences in other plant genomes.

Effective portfolio formation of business dimensions of organizations on the basis of statistical forecasts

A.V. Kryanev^{1,a)}, U.G. Pavlov², D.E. Sliva¹, U.A. Ulyanin²

¹*National Research Nuclear University "MEPhI"*

²*JSC "Tekhsnabexport"*

The problems of efficient distribution of resources among the business dimensions of an organization under uncertainty are considered. Performance indicators of the organizational business dimensions are of an uncertain nature and are assumed to be random variables with predetermined probability distribution laws. To create an effective distribution of a company's operational focus among its business dimensions, a scheme for effective portfolio formation based on the probabilities of priority and developed at NRNU MEPhI is used. For estimates of the values of performance indicators of organisation's business dimensions, their forecasts in the form of random, uniformly or normally distributed variables were taken.

1 Introduction

The report presents an implementation of the scheme for the formation of effective portfolios, presented in [1], for determining the effective resource distribution among the business dimensions of an organization. Unlike the well-known VaR schemes [2, 3, 4] and Markowitz schemes [5, 6], the scheme presented in [1] is based on the use of priority probabilities, which ensures the maximization of the probability of attaining large values of portfolio efficiency.

2 Algorithm of the numerical scheme for calculating the structure of effective portfolios of organisational business dimensions

Consider an algorithm for solving the problem of effective portfolio formation by means of priority probabilities [1].

Let the possible values of the efficiency of an i th business dimension R_i belong to the interval $[r_{imin}, r_{imax}]$, $i = 1, \dots, n$. This, in particular, means that the probability density values $\phi_i(x)$, $i = 1, \dots, n$ are zero outside the interval $[r_{imin}, r_{imax}]$, $i = 1, \dots, n$. If among the intervals $[r_{imin}, r_{imax}]$, $i = 1, \dots, n$ there are those for which the inequalities $r_{imax} < r_{jmin}$ are satisfied for some $j = 1, \dots, n$, then objects with such indices i are excluded from the structure of the portfolio in formation. Let the remaining l objects be renumbered so that the values r_{imax} are in decreasing order:

$$r_{1max} > r_{2max} > \dots > r_{lmax}. \tag{1}$$

^{a)}Email: avkryanev@mephi.ru

We impose the probabilities of priority of efficiency for objects according to equality

$$p(R_i > R_{i+1}) = \int_{r_{i+1max}}^{r_{imax}} \phi_i(x) dx / \int_{r_{imin}}^{r_{imax}} \phi_i(x) dx, i = 1, \dots, l - 1. \quad (2)$$

Formation of an effective portfolio is carried out according to the scheme of step-by-step increasing of the shares of the resource distributed among investment objects, starting with investment object with the indice 1 with the largest value of r_{1max} .

At the first stage, the share of the first object is assigned the value

$$x_1 = p(R_1 > R_2). \quad (3)$$

At the second stage, the share of the first object is assigned the value

$$x_1 = x_1 + \left(\int_{r_{3max}}^{r_{2max}} \phi_i(x) dx / \int_{r_{1min}}^{r_{1max}} \phi_i(x) dx \right) \cdot (1 - x_1), \quad (4)$$

where x_1 in the right-hand side of (4) is taken from equality (3), and the second object's value is assigned the value

$$x_2 = p(R_2 > R_3) \cdot (1 - x_1), \quad (5)$$

where x_1 on the right-hand side of (5) is taken from (4). Similarly, the assignment of shares for objects up to the object with the indice l is carried out [1]. Table 1 contains the results of calculations according to scheme (1) - (5) of the composition of effective portfolios for the organisational business dimensions based on the given forecasted values of performance indicators (the numerical values of the shares are given in percentages).

Table 1: The dynamics of organisational business focus portfolio

	2018	2019	2020	2021	2022	2023	2024	2025	2026	2027	2028	2029	2030
Area1	50,0	50,0	50,0	50,0	50,0	50,0	50,0	49,9	46,3	43,3	38,7	35,6	33,0
Area 2	50,0	50,0	50,0	50,0	50,0	50,0	50,0	49,9	46,3	43,3	38,7	35,6	33,0
Area 3	0,0	0,0	0,0	0,0	0,0	0,0	0,0	0,0	0,0	0,0	6,4	7,3	8,7
Area 4	0,0	0,0	0,0	0,0	0,0	0,0	0,0	0,2	7,4	13,4	16,2	19,3	23,0
Area 5	0,0	0,0	0,0	0,0	0,0	0,0	0,0	0,0	0,0	0,0	0,0	0,0	0,0
Area 6	0,0	0,0	0,0	0,0	0,0	0,0	0,0	0,0	0,0	0,0	0,0	2,2	2,3

3 Conclusion

The report presents an application of a scheme for effective portfolio formation, based on the probabilities of priority, used to determine the effectiveness of organisational business dimensions using the data on the forecasted values of performance indicators of business dimensions. The results of numerical calculations of effective portfolios of business dimensions of an organization are also given.

References

- [1] Kryanev A.V., Sliva D.E., Udumyan D.K. Methods for the formation of effective portfolios with the constraints and algorithms for their implementation. Vestnik Natsionalnogo Issledovatelskogo Yadernogo Universiteta "MEPhI", v. 7, №3, 2018, p. 289-293. (in Russian)
- [2] Rockafellar, R.T., Uryasev, S. Optimization of conditional value-at-risk. J. Risk, 2(3), 2000.
- [3] Lim Churlzu, Sherali Hanif D., Uryasev Stan. Portfolio optimization by minimizing conditional value-at-risk via non differentiable optimization. Computational Optimization and Applications, 46(3), 2010.
- [4] Kryanev A.V., Lukin G.V. O postanovke i reshenii zadach optimizatsii investitsionnih portfelei. Moscow: MEPhI, Preprint MEPhI 006-2001, 2001. (in Russian)
- [5] Markowitz H.M. Mean Variance Analysis in Portfolio Choice and Capital Markets. Basil. Blackwell. 1990.
- [6] Sharpe U.F., Alexander G.Dg., Baily D.V. Investment. Moscow: Infra-M, 2001.

On the possibility of implementing the Landau-Hopf-Sell scenario for a transition to turbulence

A.N. Kulikov^{1,a)}

¹*Demidov Yaroslavl State University*

F. Takens in one of his works (see Chapter 3 of [1]) proposed a concrete plan for the realization of the Landau-Hopf-Sell scenario as a cascade of Andronov-Hopf bifurcations [2-4]. This communication gives an example of a boundary value problem for a nonlinear evolution equation with partial derivatives, where this plan is realized.

Consider the boundary value problem

$$u_{tt} - \varepsilon u_t + u - \varepsilon \nu u_{txx} - \sigma^2 u_{xx} = -2\varepsilon u \int_0^\pi u_t u dx, \quad (1)$$

$$u(t, 0) = u(t, \pi) = 0, \quad (2)$$

where $u = u(t, x)$, $x \in [0, \pi]$, $\varepsilon \in (0, \varepsilon_0)$, $0 < \varepsilon_0 \ll 1$, $\sigma > 0$, $\nu > 0$. Let for some natural ν the following statement holds.

Theorem. There exists $\varepsilon_0 > 0$, such that for all $\varepsilon \in (0, \varepsilon_0)$ has $2^m - 1$ tori $T_k(\varepsilon)$ of dimension $k = 1, 2, \dots, m$. For solutions belonging to these invariant tori, the asymptotic formulas

$$u(t, x, \varepsilon) = \sum_{j=1}^k \sqrt{\frac{\nu_{n_j}}{2}} [\exp(i\sigma_{n_j} t + i\varphi_{n_j}) + \exp(-i\sigma_{n_j} t - i\varphi_{n_j})] \sin n_j x + O(\varepsilon),$$

^{a)}Email: anat_kulikov@mail.ru

where $\sigma_{n_j}^2 = \sigma^2 n_j^2 + 1$, $\nu_{n_j} = 1 - \nu n_j^2$, n_j is a set of k natural numbers for which the inequalities $1 \leq n_j \leq m$.

All tori of dimension k ($k = 1, 2, \dots, m - 1$), and the zero equilibrium state are unstable (saddle), and the torus of maximal possible dimension m is attracting (asymptotically stable).

It follows from Theorem that with decreasing ν , when $\nu \in \left[\frac{1}{(m+2)^2}, \frac{1}{(m+1)^2} \right)$ there exists $2^{m+1} - 1$ tori of dimension $p = 1, 2, \dots, m, m + 1$. Attractive is only a torus of dimension $m + 1$, which bifurcates from the torus $T_m(\varepsilon)$ with loss of stability.

The proof of the theorem and its corollary can be reduced to an analysis of an infinite-dimensional system of unbound oscillators

$$\dot{z}_n = i\sigma_n z_n + \left[\frac{\nu_n}{2} z_n - z_n |z_n|^2 \right], \quad (3)$$

where $n \in N$, $\sigma_n = \sqrt{1 + \sigma^2 n^2}$. Each of the equations of system (3) is a normal form in the analysis of the Andronov-Hopf bifurcations. For such a reduction, the method of integral manifolds, normal Poincaré forms, the modified Krylov-Bogolyubov algorithm, and the asymptotic methods of mathematical analysis are used.

Note also that Equation (1) is one of the possible variants for the Van der Pol equation with distributed parameters. Equation (3) occurs in studying a well-known mathematical model of macroeconomics, known as the multiplier-accelerator (see, for example, [5]). An example of another boundary value problem from the theory of elastic stability can be found in [6].

References

- [1] Broer H.W., Dumortier F., Van Strien S.J., Takens F. Structures in Dynamics. North-Holland, 1991.
- [2] Landau L.D. To the problems of turbulence. DAN USSR. 1944. Vol. 44. № 8. P. 339-342.
- [3] Hopf E. A mathematical example displaying the features of turbulence // Comm. Pure and Appl. Math. 1948. V.1. P. 303-322.
- [4] Sell G.R. Resonance and bifurcations in Hopf-Landau dynamical systems // Nonlinear Dynamics and turbulence. 1983. P. 305-315.
- [5] Puu T. Nonlinear Economic Dynamics. Berlin: Springer-Verlag, 1997.
- [6] Kulikov A.N. Landau–Hopf Scenario of Passage to Turbulence in Some Problems of Elastic Stability Theory // Differential equations. 2012. Vol. 48. № 9. P. 1258-1272.

The generalized Solow model

D.A. Kulikov^{1,a)}

¹Demidov Yaroslavl State University

The Solow model with the delay is consider. Existence of cycle is shown.

In the works of Nobel Prize winner in economics Solow one of the most developed models of macroeconomics at the present time was proposed. According to this model, the dynamics of the capital-labor ratio in the simplest cases is determined by an equation of the form [1-2]

$$\dot{x} = -x + x^k, \quad k \in (0, 1). \quad (1)$$

Equation (1) is given in a normed form, $x = x(t)$ – is the normalized amounts of the funds. Equation (1) has a unique positive equilibrium state $x(t) = 1$, which for the solutions with positive initial conditions $x(0) = x_0 > 0$ is the only attractor. In particular, it follows from these remarks that Equation (1) can not have t periodic solutions, i.e. can not describe economic cycles that are characteristic of the economy in a market pricing environment.

The situation will change if we take into account the delay factor. For example, if we consider the equation

$$\dot{x} = x^k - y, \quad y = x(t - h), \quad (2)$$

where $h > 0$. Equation (2), as before, has a positive equilibrium state $x(t) = 1$ ($y(t) = 1$).

Lemma. There exists $H > 0$ such that for $h > H$ this equilibrium state loses stability in oscillating manner. Wherein, $H = \frac{\arccos k}{\sqrt{1 - k^2}}$.

The proof of the Lemma can be reduced to an analysis of the characteristic equation

$$\lambda = k - \exp(-\lambda h).$$

Let $h = H(1 - \gamma\varepsilon)$, where $\varepsilon \in (0, \varepsilon_0)$, $0 < \varepsilon_0 \ll 1$, $\gamma > 0$.

Theorem. There exists $\varepsilon_0 > 0$ such that for all $\varepsilon \in (0, \varepsilon_0)$ Equation (2) has a saddle (unstable) cycle

$$x(t, \varepsilon) = 1 + 2\varepsilon^{1/2}\rho \cos(\sigma t + \varphi_0) + o(\varepsilon^{1/2}),$$

where

$$\sigma = \sqrt{1 - k^2}, \quad \rho = \sqrt{-\frac{\alpha}{d}}, \quad \alpha = -\gamma \frac{(1 - k^2)^{3/2}a}{Q}, \quad d = \frac{k(1 - k^2)^{3/2}}{(5 + 4k)Q} [(k + 5)\sqrt{1 - k^2} - 6ak] > 0,$$

$$a = \arccos k \in (0, \frac{\pi}{2}), \quad Q = ((1 - k^2)^{1/2} - ak)^2 + a^2(1 - k^2) > 0, \quad \varphi_0 \in R.$$

The asymptotic formula for self-oscillating solutions can be refined. We note that in the presented form of the problem hard excitation of oscillations (subcritical bifurcations) is realized.

A similar situation can be realized if Equation (2) is replaced by equation

$$\dot{x} = -x(t - h_1) + x^k(t - h_2), \quad h_1, h_2 > 0, \quad k \in (0, 1).$$

For example, for $h = h_1 = h_2$ the equilibrium state loses stability for $h > H = \frac{\pi}{2(1 - k)}$, and if $h = H(1 + \gamma\varepsilon)$, $\varepsilon \in (0, \varepsilon_0)$, $\varepsilon_0 \ll 1$, $\gamma \in R$ when we obtain the bifurcation problem, in the analysis of which the Andronov-Hopf theorem can be used.

Similar results were obtained in the analysis of another model of macroeconomy "demand-supply" [3-4] after taking into account the delay factor.

The reported study was funded by RFBR according to the research project № 18-01-00672.

^{a)}Email: kulikov_d_a@mail.ru

References

- [1] Solow R.M. A contribution to the theory of economic growth // The Quarterly Journal of Economics. 1956. V. 70. № 1. P. 65-94.
- [2] Puu T. Nonlinear Economic Dynamics. Berlin: Springer-Verlag, 1997.
- [3] Kulikov A.N., Kulikov D.A. The mathematical model market and the effect of delay // Matematika v Yaroslavskom univ. Sbornik obsor. statey k 40-let. Matem. Faculty. 2016. P. 132-151.
- [4] Kulikov D.A. About a mathematical model of market // IOP. Conf. Series: Journal of Physics: Conference Series. 2017. V. 788. 6pp.

Algebraic structure of special relativity

D.S. Kulyabov^{1,2,a)}, A.V. Korolkova^{1,b)}, L.A. Sevastianov^{1,3,c)}

¹*Peoples' Friendship University of Russia (RUDN University)*

²*Laboratory of Information Technologies, Joint Institute for Nuclear Research, Dubna*

³*Bogoliubov Laboratory of Theoretical Physics, Joint Institute for Nuclear Research, Dubna*

In the special relativity, the group on addition for velocities is used. However, the use of only group operations imposes restrictions on possible calculations. Variants of the extension of the group of the special theory of relativity to algebra are proposed.

The work is partially supported by Russian Foundation for Basic Research (RFBR) grants No 16-07-00556. Also the publication was prepared with the support of the "RUDN University Program 5-100".

In the presentation of the special relativity, so-called paradoxes are often singled out. One of these paradoxes is the formal appearance of velocities exceeding the speed of light. Most of these "paradoxes" arise from the incompleteness of the relativistic calculus over velocities. Namely, operations on velocities form a group by addition. The extension to algebra is usually carried out with the help of nonrelativistic operations. In addition, the noncommutativity of relativistic operations is usually not taken into account.

For example, the following paradoxes can be considered.

- Light and shadow. Let d be the distance from the source to the pointer, and D be the distance from the source to the screen. When the pointer moves parallel to the screen, the shadow velocity in D/d times is greater than the speed of the pointer.
- Light spot. An example similar to the previous one.

^{a)}Email: kulyabov_ds@rudn.university

^{b)}Email: korolkova_av@rudn.university

^{c)}Email: sevastianov_la@rudn.university

- Scissors. The intersection point of the blade guillotine shears can change the position at a superluminal velocity.
- Phase velocity. Along the direction deviated from the wave vector by an angle α :

$$v_p^\alpha = \frac{v_p}{\cos \alpha}, \quad (1)$$

where $v_p = \frac{\omega}{k}$ is the phase velocity along the wave vector.

In the special relativity, the addition of velocities is given. For simplicity, we shall consider the case of collinear velocities.

Let $c > 0$ is the speed of light.

$$u \oplus v = \frac{u + v}{1 + uv/c^2}, \quad u, v \in (-c, c). \quad (2)$$

$$\oplus : (-c, c) \times (-c, c) \rightarrow (-c, c).$$

The operation of relativistic addition has the following properties:

- \oplus is associative and commutative;
- $u \oplus v \oplus w = \frac{u + v + w + uvw/c^2}{1 + (uv + uw + vw)/c^2}$, $u, v, w \in (-c, c)$;
- $u \oplus 0 = 0 \oplus u = u$, $u \in (-c, c)$;
- $u \oplus (-u) = (-u) \oplus u = 0$, $u \in (-c, c)$;
- $\frac{\partial(u \oplus v)}{\partial u} = \frac{1 - v^2/c^2}{(1 + uv/c^2)^2} > 0$, $u, v \in (-c, c)$;
- $\lim_{u, v \rightarrow c} u \oplus v = c$, $\lim_{u, v \rightarrow -c} u \oplus v = -c$;
- $\{(-c, c), \oplus\}$ is a commutative group.

Along with the addition, we can set the subtraction:

$$v \ominus w = \frac{v - w}{1 - vw/c^2}. \quad (3)$$

To obtain an algebra, we define multiplication:

$$v \otimes w = c \frac{\exp \left[\gamma \ln \left| \frac{1+v/c}{1-v/c} \right| \ln \left| \frac{1+w/c}{1-w/c} \right| \right] - 1}{\exp \left[\gamma \ln \left| \frac{1+v/c}{1-v/c} \right| \ln \left| \frac{1+w/c}{1-w/c} \right| \right] + 1}, \quad \gamma = \ln^{-1} \left| \frac{1 + 1/c}{1 - 1/c} \right|. \quad (4)$$

Similarly, we can introduce division, as well as multiplication and division by a number.

For all these operations, the resulting velocities do not exceed the speed of light c . Thus, we can assume that the above-mentioned “paradoxes” arise from the confusion of relativistic and Galilean operations.

Bifurcation as the Coefficients of the Boundary Conditions Change in the Logistic Equation with Delay and Diffusion

D.O. Loginov^{1,a)}

¹*Yaroslavl State University*

We consider bifurcations arising in a boundary-value problem of parabolic type

$$\frac{\partial u}{\partial t} = d \frac{\partial^2 u}{\partial x^2} - r \cdot u(x, t - h)(u + 1)$$

with boundary conditions

$$\left. \frac{\partial u}{\partial x} \right|_{x=0} = 0, \quad \left. \frac{\partial u}{\partial x} \right|_{x=1} = \gamma \cdot u(1, t), \quad \gamma \in \mathbb{R}.$$

In the course of the research, a method was developed for finding the critical values of the parameters. The dependence of the bifurcation parameters on the boundary conditions is constructed. On the basis of the method of normal forms, it was possible to obtain the Lyapunov value for the values of the parameters of the problem, and also to determine the stability of the solutions constructed. It is shown that a decrease in the parameter γ makes it possible to strengthen the stability of the oscillatory regime. The maximum value of the parameter r is calculated for which there exists a periodic solution.

On the representation of electromagnetic fields in closed waveguides with discontinuous filling using four continuous potentials

M. Malykh^{1,a)}, L. Sevastianov^{1,2,b)}, N. Nikolaev^{3,c)}

¹*Department of Applied Probability and Informatics, Peoples' Friendship University of Russia (RUDN University), Moscow, Russia*

²*Bogoliubov Laboratory of Theoretical Physics of the Joint Institute for Nuclear Research, Dubna, Russia*

³*Department of Applied Physics, Peoples' Friendship University of Russia (RUDN University), Moscow, Russia*

According to the theorem of A. N. Tikhonov and A. A. Samarskii, the electromagnetic field \vec{E} and \vec{H} in a hollow waveguide of constant cross-section S can be represented by two scalar functions — potentials. In this report, we want to return to the question of the possibility of such a representation of the field in a waveguide with a complicated filling in its classical formulation.

Usually, when introducing potentials, it is possible to integrate part of Maxwell's equations and reduce the number of unknown functions. It is well known that in

^{a)}Email: dimonl@inbox.ru

^{a)}Email: malykh_md@rudn.university

^{b)}Email: sevastianov_la@rudn.university

^{c)}Email: nnikolaev@sci.pfu.edu.ru

the case of a waveguide filled with an inhomogeneous substance, this can not be done. However, the main benefit of introducing potentials is the transition from discontinuous field components to continuous potentials. From this point of view, the introduction of potentials can be viewed as a change of variables, at which the transition from discontinuous functions to continuous ones takes place.

Let's direct the Oz axis of the Cartesian coordinate system along the waveguide axis and take for brevity that

$$\vec{A}_\perp = (A_x, A_y, 0)^T \quad \text{and} \quad \nabla = (\partial_x, \partial_y, 0)^T, \quad \nabla' = (-\partial_y, \partial_x, 0)^T.$$

Instead of four discontinuous transverse components of the electromagnetic field, it is proposed to use four potentials related to the field by equations

$$\vec{E}_\perp = \nabla u_e + \frac{1}{\epsilon} \nabla' v_e, \quad \vec{H}_\perp = \nabla v_h + \frac{1}{\mu} \nabla' u_h. \quad (1)$$

Theorem on the field decomposition. Let the waveguide filling do not change along the axis and be described by piecewise-continuous functions ϵ and μ , given on the section S of the waveguide. For any electromagnetic field \vec{E}, \vec{H} satisfying the Maxwell's equations in the waveguide, the boundary conditions for the ideal conductivity on the waveguide walls and the conjugation conditions on the waveguide filling discontinuity line, there are functions $u_e, u_h \in \overset{0}{W}_2^1(S)$ and $v_e, v_h \in W_2^1(S)$ such that the equality (1) holds. This representation is unique up to additive constants.

This theorem ensures that when we move to new continuous variables, we do not lose the solutions. This replacement allows us to work immediately in classical functional spaces and bypass the main computational complexity of waveguide problems — the approximation of discontinuous functions.

For the most interesting case in practice, when waveguide filling is described by piecewise-constant functions, the system of Maxwell's equations in new variables splits into two independent systems. Moreover, the study of fields in such a waveguide reduces to the study of two scalar problems for the wave equation, since the potential u_e satisfies the boundary value problem

$$\begin{cases} \operatorname{div} \epsilon \nabla u_e + \epsilon \partial_z^2 u_e - \epsilon^2 \mu \partial_t^2 u_e = 0, \\ u_e|_{\partial S} = 0, \end{cases} \quad (2)$$

and the potential v_e — the boundary value problem

$$\begin{cases} \operatorname{div} \frac{1}{\epsilon} \nabla v_e + \frac{1}{\epsilon} \partial_z^2 v_e - \mu \partial_t^2 v_e = 0, \\ \frac{\partial v_e}{\partial n} \Big|_{\partial S} = 0. \end{cases} \quad (3)$$

This should be the case, since a waveguide with piecewise-constant filling is nothing more than several waveguides with constant filling interacting with one another through walls. Two scalar equations are sufficient for describing the field in each of the waveguides with constant filling, so it seems quite natural that the waveguide system composed of them should also be described a pair of wave equations.

The report will show how to use this splitting for the theoretical and numerical analysis of boundary value problems of the mathematical theory of waveguide systems.

Acknowledgements. The publication was prepared with the support of the "RUDN University Program 5-100".

The construction of explicit conservative difference schemes for autonomous systems of differential equations

M. Malykh^{1,a)}, L. Sevastianov^{1,2,b)}, Y. Ying^{1,3,c)}

¹*Department of Applied Probability and Informatics, Peoples' Friendship University of Russia (RUDN University), Moscow, Russia*

²*Bogoliubov Laboratory of Theoretical Physics of the Joint Institute for Nuclear Research, Dubna, Russia*

³*Department of Algebra and Geometry, KaiLI University, Kaili, China*

Standard considerations of integrability of differential equations in symbolic form refer to the computational techniques of the past centuries. We believe that all higher transcendental functions can be reconsidered as solutions of such differential equations, for which the application of the finite difference method is particularly efficient.

The elliptic functions appeared in mechanics as higher transcendental functions that provide the integration of various problems related to pendulum oscillation and top rotation. In these cases, the equations of motion can be considered as particular cases of the autonomous dynamic system

$$\dot{\vec{x}} = f(\vec{x}),$$

possessing a few integrals of motion. Standard explicit difference schemes do not conserve these integrals; therefore, their use for calculations over the time of about ten periods yields an approximate solution that is considerably aperiodic. For a top with the fixed center of gravity, the integrals of motion are quadratic, so they are conserved by the symplectic Runge-Kutta schemes. However, in the present case all these schemes will be implicit. For example, the transition from one layer to another in the single-stage scheme will require the solution of a fifth-power equation, which essentially complicates practical application of such schemes.

Problem. For a given system of differential equations and a few integrals to construct an explicit difference scheme, exactly conserving the integrals of motion.

In the present report we restrict ourselves to the case, when the integrals of motion specify a curve of the genus ρ in the space, where \vec{x} varies. In this case, any difference scheme is an algebraic transformation of this curve. Therefore, at $\rho > 1$ the desired difference scheme does not exist for purely geometric reasons (Zeuthen-Hurwitz theorems). At $\rho = 1$ (elliptic curve) the explicit formula for birational transformations are known, so that it is always possible to check, whether these formula approximate the given differential equation or not. In the case of a top, the answer is positive, and an explicit difference scheme for the approximate solutions can be constructed. Without any relation to the theory of difference schemes, this method of calculating the elliptic functions has been applied to the composition of the first tables by Ch. Gudermann. In the report, we consider the properties of this scheme.

Acknowledgements. The publication was prepared with the support of the "RUDN University Program 5-100".

^{a)}Email: malykh_md@rudn.university

^{b)}Email: sevastianov_la@rudn.university

^{c)}Email: yuying05720062@sina.com

Complex behavior of solutions of the system of three Hutchinson equations with a delayed broadcast connection

E.A. Marushkina^{1,a)}

¹*P.G. Demidov Yaroslavl State University*

Studied is the dynamics of the association consisting of three identical oscillators connected in a broadcast manner. Each single oscillator is represented by a logistic equation with a delay (the Hutchinson equation). Performed is a local asymptotic analysis of this system in the case of the proximity of the parameters of equations to the values at which the Andronov-Hopf bifurcation occurs. In addition, the coupling coefficients in the system are assumed to be small. For the constructed normal form the simplest self-similar regimes and conditions for their stability are found. Phase conversions occurring in the system are analyzed numerically. It is shown that the delay in the communication circuit of the oscillators essentially affects the qualitative behavior of the solutions in the studied system.

Consider the system of three Hutchinson Equations with a delayed broadcast connection (more about the broadcasting type of communication see, for example [1, 2]):

$$\begin{aligned} \dot{N}_1 &= r(1 - N_1(t-1))N_1, \\ \dot{N}_2 &= r(1 - N_2(t-1))N_2 + D(N_1(t-h) + N_3(t-h) - 2N_2), \\ \dot{N}_3 &= r(1 - N_3(t-1))N_3 + D(N_1(t-h) + N_2(t-h) - 2N_3). \end{aligned} \quad (1)$$

In this problem, $N_j(t)$, $j = 1, 2, 3$ can be interpreted as the density of the number of three close populations, $r > 0$ – malthusian coefficient of linear growth. Value $D > 0$ is responsible for the intensity of interaction between populations. The parameter $h > 0$ is the delay in the chain of communication. The system (1) simulates the situation from population dynamics, when populations are weakly related to each other, for example, geographically separated. In this case, one of the populations can affect the two remaining ones, which in turn are able to influence each other, but do not affect the former.

For the system (1) a local asymptotic analysis is performed if the parameters are close to the values at which the Andronov-Hopf bifurcation occurs. The parameter r is chosen equal to $\frac{\pi}{2} + \varepsilon$. Moreover, if $\varepsilon = 0$, then the stability spectrum of the system (1) contains a pair of purely imaginary eigenvalues $\lambda = \pm i\frac{\pi}{2}$ multiplicity 3, which correspond to three linearly independent eigenfunctions. The interaction $D = \varepsilon d$ between kinds selected weak, proportional to the small parameter $0 < \varepsilon \ll 1$.

Asymptotics of the stable periodic solution $N_1(t)$ of the system (1) is well known and written out as follows:

$$\begin{aligned} N_1(t) &= 1 + \sqrt{\varepsilon} \sqrt{\frac{40}{3\pi - 2}} \cos\left(\left(\frac{\pi}{2} - \varepsilon \frac{2}{3\pi - 2}\right)t + c\right) + \\ &\quad + \varepsilon \frac{4\sqrt{5}}{3\pi - 2} \cos\left(\left(\pi - \varepsilon \frac{4}{3\pi - 2}\right)t - \gamma + 2c\right) + O(\varepsilon^{3/2}), \end{aligned}$$

where $\gamma = \arctan(1/2)$, and c – any constant.

For further local analysis of the system (1), a standard replacement of the normal form method was used (see [3, 4]):

$$N_j(t) = 1 + \sqrt{\varepsilon}(z_j(\tau)e^{i\frac{\pi}{2}t} + \bar{z}_j(\tau)e^{-i\frac{\pi}{2}t}) + \varepsilon u_{j1}(t, \tau) + \varepsilon^{3/2} u_{j2}(t, \tau) + \dots, \quad (2)$$

^{a)}Email: marushkina-ea@yandex.ru

where $z_j(\tau)$ – complex-valued functions of the slow time $\tau = \varepsilon t$, ($j = 2, 3$).

On the third step of the algorithm, from the solvability conditions of the tasks for $u_{j2}(t, \tau)$ in the class of 4-periodic in t functions we obtained the following normal form:

$$\begin{aligned} \left(1 + i\frac{\pi}{2}\right)z_2' &= iz_2 + \frac{(1-3i)\pi}{10}z_2|z_2|^2 + d\left(z_1e^{-i\frac{\pi}{2}h} + z_3e^{-i\frac{\pi}{2}h} - 2z_2\right), \\ \left(1 + i\frac{\pi}{2}\right)z_3' &= iz_3 + \frac{(1-3i)\pi}{10}z_3|z_3|^2 + d\left(z_1e^{-i\frac{\pi}{2}h} + z_2e^{-i\frac{\pi}{2}h} - 2z_3\right). \end{aligned} \quad (3)$$

The self-similar solutions of the system (3) next form: $z_j(\tau) = \rho_j^* e^{i\varphi_j^* \tau}$ – self-similar cycles, where ρ_j^* and φ_j^* – real numbers, and $z_j(\tau) = \rho_j^*(\tau) e^{i\varphi_j^* \tau}$ – self-similar torus, where $\rho_j^*(\tau)$ – periodic on the τ functions, are studied by numerically-analytical methods. The stability of the found periodic solutions is investigated. The scenario of phase reconstructions occurring in the system at $h = 0$ is constructed (see also [3, 4, 5]). An important feature of this scenario is the presence in it of complex disordered oscillations for sufficiently small values of the parameter d . There are no such oscillations in the problem of the interaction of a pair of Hutchinson equations [3]. The problem of changes in the scenario of phase rearrangements of the system (3) for $h > 0$ is of greater interest. It was found that the presence of delay in the communication circuit leads to a complication of oscillations and the appearance of solutions in which the phase difference between the oscillatory solutions $z_3(\tau)$ and $z_2(\tau)$ increases without limit with the growth τ .

Acknowledgment. The reported study was funded by RFBR, according to the research project No. 16-31-60039 mol_a_dk.

References

- [1] Milo R., Shen-Orr S., Itzkovitz S., et al. Network motifs: Simple Building Blocks of Complex Networks // Science. – 2002. – V. 298. – No. 5594. – P. 824–827.
- [2] Glyzin S. D., Kolesov A. Yu., Rozov N. Kh. Self-excited relaxation oscillations in networks of impulse neurons // Russian Math. Surveys. – 2015. – V. 70. – No. 3. – P. 383–452
- [3] Glyzin S. D. Dynamical properties of the simplest finite-difference approximations of the "reaction-diffusion" boundary value problem // Differential Equations. – 1997. – V. 33. – No. 6. – P. 808–814
- [4] Glyzin S. D. A registration of age groups for the Hutchinson's equation // Model. Anal. Inform. Syst. – 2007. – V. 14. – No. 3. – P. 29–42 (in Russian)
- [5] Tolbey A. O. Local Dynamics of Three Coupled Oscillators with a Feedback Loop // Model. Anal. Inform. Syst. – 2012. – V. 19. – No. 3. – P. 105–112 (in Russian)

Integrated control of a robotic group with partial dominance of decision variants

S.Y. Misyurin^{1,3,a)}, M.A. Potapov^{2,b)}, A.P. Nelyubin^{3,c)}

¹*NRNU "MEPhI"*

²*ICAD RAS*

³*IMASH RAN*

^{a)}Email: SYMisyurin@mephi.ru

^{b)}Email: pmatarus@gmail.com

^{c)}Email: nelubin@gmail.com

The problem of control of a robotic group is considered as a special formulation of the goal programming problem. An approach to solve it is proposed by introducing zones of partial dominance of decision variants over the goal.

A special formulation of the goal programming problem is considered. In practice, there are often situations where available resource and other constraints do not allow achieving or dominating the goal by possible decision variants. In our case, each decision variant is expressed in the ranges of technical characteristics of a group of robots. Each set of technical characteristics can be presented as a specific decision variant in the conditions of a (multicriteria) model of goal programming.

In general, the areas of change of alternatives are divided into zones of partial dominance and the zone of complete domination of the goal. In areas of partial dominance, our decision variants (individual robots) provide an advantage over the indicators (criteria) of the selected variants over the corresponding goal indicators. Thus, the general functioning area is divided into two unequal parts: the zone of partial dominance of our decision variants (robots) and the zone of complete domination of the goal. As a rule, the measure of the set of complete domination of the goal is substantially less than that of the sum of sets of partial dominance.

When organizing an integrated (coordinated) functioning of a group of robots and ensuring the transfer of control to that part of the robots that currently partially dominates the goal, it is possible to achieve the mode of full dominance of a group of robots in the overwhelming volume of the functioning space. The integrated control provides, in general, complete dominance over the goal with limited resource capabilities to increase the ranges of characteristics of each robot by most effectively control a robotic group.

Application of the improved polycrystalline model in the framework of the EBSD experiment simulation

A.O. Ovchinnikova^{1,a)}, T.I. Savyolova^{1,b)}

¹*National Research Nuclear University "MEPhI"*

In this work the influence of the grain structure model in polycrystalline specimen on the results of the simulated EBSD experiment is studied. In the framework of EBSD experiment simulation the improved model of the polycrystalline with the grains in form of ellipses is used. Such a model is proposed to describe structural features of the real specimen more elaborately than one with grains as circles. Matching the improved polycrystalline model with the initial one is performed by comparison of the texture index, calculated from the EBSD measurements, conducted for both models under varying of the experiment parameters: scanning step and tolerance angle.

Experimental nature of material investigations by means of EBSD (Electron Back Scattering Diffraction) does not allow to compare the experiment results with the original specimen characteristics to tune the parameters of measurements: scanning step and tolerance angle [1]. The specimen and experiment simulation makes it possible to compare texture entities calculated

^{a)}Email: aoantonova@mail.ru

^{b)}Email: TISavelova@mephi.ru

directly from specimen with corresponding ones obtained from model measurements. In this work the attempt to improve the model of EBSD experiment proposed earlier in [2, 3] was performed by utilizing the novel polycrystalline model, in which grains were considered as rotated ellipses. Such a model of the grain structure is based on the EBSD experiment specificity, as in the commercial software [4] the plane cross sections of grains are approximated by ellipses.

Two distinct model specimens \vec{S}_{cir} and \vec{S}_{el} consisting of $N = 3000$ grains were created:

$$\vec{S}_{cir} = \{\vec{U}_{cir_i}, i = 1, \dots, N\}, \vec{U}_{cir} = [x_{cir}, \omega, g(\phi, \theta, \psi), \delta], \quad (1)$$

$$\vec{S}_{el} = \{\vec{U}_{el_i}, i = 1, \dots, N\}, \vec{U}_{el} = [x_{el}, \omega, g(\phi, \theta, \psi), \delta]. \quad (2)$$

The vectors \vec{U}_{cir} and \vec{U}_{el} so defined were proposed to be the grain models, where x_{cir} was the size of the grain determined as a diameter of a circle equal to the grain's cross section with respect to its area, and the size x_{el} was modeled as a chord of ellipse approximating the plane cross section of the grain; $g(\phi, \theta, \psi)$ – an orientation of the grain; ω – disorientation angle with the following grain; δ – a boundary between the given grain and the following one.

For both specimens the same orientations sample was utilized, orientations were modeled by Monte-Carlo method with orientation distribution function (ODF) in the form of central normal distribution (CND) [5] with texture sharpness equal to 1/8. Thus, the specimens \vec{S}_{cir} and \vec{S}_{el} had equal texture characteristics and equal mean grain size $\bar{x}_{cir} = \bar{x}_{el} = 2.0\mu m$, but different grain structure (rotated ellipses and circles).

Define an operator $\Phi(\vec{S}, h, \omega_0)$, modelling the result of EBSD study of the specimen \vec{S} under the parameters (h, ω_0) , where $h \in (0, H)$, $H > 0$ – scanning step over the surface of specimen, $\omega_0 \in \Omega_0 \subseteq (0, \pi)$ – threshold disorientation angle. We assumed, that for \vec{S}_{cir} the measurements are made during diameters, whereas for specimen \vec{S}_{el} orientation scanning was performed along the ellipses chords. The last approach seemed to be more reliable according to a procedure of the real EBSD experiment.

The results of simulated EBSD measurements of both specimen \vec{S}_{cir} , \vec{S}_{el} can be presented as

$$\vec{S}_{cir} = \{[\tilde{x}_{cir_i}, \tilde{\omega}_i, \tilde{g}_i(\tilde{\phi}_i, \tilde{\theta}_i, \tilde{\psi}_i)], i = 1, \dots, \tilde{N}\}. \quad (3)$$

$$\vec{S}_{el} = \{[\hat{x}_i, \hat{\omega}_i, \hat{g}_i(\hat{\phi}_i, \hat{\theta}_i, \hat{\psi}_i)], i = 1, \dots, \hat{N}\}. \quad (4)$$

As it can be seen from Eqs. 3,4 different approaches of specimen modeling result in the difference of simulated measurements procedure, causing the change of all grain properties, restored from measurements.

The simulation of EBSD experiment results was performed for the given set of parameters meanings [2, 3]: $h = 0.5\mu m; 1.0\mu m; 2.0\mu m; \omega_0 = 5^\circ, 10^\circ, 20^\circ$.

To compare considered grain structure models the behaviour of texture index (TI) under varying the parameters (h, ω_0) was investigated. For calculation of TI from the set of individual orientations the kernel estimation method was used. The TI calculation from the EBSD measurements demonstrated slightly different results for both modeled specimens. The dependence of the TI relative error on the experiment parameters (h, ω_0) is presented on Fig. 1 for both specimens. It can be noticed that the TI behaviour under parameters varying was saved when the new specimen model was utilized.

The dependence of TI on experiment parameters, obtained by modelling, was compared with one, calculated for ferritic-martensitic steel EP823 (12Cr-Mo-W-Si-V-Nb-B). EBSD measurements for steel EP823 were performed with the same parameters meanings as in modelling. The dependence of IT on measurement parameters in model experiment was confirmed by the dependence calculated for steel EP823.

The reported study was funded by RFBR according to the research project № 18-31-00036.

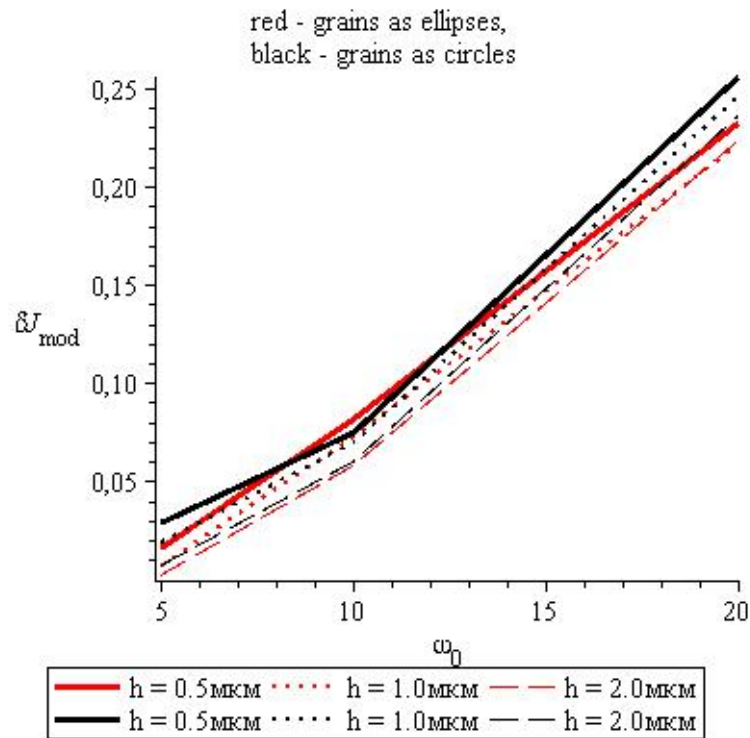


Fig. 1: Dependence of the TI relative error on the tolerance angle ω_0 .

References

- [1] Randle V. Introduction to texture analysis: macrotexture, microtexture and orientation mapping: 2nd ed (Boca Raton, CRC Press, 2010).
- [2] Antonova A.O., Savyolova T.I. Comput. Math. Math. Phys. 2015. 55 (2). pp. 317–29.
- [3] Antonova A.O., Savyolova T.I. Cristallogr. Rep. 2016. 61 (3). pp. 523–31.
- [4] Software channel 5, www.hkltechnology.com
- [5] Savyolova T I, Ivanova T M and Sypchenko M V 2012 Methods for Solving Ill-Posed Problems in Texture Analysis and Their Applications (Moscow: NRNU MEPhI) [in Russian]

Application of the statistical tests method for calculation of the hardware function model estimates for streamer detector systems

D.V. Peregoudov^{1,a)}, A.D. Gvishiani^{1,2,b)}, I.I. Yashin^{3,c)}, V.V. Shutenko^{3,d)}

¹*Geophysical Center RAS*

²*Schmidt Institute of Physics of the Earth RAS*

³*National Research Nuclear University MEPhI*

The application of the statistical tests method for calculation of the hardware function model estimates for streamer detector systems performing the measurements of the muon flux intensity distribution functions is discussed. The component model describing the detector system functioning is formed. The statistical tests method is implemented for calculation of the hardware function models. The estimate for the URAGAN muon hodoscope hardware function model is analyzed.

The streamer detector (SD) systems are overviewed, intended for measuring the muon flux intensity distribution functions. The bases of the SD systems are the detectors – the stream tubes located in several parallel planes. Getting into the tube, a muon causes an electric discharge in it. The signal from the discharge is detected using the conductive strips paved above and below each plane; the triggered strips are defined. SD systems consist of sets of detecting and non-detecting parallelepipedic gaps, forming a kind of "frame" construction. Intensity measurements correspond to the output function $Y(i, j, Tk)$. In the SD, the number of muons registered in each solid angle $\varphi_1 = \Delta\varphi(i-1)$, $\vartheta = \Delta\vartheta$, $i = 1, \dots, N_1$, $j = 1, \dots, N_2$ during a predefined time interval, is counted. On Fig.1, the URAGAN hodoscope [1] output function 2D image is represented. The initial muon flux intensity is represented by the input function $Y_0(i, j, Tk)$. The hardware function (HF) $A(i, j)$ for the SD establishes the relation between the input $Y_0(i, j, Tk)$ and output $Y(i, j, Tk)$ functions:

$$Y(i, j, Tk) = A(i, j)Y_0(i, j, Tk), \quad i = 1, \dots, N_1, \quad j = 1, \dots, N_2.$$

The HF model is represented by the multiplication $A_M(i, j, c_1, c_2) = A_{M1}(i, j, c_1)A_{M2}(j, c_2)$. The component $A_{M1}(i, j, c_1)$ determined by the SD geometry, the component $A_{M2}(j, c_2)$ determines the attenuation in the atmosphere and is assumed to be known c_1, c_2 are the parameters.

The calculation of the first component is quite a challenge. Simplification is achieved by determining the facts of registration of muons during the passage of their random tracks through the SD system.

The application of the statistical tests method [2] is performed to evaluate the first component. The vector w of random angles and coordinates of the muon track is generated. The first indicator function $A_{M11}(i, j, c_1, w)$ is calculated, corresponding to the SD output: when the angles φ, ϑ of the muon track match the solid angle i_0, j_0 two events are possible: when registering a muon, the indicator function is assumed equal to 1 for $i = i_0, j = j_0$, and zero for $1 \leq i < i_0, i_0 < i \leq N_1, 1 \leq j < j_0, j_0 < j \leq N_2$; when not registering a muon the function is equal to 0 for $i = 1, \dots, N_1, j = 1, \dots, N_2$. The second indicator function $A_{M12}(i, j, c_1, w)$, corresponding to the SD input, is calculated in a similar way.

^{a)}Email: d.peregoudov@gcras.ru

^{b)}Email: a.gvishiani@gcras.ru

^{c)}Email: IYashin@mephi.ru

^{d)}Email: VVShutenko@mephi.ru

The random vectors $w_s, s = 1, \dots, \bar{s}$ are formed for the statistical tests. The $A_{M1n}^\circ(i, j, c_1, c_2, \bar{s}), n = 1, 2$ are calculated, their summation and subsequent division is performed:

$$A_{M1n}^\circ(i, j, c_1, c_2, \bar{s}) = \sum_{s=1}^{\bar{s}} A_{M1n}(i, j, c_1, w_s), n = 1, 2,$$

$$A_{M1}^\circ(i, j, c_1, \bar{s}) = A_{M11}^\circ(i, j, c_1, \bar{s})/A_{M12}^\circ(i, j, c_1, \bar{s}).$$

The HF model estimate as a result of \bar{s} statistical tests is the following:

$$A_M^\circ(i, j, c_1, c_2, \bar{s}) = A_M^\circ(i, j, c_1, \bar{s})/A_{M2}(j, c_2).$$

For the parameters c_1, c_2 as a result of statistical test series \bar{s} , the HF estimate A was calculated, its 2D image for the URAGAN hodoscope is presented on Fig.2.

figureone

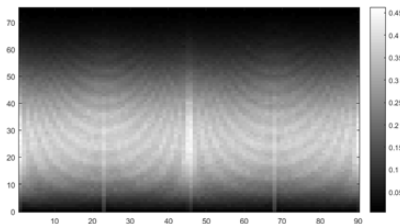


Fig. 1: An example of the URAGAN hodoscope output function.

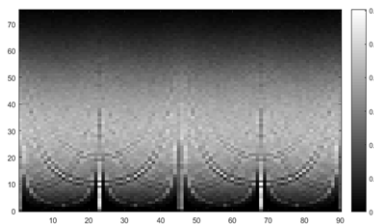


Fig. 2: The HF evaluation using the statistical tests method.

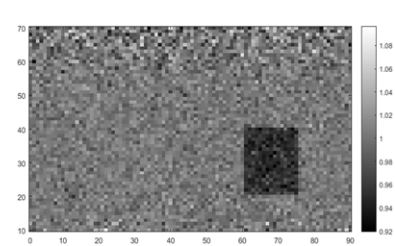


Fig. 3: The model input function estimate.

The analysis of the HF estimate was made in order to determine the possibility of its use for the recognition of intensity decrease areas. The input function $Y_M(i, j)$ was modelled, based on which the output model function $Y_M(i, j, c_1, c_2, \bar{s})$ was calculated. The estimate $Y_{M0}^\circ(i, j, c_1, c_2, \bar{s}, \bar{s}_0) = Y_M(i, j, c_1, c_2, \bar{s}_0)/A_M^\circ(i, j, c_1, c_2, \bar{s})$ was defined.

Recognition of intensity decrease in the input muon flux was made for a given range of angles. The model input function was set as $Y_{M0}(i, j) = Y_0(1 - p)$ for $i \in [i_1, i_2], j \in [j_1, j_2]$ and $Y_{M0}(i, j) = Y_0$ for other points, the values $i_1 = 60, i_2 = 75, j_1 = 22, j_2 = 40, p = 0.05$ were set, and the output function $Y_M(i, j, c_1, c_2, \bar{s})$ was formed. On Fig.3, the 2D image of the estimate for the function $Y_{M0}^\circ(i, j, c_1, c_2, \bar{s}, \bar{s}_0)$ is presented. Analysis of Fig.3 shows that, based on the calculated HF, the recognition of of the mentioned intensity decrease area was carried out.

This research was conducted in the framework of the Russian Science Foundation project No. 17-17-01215.

References

- [1] I.I. Yashin, I.I. Astapov, N.S. Barbashina, V.V. Borog, D.V. Chernov, A.N. Dmitrieva, R.P. Kokoulin, K.G. Kompaniets, Yu.N. Mishutina, A.A. Petrukhin, V.V. Shutenko, E.I. Yakovleva. *Real-time data of muon hodoscope URAGAN.* // Advances in Space Research. 2015. Vol. 56. P. 2693–2703.
- [2] Mikhailov G.A., Voytishchek A.V. *Chislennoe statisticheskoe modelirovanie. Metod Monte-Karlo (Numerical statistical modelling. The Monte-Carlo method).* //Moscow.: Yurait. 2018. Vol. 681. P. 693–707.

Stability of Antiphase Regime in a System of Two Coupled Nonlinear Relaxation Oscillators

M.M. Preobrazhenskaia^{1,2,a)}

¹Yaroslavl State University

²Scientific Center in Chernogolovka RAS

Let us consider the system of non-linear differential-difference equations (see [1, 2, 3])

$$\begin{aligned} \dot{u}_1 &= [\lambda f(u_1(t-1)) + b g(u_2(t-h)) \ln(u_*/u_1)]u_1, \\ \dot{u}_2 &= [\lambda f(u_2(t-1)) + b g(u_1(t-h)) \ln(u_*/u_2)]u_2, \end{aligned} \quad (1)$$

which is used to model the association of two neurons with a synaptic connection. Here $h > 0$ characterizes the delay in the connection chain, $u_1(t), u_2(t) > 0$ are the normalized membrane neurons potentials, the parameter $\lambda \gg 1$ characterizes the electrical processes rate in the system, $b = \text{const} > 0$, $u_* = \exp(c\lambda)$ is the threshold value for control interaction, $c = \text{const} \in R$, the terms $bg(u_{j-1}) \ln(u_*/u_j)u_j$ model synaptic interaction. The functions $f(u), g(u) \in C^2(R_+)$, where $R_+ = \{u \in R : u \geq 0\}$, and satisfy the following conditions:

$$\begin{aligned} f(0) &= 1; f(u) + a, uf'(u), u^2f''(u) = O(u^{-1}) \text{ as } u \rightarrow +\infty, a = \text{const} > 0; \\ \forall u > 0 \quad g(u) &> 0, g(0) = 0; g(u) - 1, ug'(u), u^2g''(u) = O(u^{-1}) \text{ as } u \rightarrow +\infty. \end{aligned} \quad (2)$$

For any natural n we find a periodic solution of the system (1) containing n asymptotically high bursts on the period.

Let us show that it has solution in the form $u_1(t) = \exp(\lambda x(t))$, $u_2(t) = \exp(\lambda x(t + \Delta))$, where $\Delta \geq 0$, $x(t)$ is the periodic solution of equation

$$\dot{x} = f(\exp(x(t-1)/\varepsilon)) + b(c-x)g(\exp(x(t+\Delta-h)/\varepsilon)), \varepsilon, \quad (3)$$

$\varepsilon \ll 1$. Using (2) we obtain that it has limited equation

$$\dot{x} = R(x(t-1)) + b(c-x)H(x(t+\Delta-h)), \quad (4)$$

where $R(x) = 1$ and $H(x) = 0$ as $x < 0$, $R(x) = -a$ and $H(x) = 1$ as $x > 0$.

Denote the solution of the relay equation (4) by $x_*(t)$, and its period by T_* .

Theorem. *The parameters a, b, c, h, Δ exist such that for any natural n and small enough $\varepsilon > 0$ the equation (3) has an orbital exponential stable cycle $x_*(t, \varepsilon)$ with period $T_*(\varepsilon)$, at that*

$$\lim_{\varepsilon \rightarrow 0} \max_{0 \leq t \leq T_*(\varepsilon)} |x_*(t, \varepsilon) - x_*(t)| = 0, \quad \lim_{\varepsilon \rightarrow 0} T_*(\varepsilon) = T_*$$

and period of the function $x_*(t, \varepsilon) > 0$ has n segments where it is positive.

Proved theorem allows us to justify the existence and stability of a periodic solution with n asymptotically high bursts on the period for the system (1). If $\Delta = 0$, then the system (1) has a homogeneous solution $u_1 \equiv u_2$. And if constant Δ satisfy the matching condition $\Delta = T_*/2$, then (1) has anti-phase solution. Thus, it is shown that the appearance of bursting in a system of coupled oscillators is a consequence of the delay in the connection chain between them.

This work was partly supported by the Russian Science Foundation (project nos. No 14-21-00158).

^{a)}Email: rita.preo@gmail.com

References

- [1] Glyzin S. D., Kolesov A. Y., Rozov N. K. On a method for mathematical modelling of chemical synapses, *Differential Equations*, 2013, 49:10, 1227–1244.
- [2] Glyzin S. D., Kolesov A. Y., Rozov N. K. Modeling the bursting effect in neuron systems, *Mathematical Notes*, 2013, 93:5, 676–690.
- [3] Glyzin S. D., Kolesov A. Y., Rozov N. K. Self-excited relaxation oscillations in networks of impulse neurons, *Russian Mathematical Surveys*, 2015, 70:3, 383–452.

Electricity load forecasting with clustering consumers in smart energy grids

E. Y. Shchetinin^{1,a)}, M. S. Berezhkov^{1,b)}

¹*Financial University under Government of Russian Federation*

Clustering is a well-known machine learning algorithm which enables the determination of underlying groups in datasets. In electric power systems it has been traditionally utilized for different purposes like defining consumer individual profiles, tariff designs and improving load forecasting. A new age in power systems structure such as smart grids determined the wide investigations of applications and benefits of clustering methods for smart meter data analysis. This paper presents an improvement of energy consumption forecasting methods by performing cluster analysis. For clustering the centroid based method K-means with K-means++ centroids was used. Various forecasting methods were applied to find the most effective ones with clustering procedure application.

1 Introduction

The development of intelligent networks in manufacturing, finance, and services creates new opportunities for the development and application of effective methods of machine learning and data analysis. Smart technologies for collecting, recording and monitoring data on energy consumption create a huge amount of data of different nature. These data can be used for optimal network management, improving the accuracy of the forecasting load, detection of abnormal effects of power supply (peak load conditions), the formation of flexible price tariffs for different groups of consumers [1, 2]. One of the most important issues in this area is to predict the power load consumption as accurately as possible. In order to improve the accuracy, our goal is to investigate the possible benefits of combining clustering procedures with forecasting methods.

2 Energy consumption time series modeling

The time series X is an ordered sequence of n real variables

$$X = (x_1, x_2, \dots, x_n), \quad x_i \in R. \quad (1)$$

^{a)}Email: riviera-molto@mail.ru

^{b)}Email: berezhkov.m@gmail.com

Four different model-based representation methods were chosen: (a) Robust Linear Model (RLM), (b) Generalized Additive Model (GAM), (c) Holt-Winters Exponential Smoothing, and (d) Median Filter. The first presentation is based on a robust linear model (RLM). Like other regression methods, it is aimed at modeling the dependent variable by independent variables

$$x_i = \beta_1 u_{i1} + \beta_2 u_{i2} + \dots + \beta_s u_{is} + \varepsilon_i, \quad (2)$$

where $i = 1, \dots, n$, u_i is energy consumption, β_1, \dots, β_s are the regression coefficients, u_{i1}, \dots, u_{is} are independent binary variables, $u_{ij}, j = 1, 2, \dots, s$, ε_i is a white noise. Extensions for RLM are generalized additive models (GAM) [3]

$$E(x_i) = \beta_0 + f_1(u_{i1}), \quad (3)$$

where f_1 is cubic spline, $u_1 = (1, 2, \dots, s, 1, \dots, s, \dots)$. Next method is exponential smoothing Holt-Winters [5]. Last presentation for time series model is a median filter as following

$$\hat{x}_k = \text{median}(x_k, x_{k+s}, \dots, x_{k+s \times (d-1)}), \quad (4)$$

where $k = (1, \dots, s)$, and d – time series dimension.

In our paper we used next methods to improve forecasting energy consumption time series: Support Vector Regression (SVR), a method based on a combination of STL decomposition, Holt-Winters exponential smoothing and ARIMA model. Seasonal decomposition of time series based on loess regression (STL) is a method, which decomposes seasonal time series into three parts: trend, seasonal component and remainder (noise). For the final three time series any of the forecast methods is used separately, in our case either Holt-Winters exponential smoothing or ARIMA model. Also Random Forest(RF) algorithm is suitable for classification and regression. This method constructs the large number of decision trees at training time. Its output is the class that is the mode of the classes (classification) or mean prediction (regression) of the individual trees. We considered Extreme Gradient Boosting (XGB) as an efficient and scalable implementation of gradient boosting framework. Bagging (Bagg) predictors generate multiple versions of predictors and use them for determination an aggregated predictor. The accuracy of the forecast of electricity consumption was measured by MAPE (Mean Absolute Percentage Error).

3 Computer experiments for customer energy consumption

We performed several computer experiments to evaluate the profit of using clustering procedures on four time series representation methods for one day ahead forecast. Our testing data set contains measurements from customers of Central Russia Region. Each forecasting method was evaluated on 5 datasets; 4 datasets are clustered with different representation methods (*Median, HW, GAM, RLM*) and aggregated electric load consumption (Sum). Optimized clustering of consumers significantly improves accuracy of forecast with forecasting methods *SVR, Bagging, XGB*. Despite this, clustering with STL+ARIMA, RF does not really improves accuracy of forecast. Three robust representation methods of time series Median, GAM and RLM performed best among all representations, while *HW* was the worst in most of the cases. The best result of all cases achieved by *Bagging* with optimized clustering using *GAM* representation with mean daily MAPE error under 3,17%.

4 Conclusion

The main purpose of this paper is to show that the application of the clustering procedure of consumers to the representation of time series of energy consumption can improve the accuracy

of their forecasts for energy consumption. Robust linear model, generalized additive model, exponential smoothing and median linear filter were used as such representations. We applied a modified K-means++ algorithm to more accurately select centroids and the Davis-Boldin index to evaluate clustering results. Numerical experiments have shown that the methods of forecasting such as STL+ARIMA, SVR, RF, Bagging considered in the paper are more effective for improving forecast accuracy if used together with clustering. The most accurate prediction result is obtained by Bagging with the GAM presentation. Among the perspective applications of clustering for smart grids are benefits for tariff design, compilation smart demand response programs, improvement of load forecast, classifying new or non-metered customers and other tasks.

References

- [1] Haben S., Singleton C., Grindrod P., Analysis and Clustering of Residential Customers Energy Behavioral Demand Using Smart Meter Data // IEEE Transactions on Smart Grid. 2015. V.PP. no.99. P.1-9.
- [2] Chicco G., Napoli R. and Piglione F., Comparisons Among Clustering Techniques for Electricity Customer Classification // IEEE Trans. Power Sys., 2013, vol. 21. P.933-940.
- [3] Shchetinin Eu.Yu., Lyubin P.G., Fast two-dimensional smoothing with discrete cosine transform, Springer Communications in Computer and Information Science (CCIS), Springer: Berlin, 2016, 678, P. 646-656.
- [4] Arthur D. and Vassilvitskii S., K-means++: The Advantages of Careful Seeding, in SODA '07 Proceedings of the eighteenth annual ACM-SIAM symposium on discrete algorithms, 2007, P. 1027–1035.
- [5] Taylor J.W., Short-term electricity demand forecasting using double seasonal exponential smoothing, Journal of Operational Research Society, 2003, vol. 54, P. 799–805.

On Some Properties of Tail Dependence Coefficient Nonparametric Estimators

E. Shchetinin^{1,a)}, N. Rassakhan¹

¹*Financial University under Government of Russian Federation*

Significant damage to national economies, the environment and society. The development of models and methods for quantifying extremes and their dependence structure can lead to a better understanding of extreme events. A key paradigm in extreme events analysis is the tail dependence coefficient (TDC) that describes the degree of association between pairs of different extremes. Knowledge of the characteristics of TDC can help to improve existing models of the probability of occurrence of extremes. In this study efficient estimation of the TDC in rainfall is investigated. Different nonparametric TDC estimators are implemented on the rain gauge data

^{a)}Email: riviera-molto@mail.ru

and their advantages and disadvantages are discussed. Our results indicate that tail dependency significance cannot be ignored for modeling of multivariate rainfall fields, that contradicts with the assumption of joint normality, usually applied in hydrologic applications.

Numerical analysis of invariant characteristics of buckling beam driven oscillations

D.M. Sirotin^{1,2,a)}

¹*P.G. Demidov Yaroslavl State University*

²*Scientific Center in Chernogolovka RAS*

Oscillation of a resilient beam with longitudinal compression were considered. The law of motion with a change in the frequency of the harmonic action was registered. As a result of the full-scale experiment a set of data was obtained that consists of ordered periodic oscillations as well as disordered oscillations specific to dynamical systems with chaotic behavior. To study the invariant numerical characteristics of the attractor of the corresponding dynamical system β -statentropy and the first Lyapunov exponent were calculated. Based on the developed algorithms the dependence of β -statentropy on the frequency of the external action was constructed. A phenomenological model was proposed. Estimation of its adequacy was carried out by comparing dependences of β -statentropy and the first Lyapunov exponent on the frequency of the external action constructed for experimental system and model.

In the course of a volumetric numerical experiment, an array of data was processed, representing both ordered periodic oscillations and disordered oscillations specific to dynamical systems with chaotic behavior.

The data considered were obtained as a result of a full-scale experiment with an elastic beam with longitudinal compression. The beam consists of two steel strips connected on free ends and fixed on opposite ones. Compression is achieved by a strained string. Excitation of oscillations is performed by exposure of alternating magnetic field on a magnet placed on the loose end. The law of motion with a change in the frequency of the harmonic action was registered [1].

To study the invariant numerical characteristics of the attractor of the corresponding dynamical system β -statentropy were calculated [2]. Based on the dependence of β -statentropy on the frequency of the external action and the nature of the phase portraits a phenomenological model was proposed.

To simulate this situation the two most important assumptions are made. First, the motion of the elastic beam is replaced by the motion of a material point in a certain force field. Second, the form of the potential function was chosen from the following considerations: it should have a maximum at deflection $x = 0$ and two minimums at $x = \pm x_0$, that is equilibrium position at $x = 0$ is unstable, and equilibriums at $x = \pm x_0$ are stable. These conditions are satisfied by the Duffing equation

$$\ddot{y} + \alpha\dot{y} + \frac{1}{2}y(y^2 - 1) = f \cos(\Omega\tau),$$

^{a)}Email: hhiks@yandex.ru

where α is the dissipation parameter, f is the parameter of the intensity of the external action, Ω is the frequency of the external action normalized to the frequency of small free oscillations.

In this equation, when the parameters are changed, a well-known Feigenbaum scenario of transition to chaos through the chain of doubling bifurcations is realized. This circumstance allows us to propose the following method of selecting the parameters of the problem so that the properties of the attractor of the dynamic system and the experimental model described above are close. To this end, in the region where the Feigenbaum scenario of the transition to chaos is realized, the parameters α and f equations are fixed. Then the frequency Ω , at which the first doubling of the period occurs, is determined, this value is compared with the frequency at which the period doubles in the experimental system. Next, the values of Ω were determined under which the system has a chaotic attractor. Estimation of adequacy of the choice of α and f was carried out by comparing dependences of β -statentropy and the first Lyapunov exponent [3] on the frequency of the external action constructed for experimental system and model

Acknowledgments:

This work was supported by the Russian Science Foundation (project 14-21-00158).

References

- [1] Glyzin S. D., Lokhanin M. V., Sirotin D. M., Invariant Characteristics of Forced Oscillations of a Beam with Longitudinal Compression, *Modelling and Analysis of Information Systems*, 25(1), 2018, 54-62.
- [2] E. A. Timofeev, Invariants of Measures Admitting Statistical Estimates, *St. Petersburg Mathematical Journal*, 17(3), 2005, 204–236.
- [3] Glyzin D. S., Glyzin S. D., Kolesov A. Yu., Rozov N. Kh., The Dynamic Renormalization Method for Finding the Maximum Lyapunov Exponent of a Chaotic Attractor, *Differ. Equ.*, 41(2), 2005, 284–289.

Regression analysis of the results of planned computer experiments in machine mechanics

I.N. Statnikov^{1,a)}, G.I. Firsov^{1,b)}

¹*Blagonravov Engineering Research Institute of RAS*

The possibility is considered on the basis of the planned computational experiment at the stage of mathematical modeling to efficiently construct convolutions of the received information. This allows us to build a direct functional relationship between the parameters and the quality criteria of the dynamic system. formulas for calculating the coefficients for some types of regression dependencies are obtained, pre-calculated estimates of the variances from below and from above are given both for the coefficients and for the values of the regression function (i.e., the error forecast of the quality criterion). The results of research on the mathematical model of acoustic emission of loom elements are presented; a mathematical model for the

^{a)}Email: firsovgi@mail.ru

^{b)}Email: firsovgi@mail.ru

propagation of acoustic energy by the design of the machine is constructed; Such assessments made it possible to develop recommendations for reducing machine noise.

Conducting mathematical experiments should be purposeful and optimal. The specific nature of the various fields of scientific research led to the development of a variety of methods and their modifications to the planning of extreme experiments. In the study of machines and mechanisms, the specificity of this field of scientific knowledge is associated with the construction on the basis of classical mechanics of mathematical models in the form of a set of differential equations (ordinary, linear and nonlinear, in partial derivatives), and analysis of the solutions of these equations, depending on the parameters of the system and the specified quality criteria cars [1]. Using the methods of simulation in the problems of analysis and synthesis of dynamic systems, they face the problem of obtaining a large amount of information, and hence with the problems of processing and interpreting the results obtained. The report considers the application of the method of planned LP-search (PLP-search) [2] for collapsing the obtained information on the basis of statistical processing of simulation results. The PLP search allows one, on the one hand, to perform a quasi-uniform survey of the region of the investigated parameters; on the other hand, as a result of special planning of these experiments, quantitative estimates of the influence of variable parameters on the analyzed properties of the machine developed in mathematical statistics [3] are applied. The relationship between the considered quality criteria and the system parameters is proposed to be formed, for example, in the form of a generalized power-law Kolmogorov-Gabor polynomial [4]. The complexity of using such an approximation lies in the cumbersomeness of the expressions obtained even with a relatively small dimension of the parameter space. In the PLP-search method, this problem is solved on the basis of the constructed procedure for performing computer experiments and using the variance analysis. The specificity of the PLP search method allows us to calculate in advance various parameters functions necessary for the formation of a system of linear equations by the method of least squares. This is possible, since in PLP-search all the number of experiments is carried out in series, and pseudo-random numbers of the LP-sequence are used [5]. The report details the derivation of formulas for calculating the sums of variable parameters and estimates the variance of the calculation error in calculations using approximate formulas. It is shown that the value of the dispersion does not depend on the dimensionality of the space of the variable parameters, but depends on the range of variation of the parameters, while the dispersion value decreases significantly after 5-7 series of experiments. To significantly reduce the variance of the error, it is necessary to increase the number of experiments in the series. The real possibilities of the obtained dependences in terms of the accuracy attained were verified on the test linear functions without "noise" and with it, where as the noise an "additive" of randomly distributed random numbers in the given interval with a dispersion calculated in advance was used. The accuracy of the approximation was verified by the sum of two criteria: the root-mean-square deviation between the given and received functions and the average value of the modulus of deviations between these functions. For the used functions, let's say that they were combined with different combinations of coefficients (positive and negative, different orders) to refine the algorithm for calculating the estimates of the components of the parameter vector. In addition, the results show that, for most of the functions studied, the criteria in many cases achieve better values at different levels of planning than with a level-based one. This fact is explained by the unequal (probabilistic) influence of the variable parameters on the magnitude of the criterion. Therefore, when researching mathematical models with a further aim at constructing regression dependencies, significant savings in computational experiments are possible with the following tactics: first a small computational experiment (several hundreds of computational experiments) is carried out using PLP search, then the degree of probabilistic influence on those or other

accuracy criteria, and then a vector of quantities of the levels of variable parameters is assigned, which will allow for the total (total) number of subtractions experimental experiments, less than if we were to carry out the computational experiment "blindly", to achieve the desired accuracy of approximation. Summarizing the presented material, we assume that the obtained formulas of linear, quadratic and cubic approximation of the results of computational experiments obtained on mathematical models, while observing the recommendations described, ensure the given accuracy beforehand if the fact itself of the corresponding dependence of design parameters on the criteria is established. This allows in many cases to move from complex differential dependencies to simple ones (for example, algebraic ones) and use the latter as preliminary in designing the object, and sometimes, as final ones. The proposed technique is illustrated by the example of solving a two-criteria problem of optimal design of the vibration damping system of a loom. On the basis of the application of the PLP search, it was possible to isolate a range of variable parameters (for which the damping coefficients of the machine nodes were adopted) for a relatively small number of machine experiments, in which the normalized quality criteria estimating the noise levels and consumption of the vibration isolation material exceed 0,5. On the basis of identifying this area and understanding the physical processes, it was possible to construct mathematical models that reliably relate the values of the criteria to the values of the variable parameters. On the other hand, based on the constructed mathematical models for the quality criteria, the functions of the sensitivity [6] of the criteria for variable parameters were constructed and, thus, the objective possibilities of a preliminary choice of the compromise coverage option by the noise level criteria and noise protection costs were created.

References

- [1] Misyurin S.Yu., Kreinin G.V.. On Choosing the Drive Type for the Power Unit of a Mechatronics System // Journal of Machinery Manufacture and Reliability, 2015, Vol. 44, No. 4, pp. 305–311.
- [2] Statnikov I.N., Firsov G.I. Using sobol sequences for planning experiments // Journal of Physics: Conference Series. - 937 – 2017. – 012050. - P. 1-3.
- [3] Kryanev A.V., Lukin G.V. Mathematical methods for processing indeterminate data. Moscow: Phymathlit, 2006. 213 p. (In Russian).
- [4] Nalimov V.V. Theory of experiment. Moscow: Nauka, GRFML, 1982. 256 p. (In Russian).
- [5] Sobol I.M. Multidimensional quadrature formulas and functions Haar. Moscow: Phymathlit, 1969. 288 p. (In Russian).
- [6] Sobol I.M., Tarantola S., Gatelli D., Kucherenko S.S., Mauntz W. Estimating the Approximation Error when fixing Unessential Factors in Global Sensitivity Analysis // Reliability Engineering and System Safety. 2007, v.92, №7, p.957-960.

A new method for triplet periodicity change point detection

Y.M. Suvorova^{1,a)}, K.G. Skryabin¹, E.V. Korotkov^{1,2}

¹*Research Center of Biotechnology RAS*

²*National Research Nuclear University MEPhI*

Gene fusion - the process of creating new genes by combining previously independent sequences - one of the main mechanisms of the evolution of protein sequences. Earlier, we developed a method for triplet periodicity change points detection in protein-coding sequences and showed their relationship with the formation of this sequence as a result of gene fusion. In the present work, the method for finding the triplet periodicity change point was significantly improved by using the informational measure of the difference of the triplet periodicity matrices and using the Monte-Carlo method. Analysis of the coding sequences from the *A.thaliana* genome showed that the new method finds about four times more the triplet periodicity change points, than in the previous work, at the same level of statistical significance (95%). An additional analysis of the found sequences with TP change points was performed.

The study of the evolution of protein coding sequences of DNA is the subject of interest of scientists for several decades. It was shown that one of the mechanisms of the formation of new proteins is a fusion (concatenation) of two previously independent sequences or their parts [1]. Also the property of triplet periodicity (TP) is closely associated [2, 3] with protein-coding sequences. Earlier, we developed a method for finding the triplet periodicity change point in a protein coding sequence and showed a possible relationship between this phenomenon and the formation of a gene as a result of a fusion [4, 5]. In this work, the previously developed method for finding the TP change point has been significantly improved.

The TP change point is a position in a sequence in which the TP of the left part from the point is significantly different from TP of all the three reading frames of the right part. The triplet periodicity of a DNA sequence (or its part) is usually represented as a 4×3 frequency matrix, where the columns correspond to three codon positions, and the rows to the four DNA bases ('a', 't', 'c', 'g'). In this paper, to determine the difference between two TP matrixes, an information-based measure was used [6]. Also, we introduce Monte Carlo simulations for each studied sequence. To do this, each gene under investigation was 100 times shuffled with the retention of the TP level of the gene. On the obtained shuffled sequences set, the mean and variance for the objective function was calculated. Then the resulting value obtained on real gene was reduced to the normal form. This allowed to avoid the influence of the length of the gene on the result and to find statistically significant cases on shorter sequences.

The genome of the *A.thaliana* plant was chosen as the object of the study. All protein-coding sequences of this genome were downloaded from the Ensembl database - a total of 48321 sequences. Next, to select a threshold value, we generated a random dataset with the same length and TP level as in real genes by special trio-shuffling every studied gene sequence [4]. Using the developed program, the shuffled and real coding sequences were studied and 15202 sequences were found at a significance level of 95%. This is much more than we received earlier. In the previous study, for the *A.thaliana* genome, 2224 genes containing a TP change point were found.

Since the coding sequences were used in this work, and it is known that the variants of alternative splicing of a eukaryotic gene may be very similar, it is necessary to evaluate their

^{a)}Email: suvorovay@gmail.com

influence on the result. Duplicate sequences (splice variants) were excluded as a result of leaving 9131 unique genes. It is important to note that even considering alternative splicing the method finds about four times more the TP change points, than we found in the previous work. Next, the effect of amino acid repeats and low-complexity sequences on the result of our program was investigated. Using the *Seg* tool [7], we found that up to 37% of the TP change points can be explained by the effect of different kind of repeats. Similar results were obtained on other eukaryotic genomes. - *C. Elegance, D.melanogaster, H.sapiens, R.Norvegicus.*

References

- [1] Kummerfeld S K and Teichmann S A 2005 Relative rates of gene fusion and fission in multi-domain proteins. *Trends Genet.*21 25–30
- [2] Frenkel F E and Korotkov E V 2009 Using Triplet Periodicity of Nucleotide Sequences for Finding Potential Reading Frame Shifts in Genes *DNA Res.* 16 105–14
- [3] Frenkel F E and Korotkov E V 2008 Classification analysis of triplet periodicity in protein-coding regions of genes *Gene*421
- [4] Suvorova Y M, Rudenko V M and Korotkov E V 2012 Detection change points of triplet periodicity of gene *Gene*491 58–64
- [5] Suvorova Y, Korotkova M and Korotkov E 2014 Study of the Paired Change Points in Bacterial Genes *IEEE/ACM Trans. Comput. Biol. Bioinforma.* 1–1
- [6] Kullback S 1997 *Information Theory and Statistics.* ed S Kullback (New York: Dover publications.)
- [7] Wootton J C and Federhen S 1996 Analysis of compositionally biased regions in sequence databases *Methods Enzymol.*266 554–71

The Monte-Carlo method for modeling of grains, their disorientation for polycrystal

N.S. Tolmacheva^{1,a)}, T.I. Savyolova^{1,b)}

¹*National Research Nuclear University "MEPhI"*

EBS D experiment is widely used in metal science to study the structure and texture of materials. An up-to-date task is to study the adequacy of measuring the characteristics of materials. To do this, scientists create mathematical models of the sample and the measurement results, and EBS D technology can help in this. In this article, we develop a mathematical model of the grain structure of a polycrystalline sample in the form of ellipses and derive the calculation formulas. Random variables are the small semi-axis, the coefficient of elongation (the ratio of the large and small semi-axes), the angle of rotation of the ellipse. Numerical examples of the lengths

^{a)}Email: tniserg@gmail.com

^{b)}Email: TISavelova@mephi.ru

of the chords of ellipses are obtained using the Monte-Carlo method. Results of a numerical experiment are presented in the form of histograms. The choice of the simulation parameters is based on the experimental data measured with the EBSD experiment for some steels.

Introduction

In recent years, the automation and development of diffraction of reflected electrons (EBSD) makes it possible to obtain a large number of measurements of crystallographic orientations and sizes of individual grains, in contrast to x-ray and neutron methods. The spatial arrangement of grains and the value of their orientations affect the microstructure and macrostructure of the material. One of the main and most important parameters of EBSD experiment is scanning step and threshold angle between neighboring grains. The result of the system is an array of data (x,y) , which can be represented as a raster image, called the orientation map of the crystal lattice of the sample, the pixel position of which corresponds to the beam positions on the sample, and the color coded values of the Eulerian angles.

Results

Designations used in the article:

- a large semi-axis,
- b small semi-axis,
- $k = \frac{a}{b} \geq 1$ coefficient of elongation,
- φ angle of rotation of the ellipse (between the axis OX and the big semi-axis),
- c chord, a segment from the origin to the intersection with the ellipse boundary along the OX axis.

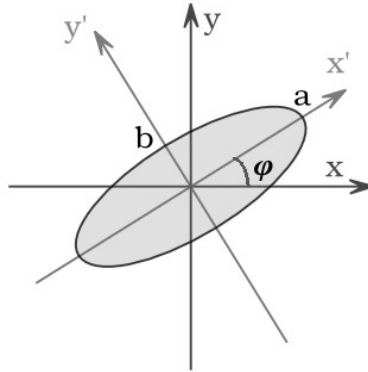


Fig. 1: Rotation of an ellipse around center.

Random parameters of the ellipse (r, k, φ) are mutually independent and have distribution laws $p_1(r), p_2(k), p_3(\varphi)$, where

$$p_1(r) = ae^{-ar}, \quad r \geq 0, \quad (a > 0),$$

$$p_2(k) = \frac{1}{K-1}, \quad k \in (1, K), \quad K > 1,$$

$$p_3(\varphi) = \frac{1}{\pi}, \quad \varphi \in (0, \pi).$$

If these conditions are met, the density of the ellipse section is calculated by the formula (1) and the chord is modeled by the formula (2). Similar results were obtained for grain size.

$$p_4(z) = \int_1^K \frac{dk}{K-1} \int_0^{\frac{\pi}{2}} \frac{2}{\pi} a e^{-za\sqrt{1-(1-\frac{1}{k^2})\cos^2\varphi}} \sqrt{1-(1-\frac{1}{k^2})\cos^2\varphi} d\varphi \quad (1)$$

$$x = \left[\left(\frac{a \cos(\pi\gamma_3)}{(-\ln\gamma_1)(1+\gamma_2(K-1))} \right)^2 + \left(\frac{a \sin(\pi\gamma_3)}{(-\ln\gamma_1)} \right)^2 \right]^{-\frac{1}{2}} \quad (2)$$

Using the obtained results, a random chord and grain size were modeled.

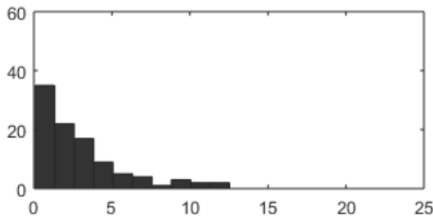


Fig. 2: Histogram of the distribution of chords for $a = 0.5, K = 3$.

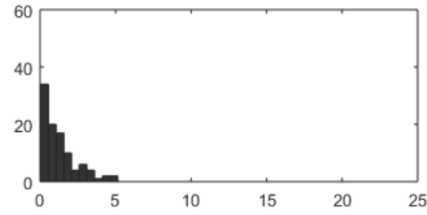


Fig. 3: Histogram of the distribution of chords for $a = 1, K = 2$.

References

- [1] Varyukhin V.N., Pashinskaya E.G., Zavdoveev A.V.,Burkhovetsky V.V. Possibilities of the diffraction method for backscattered electrons for analyzing the structure of deformed materials. Kiev. Naukova Dumka, 2014, p. 104.
- [2] Antonova A.O. The influence of parameters of the EBSD experiment on the accuracy of the calculation of textural characteristics of polycrystalline material. Dissertation for the degree of candidate of physical and mathematical sciences. 2017, 148p.
- [3] Savyolova T.I. Monte Carlo Method.] National Research Nuclear University MEPhI, Moscow, 2011, 150p.

The determination of the coefficients of harmonic linearization for deterministic nonlinear system with control

A.V. Zavozina^{1,a)}, T.R. Velieva^{1,b)}, A.V. Korolkova^{1,c)}

¹*Peoples' Friendship University of Russia*

^{a)}Email: 1032171772@rudn.university

^{b)}Email: velieva_tr@rudn.university

^{c)}Email: akorolkova@sci.pfu.edu.ru

The study of systems with management revealed the phenomenon of global synchronization of nodes in the network, which manifested in the form of a self-oscillating mode. The existence of this mode impares the characteristics of the network, for example, bandwidth. Our research team have decided to apply the method of harmonic linearization for determination of the parameters of the self-oscillating regime.

To describe a system with control, we will use the following continuous model of interaction between an incoming TCP traffic and a router that processes TCP-packages using RED protocol [1, 3]:

$$\begin{cases} \dot{W}(t) = \frac{1}{T(Q,t)} - \frac{W(t)W(t-T(Q,t))}{2T(t-T(Q,t))}p(t-T(Q,t)); \\ \dot{Q}(t) = \frac{W(t)}{T(Q,t)}N(t) - C; \\ \dot{\hat{Q}}(t) = -w_q C \hat{Q}(t) + w_q C Q(t). \end{cases} \quad (1)$$

Here the following notation is used: W is the average TCP window size, Q is the average queue size, \hat{Q} is the exponentially weighted moving average (EWMA) of the queue size average, C is the queue service intensity, T is the full round-trip time, $T = T_p + \frac{Q}{C}$, where T_p is the round-trip time for free network (excluding delays in hardware), $\frac{Q}{C}$ is the time which batch spent in the queue, N is the number of TCP sessions, p is the packet drop function. Before applying the harmonic linearization method, it is necessary to linearize the packet drop function for the RED algorithm [2, 4]. The linearized function of the P_{RED} packet drop looks like this:

$$P_{RED} = \begin{cases} 0, & 0 < \hat{Q} \leq Q_{\min}, \\ \frac{p_{\max}}{Q_{\max} - Q_{\min}}, & Q_{\min} < \hat{Q} \leq Q_{\max}, \\ 0, & \hat{Q} > Q_{\max}. \end{cases} \quad (2)$$

Here \hat{Q} is the exponentially-weighted moving average of the queue size average, Q_{\min} and Q_{\max} are the thresholds for the weighted average of the queue length, p_{\max} is the the maximum level of packet drop. We calculate the coefficients of harmonic linearization $\varkappa_0(A, \omega, x_0)$, $\varkappa(A, \omega, x_0)$ and $\varkappa'(A, \omega, x_0)$ for static nonlinearity P_{RED} :

$$\begin{aligned} \varkappa_0(A, \omega, x_0) &= \frac{1}{2\pi} \int_0^{2\pi} P_{RED}(x_0 + A \sin(\omega t))(\omega t); \\ \varkappa(A, \omega, x_0) &= \frac{1}{A\pi} \int_0^{2\pi} P_{RED}(x_0 + A \sin(\omega t)) \sin(\omega t)(\omega t); \\ \varkappa'(A, \omega, x_0) &= \frac{1}{A\pi} \int_0^{2\pi} P_{RED}(x_0 + A \sin(\omega t)) \cos(\omega t)(\omega t). \end{aligned} \quad (3)$$

Let us demonstrate the case when:

$$Q_{\min} < x_0 < Q_{\max}, \quad x_0 - A < Q_{\min}, \quad x_0 + A > Q_{\max}. \quad (4)$$

Let us find the values of the limits of integration α_{\min} and α_{\max} :

$$\begin{aligned} x_0 + A \sin \alpha_{\min} &= Q_{\min}, \quad \sin \alpha_{\min} = \frac{Q_{\min} - x_0}{A}; \quad \cos \alpha_{\min} = \sqrt{1 - \frac{(Q_{\min} - x_0)^2}{A^2}}; \\ x_0 + A \sin \alpha_{\max} &= Q_{\max}, \quad \sin \alpha_{\max} = \frac{Q_{\max} - x_0}{A}; \quad \cos \alpha_{\max} = \sqrt{1 - \frac{(Q_{\max} - x_0)^2}{A^2}}. \end{aligned} \quad (5)$$

Thus, by integrating in this area, we will get:

$$\begin{aligned} \varkappa_0(A, x_0) &= \frac{p_{\max}}{2\pi(Q_{\max} - Q_{\min})} [2 \arcsin(\frac{Q_{\max} - x_0}{A}) + 2 \arcsin(\frac{Q_{\min} - x_0}{A})]; \\ \varkappa(A, x_0) &= -\frac{2p_{\max}}{\pi A(Q_{\max} - Q_{\min})} [\sqrt{1 - \frac{(Q_{\min} - x_0)^2}{A^2}} - \sqrt{1 - \frac{(Q_{\max} - x_0)^2}{A^2}}]; \\ \varkappa'(A, x_0) &= 0. \end{aligned} \tag{6}$$

Since the derivation of harmonic linearization coefficients by analytical methods for all possible cases of relations between the thresholds Q_{\min} and Q_{\max} , the shift x_0 and the amplitude A , is a time-consuming task. Our team has developed a software package, which involves the computer algebra SymPy. With the help of this system all the time-consuming processing of the formulas is carried out. The result of the program is the analytical expression of the harmonic linearization coefficients, which will be used subsequently to generate computational programs in the Julia programming language for further investigation of the original system for determining the regions of self-oscillations.

The work is partially supported by RFBR grant No 16-01-20379. Also the publication was prepared with the support of the "RUDN University Program 5-100".

References

- [1] Misra V., Gong W. B., Towsley D., Fluid-Based Analysis of a Network of AQM Routers Supporting TCP Flows with an Application to RED // ACM SIGCOMM Computer Communication Review. "– 2000. – Vol. 30, No 4. – Pp. 151–160.
- [2] Floyd S., Jacobson V., Random Early Detection Gateways for Congestion Avoidance // IEEE/ACM Transactions on Networking."– 1993. – Vol. 1, No 4. – Pp. 397–413.
- [3] T. R. Velieva, A. V. Korolkova, D. S. Kulyabov, B. A. Dos Santos. Model Queue Management on Routers // Vestnik RUDN. Series "Mathematics. Computer science. Physics."– 2014. – № 2. – Pp. 81–92.
- [4] D. S. Kulyabov, A. V. Korolkova, T. R. Velieva. Application of the Harmonic Linearization Method to the Study a Control Systems with a Self-Oscillatory Regime // Vestnik RUDN. Series "Mathematics. Computer science. Physics." – 2017. – T. 25. – № 3. – Pp. 234–252.

Issues of medical datasets classification

V.V. Zhukov^{1,a)}, L.V. Aleksandrova¹, A.M. Mardashev¹, V.A. Petrov¹, I.L. Tolmachev¹

¹*Peoples' Friendship University of Russia (RUDN University)*

In this paper, we consider the main features and issues associated with medical datasets. The principal interest is the influence of these issues on the process of classification for such datasets. This work aims to develop general recommendations for the construction of classifiers for medical datasets.

^{a)}Email: zhukov_vv@rudn.university

The methods of machine learning in the field of medicine and biomedical research are gaining increasing popularity, especially with regard to solving the classification problem. Classification is an important part and area of research in the data mining [1]. Recently published works demonstrate the possibilities of machine learning for the classification of benign and malignant neoplasms of the breast, as well as prediction of survival after chemo- or radiotherapy depending on several tumor characteristics [2, 3]. However, the construction of good classifiers with sufficient generalization ability is associated with some difficulties that arise from the characteristics of medical and biomedical data.

1 Medical datasets issues

Due to the specifics of the observation and collection of medical and biomedical data, such datasets have some issues.

Medical datasets are relatively small comparing to datasets from other fields [4]; they also may be collected from a non-reproducible situation [5]. The term “small” is referred to the situation in which the number of observations in dataset and number of features are comparable (we use the simplified definition given in [4]).

Medical datasets are often highly imbalanced [6]. Imbalanced data means where one class severely out-represent another class (or a dataset whose classification categories are not equally represented) [7].

Medical datasets are usually incomplete, containing missing values [5, 8]. There are many reasons for the missing values appearance: data can be missed due to their actual absence; errors in the data collection process may be made; data cannot be measured by technical means, etc.

Besides, other characteristics are also inherent for medical data. For example, structure (since data are usually collected according to specified protocols [5]). However, we are going to consider only three mentioned issues, since they have the most significant impact on the classification problem.

2 The impact of datasets issues on the classification problem

These issues significantly affect the process of solving the classification problem.

Inference in machine learning is based on a strong assumption: using a representative training set of samples to infer model. When available sample size is small, learning from a given dataset to build a classification model becomes difficult [9]. Sometimes the learning task can even not be accomplished [4]. First of all, we are talking about the so-called "curse of dimensionality". Also, the question arises of the correct calculation of efficiency metrics (at least with low bias).

Most classifiers work well when the class distribution in the response variable of the dataset is well balanced [10]. Data imbalance is a crucial source of performance degradation. The reason behind this is that all algorithms assume a balanced class distribution for learning. They aim to optimize the overall accuracy without considering the relative distribution of each class, so they tend to bias toward the less important negative class or majority class with larger instances [7].

Data with missing values cannot be used to build classifiers. Although the simplest and most overused way to handle missing values is to remove the cases with missing values, it is usually not applicable for medical datasets due to several reasons. First, it is valid only when missing values are assumed to be independent of both observed and unobserved data (which is not realistic in most situations). Second, it further reduces the number of data points available for analysis (which is essential for medical datasets) [5].

3 Working with datasets issues

Some methods can help resolve these issues. For example, there are techniques for small datasets classification, such as Diffusion-neural-network (DNN), Generalized Trend Diffusion Modeling, Bootstrap Method, Mega Trend Diffusion Function. It is shown that after the data preprocessing and dataset extension, the accuracy of classification is increased [9].

Since accuracy rate of the predictive model is not an appropriate measure when there is an imbalance problem, the performance of the classifier is usually measured using precision and sensitivity [10]. Besides, there are ways to solve imbalanced datasets learning issue. They include methods such as Oversampling, Undersampling, Bagging and Boosting.

Handling missing values in medical datasets is challenging. Despite there are many different types of imputation algorithms mentioned in the literature, due to subject specificity the role of the domain knowledge may be dominant in both analyzing the data and interpreting the results [5]. It is also may be useful to perform data preprocessing before imputation as it may increase classification performance than imputation alone [8].

4 Conclusion

In this paper, we summarized key characteristics of most medical datasets: small size, imbalance, and missing values. Their impact on the process of solving the classification problem is shown – the use of standard metrics and techniques does not allow reaching a sufficient level of generalizing ability. Possible ways of solving these problems are mentioned.

References

- [1] J. Hu, J. Deng and M. Sui, "A New Approach for Decision Tree Based on Principal Component Analysis," 2009 International Conference on Computational Intelligence and Software Engineering, Wuhan, 2009, pp. 1–4.
- [2] H. Asri, H. Mousannif, H. Al Moatassime, T. Noel, Using machine learning algorithms for breast cancer risk prediction and diagnosis, *Procedia Computer Science* 83 (2016) 1064–1069.
- [3] M. Montazeri, M. Montazeri, M. Montazeri, A. Beigzadeh, Machine learning models in breast cancer survival prediction, *Technology and Health Care* 24 (1) (2016) 31–42.
- [4] R. Andonie, *Extreme Data Mining: Inference from Small Datasets*, *International Journal of Computers Communications & Control*, Vol. V (2010), No. 3, pp. 280–291
- [5] Lee CH, Yoon H-J. Medical big data: promise and challenges. *Kidney Research and Clinical Practice*. 2017;36(1):3–11
- [6] Rahman, N.N., Davis, D.N.: Addressing the Class Imbalance Problems in Medical Datasets. *International Journal of Machine Learning and Computing*, 3(2), 224–228, (2013).
- [7] Miss. Reshma K. Dhurjad, Prof. Mr. S. S. Banait , " A survey on Oversampling Techniques for Imbalanced Learning " , *International Journal of Application or Innovation in Engineering & Management (IJAIEEM)*, Volume 3, Issue 10, October 2014 , pp. 279–284
- [8] Huang, M.-W., Lin, W.-C., Chen, C.-W., Ke, S.-W., Tsai, C.-F., and Eberle, W. (2016) Data preprocessing issues for incomplete medical datasets. *Expert Systems*, 33: 432–438.

- [9] Ruparel, N. H., Shahane, N. M., & Bhamare, D. P. (2013, May). Learning from small data set to build classification model: A survey. In Proc. IJCA Int. Conf. Recent Trends Eng. Technol.(ICRTET) (pp. 23–26).
- [10] Yap B.W., Rani K.A., Rahman H.A.A., Fong S., Khairudin Z., Abdullah N.N. (2014) An Application of Oversampling, Undersampling, Bagging and Boosting in Handling Imbalanced Datasets. In: Herawan T., Deris M., Abawajy J. (eds) Proceedings of the First International Conference on Advanced Data and Information Engineering (DaEng-2013). Lecture Notes in Electrical Engineering, vol 285. Springer, Singapore

New functional-separable solutions to unsteady axisymmetric boundary-layer equations in terms of elementary functions

A.I. Zhurov^{1,2,a)}

¹*Ishlinsky Institute for Problems in Mechanics of the Russian Academy of Sciences, Moscow*

²*Cardiff University, Cardiff, United Kingdom*

The study is concerned with nonlinear equations describing the unsteady axisymmetric boundary layer of a power-law non-Newtonian fluid on a body of revolution. The equation for the stream function, w , is shown to reduce to a single third-order partial differential equation of the form $w_{tz} + w_z w_{xz} - w_x w_{zz} = \kappa r^{n+1}(x) w_{zz}^{n-1} w_{zzz} + F(t, x)$, where n is a rheological parameter of the fluid; the function $r(x)$, determining the shape of the body, is assumed arbitrary. The focus is on new exact solutions that can be expressed in terms of elementary functions or by quadrature with significant arbitrariness. Solutions are sought in the functional separable form $w = fu(\xi) + gz + h$, $\xi = \varphi z + \psi$. The functions $f(t, x)$, $g(t, x)$, $h(t, x)$, $\varphi(t, x)$, $\psi(t, x)$, and $u(\xi)$ are determined in the analysis. A number of new exact solutions have been obtained with several arbitrary functions.

Introduction

Boundary-layer equations are important in many areas of science and engineering. Apart from the classical Newtonian fluid [1, 2, 3], more complex rheological models are frequently used in applications [4, 5, 6, 7]. Exact solutions to the Navier–Stokes and boundary-layer equations promote a better understanding of qualitative features of steady and unsteady fluid flows. Exact solutions with significant functional arbitrariness are of particular interest, as they may provide solutions to model problems and a means for effective assessment of numeric, asymptotic, and approximate analytical methods.

Equations

The axisymmetric unsteady hydrodynamic laminar boundary layer of a power-law non-Newtonian fluid is described by the equations

$$U_t + UU_x + VU_y = \kappa U_y^{n-1} U_{yy} + F(t, x), \quad (rU)_x + (rV)_y = 0, \quad (1)$$

^{a)}Email: alexei.zhurov@mail.ru

where x and y are the longitudinal (streamwise) and transverse coordinates, U and V are the streamwise and transverse fluid velocity components, $F(t, x) = -p_x/\rho$ is a given function, p is the pressure, ρ is the mass density, κ is the effective viscosity, n is a rheological parameter, and $r(x)$ is the dimensionless cross-sectional radius perpendicular to the axis of rotation and defining the shape of the body.

With the stream function W defined by

$$U = W_y, \quad V = -W_x - (r'_x/r)W, \quad r = r(x)$$

and the new variables $z = r(x)y$ and $w = r(x)W$, system (1) can be rewritten in the form [8]

$$w_{tz} + w_z w_{xz} - w_x w_{zz} = \kappa r^{n+1}(x) w_{zz}^{n-1} w_{zzz} + F(t, x). \quad (2)$$

Equation (2) is known to have a large number of exact solutions [9] for $n = 1$ (Newtonian fluid) and $n \neq 1, r = 1$ (non-Newtonian fluid, plane case) as well as relatively few exact solutions for $n \neq 1, r \neq \text{const}$ (non-Newtonian fluid, axisymmetric case). The current study looks for new exact solutions in terms of elementary functions (with quadratures) for $n \neq 1$ and $r \neq \text{const}$.

Solution method

Like in [10, 11], exact solutions to equation (2) are sought in the functional separable form

$$w = fu(\xi) + gz + h, \quad \xi = \varphi z + \psi, \quad (3)$$

with the functions $f = f(t, x), g = g(t, x), h = h(t, x), \varphi = \varphi(t, x), \psi = \psi(t, x)$, and $u = u(\xi)$ to be determined in the subsequent analysis.

Substituting (3) into (2), replacing z with $(\xi - \psi)/\varphi$, and rearranging, gives the functional equation

$$\begin{aligned} g_t + gg_x - F + [(f\varphi)_t + (fg\varphi)_x]u' + f\varphi(f\varphi)_x(u')^2 \\ + f(\varphi\psi_t - \psi\varphi_t + g\varphi\psi_x + g_x\varphi\psi - g\varphi_x\psi - h_x\varphi^2)u'' \\ + f(\varphi_t + g\varphi_x - g_x\varphi)\xi u'' - ff_x\varphi^2uu'' = \kappa r^{n+1}f^n\varphi^{2n+1}(u'')^{n-1}u'''. \end{aligned} \quad (4)$$

By setting all coefficients (dependent on t and x) of the different functions dependent on ξ to be proportional to $r^{n+1}f^n\varphi^{2n+1}$, one arrives at the nonlinear third-order ODE for $u = u(\xi)$

$$a_1 + a_2u' + a_3(u')^2 + a_4u'' + a_5\xi u'' + a_6uu'' = \kappa(u'')^{n-1}u''', \quad (5)$$

where a_1, \dots, a_6 are arbitrary constants. Any consistent solution to the determining system resulting from (4) together with a corresponding solution to equation (5) generates an exact solution (3) to Eq. (2).

The primarily focus of the current study is to find exact solution to Eq. (5), expressible in terms of elementary functions or quadratures, other than those described previously in [10, 9].

Results

The proposed approach has resulted in a number of new solutions with $n = 1 + \frac{1}{m}$ (with integer $m \neq -1, 0$), $n = \frac{1}{3}$, and $n = 3$. Here are a few examples:

$$\begin{aligned} n = \frac{1}{3}: \quad u = \sqrt{\xi^2 \pm 1}; \quad n = \frac{1}{2}: \quad u = \xi \ln \left| \frac{\xi + 1}{\xi - 1} \right|, \quad u = \xi \arctan \xi; \\ n = \frac{2}{3}: \quad u = \xi \ln \left| \frac{\xi - 1}{\xi + 1} \right| + \frac{2}{3}(\xi^2 - 1)^{-1}, \quad u = \xi \arctan \xi - \frac{1}{3}(\xi^2 + 1)^{-1}; \\ n = \frac{3}{2}: \quad u = \xi^6 \pm 5\xi^4 + 15\xi^2; \quad n = 2: \quad u = C_1 e^{2\xi} + [C_2 \sin(\sqrt{3}\xi) + C_3 \cos(\sqrt{3}\xi)] e^{-\xi}, \end{aligned}$$

The corresponding functions f , g , h , φ , ψ , F , and r are found from the determining system following from Eq. (4) considering the fact that some of the terms in (5) are linearly dependent.

References

- [1] H. Schlichting, *Boundary Layer Theory*, McGraw-Hill, New York, 1981.
- [2] L.G. Loitsyanskiy, *Mechanics of Liquids and Gases*, Begell House, New-York, 1995.
- [3] F.L. Crabtree, D. Küchemann, L. Sowerby, In: *Laminar Boundary Layers* (Ed. L. Rosenhead), Oxford University Press, Oxford, 1963.
- [4] A. Acrivos, M.J. Shah, E.E. Petersen, Momentum and heat transfer in laminar boundary-layer flows of non-Newtonian fluids past external surfaces, *AIChE J.*, 1960, Vol. 6, No. 2, pp. 312–317.
- [5] Z.P. Shulman, *Convective Heat and Mass Transfer in Reologically Complicated Fluids* [in Russian], Energiya, Moscow, 1975.
- [6] G. Böhme, *Non-Newtonian Fluid Mechanics*, Elsevier, Amsterdam, 1987.
- [7] A.D. Polyanin, A.M. Kutepov, A.V. Vyazmin, D.A. Kazenin, *Hydrodynamics, Mass and Heat Transfer in Chemical Engineering*, Taylor & Francis, London, 2002.
- [8] A.D. Polyanin, Exact solutions of unsteady boundary layer equations for power-law non-Newtonian fluids, *Doklady Physics*, 2015, Vol. 60, No. 8, pp. 372–376.
- [9] A.D. Polyanin, A.I. Zhurov, One-dimensional reductions and functional separable solutions to unsteady plane and axisymmetric boundary-layer equations for non-Newtonian fluids, *Int. J. Non-Linear Mechanics*, 2016, Vol. 85, pp. 70–80.
- [10] A.D. Polyanin, A.I. Zhurov, Unsteady axisymmetric boundary-layer equations: Transformations, properties, exact solutions, order reduction and solution method, *Int. J. Non-Linear Mechanics*, 2015, Vol. 74, pp. 40–50.
- [11] A.D. Polyanin, A.I. Zhurov, Direct functional separation of variables and new exact solutions to axisymmetric unsteady boundary-layer equations, *Commun. Nonlinear Sci. Numer. Simulat.*, 2016, Vol. 31, pp. 11–20.

7th International conference
“Problems of Mathematical Physics
and Mathematical Modelling”

Book of abstracts
(Moscow, NRNU MEPhI, 25–27 June 2018)

Decision on publication 18.06.2018. Format 60x84 1/8.
Quires 27. Circulation 120. Order №80.

National Research Nuclear University MEPhI
Printing house NRNU MEPhI
115409, Moscow, Kashirskoe shosse, 31